

INFORMATION TO USERS

This manuscript has been reproduced from the microfilm master. UMI films the text directly from the original or copy submitted. Thus, some thesis and dissertation copies are in typewriter face, while others may be from any type of computer printer.

The quality of this reproduction is dependent upon the quality of the copy submitted. Broken or indistinct print, colored or poor quality illustrations and photographs, print bleedthrough, substandard margins, and improper alignment can adversely affect reproduction.

In the unlikely event that the author did not send UMI a complete manuscript and there are missing pages, these will be noted. Also, if unauthorized copyright material had to be removed, a note will indicate the deletion.

Oversize materials (e.g., maps, drawings, charts) are reproduced by sectioning the original, beginning at the upper left-hand corner and continuing from left to right in equal sections with small overlaps.

ProQuest Information and Learning
300 North Zeeb Road, Ann Arbor, MI 48106-1346 USA
800-521-0600

UMI[®]

The University of Alberta

**SUBCELLULAR CONTROL OF MYOCARDIAL ENERGY
METABOLISM**

by



Teresa Ann Hopkins

A thesis submitted to the Faculty of Graduate Studies and Research in partial
fulfillment of the requirements for the degree of
Doctor of Philosophy

Department of Pharmacology

Edmonton, Alberta

Fall 2005



Library and
Archives Canada

Bibliothèque et
Archives Canada

0-494-08656-4

Published Heritage
Branch

Direction du
Patrimoine de l'édition

395 Wellington Street
Ottawa ON K1A 0N4
Canada

395, rue Wellington
Ottawa ON K1A 0N4
Canada

Your file *Votre référence*

ISBN:

Our file *Notre référence*

ISBN:

NOTICE:

The author has granted a non-exclusive license allowing Library and Archives Canada to reproduce, publish, archive, preserve, conserve, communicate to the public by telecommunication or on the Internet, loan, distribute and sell theses worldwide, for commercial or non-commercial purposes, in microform, paper, electronic and/or any other formats.

The author retains copyright ownership and moral rights in this thesis. Neither the thesis nor substantial extracts from it may be printed or otherwise reproduced without the author's permission.

AVIS:

L'auteur a accordé une licence non exclusive permettant à la Bibliothèque et Archives Canada de reproduire, publier, archiver, sauvegarder, conserver, transmettre au public par télécommunication ou par l'Internet, prêter, distribuer et vendre des thèses partout dans le monde, à des fins commerciales ou autres, sur support microforme, papier, électronique et/ou autres formats.

L'auteur conserve la propriété du droit d'auteur et des droits moraux qui protègent cette thèse. Ni la thèse ni des extraits substantiels de celle-ci ne doivent être imprimés ou autrement reproduits sans son autorisation.

In compliance with the Canadian Privacy Act some supporting forms may have been removed from this thesis.

Conformément à la loi canadienne sur la protection de la vie privée, quelques formulaires secondaires ont été enlevés de cette thèse.

While these forms may be included in the document page count, their removal does not represent any loss of content from the thesis.

Bien que ces formulaires aient inclus dans la pagination, il n'y aura aucun contenu manquant.


Canada

DEDICATION

This thesis is dedicated to my grandmother Amelia Elizabeth Bruins who passed away in April 2004. She was a woman of great wisdom and strength (with a stubborn streak a mile wide).

My grandmother taught me the importance of love, laughter, family, and above all courage. Whenever I feel as though a task is too difficult, I can hear her say *'For goodness sake, why not try?'*

I hope that one day I will be half the woman that she was.

ABSTRACT

The heart derives a majority of its energy requirements from the oxidation of fatty acids and glucose. Following an ischemic episode, high rates of fatty acid oxidation may impair cardiac recovery. These high fatty acid oxidation rates can inhibit glucose oxidation and are important for cardiac metabolic substrate preference.

Since fatty acid oxidation inhibits glucose oxidation at the level of the pyruvate dehydrogenase complex (PDC), the control of PDC activity is one important factor influencing cardiac energy metabolism. This study investigated the subcellular control of PDC activity by phosphorylation and allosteric inhibition. Mice overexpressing peroxisome proliferator activated receptor alpha (PPAR α) were utilized, since these mice have increased levels of an associated PDC kinase (PDK) that phosphorylates and inhibits PDC activity. Glucose oxidation rates and PDC activity were measured in the heart and despite significant changes in glucose oxidation rates, PDC activity was unchanged. Since the *in vitro* PDC activity assay reflects phosphorylation status but not flux, these data suggest that PDC flux is an important determinant of glucose oxidation rates in the heart.

An important determinant of fatty acid oxidation rates and myocardial substrate preference is malonyl CoA, which inhibits mitochondrial fatty acid

uptake by carnitine palmitoyltransferase isoform 1 (CPT-1). Since malonyl CoA decarboxylase (MCD) degrades malonyl CoA, MCD may regulate myocardial substrate preference. We investigated the localization of MCD using novel techniques in order to further predict the function and subcellular control of MCD and malonyl CoA levels. This study indicated that a large proportion of MCD was found in cardiac peroxisomes, however the role of peroxisomal MCD remains unclear.

Although the exact role of MCD is unknown, it has been shown that inhibition of MCD improves functional recovery following ischemia. MCD knockout mice were generated to further explore MCD function and were genotyped and characterized in this study. These mice show decreased reliance on fatty acids for energy production, however no changes in expression of enzymes involved in malonyl CoA regulation were observed.

Data provided by this study indicate that both PDK and MCD may be important pharmacological targets to enhance glucose use and improve recovery following ischemia.

ACKNOWLEDGEMENTS

I would like to thank my supervisor Dr. Gary Lopaschuk for taking a chance on me as a summer student even though my undergrad grades were not 'stellar'.

Thank you to my supervisor Dr. Jason Dyck for always having an open door for any problem and for toughening me up to prepare me for a career in science.

Thanks so much to Dr. Sandy Clanachan for always having a third opinion in every supervisory committee meeting, for all of the advice on finding a post-doctoral fellowship and for always standing by me to offer help.

I would like to thank my parents (Brian and Donna) for supporting me even if they won't admit that they don't know what Pharmacology is and for always being just a phone call away for any reason.

I would like to thank my little sister Krista for loving Harry Potter, movies and books that remind me there is more to life than just science. It's great to have a sister that understands my thesis woes.

Thanks so much to Jason Iden for helping me with everything from computer programs to skydiving to car washes. If it were not for your support I would not be here today. Your courage and relaxed view of life have changed my entire outlook and I am so thankful to know you.

And last but not least thank you so much to the following friends that have made such a difference during my time here:

Miss Emily Manning for all-you-can-eat-sushi-nights-of-fun

Donna Beker for coffee breaks and talks about life

Jay Jaswal for making O'Byrnes extra fun

Rohit Moudgil for the experience-of-a-lifetime-wedding-extravaganza

Grant Wickman and Debbie Iden for making me participate in the
Pharmacology nights out at Avenue Pizza

Karalyn Cuthbert for being a spectacular friend both in and
out of the lab

Brandy Hyndman for Dairy Queen ice cream and our trip to Ottawa

Lynn McLernon for keeping me sane in 2001

Mike Kuang for sharing the 'best' parts of the Dyck lab with me

Suzanne Kovacic (Suzy Q) for making me laugh every day

Brandi Holman and Kim Forrest for believing in me since Senator
Riley High School in High River... I love you guys.

Heather Platt for being my best friend, cooking me dinners, listening
to my problems and offering to help me move to Boston. I could
never have finished my thesis without your support.

TABLE OF CONTENTS

1. INTRODUCTION	1
<i>Fatty acids as a source of energy.....</i>	<i>3</i>
Fatty acid uptake.....	3
Mitochondrial fatty acid uptake.....	5
Mitochondrial β -oxidation of fatty acids	6
The Krebs' Cycle	7
Peroxisomal β -oxidation of fatty acids.....	8
<i>Control of fatty acid oxidation rates</i>	<i>3</i>
Malonyl CoA inhibition of CPT-1.....	10
Malonyl CoA production by ACC.....	11
Malonyl CoA degradation by MCD	13
Peroxisomal production of malonyl CoA and regulation of mitochondrial fatty acid oxidation rates	15
<i>Glucose as a source of energy</i>	<i>16</i>
Glucose uptake.....	16
Glycolysis	17
Control of Glycolysis by PFK-2 phosphorylation via AMPK...	17
Glucose oxidation	19
Control of glucose oxidation rates by the Randle cycle	19
Control of glucose oxidation by PDC phosphorylation.....	21
<i>Regulation of metabolic pathways by gene expression</i>	<i>23</i>
Peroxisome proliferator activated receptors.....	23
PPAR α control of fatty acid oxidation gene expression	24
PPAR α control of glucose oxidation gene expression	25

<i>Metabolic substrate preference during ischemia/reperfusion</i>	26
Fatty acid oxidation.....	26
Glycolysis	27
Glucose oxidation	27
Impact of incomplete glucose oxidation during I/R.....	28
Pharmacological treatments	29
<i>PDK and MCD and cardiac substrate preference</i>	32
PDK activity, expression and tissue distribution.....	32
MCD activity, expression and tissue distribution	34
MCD deficiency.....	34
MCD subcellular localization.....	35
MCD inhibition.....	37
<i>Hypothesis and Objectives</i>	38
<i>References</i>	38

2. CONTROL OF PYRUVATE DEHYDROGENASE ACTIVITY IN PPAR α TRANSGENIC MICE 56

<i>Introduction</i>	57
<i>Methods</i>	60
Transgenic animals	60
Isolated working mouse heart model	60
PDC activity measurements	61
Immunoblotting	62
Statistics.....	62
<i>Results</i>	64
Contractile function of isolated perfused mouse hearts	64
Metabolism and PDC activity measurements	64
Expression levels of PDK and PDH E1- α	65

Metabolism and PDC activity measurements in WY14, 643 treated animals	67
Discussion	73
Diabetic phenotype and metabolic control by PPAR α	73
PPAR α increases PDK4 expression and decreases glucose oxidation rates in the absence of depressed PDC activity .	73
<i>In vitro</i> assays do not measure PDC flux.....	74
Fasting and WY14,643 alter glucose oxidation rates with only minor changes in PDC activity.....	75
Diminished pyruvate supply and effect on glucose oxidation rates.....	76
WY 14,643 treatment of MHC-PPAR α mice.....	76
Contribution of PDC phosphatase is unknown.....	77
Limitations	78
Summary	79
References	80

3. SUBCELLULAR LOCALIZATION OF MALONYL COA DECARBOXYLASE

83

Introduction.....

84

Methods

87

Subcellular fractionation using an Optiprep gradient..... 87

Immunoblot analysis of fractions

86

Isolated working rat heart model for fractionation..... 88

Isolation of pure peroxisomes using a vertical rotor

89

Production of MYC labelled MCD constructs by PCR..... 90

Preparation of MYC tagged constructs for sub-cloning into the mammalian expression vector pcDNA3.1(+)

..... 92

Ligation and transformation of MYC tagged constructs

92

Transfection of MYC tagged constructs into CHO cells and

analysis by immunoblotting	93
Determination of MCD construct activity in CHO cells	94
Isolation of neonatal rat cardiac myocytes.....	95
Culture of neonatal rat cardiac myocytes.....	96
Transfection of MYC tagged MCD constructs into neonatal rat cardiac myocytes	97
Immunocytochemistry of neonatal rat cardiac myocytes	97
Visualization of MCD localization using confocal microscopy	98
Results	99
MCD protein localization by subcellular fractionation of rat heart tissue	99
Localization of endogenous MCD in isolated neonatal rat rat cardiac myocytes	106
Transfection, intracellular processing and activity measurements of MYC tagged MCD constructs in CHO cells.....	112
Immunocytochemistry and localization of MCD fusion proteins in neonatal rat cardiac myocytes	118
Summary of MCD localization using MCD-MYC fusion proteins	123
Discussion	124
Subcellular fractionation of MCD	124
Translocation of MCD	124
Putative targeting sequences of MCD	125
Peroxisomal localization of MCD in the heart	125
Mitochondrial localization of MCD in the heart.....	127
What is the role of peroxisomal MCD?.....	129
Signaling events and MCD localization	131
Initiation of MCD translation.....	132
Neonatal rat cardiac myocytes as a model.....	133
Limitations	133
Summary	134
References	135

4. MALONYL COA DECARBOXYLASE KNOCKOUT MICE: GENOTYPING AND GENE EXPRESSION.....	138
<i>Introduction.....</i>	<i>139</i>
<i>Methods</i>	<i>141</i>
Production of MCD knockout mice.....	141
MCD activity measurements.....	141
Measurements of malonyl CoA levels.....	142
Isolation of genomic DNA from ear notches.....	143
Precipitation of genomic DNA.....	143
Genomic DNA amplification using the Genomiphi system.....	144
Genotyping of animals by PCR.....	145
Backcrossing strategy for MCD knockout mouse breeding lines.....	148
Isolated working mouse heart model.....	149
Isolation of tissue from MCD knockout mice.....	149
Quantitative RT-PCR analysis of gene expression.....	150
Immunoblotting protocol for protein expression.....	150
PDC activity measurements.....	151
Statistics.....	152
<i>Results</i>	<i>154</i>
Production of MCD knockout mice and genomic primer design.....	154
Genotyping of the MCD knockout mice is accurate.....	155
Metabolic profile of isolated working mouse hearts from MCD knockout mice and control mice.....	160
mRNA expression analysis by quantitative RT-PCR.....	165
Protein expression of PPAR α regulated enzymes.....	165
Protein expression of the enzymes involved in regulation of malonyl CoA levels.....	168

PDC activity in MCD knockout mice	168
Discussion	174
Accuracy of the PCR genotyping method	174
Phenotype of MCD knockout mice	174
Backcrosses	175
Metabolic profile of MCD knockout mice	176
Expression of proteins involved in malonyl CoA regulation ..	177
mRNA and protein expression of PPAR α regulated genes.....	177
Limitations	178
Summary	179
References	180
5. GENERAL DISCUSSION	183
<i>MCD localization, control of MCD activity and the role of peroxisomal</i>	
<i>MCD</i>	184
Peroxisomal oxidation and MCD	184
Malonyl CoA compartmentalization issues	187
Control of MCD localization	188
<i>MCD knockout mice</i>	190
<i>Treatment of ischemic heart disease</i>	191
Metabolic modulation in the treatment of ischemic heart	
disease	191
Modulation of PDK activity.....	192
Modulation of PPAR α activity	193
Modulation of MCD activity.....	195

<i>Metabolic modulation of insulin sensitivity</i>	196
<i>Summary</i>	198
<i>References</i>	200

LIST OF TABLES

Table 2-1. Contractile parameters of isolated working hearts from wild-type and MHC PPAR α hearts.....	64
Table 2-2. Activity of PDC in the active form (PDCa) in untreated, fasted and WY 14, 643 treated wild-type and MHC-PPAR α hearts.....	71
Table 3-1. Antibody dilutions and protocols for immunoblotting and immunocytochemistry	88
Table 3-2. PCR primer sequences for the development of MYC tagged MCD constructs	91
Table 4-1. Primer sequences for genotyping of MCD knockout mice by PCR .	145
Table 4-2. Antibody dilutions and protocols for immunoblot analysis of MCD knockout mice	151

LIST OF FIGURES

Figure 1-1. Uptake, activation and intracellular trafficking of fatty acids and glucose	5
Figure 1-2. Mitochondrial β -oxidation in the heart	6
Figure 1-3. The Krebs' cycle	8
Figure 1-4. Regulation of cytosolic malonyl CoA levels by AMPK, MCD and ACC	12
Figure 1-5. The glycolytic pathway	18
Figure 1-6. The glucose oxidation pathway	20
Figure 1-7. The roles of the three PPAR isoforms in whole body energy metabolism.....	25
Figure 2-1. Palmitate oxidation, glucose oxidation, tricarboxylic acid cycle production and PDC activity of wild-type and MHC-PPAR α mouse hearts.....	66
Figure 2-2. Expression levels of the cardiac PDK isoforms and PDC E1- α	68

Figure 2-3. Glucose oxidation and PDC activity of fasted and WY 14,643 treated animals	70
Figure 2-4. Correlation curves	72
Figure 3-1. Subcellular fractionation protocol.....	100
Figure 3-2. Immunoblots of the cytosol, nuclear, microsomal and mitochondrial enriched fractions	101
Figure 3-3. Translocation of MCD in response to ischemia/reperfusion.....	102
Figure 3-4. Isolation of pure peroxisomes	104
Figure 3-5. Immunoblot analysis of pure peroxisomes.....	105
Figure 3-6. Confocal configuration of Zeiss 510 confocal microscope system for immunocytochemistry	107
Figure 3-7. Immunocytochemistry of endogenous MCD in ITS treated myocytes	108
Figure 3-8. Immunocytochemistry of endogenous MCD in myocytes grown in 10% fetal bovine serum	110

Figure 3-9. MCD expression in myocytes treated with ITS buffer or serum.....	111
Figure 3-10. Nile red analysis of lipid accumulation in serum treated cells	113
Figure 3-11. Design and transfection of MYC tagged MCD constructs in CHO cells.....	115
Figure 3-12. MCD activity of MCD fusion proteins in CHO cells	117
Figure 3-13. Co-localization of the MYC-MCDtr construct.....	119
Figure 3-14. Co-localization of the MCDtr-MYC construct.....	120
Figure 3-15. Co-localization of the MYC-MCDfl construct.....	121
Figure 3-16. Co-localization of the MCDfl-MYC construct.....	122
Figure 4-1. Production of MCD knockout mice by a directed homologous recombination event	156
Figure 4-2. Primer design for specific genotyping of each allele.....	157
Figure 4-3. Genomic DNA isolation protocol using Genomiphi system.....	158

Figure 4-4. Genomic DNA amplification of isolated genomic DNA from MCD knockout mice	159
Figure 4-5. Confirmation of genotyping strategy.	161
Figure 4-6. MCD knockout mouse backcross strategy	162
Figure 4-7. Characterization of MCD knockout mice.....	163
Figure 4-8. Palmitate oxidation rates of wild-type and MCD knockout mouse hearts.....	164
Figure 4-9. Cardiac mRNA expression of several metabolic genes	166
Figure 4-10. Immunoblot analysis of PPAR α regulated genes	167
Figure 4-11. Immunoblot analysis of genes involved in malonyl CoA regulation	170
Figure 4-12. Densitometry of immunoblot analysis	171
Figure 4-13. Cardiac PDC activity of wild-type and MCD knockout mouse hearts.....	172

Figure 4-14. Relationship between number of backcrosses and level of homozygosity to background strain173

Figure 5-1. Summary of subcellular control of malonyl CoA levels in the myocyte at the current level of understanding, assuming a peroxisomal distribution of MCD186

SYMBOLS AND ABBREVIATIONS

α	alpha
β	beta
γ	gamma
$^{\circ}\text{C}$	degrees celcius
%	percent
x g	times gravity – centrifugation speed
ABC transporter	ATP binding cassette transporter
ACBP	acyl CoA binding protein
ACC	acetyl CoA carboxylase
Acetyl CoA	acetyl coenzyme A
AMP	adenosine monophoshate
AMPK	5' AMP activated protein kinase
ANOVA	analysis of variance
ATP	adenosine triphosphate
BAC	bacterial artificial chromosome
BSA	bovine serum albumin
bp	base pair (s)
[^{14}C]	^{14}C Carbon
C57 BL6	C57 Black 6
cDNA	complementary deoxyribonucleic acid
CHO cells	Chinese Hamster Ovary cells
CO_2	carbon dioxide
CoA	coenzyme A
CPT-1	Carnitine palmitoyltransferase isoform 1
CPT-2	Carnitine palmitoyltransferase isoform 2
Da	Dalton (1 atomic mass unit)
DCA	dichloroacetic acid
ddH $_2\text{O}$	double distilled water
DTT	dithiothreitol
DNA	deoxyribonucleic acid

<i>E. coli</i>	<i>Escherichia coli</i>
EDTA.....	ethylenediaminetetraacetic acid di-sodium salt
<i>e.g.</i>	<i>exempli gratia</i> (Latin, 'for example')
EGTA.....	ethylene glycol-bis(β-aminoethylether)-N,N,N',N'-tetraacetic acid
et al.	et alii (Latin, 'and others')
ES.	embryonic stem cells
FABP _{pm}	plasma membrane fatty acid binding protein
FACS	fatty acyl coA synthetase
FAT/CD36	fatty acid translocase
FATP	fatty acid transport protein
FADH ₂	flavin adenine dinucleotide
g.....	gram(s)
GLUT-4	glucose transporter-4
GTP.....	guanosine dinucleotide
[³ H]	³ Hydrogen (Tritium)
H ₂ O.....	water
HEPES	4-(2-hydroxyethyl) piperazine-1-ethane sulphonic acid
HPLC	high performance liquid chromatography
ICC	immunocytochemistry
<i>i.e.</i>	<i>id est</i> (Latin, 'that is')
ITS	insulin-transferrin-selenium
Kb	kilobase(s)
kg	kilogram
K _m	Michaelis Menton constant
l.....	litre(s)
LB broth.....	Luria-Bertani broth
LDH.....	lactate dehydrogenase
M.....	moles·l ⁻¹
Malonyl CoA.....	malonyl coenzyme A
MCD	malonyl CoA decarboxylase
mg	milligram
MgCl ₂	magnesium chloride
MgSO ₄	magnesium sulphate
MHC-PPARα.....	mice with cardiac overexpression of PPARα
ml.....	milliliter

mM	millimolar
mmHg	millimeters of mercury
mol	moles
mRNA	messenger ribonucleic acid
n	number of samples
N ₂	nitrogen
NaCl	sodium chloride
NADH	nicotinamide adenine dinucleotide
NaF	sodium fluoride
nm	nanometer
nmol	nano mole
NaOH	sodium hydroxide
NaPPi	sodium pyrophosphate
O ₂	molecular oxygen
PBS	phosphate buffered saline
PCR	polymerase chain reaction
PDC	pyruvate dehydrogenase complex
PDK	pyruvate dehydrogenase kinase
PDP	pyruvate dehydrogenase phosphatase
PFK-1	phosphofructokinase-1
PFK-2	phosphofructokinase-2
PPAR α	peroxisome proliferator activated receptor alpha
PTS-1	peroxisomal targeting sequence type 1
rpm	revolutions per minute
RT-PCR	reverse transcription-polymerase chain reaction
RXR	retinoid X receptor
SDS	sodium dodecylsulphate
SDS-PAGE	sodium dodecylsulphate polyacrylamide gel electrophoresis
SEM	standard error of the mean
TBS	tris buffered saline
TCA	tricarboxylic acid
TPP	thiamine pyrophosphate
tris HCl	tris[hydroxymethyl]-amino methane hydrochloride
U	units
UCP	uncoupling protein

μ l..... microliter
 μ mol.....micromole
V..... Volts
VDAC-1.....voltage dependent anion channel isoform 1
vs..... versus

Mathematical prefixes

M..... mega (10^6)
k.....kilo (10^3)
c..... centi (10^{-1})
m..... milli (10^{-3})
 μmicro (10^{-6})
n..... nano (10^{-9})
p.....pico (10^{-12})

Chapter 1

Introduction

Cardiovascular disease is the leading cause of death in Canada and despite current treatments the incidence continues to rise ¹. Ischemic heart disease is a major contributor to this incidence of cardiovascular disease. The current treatment of ischemic heart disease is aimed at either increasing oxygen supply to the heart, or lowering the oxygen requirement of the heart by decreasing cardiac work. A novel approach in the treatment of ischemic heart disease is to target cardiac efficiency, which would yield the same amount of cardiac work with a reduced oxygen demand. Therefore, our laboratory continues to search for new treatments directed towards optimizing cardiac energy metabolism.

To provide energy for maintenance of contraction and ionic homeostasis, the heart has a very high demand for high energy phosphates, such as adenosine tri-phosphate (ATP). While the heart does not have a long-term storage mechanism for ATP, phosphate groups can be provided from phosphocreatine to temporarily restore ATP levels. In the absence of constant ATP production, the heart is unable to maintain contractile function and blood supply to systemic tissues may become compromised. The heart maintains this ATP production from several different sources including fatty acids and glucose.

60-90% of the energy production in the aerobic heart comes from the utilization of fatty acids ². While glucose and lactate are other major sources of energy, the heart can also use pyruvate or ketone bodies such as 3-hydroxybutyrate, acetoacetate and acetone. The amount of glucose and lactate used depends on the rate of fatty acid utilization. Although the heart is capable of using various substrates, the choice of substrate plays an important role in certain types of ischemic settings such as myocardial infarction.

The substrate preference of the heart determines the functional recovery following an ischemic episode. This feature of the heart allows us to target metabolism in the treatment of heart disease and potentially improve clinical outcomes. There are currently two drugs on the market world-wide, trimetazidine and ranolazine, which target energy preference in the heart and have shown efficacy in the setting of angina. Therefore, understanding the basic science involved in cardiac energy metabolism is essential for the design of new pharmacological treatments.

Fatty Acid Utilization and Acute Control of Fatty Acid Oxidation

1.1 Fatty acids as a source of energy

1.1.1: Fatty acid uptake

Fatty acids are delivered to the heart either as free fatty acids bound to albumin or in the form of triglycerides supplied by very low density lipoprotein (VLDL) or chylomicrons. Fatty acids are liberated from triglycerides by lipoprotein lipase present on the external surface of the endothelial cell³ and/or on the cardiac myocyte⁴. Free fatty acids enter into the cardiac myocyte by plasma membrane fatty acid transporters including fatty acid translocase (FAT/CD36)^{5,6}, fatty acid transport protein (FATP)⁷⁻¹¹, plasma membrane fatty acid binding protein (FABPpm)¹² or by passive diffusion across the membrane¹³⁻¹⁵. Although the relative contribution of these pathways (protein-mediated fatty acid transport and flip-flop diffusion of fatty acids) remains a subject of debate, it appears that protein mediated transport is a major mechanism by which the heart takes up fatty acids.

In support of protein mediated uptake of fatty acids, FAT/CD36 knockout mice exhibit a 50-80% loss of fatty acid uptake in the heart ^{16, 17}, which is accompanied by a 40% reduction in fatty acid oxidation rates ¹⁸. This suggests an important role of FAT/CD36 in protein-mediated uptake of fatty acids into the myocyte. FAT/CD36 is stored in endosomal vesicles within the myocyte ¹⁹ and can be mobilized to the plasma membrane by insulin ²⁰, 5'AMP-activated protein kinase (AMPK) ²¹ and muscle contraction ²². Therefore, the uptake of fatty acids by FAT/CD36 can be increased during periods of high energy demand.

The role of the other two putative fatty acid uptake proteins, FABPpm and FATP is less well known. It has been suggested that FABPpm may act as an acceptor for fatty acids, which then either enter the cell by FAT/CD36 transport or passive diffusion ²³. While FABPpm may target fatty acids to the membrane to allow uptake into the cell, it appears that the role of FATP may be to drive fatty acid uptake into the heart by promoting metabolism, since FATP can activate fatty acids to fatty acyl CoA ¹⁰. These transport mechanisms are important for fatty acid uptake and activation in the cardiac myocyte.

Regardless of the transport mechanism, once inside the myocyte fatty acids are either bound to fatty acid binding proteins ²⁴⁻²⁸ or are converted to fatty acyl CoA by the enzyme fatty acyl CoA synthetase (FACS). Fatty acyl CoAs are bound to acyl CoA binding proteins (ACBP) in the cytosol (the predominant carrier of acyl CoA in the heart ²⁹) and are either transported into the mitochondria for energy production, used as a substrate for triglycerides, or complex lipid synthesis (phospholipids). Figure 1-1 depicts

the uptake and intracellular trafficking of fatty acids in the heart. Fatty acids may be directed toward mitochondria where further metabolism of the fatty acyl CoA occurs.

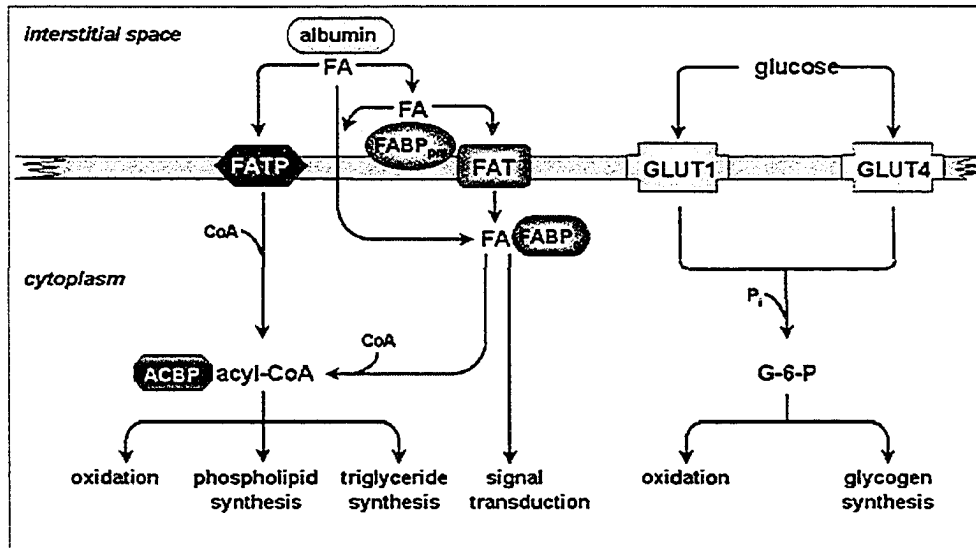


Figure 1-1: The uptake, activation and intracellular trafficking of fatty acids and glucose in the heart (Figure from Luiken et al, 2004³⁰)

1.1.2: Mitochondrial fatty acid uptake

Since the Coenzyme A (CoA) moiety of fatty acyl CoAs does not readily cross membranes, the uptake of fatty acyl CoA into mitochondria requires a specialized enzyme shuttle system. This system consists of three components, which allows the movement of fatty acyl CoAs into the mitochondrial matrix. The first step of this uptake process involves the conversion of fatty acyl CoA to fatty acyl carnitine by carnitine palmitoyl transferase-1 (CPT-1), which is localized to the outer mitochondrial membrane^{31, 32}. Carnitine acyl translocase transports the fatty acyl carnitine conjugate into the mitochondrial matrix and carnitine palmitoyl transferase-2 (on the inner mitochondrial membrane³²) regenerates the fatty acyl CoA by replacing the existing carnitine group

with a CoA molecule. Following these enzymatic processes the fatty acyl CoA is reconstituted in the same form in the mitochondria as it was in the cytosol, with the exception that the CoA moiety is derived from separate cytosolic and mitochondrial pools. Since the metabolism of fatty acyl CoA occurs in the mitochondria, mitochondrial uptake of fatty acids dictates the rate of oxidation through the β -oxidation pathway.

1.1.3 Mitochondrial β -oxidation of fatty acids

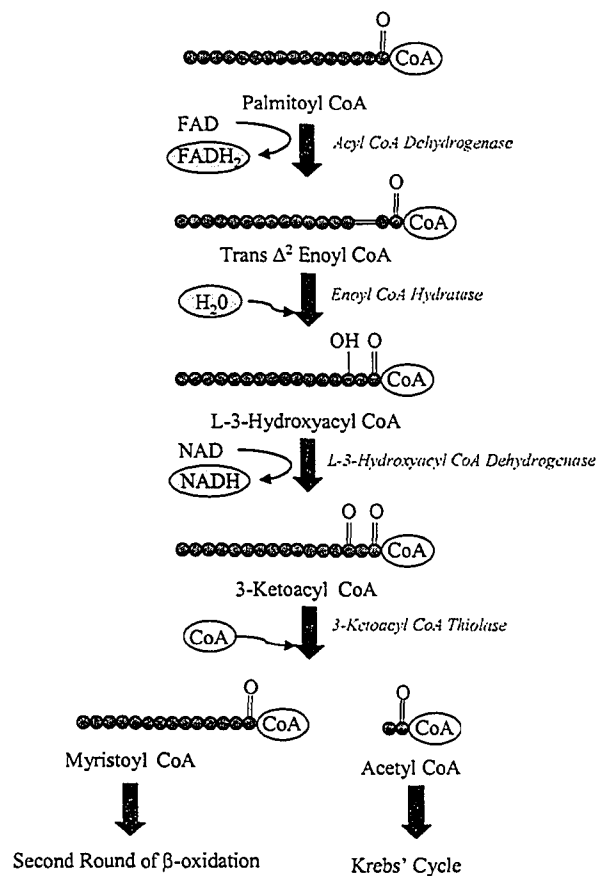


Figure 1-2: A schematic representation of the enzymatic reactions of mitochondrial β -oxidation in the heart

As suggested by the term 'β-oxidation' the utilization of fatty acids has a strict oxygen requirement. Fatty acyl CoAs within the mitochondrial matrix are catabolized by a series of four enzymatic reactions as depicted in Figure 1-2. The fatty acyl CoA goes through several rounds of β-oxidation and is shortened by a two-carbon acetyl CoA molecule for each turn of the oxidation spiral. The remainder of the fatty acyl CoA undergoes these same four steps until completion. For example, palmitoyl CoA (C16) undergoes 8 rounds of β-oxidation to produce 8 acetyl CoA molecules. Unsaturated fatty acids such as linolenic acid require additional enzymes such as enoyl CoA isomerase for complete oxidation to acetyl CoA. The acetyl CoA produced from mitochondrial oxidation of fatty acids is further coupled to the Krebs' cycle, described below.

1.1.4 The Krebs' cycle

The Krebs' cycle consists of an efficient group of enzymes, which produce reducing equivalents such as NADH, FADH₂ and GTP that are eventually used for ATP production. The cycle is initiated by the entry of acetyl CoA from both the fatty acid oxidation and glucose oxidation pathways (see Section 1.3.4). The acetyl CoA groups produced by these oxidative pathways combine with oxaloacetate to form citrate, a reaction catalyzed by the enzyme citrate synthase. The remainder of the Krebs' cycle and the reducing equivalents produced is depicted in Figure 1.3. The reducing equivalents produced by fatty acid oxidation, glucose oxidation and the Krebs' cycle feed into the electron transport chain allowing the mitochondria to establish a proton gradient. This gradient produces ATP by the movement of protons down the concentration gradient

through a mitochondrial ATP synthase. ATP production can occur from the oxidation of substrates in both the mitochondrial and peroxisomal compartments of the myocyte.

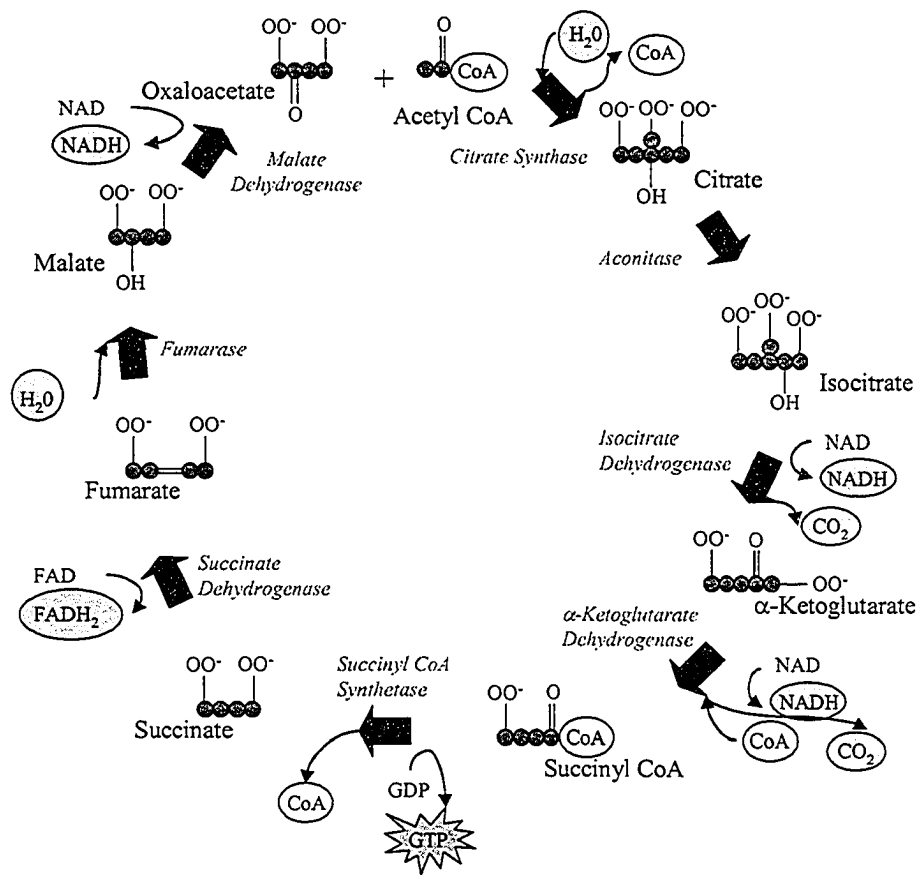


Figure 1-3: A schematic representation of the enzymatic reactions of the mitochondrial Krebs' Cycle in the heart

1.1.5 Peroxisomal β-oxidation of fatty acids

Mitochondria are not the only organelles that oxidize fatty acids in the heart. Peroxisomes also have a role in fatty acid metabolism, although peroxisomal β-oxidation is not as well understood. Uptake of fatty acids into peroxisomes is not very well characterized, but a malonyl CoA-sensitive carnitine acyltransferase system has been

reported in liver peroxisomes³³. Another proposed mechanism of fatty acid uptake exists for the peroxisomal entry of fatty acids. Since the uptake of very long chain fatty acids into peroxisomes is impaired in X-linked adrenoleukodystrophy (a peroxisomal disorder characterized by accumulation of very long chain fatty acids) and the adrenoleukodystrophy gene has high homology to an ABC (ATP binding cassette) transporter³⁴, this suggests that the uptake of very long chain fatty acids in peroxisomes occurs through an ABC transporter mediated mechanism. The mitochondria and peroxisomes not only have different mechanisms for fatty acid uptake but they also have differences in how these fatty acids are oxidized.

The first enzyme in the peroxisomal β -oxidation pathway is catalyzed by acyl CoA oxidase rather than acyl CoA dehydrogenase as seen in the mitochondria. Since acyl CoA oxidase does not produce FADH_2 , peroxisomal β -oxidation produces less ATP than mitochondrial oxidation and is not as energetically efficient. Another unique aspect of peroxisomal oxidation is that peroxisomes do not contain the enzymes of the Krebs' cycle for complete utilization of acetyl CoA. Peroxisomal acetyl CoA has been shown in yeast to be directed into the mitochondrial Krebs' cycle³⁵. However, recent ^{13}C -NMR data suggest that in the rat heart there is no entry of peroxisomal acetyl CoA into the mitochondrial Krebs' cycle³⁶. Another difference between the mitochondrial and peroxisomal fatty acid oxidation pathways is the different chain length affinity for fatty acid intermediates. β -oxidation within peroxisomes does not reach completion as the enzymes involved have very low affinity for short chain fatty acids below butyryl CoA³⁷. Therefore, it has been postulated that peroxisomal oxidation exists to reduce chain length of very long chain fatty acids, which are then shunted to the mitochondria for further

metabolism. The mitochondrial uptake of free fatty acids and partially oxidized fatty acids from peroxisomes is tightly regulated by the control of CPT-1 activity.

1.2 Control of fatty acid oxidation rates

1.2.1 Malonyl CoA inhibition of CPT-1

As previously mentioned, the rate of fatty acid oxidation is controlled by entry of fatty acids into the mitochondria through the CPT-1 carnitine shuttle system. There are two isoforms of CPT-1 in the heart: the muscle isoform M-CPT-1, and the liver isoform L-CPT-1³⁸. In the heart, the majority of CPT-1 activity is derived from the muscle isoform while a small amount of L-CPT-1 exists³⁸. M-CPT-1 is more sensitive to inhibition by malonyl CoA, a potent inhibitor of CPT-1^{39, 40}, suggesting that malonyl CoA is an important regulator of fatty acid oxidation rates in the heart.

While the production of malonyl CoA is important for fatty acid biosynthesis in the liver, the role of malonyl CoA in the heart appears primarily to be regulation of mitochondrial fatty acid uptake⁴¹ and possibly peroxisomal fatty acid transport⁴². However, there appears to be a discrepancy between the total cellular content of malonyl CoA in the heart and the K_m for inhibition of CPT-1 such that malonyl CoA levels are higher than the K_m for CPT-1⁴³. This suggests that CPT-1 should be completely inhibited in the heart⁴³. However, Hoppel and colleagues have shown that malonyl CoA sensitivity of CPT-1 can be altered by phosphorylation⁴⁴, which could alter malonyl CoA control of CPT-1 activity despite these high levels of cellular malonyl CoA. In addition, since inhibition of CPT-1 occurs on the cytosolic face of the enzyme⁴⁵⁻⁴⁸ it has been suggested that only cytosolic malonyl CoA is able to inhibit fatty acid uptake into the

mitochondria. Malonyl CoA may therefore exist in distinct cellular pools and cytosolic levels may be much lower than that required to inhibit CPT-1. While the subcellular control of malonyl CoA concentrations has not been fully elucidated, strong evidence suggests that malonyl CoA regulates fatty acid oxidation rates in the heart.

The mechanisms by which malonyl CoA regulates fatty acid uptake and oxidation in the heart are not completely understood. During conditions when malonyl CoA levels are high, fatty acid oxidation rates are low. Conversely, fatty acid oxidation rates are high under conditions where malonyl CoA levels are reduced. Taken together this correlation suggests an important role for malonyl CoA in the regulation of fatty acid oxidation rates in the heart. Since the turnover rate of malonyl CoA is very fast (less than 3 minutes⁴⁹) the steady state levels of malonyl CoA are dynamically regulated by its synthesis, degradation and supply of acetyl CoA. The enzymes responsible for the production and degradation of malonyl CoA are acetyl CoA carboxylase (ACC) and malonyl CoA decarboxylase (MCD), respectively. Both of these enzymes have been shown to be major regulators of cardiac fatty acid oxidation rates^{50, 51}. Figure 1-4 shows the regulation of malonyl CoA levels by these enzymes and the impact on mitochondrial fatty acid oxidation rates.

1.2.2 Malonyl CoA production by acetyl CoA carboxylase (ACC)

Acetyl CoA carboxylase catalyzes the conversion of acetyl CoA to malonyl CoA. There are two isoforms of ACC in the heart encoded by different genes^{52, 53}. ACC-1 is a protein with a molecular weight of 266 kDa⁵³⁻⁵⁵ and is localized to the cytosol⁵⁶,

whereas ACC-2 has a molecular weight of 280 kDa⁵³⁻⁵⁵ and is associated with the outer mitochondrial membrane⁵⁶.

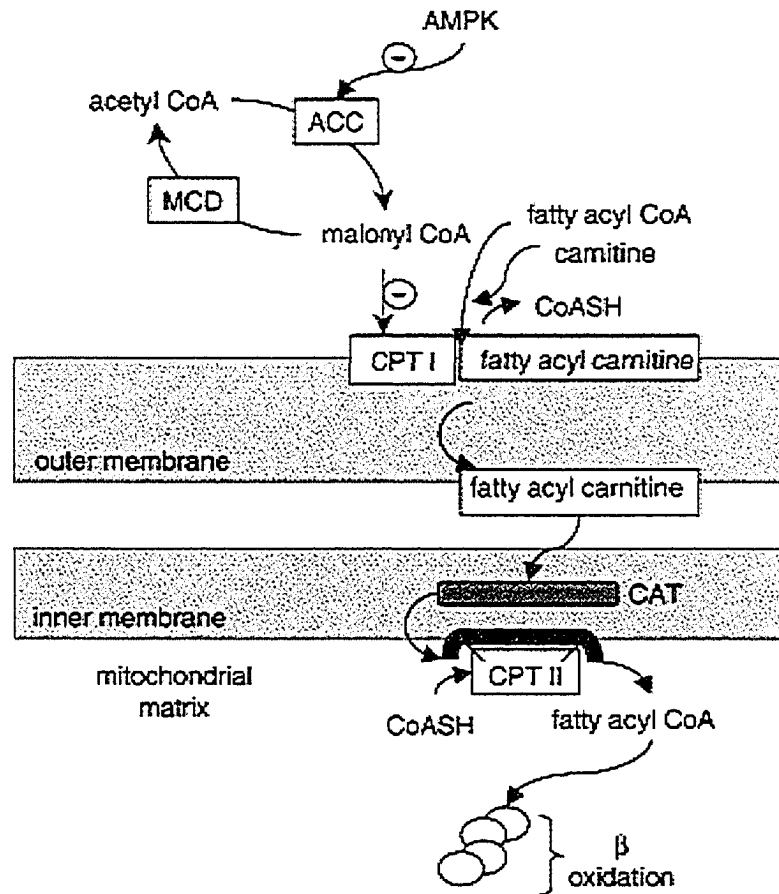


Figure 1-4: Regulation of cytosolic malonyl CoA levels by AMPK, ACC, and MCD alters mitochondrial fatty acid oxidation rates. (Figure from Fukao et al, 2004⁵⁷)

The role of each isoform is postulated to be unique such that ACC-1 produces malonyl CoA for fatty acid biosynthesis, while ACC-2 produces malonyl CoA for inhibition of CPT-1⁵⁸. ACC-2 null mice have been generated and both skeletal muscle and heart tissues extracted from these mice have very low levels of malonyl CoA⁵⁹. In accordance, the rate of skeletal muscle fatty acid oxidation is much higher in ACC-2 null

mice than in their wild-type counterparts⁵⁹ indicating the important role of ACC-2 in the control of malonyl CoA levels and regulation of fatty acid oxidation.

In addition to the intracellular localization of ACC being able to control its function, ACC can also be controlled via phosphorylation by a number of kinases⁶⁰⁻⁶². One such kinase is 5' AMP activated protein kinase (AMPK), a stress kinase that is activated by increased levels of AMP and plays an important role in the control of fatty acid oxidation rates^{51, 63}. When AMPK activity is high, such as during ischemia/reperfusion and exercise⁶³⁻⁶⁵ malonyl CoA production by ACC is inhibited and fatty acid oxidation rates are accelerated.

Another mechanism of ACC control is through allosteric regulation of ACC by citrate. ACC activity is dramatically increased by the presence of citrate⁶⁶ and citrate produced from the Krebs' cycle feeds-back to accelerate ACC production of malonyl CoA. ACC activity is also acutely regulated by the presence of the reaction substrate, acetyl CoA. High levels of acetyl CoA increases flux through ACC and increases malonyl CoA production. These mechanisms are important regulators of fatty acid oxidation in the myocyte.

1.2.3 Malonyl CoA degradation by malonyl CoA decarboxylase (MCD)

Malonyl CoA decarboxylase catalyzes the conversion of malonyl CoA to acetyl CoA and effectively lowers malonyl CoA levels. There is only one isoform of MCD found in the heart and this isoform has a molecular weight of approximately 50.7 kDa⁶⁷. MCD in the heart has been shown to play an important role in the regulation of cardiac fatty acid oxidation rates through the control of malonyl CoA levels⁵⁰. Pharmacological

inhibition of MCD causes a rise in malonyl CoA levels and improved recovery following ischemia/reperfusion injury ⁶⁸. As well, hearts from mice lacking the MCD protein are more resistant to an ischemic insult ⁶⁹ suggesting that the regulation of fatty acid oxidation rates by MCD may be an important target for future therapies for ischemic heart disease or left ventricular dysfunction following cardiovascular surgery.

Although the role of MCD in the control of fatty acid oxidation rates is becoming clearer, the localization of the enzyme is still a matter of controversy. Much of this controversy is due to the presence of two potential targeting sequences on the MCD protein: (1) an N-terminal mitochondrial sequence and (2) a C-terminal peroxisomal targeting sequence type 1 (PTS-I) ⁷⁰. A second, confounding factor is the presence of two potential translational start sites on the MCD mRNA transcript ⁶⁷. Pancreatic islet cells express both a 54.7 and 50.7 kDa form of MCD ⁶⁷, suggesting that both translational start sites may be operational. Since only one of the MCD translational start sites allows synthesis of MCD with the N-terminal mitochondrial targeting sequence, the translational start site utilized *in vivo* will affect the localization of MCD in the heart. A potential cleavage site also exists on the MCD protein ⁷⁰, which may represent cleavage of the full-length isoform of the MCD protein and thus may impact the localization of MCD. Experimental data suggest that the localization of MCD is mitochondrial, peroxisomal, cytosolic or a combination of these three ⁷¹⁻⁷⁴. The localization of MCD will be further addressed in Section 1.8.3 of this chapter.

Although the extent to which post-translational modification can regulate cardiac MCD is currently unknown, *in vitro* dephosphorylation with alkaline phosphatase has been shown to enhance MCD activity ⁶⁷, suggesting that MCD is regulated via

phosphorylation by an unknown enzyme. MCD in skeletal muscle is phosphorylated by AMPK^{75,76}, however conflicting evidence suggests that AMPK does not phosphorylate MCD in skeletal muscle or the heart⁷⁷. The post-translational regulation of MCD in the heart by cleavage, subcellular localization and phosphorylation is currently unclear, despite the fact that MCD plays an important role in substrate preference of the heart by altering malonyl CoA levels.

1.2.4 Peroxisomal production of malonyl CoA regulates mitochondrial fatty acid oxidation

The production of malonyl CoA is an important determinant of mitochondrial fatty acid oxidation rates in the heart and recent studies in the Langendorff perfused rat heart suggest that at least 50% of the malonyl CoA produced within the cardiac myocyte is derived from peroxisomal acetyl CoA⁷⁸. Therefore, the production of malonyl CoA from peroxisomal derived acetyl CoA may represent another level of control for mitochondrial fatty acid uptake through CPT-1. Since the concentration of acetyl CoA in these studies remains below the Km for ACC, the supply of acetyl CoA from both mitochondria⁷⁹ and peroxisomes may be rate-limiting for production of malonyl CoA⁷⁸. Long chain fatty acids such as palmitate are partially oxidized in the peroxisome, therefore acetyl CoA is produced by the oxidation of both very long chain fatty acids and long chain fatty acids. Therefore, high rates of peroxisomal oxidation may turn off uptake of long chain fatty acids into the mitochondria by the production of malonyl CoA. However, the shorter chain fatty acids derived from this peroxisomal oxidation may not require CPT-1 mediated fatty acid uptake, suggesting that high rates of peroxisomal

oxidation of fatty acids may allow CPT-1 independent mitochondrial uptake of short chain fatty acids to occur.

Taken together, these data suggest that an important regulator of mitochondrial fatty acid oxidation is the rate of peroxisomal acetyl CoA production. Therefore, the capability of the heart for peroxisomal oxidation could determine the level of mitochondrial fatty acid oxidation.

Glucose Utilization and Acute Control of Glycolysis and Glucose Oxidation

1.3 Glucose as a source of energy

1.3.1 Glucose uptake

Glucose uptake into the myocyte occurs via two main glucose transporters (GLUT-1 and GLUT-4) present in the heart. Figure 1-1 shows the uptake and activation of glucose in the heart by these transporters. GLUT-1 is present on the plasma membrane and is responsible for the basal uptake of glucose into the myocyte, while GLUT-4 resides within intracellular vesicles and is mobilized to the plasma membrane upon stimulation. The stimuli that cause acute GLUT-4 translocation are insulin⁸⁰⁻⁸², AMPK activation due to ischemia⁸³ and exercise⁸⁴⁻⁸⁷, as well as activation by AMPK directly⁸⁸. GLUT-4 mobilization in response to insulin requires the activation of PI-3 kinase⁸⁹, whereas the mobilization by AMPK is PI-3 kinase independent⁸⁸. While GLUT-4 is acutely regulated by its mobilization to the plasma membrane, GLUT-1 seems to be predominantly regulated by expression levels under specific conditions. For instance, during fasting expression of GLUT-1 is decreased, while GLUT-4 expression is not altered⁹⁰. Thus due to the differential regulation of the two glucose transporters, glucose

uptake into the myocyte can be acutely increased and chronically regulated to alter glucose uptake.

Following glucose transport into the myocyte through either GLUT-1 or GLUT-4 the glucose molecule is rapidly converted to glucose 6-phosphate by hexokinase, which traps glucose inside the myocyte for either storage in the form of glycogen or energy utilization. This utilization of glucose can be divided into two processes, namely glycolysis and glucose oxidation.

1.3.2 Glycolysis

Glucose catabolism through the glycolytic pathway is unique from that of the cardiac oxidative pathways. For example the enzymes of glycolysis are localized exclusively in the cytosol, whereas the oxidative enzymes are either mitochondrial or peroxisomal. Another example is that glycolysis can operate in the absence of oxygen although it is much less efficient than the oxidation pathways (produces only two ATP molecules per glucose molecule). Glucose catabolism through the glycolytic pathway culminates in the production of pyruvate as depicted in Figure 1-5, which in the presence of oxygen can undergo further metabolism through the glucose oxidation pathway.

1.3.3 Control of glycolysis by regulation of phosphofructokinase-2 via AMPK

The rate limiting step of glycolysis is phosphofructokinase isoform 1 (PFK-1) which converts fructose 6-phosphate to fructose 1,6 bisphosphate. PFK-1 is an important point of control in the glycolytic pathway and is allosterically activated by fructose 2,6 bisphosphate. The production of fructose 2,6 bisphosphate by phosphofructokinase

isoform 2 (PFK-2) is enhanced by the phosphorylation of PFK-2 by AMPK^{91, 92}. Fructose 2,6 bisphosphate is not the only molecule that controls glycolytic catabolism of glucose. Citrate produced from the Krebs' cycle inhibits PFK activity and glycolysis, which re-directs the glucose towards glycogen production^{93, 94}. Therefore, accumulation of several allosteric mediators of the PFK enzymes regulates the rate of glycolysis in the heart. A similar control via allosteric inhibition exists for the glucose oxidation pathway.

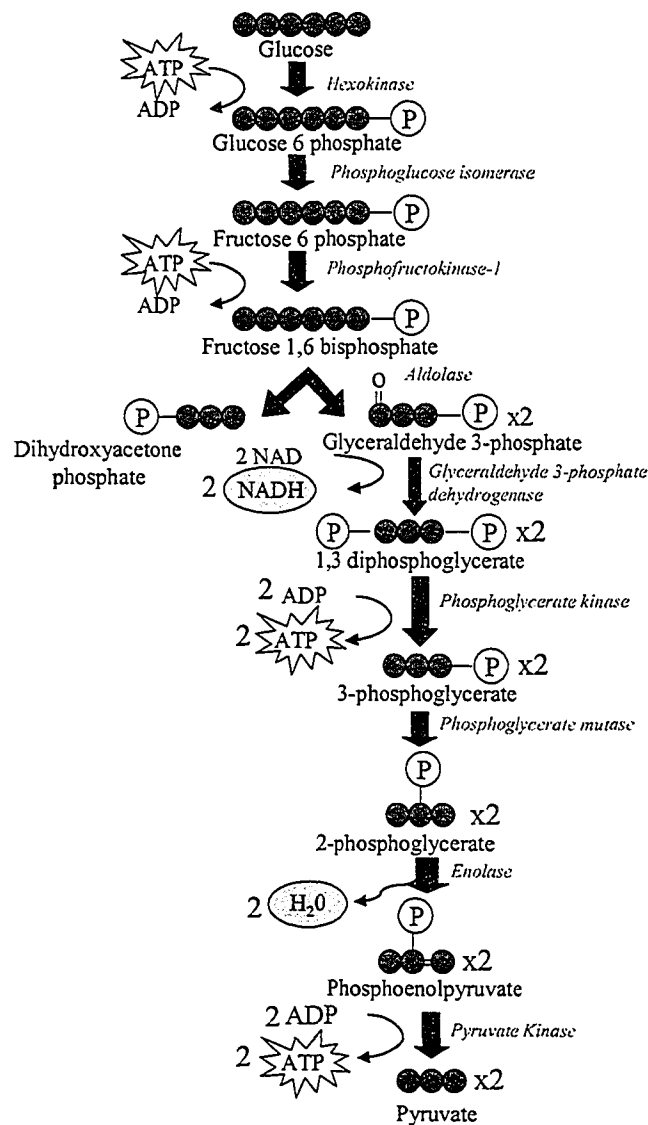


Figure 1-5: A schematic representation of the enzymatic reactions of the cytosolic glycolytic pathway

1.3.4 Glucose oxidation

Glucose oxidation is defined in this document as the complete oxidation of glucose to CO₂ and water, which encompasses both the glycolytic pathway and the entry of the resulting acetyl CoA into the Krebs' cycle. This acetyl CoA is derived from the conversion of glycolytic pyruvate to acetyl CoA by the multi-enzyme pyruvate dehydrogenase complex (PDC). The PDC complex is localized to the inner mitochondrial membrane⁹⁵ and is rate-limiting for the glucose oxidation pathway. The complex is composed of three enzymes, which together have pyruvate dehydrogenase activity (pyruvate decarboxylase, dihydrolipoate acetyltransferase and dihydrolipoyl dehydrogenase) and two regulatory enzymes (pyruvate dehydrogenase kinase and pyruvate dehydrogenase phosphatase). The production of acetyl CoA by PDC is reduced by phosphorylation of the complex and is restored upon dephosphorylation. Therefore, the rate of acetyl CoA production is dependent on the phosphorylation status of the PDC complex. The acetyl CoA molecules produced by PDC enter into the Krebs' cycle as depicted in Fig 1.6. This cycle is the common endpoint for both the fatty acid and glucose oxidative pathways. The acetyl CoA derived from fatty acid oxidation also has an important role in the allosteric inhibition of PDC, which may cause a shift towards fatty acid substrate preference in the heart (described in Section 1.5).

1.3.5 Control of glucose oxidation rates by the Randle cycle

Glucose oxidation rates are controlled at the level of the pyruvate dehydrogenase complex, which is the rate-limiting step of glucose oxidation and is regulated by the end-products of glucose and fatty acid oxidation⁹⁶. These end-products include the acetyl

CoA/CoA ratio and the NADH/NAD⁺ ratio, which exert allosteric control on the second enzyme of the PDC complex ⁹⁷. Therefore high rates of fatty acid oxidation can inhibit glucose oxidation rates by the production of acetyl CoA. The switch in substrate preference that occurs by the inhibition of glucose oxidation by fatty acid oxidation was originally suggested by Phillip Randle ⁹⁸ and would allow for the preferential use of fatty acids when plasma fatty acid levels are high. The reduction in cardiac glucose use would allow glucose to be spared in the heart upon starvation to make glucose available to organs such as the brain. The Randle cycle inhibition of cardiac glucose use is achieved by the allosteric regulation of PDC by acetyl CoA and NADH, which is associated with a switch in cardiac substrate preference towards the use of fatty acids.

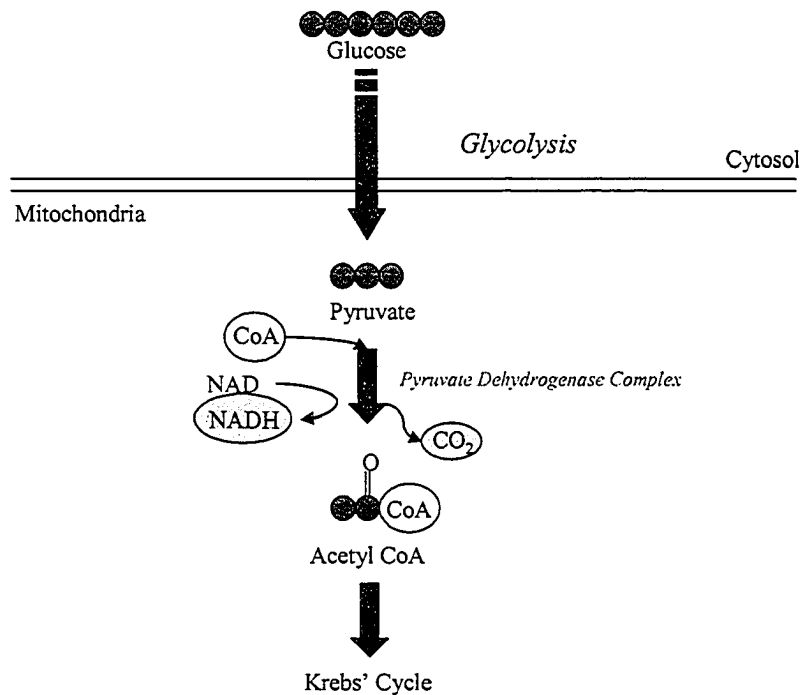


Figure 1-6: A schematic representation of the enzymatic reactions of the complete oxidation of glucose in the heart

1.3.6 Control of glucose oxidation rates by phosphorylation of PDC

As well as allosteric modulation of glucose oxidation rates, PDC is also regulated by phosphorylation status. The multi-enzyme complex is associated with an intrinsic kinase (pyruvate dehydrogenase kinase) and a loosely bound phosphatase (pyruvate dehydrogenase phosphatase). Phosphorylation of PDC by its kinase is associated with a decline in PDC activity, while dephosphorylation restores PDC activity^{99, 100}.

Inactivation of PDC activity occurs via pyruvate dehydrogenase kinase (PDK) mediated phosphorylation¹⁰¹. There are currently four known isoforms of PDK but only PDK-1, PDK-2, and PDK-4 are present in the heart^{102, 103}. PDK-2 activity and to a lesser extent PDK-1 comprise the majority of PDK activity in the normal heart¹⁰³, while PDK-4 expression is highly inducible during the fasted state¹⁰⁴⁻¹⁰⁷. These studies suggest that both acute regulation of PDK as well as chronic induction of PDK expression can impact PDC activity. Acute regulation of PDK is controlled by the end-products of oxidation, as well as the substrate of the PDC reaction. The kinase is activated by acetyl CoA/CoA and NADH/NAD⁺ ratios, while pyruvate inhibits PDK activity^{101, 108}. Pharmacological inhibition of the PDK isoforms with dichloroacetate (a pyruvate analog) promotes glucose utilization in the heart¹⁰⁹, suggesting that PDK phosphorylation of PDC is important for substrate preference in the heart. There are three suggested sites of phosphorylation of the PDC complex by PDK, however phosphorylation at a single site is sufficient for loss of PDC activity^{110, 111}.

Phosphorylation of PDC by PDK decreases PDC activity, while dephosphorylation of the complex by the associated phosphatase restores PDC activity. Dephosphorylation is achieved by two different isoforms of PDC phosphatase, which are

both capable of dephosphorylation at all three PDC phosphorylation sites ¹¹². Acute regulation of the PDC phosphatase (PDP) is unique from the regulation of PDK. PDP is activated by high magnesium and calcium concentrations, which increases PDP binding to the complex and enhances dephosphorylation of PDC ^{113, 114}. Since phosphorylation alters PDC activity, the balance of PDK and PDP activities is one determinant of PDC activity and glucose oxidation rates.

Despite considerable data showing a correlation between PDC activity and glucose oxidation rates, the inactivation of PDC and a reduction in glucose oxidation rates is not correlative in some studies ^{115, 116}. Therefore it is currently not known whether the most important regulator of PDC activity in the heart is due to phosphorylation of the enzyme complex or allosteric control by end-product inhibition.

Gene Expression and Control of Metabolic Pathways

The allosteric and phosphorylation control of the fatty acid oxidation, glycolysis, and glucose oxidation pathways previously discussed is one method to control substrate preference. However, another important level of control is the alteration of metabolic gene expression. There are a number of transcriptional control mechanisms to alter metabolic gene expression including the nuclear receptor peroxisome proliferator activated receptor isoform alpha (PPAR α).

1.4 Regulation of metabolic pathways by gene expression

1.4.1 Peroxisome proliferator activated receptors (PPAR)

The PPAR family of nuclear receptors has emerged as an important regulator of metabolic gene expression^{117, 118}. PPARs are nuclear receptors that are activated by long chain fatty acids¹¹⁹⁻¹²¹ or can be pharmacologically activated by the fibrate drugs (PPAR α agonists)¹²² or the thiazolidinedione drugs (PPAR γ agonists)^{123, 124}. The activation of PPAR by these agents or endogenous fatty acids causes the PPAR to heterodimerize with the retinoid X receptor (RXR)¹²⁵ and bind to peroxisome proliferator response elements (PPREs) in the promoter region of a gene^{117, 122, 126}. Binding of this dimer to the promoter region recruits transcriptional machinery to the target gene and increases mRNA expression. Expressional control of target genes in different tissues is achieved by tissue specific regulation by three different PPAR isoforms. These three different PPARs appear to have different metabolic functions.

The three forms of PPAR¹¹⁷ are designated PPAR α , PPAR γ and PPAR β/δ . PPAR α is highly expressed in tissues that oxidize fatty acids such as heart and skeletal

muscle, while PPAR γ is highly expressed in adipocytes¹²⁷. PPAR β/δ is ubiquitously expressed but the expression level is especially high in the heart¹²⁷. The high level of expression of PPAR α and PPAR β/δ in heart suggests an important role for each of these isoforms in the control of cardiac energy metabolism. PPAR α in particular is an important regulator of cardiac energy metabolism due to the expressional regulation of several fatty acid oxidizing enzymes. PPAR β/δ appears to play an important role in the inhibition of cardiac hypertrophy by preventing NF κ B activation and cardiac apoptosis¹²⁸. Studies from cardiac specific PPAR β/δ knockout mice indicate that PPAR β/δ controls basal fatty acid oxidation rates and deletion of this protein can result in cardiac dysfunction as well as myocardial lipid accumulation¹²⁹. Thus both PPAR β/δ and PPAR α are important regulators of cardiac energy metabolism. While both PPAR α and PPAR β/δ affect cardiac gene expression, the role of the PPAR γ isoform does not occur through a direct action on cardiac gene targets. The PPAR γ isoform is most highly expressed in adipose tissue and plays a role in fatty acid storage in the adipocyte. Other tissue specific roles of the PPAR isoforms are indicated in Figure 1-7, but PPAR α seems to play the predominant role in the control of cardiac energy metabolism.

1.4.2 PPAR α control of fatty acid oxidation gene expression

PPAR α increases the expression of several fatty acid oxidation genes important for substrate preference in the heart. Such genes include FAT/CD36^{130, 131}, FABPpm^{132, 133}, FACS^{134, 135}, CPT-1¹³⁶, acyl CoA oxidase^{126, 137}, lipoprotein lipase^{138, 139}, MCD¹⁴⁰ and uncoupling proteins¹⁴¹⁻¹⁴⁶. Overall, the effect of PPAR α in the heart is to accelerate the oxidation of fatty acids by affecting almost all areas of fatty acid utilization as

observed with these changes in expression. These areas include the hydrolysis of triglycerides, myocyte fatty acid uptake, activation to CoA esters, mitochondrial fatty acid uptake and β -oxidation. In addition to expressional changes in genes involved in fatty acid oxidation, PPAR α also regulates genes important for control of glucose oxidation rates.

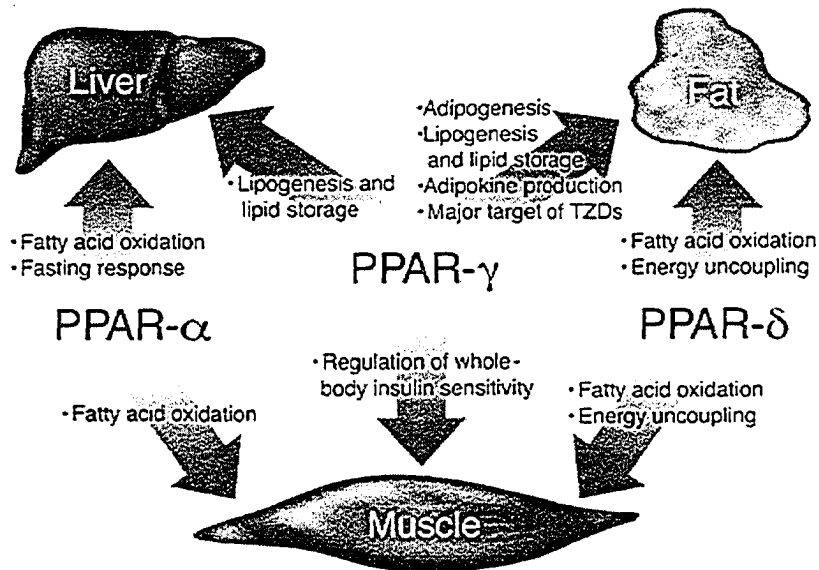


Figure 1-7: The roles of the three isoforms of PPAR in whole-body regulation of energy metabolism (Figure from Evans et al, 2004¹⁴⁷)

1.4.3 PPAR α control of glucose oxidation gene expression

PPAR α regulates the expression of PDK¹⁰⁷, another important indirect regulator of fatty acid substrate preference in the heart, due to the effect of PDK in inhibiting glucose oxidation rates. The expression of PDK is increased during fasting and re-feeding^{104, 106} due to an increase in PPAR α activity¹⁰⁷. This increased expression of PDK-4 inhibits PDC conversion of pyruvate to acetyl CoA¹⁰⁵ and glucose oxidation rates. Taken

together, the overall effect of PPAR α activation is to switch substrate preference in the heart towards the utilization of fatty acids by inhibition of glucose oxidation at the level of PDC and enhancing expression of fatty acid metabolizing enzymes.

Ischemia/Reperfusion and Metabolism

1.5 Metabolic substrate preference during ischemia/reperfusion

1.5.1 Fatty acid oxidation

During ischemia, the heart muscle is deprived of oxygen and has a decreased ability to utilize fatty acids as a source of energy due to the oxygen requirement of the β -oxidation pathway. However, upon reperfusion of the heart fatty acid oxidation dominates over all other substrates¹⁴⁸⁻¹⁵⁰. This high rate of fatty acid oxidation is a result of high plasma fatty acid levels¹⁵¹⁻¹⁵³ due to (1) catecholamine release and (2) heparin administration during surgery, which releases lipoprotein lipase and activates triglyceride breakdown. The increase in fatty acid supply is not the only contributing factor for acceleration of fatty acid oxidation rates. Malonyl CoA levels are decreased during ischemia and following reperfusion^{41, 63, 79, 154}, which relieves CPT-1 inhibition³⁹, promotes fatty acid uptake into the mitochondria, and results in an acceleration of fatty acid oxidation rates. Since both synthesis and degradation of malonyl CoA controls malonyl CoA levels, the enzyme activities of ACC and MCD are important regulators of malonyl CoA during ischemia/reperfusion. Malonyl CoA production is decreased during ischemia and reperfusion due to the phosphorylation and inactivation of ACC by AMPK⁴¹, which is activated in response to an increase in the AMP/ATP ratio and Cr/PCr levels⁶³. Furthermore, malonyl CoA degradation and activity of MCD is unchanged by

ischemia or reperfusion⁵⁰. The net effect of reduced ACC activity and unchanged MCD activity is a reduction in malonyl CoA levels. During reperfusion of previously ischemic hearts, low levels of malonyl CoA allow the heart to rely almost completely on fatty acids as a source of energy, which contributes to ischemic damage.

1.5.2 Glycolysis during ischemia/reperfusion

The catabolism of glucose by glycolysis is activated during ischemia and is responsible for the majority of energy production in the absence of oxygen¹⁵⁵⁻¹⁵⁷. High rates of glycolysis during ischemia are attributed to the activation of AMPK, which increases glucose uptake through GLUT-4 and accelerates glycolysis due to the phosphorylation of PFK-2⁹¹. Upon reperfusion both glycolytic rates and AMPK activity remain high, suggesting that glycolysis acts as a continuous energy production pathway to produce ATP throughout both ischemia and reperfusion.

1.5.3 Glucose oxidation during ischemia/reperfusion

Unlike glycolysis, glucose oxidation is unable to provide ATP during severe ischemia. In the absence of oxygen glucose oxidation rates are reduced and do not account for much of the ATP production during severe ischemia. These low glucose oxidation rates during ischemia are likely due to the inhibition of pyruvate dehydrogenase in the absence of oxygen, due to NADH and acetyl CoA accumulation from a decreased Krebs' cycle activity and electron transport chain activity¹⁵⁸.

Glucose oxidation is also depressed upon reperfusion of the heart. During reperfusion glucose oxidation rates remain low due in part to the high rates of fatty acid

oxidation and inhibition of PDC by the Randle cycle ¹⁰⁹. Therefore, the complete oxidation of glucose does not readily occur in the ischemic/reperfused heart. This incomplete oxidation of glucose increases the reliance of the heart on fatty acids, which can impact the functional recovery of the heart after an ischemic episode.

1.5.4 Impact of incomplete glucose oxidation during ischemia/reperfusion

The uncoupling of glycolysis and glucose oxidation that occurs with high fat is proposed to worsen cardiac recovery following an ischemic episode ¹⁵⁹, due to proton accumulation ¹⁶⁰. The protons are produced by the hydrolysis of ATP during ischemia at the rate of two protons for each molecule of glucose utilized. Proton production does not affect the aerobic heart because in the aerobic setting the oxidation of glucose utilizes these protons and allows complete oxidation of glucose to CO₂ and water. However, during ischemia/reperfusion in the presence of fatty acids the utilization of excess protons is delayed, which causes the cardiac tissue to become acidic ¹⁶⁰. Major problems associated with this acidity occur upon reperfusion of the heart tissue. As the blood reperfuses the heart, the environment between the cytosol and the external surface of the cell is altered such that a large proton gradient exists. The high concentration of intracellular protons causes a rapid efflux of protons out of the cell through the sodium-hydrogen exchanger, which in turn causes an influx of sodium ions into the myocyte ¹⁶¹. The myocyte responds by removing the sodium through the sodium/calcium exchanger or the sodium/potassium ATPase ¹⁶¹ to correct ionic homeostasis. However, a rapid influx of calcium into the cell can occur via the reverse mode sodium/calcium exchanger, which leads to calcium overload and cell death ¹⁶¹. Therefore, in the absence of complete

glucose oxidation during ischemia/reperfusion, the resulting accumulation of protons can lead to poor functional recovery of the heart ¹⁶⁰. Since the levels of ATP recover to normal very rapidly during reperfusion following ischemia, this poor functional recovery is attributed to the use of a majority of the ATP produced to re-establish ionic homeostasis, instead of maintenance of contractile function of the heart ¹⁶². Therefore, cardiac efficiency is reduced in post-ischemic hearts utilizing fatty acids as the primary source of energy. The cardiac energy metabolism pathways in the aerobic and ischemic heart are shown in Figure 1-8.

Taken together these observations suggest that the relative use of fatty acids and glucose following a period of ischemia determines the functional recovery of the heart. Therefore, inhibition of fatty acid oxidation or the acceleration of glucose oxidation may improve cardiac recovery, and pharmacological approaches aimed at switching substrate preference of the heart from fatty acids to glucose may improve recovery post-ischemia.

1.5.5 Pharmacological treatments aimed at the acceleration of glucose oxidation rates or inhibition of fatty acid oxidation rates

Pharmacological inhibition of fatty acid oxidation using etomoxir (CPT-1 inhibitor) ^{163, 164}, trimetazidine or ranolazine (3-ketoacyl CoA thiolase inhibitors) ^{165, 166} during reperfusion indirectly accelerates glucose oxidation rates and improves the functional recovery of the heart. The direct acceleration of glucose oxidation rates by treating hearts with dichloroacetate, a PDK inhibitor, also causes a marked improvement in proton production and cardiac efficiency following ischemia ^{159, 160, 167}. Therefore, directly accelerating the glucose oxidation pathway or indirectly accelerating glucose use

by the inhibition of fatty acid oxidation are both potential treatments for ischemia/reperfusion injury.

A novel approach to inhibit fatty acid oxidation rates and promote glucose utilization is to maintain malonyl CoA levels through the inhibition of malonyl CoA degradation. MCD inhibitors cause an increase in malonyl CoA levels and are correlated with an improvement in cardiac recovery following ischemia ⁶⁸. Another approach to increase malonyl CoA is to inhibit AMPK to relieve ACC inhibition. While the activation of MCD and AMPK have been proposed as treatments for diabetes ^{168, 169}, the inhibition of both MCD and AMPK may be novel approaches to improve recovery of the heart following an ischemic episode.

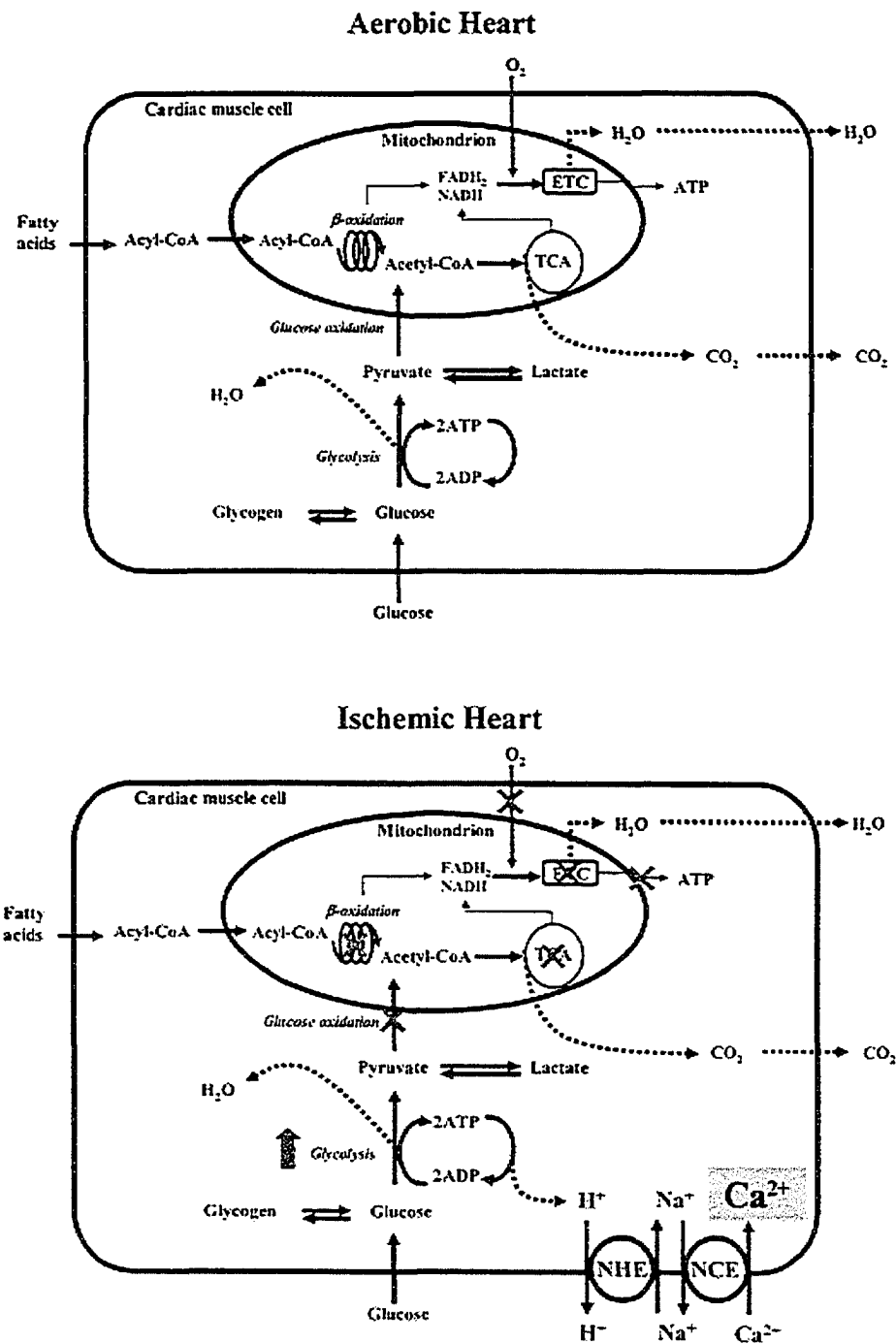


Figure 1-8: Pathways of cardiac energy metabolism during aerobic metabolism (upper panel) and an ischemic insult (lower panel). (Figure from Sambandam et al, 2003¹⁷⁰)

Important targets for Metabolic Manipulation: PDK and MCD

1.6 PDK and MCD are important regulators of cardiac substrate preference

Due to the importance of cardiac substrate preference during ischemia/reperfusion (as discussed in Section 1.5) the aim of this thesis is to help elucidate the mechanisms that control energy metabolism in the heart. This aim will be achieved by experiments to study the regulation of two enzymes, which are important determinants of energy substrate preference in the heart. PDK is important for the regulation of glucose oxidation rates, while MCD plays an important role in the regulation of fatty acid oxidation rates. Expression of these enzymes is increased by the activation of PPAR α , and therefore PPAR α may mediate a coordinated control of substrate preference in the heart. For that reason the studies presented in subsequent chapters involve the regulation and activity of both PDK and MCD, both acutely and chronically via PPAR α .

1.7 PDK

1.7.1 PDK expression, activity and tissue distribution

As alluded to earlier in this chapter, there are four isoforms of PDK, which have unique tissue distributions. PDK1 mRNA is highly expressed in heart, liver, and skeletal muscle but has modest expression in pancreas, brain, placenta, lung and kidney^{102, 103}. PDK2 has the highest expression in heart and skeletal muscle but has intermediate expression in brain, kidney, pancreas and liver^{102, 103}. PDK3 is highly expressed in the testes¹⁰², while PDK4 mRNA expression is found only in heart and skeletal muscle^{102, 103}. This tissue specific PDK isoform expression suggests that energy metabolism can be

varied by PDK in a tissue dependent manner. While the tissue distribution of the PDK isoforms represents one level of control, the acute regulation of PDK is another way to control PDC activity.

Although PDK is acutely activated by high ratios of NADH/NAD⁺ and acetyl CoA/CoA ratios ^{101, 108}, each isoform has a different sensitivity for these molecules with PDK4 being most highly activated by NADH ¹⁰². Similarly, these isoforms also have different sensitivity for inhibition by dichloroacetate and pyruvate, with PDK2 being the most sensitive to inhibition ^{102, 171}. Taken together these data suggest that expression of different PDK isoforms with varying sensitivity to regulation may be a mechanism of control for PDC activity in different tissues ¹⁰² or pathological states.

In addition to acute regulation of PDK activity there is also a chronic control of PDK isoform expression, which allows long-term control of PDC activity. PDK4 is a highly inducible isoform and its mRNA and protein expression is increased during both fasting and diabetes in the rat heart ¹⁰⁴, as well as during fasting in skeletal muscle ¹⁷². Several studies demonstrate an increase in PDK4 expression upon stimuli such as high fat feeding, low carbohydrate diets, and lipid supply ¹⁷³⁻¹⁷⁵. The mechanism behind this increase in PDK expression has been suggested to be regulation by PPAR α ^{105, 107}. However, despite these dramatic changes in PDK4 expression it is unknown if this translates into an alteration in glucose oxidation rates in the heart.

1.8 MCD

1.8.1 MCD expression, activity and tissue distribution

MCD mRNA is found in almost every tissue with the highest expression in the heart, liver, kidney and adipose tissues⁷⁰. Similarly the highest MCD activity was found in the heart and liver⁷⁰, suggesting that MCD plays an important role regulating oxidative metabolism.

1.8.2 MCD deficiency

Much of the initial interest in MCD can be attributed to the development of severe metabolic disorders upon mutation of the MCD gene. These mutations produce symptoms such as malonic aciduria, micropenis, cardiomyopathy, metabolic acidosis, vomiting, hypoglycemia, and mild mental retardation¹⁷⁶⁻¹⁸². The cause of these symptoms is attributed to several different genetic mutations described in MCD deficiencies including a frame shift which results in a truncated MCD protein with reduced activity^{71, 177, 182}. Another interesting feature of two patients with MCD deficiency is the evidence of cardiomyopathy¹⁸², suggesting that MCD plays a role in normal cardiac development and function. While a loss of MCD activity is likely the main cause of MCD deficiency, it has been proposed that an abnormal subcellular distribution of MCD may also play a role in the manifestation of MCD deficiency. In fact, mistargeting of MCD to the plasma membrane has been suggested to be responsible for the symptoms of MCD deficiency in one patient¹⁸³. This suggests that the subcellular localization of MCD is important for its proper function.

1.8.3 MCD subcellular localization

The issue of subcellular localization of MCD remains very controversial. The initial work by Kollatukudy and colleagues delineated the subcellular localization and intracellular processing of MCD in the goose uropygial gland¹⁸⁴⁻¹⁸⁷. The goose MCD has two potential methionine start sequences that would allow the translation of either a 54.7 or 50.7 kDa protein¹⁸⁶. In the goose liver it appears that MCD is expressed from the first methionine start sequence and upon import into the mitochondria is cleaved to the smaller isoform¹⁸⁶. However, in the uropygial gland MCD is expressed from both methionine start sequences allowing accumulation of MCD in both the mitochondria and the cytosol¹⁸⁶. The role of MCD in this specialized gland is to ensure that fatty acid synthase uses methmalonyl CoA as a precursor molecule rather than malonyl CoA and allows the production of goose grease for feather preening^{185, 187}. The mitochondrial MCD of goose liver has also been proposed to protect mitochondrial enzymes from inhibition by malonyl CoA¹⁸⁸. Although the evidence learned from the localization of goose MCD is well accepted and may be applied to cardiac MCD, the actual localization of MCD has not been established in the heart.

Previous studies investigating the subcellular localization of MCD are conflicting. An antibody generated against a human MCD clone recognizes a peroxisomal and cytosolic form of MCD in rat and human liver, however no MCD was detected in the mitochondria⁷⁴. However, a second study using subcellular fractionation techniques in rat liver indicates the presence of MCD in both mitochondria and peroxisomes, but not the cytosol⁷¹. These two studies are in direct contrast to one another and it is difficult to conclude the localization of MCD in these tissues. In the heart MCD localization has only

been approached through activity studies of subcellular fractions suggesting that at least 50% of MCD activity is mitochondrial ⁷². However, the localization of the MCD protein in the heart has not been fully explored. As well, the use of subcellular fractionation as a method for isolation of peroxisomes from mitochondria is often misleading due to the contamination among fractions. Taken together, the lack of definitive evidence has not allowed the exact subcellular distribution of MCD in the heart to be elucidated.

Part of the confusion surrounding MCD localization may be due to the unique qualities of the MCD protein. As previously mentioned, MCD contains both a putative mitochondrial and peroxisomal targeting sequence ⁷⁰. Since the localization of cardiac MCD is currently unknown, it remains to be determined if either of these sequences is functional in the heart. Furthermore, it is unclear if a cleavage event regulates the localization of MCD such that one targeting sequence is removed.

As previously described, MCD is an important regulator of fatty acid oxidation rates in the heart due to modulation of cytosolic malonyl CoA levels and CPT-1 activity. The question remains as to how a protein that may be localized to mitochondria/peroxisomes can modulate these cytosolic malonyl CoA concentrations. Currently there has not been a mechanism described for the movement of malonyl CoA from the mitochondria to the cytosol. Therefore, it is important to determine the subcellular localization of MCD in order to understand the cellular mechanisms involved in the control of malonyl CoA levels and fatty acid oxidation rates.

1.8.4 MCD inhibition

While a novel approach for treatment of ischemic heart disease is inhibition of MCD, MCD activation has been proposed as a treatment for diabetes since overexpression of MCD in rat liver has been shown to reverse whole-body insulin resistance¹⁸⁹. Since MCD isoforms in several tissues are very similar, activation of MCD in skeletal muscle, but not the heart, is difficult. Therefore MCD activation in skeletal muscle may lead to activation of fatty acid oxidation in the heart and poor functional recovery following cardiac ischemia. In fact, data from our group suggest that inhibition of MCD in the heart raises malonyl CoA levels and improves functional recovery upon reperfusion⁶⁸. Interestingly, inhibition of MCD *in vivo* does not seem to produce any metabolic disorders such as those observed with MCD deficiencies (unpublished observations) suggesting that acute inhibition of MCD may be less detrimental than chronic inhibition. In addition, the MCD knockout mice discussed in Chapter 4 do not exhibit a pathogenic phenotype (unpublished observations). Since MCD deficiency in these mice is not lethal in the embryonic stage, MCD may not be absolutely required during development. Taken together, MCD inhibition may be a novel approach to the treatment of ischemic heart disease.

Hypothesis and Objectives of this study

1.9.1 General hypothesis and objectives

Evidence described in Section 1.7 indicates the importance of substrate preference in the recovery of the heart following ischemia/reperfusion injury. Our laboratory continues to investigate the **general hypothesis** that inhibiting fatty acid oxidation or accelerating glucose oxidation improves cardiac functional recovery post-ischemia. The **general objective** of this thesis is to investigate the co-ordinated control of two reciprocal oxidative pathways by PPAR α through the control of PDK and MCD.

1.9.2 General aims

The general aims of this thesis are (i) to determine the role of PPAR α in the regulation of PDC activity in the heart, (ii) to determine the subcellular localization of MCD in the heart, and (iii) to determine the effect of chronic MCD activity loss on PPAR α activation. These aims are discussed in the following three chapters.

Literature Cited

1. The Growing Burden of Heart Disease and Stroke. 2003.
Ref Type: Pamphlet
2. Lopaschuk,G.D., Belke,D.D., Gamble,J., Itoi,T., & Schonekess,B.O. Regulation of fatty acid oxidation in the mammalian heart in health and disease. *Biochim. Biophys. Acta* **1213**, 263-276 (1994).
3. Pedersen,M.E., Cohen,M., & Schotz,M.C. Immunocytochemical localization of the functional fraction of lipoprotein lipase in the perfused heart. *J. Lipid Res.* **24**, 512-521 (1983).
4. Yagyu,H. *et al.* Lipoprotein lipase (LpL) on the surface of cardiomyocytes increases lipid uptake and produces a cardiomyopathy. *J. Clin. Invest.* **111**, 419-426 (2003).
5. Irie,H. *et al.* Myocardial recovery from ischemia is impaired in CD36-null mice and restored by myocyte CD36 expression or medium-chain fatty acids. *Proc. Natl. Acad. Sci. U. S. A* **100**, 6819-6824 (2003).
6. Van Nieuwenhoven,F.A. *et al.* Putative membrane fatty acid translocase and cytoplasmic fatty acid-binding protein are co-expressed in rat heart and skeletal muscles. *Biochem. Biophys. Res. Commun.* **207**, 747-752 (1995).
7. Berger,J., Truppe,C., Neumann,H., & Forss-Petter,S. A novel relative of the very-long-chain acyl-CoA synthetase and fatty acid transporter protein genes with a distinct expression pattern. *Biochem. Biophys. Res. Commun.* **247**, 255-260 (1998).
8. Fitscher,B.A., Riedel,H.D., Young,K.C., & Stremmel,W. Tissue distribution and cDNA cloning of a human fatty acid transport protein (hsFATP4). *Biochim. Biophys. Acta* **1443**, 381-385 (1998).
9. Gimeno,R.E. *et al.* Characterization of a heart-specific fatty acid transport protein. *J. Biol. Chem.* **278**, 16039-16044 (2003).
10. Herrmann,T. *et al.* Mouse fatty acid transport protein 4 (FATP4): characterization of the gene and functional assessment as a very long chain acyl-CoA synthetase. *Gene* **270**, 31-40 (2001).
11. Van Nieuwenhoven,F.A., Willemsen,P.H., van,d., V, & Glatz,J.F. Co-expression in rat heart and skeletal muscle of four genes coding for proteins implicated in long-chain fatty acid uptake. *Int. J. Biochem. Cell Biol.* **31**, 489-498 (1999).

12. Sorrentino, D. *et al.* Oleate uptake by cardiac myocytes is carrier mediated and involves a 40-kD plasma membrane fatty acid binding protein similar to that in liver, adipose tissue, and gut. *J. Clin. Invest.* **82**, 928-935 (1988).
13. Cooper, R., Noy, N., & Zakim, D. A physical-chemical model for cellular uptake of fatty acids: prediction of intracellular pool sizes. *Biochemistry* **26**, 5890-5896 (1987).
14. Kamp, F., Zakim, D., Zhang, F., Noy, N., & Hamilton, J.A. Fatty acid flip-flop in phospholipid bilayers is extremely fast. *Biochemistry* **34**, 11928-11937 (1995).
15. Zakim, D. Fatty acids enter cells by simple diffusion. *Proc. Soc. Exp. Biol. Med.* **212**, 5-14 (1996).
16. Coburn, C.T. *et al.* Defective uptake and utilization of long chain fatty acids in muscle and adipose tissues of CD36 knockout mice. *J. Biol. Chem.* **275**, 32523-32529 (2000).
17. Coburn, C.T., Hajri, T., Ibrahimi, A., & Abumrad, N.A. Role of CD36 in membrane transport and utilization of long-chain fatty acids by different tissues. *J. Mol. Neurosci.* **16**, 117-121 (2001).
18. Kuang, M., Febbraio, M., Wagg, C., Lopaschuk, G.D., & Dyck, J.R. Fatty acid translocase/CD36 deficiency does not energetically or functionally compromise hearts before or after ischemia. *Circulation* **109**, 1550-1557 (2004).
19. Bonen, A., Luiken, J.J., Arumugam, Y., Glatz, J.F., & Tandon, N.N. Acute regulation of fatty acid uptake involves the cellular redistribution of fatty acid translocase. *J. Biol. Chem.* **275**, 14501-14508 (2000).
20. Luiken, J.J. *et al.* Insulin stimulates long-chain fatty acid utilization by rat cardiac myocytes through cellular redistribution of FAT/CD36. *Diabetes* **51**, 3113-3119 (2002).
21. Luiken, J.J. *et al.* Contraction-induced fatty acid translocase/CD36 translocation in rat cardiac myocytes is mediated through AMP-activated protein kinase signaling. *Diabetes* **52**, 1627-1634 (2003).
22. Luiken, J.J., Willems, J., van, d., V, & Glatz, J.F. Electrostimulation enhances FAT/CD36-mediated long-chain fatty acid uptake by isolated rat cardiac myocytes. *Am. J. Physiol. Endocrinol. Metab.* **281**, E704-E712 (2001).
23. Luiken, J.J., Turcotte, L.P., & Bonen, A. Protein-mediated palmitate uptake and expression of fatty acid transport proteins in heart giant vesicles. *J. Lipid Res.* **40**, 1007-1016 (1999).

24. Fournier,N., Geoffroy,M., & Deshusses,J. Purification and characterization of a long chain, fatty-acid-binding protein supplying the mitochondrial beta-oxidative system in the heart. *Biochim. Biophys. Acta* **533**, 457-464 (1978).
25. Fournier,N.C. & Rahim,M. Control of energy production in the heart: a new function for fatty acid binding protein. *Biochemistry* **24**, 2387-2396 (1985).
26. Glatz,J.F., Paulussen,R.J., & Veerkamp,J.H. Fatty acid binding proteins from heart. *Chem. Phys. Lipids* **38**, 115-129 (1985).
27. Glatz,J.F., Janssen,A.M., Baerwaldt,C.C., & Veerkamp,J.H. Purification and characterization of fatty-acid-binding proteins from rat heart and liver. *Biochim. Biophys. Acta* **837**, 57-66 (1985).
28. Said,B. & Schulz,H. Fatty acid binding protein from rat heart. The fatty acid binding proteins from rat heart and liver are different proteins. *J. Biol. Chem.* **259**, 1155-1159 (1984).
29. Rasmussen,J.T., Borchers,T., & Knudsen,J. Comparison of the binding affinities of acyl-CoA-binding protein and fatty-acid-binding protein for long-chain acyl-CoA esters. *Biochem. J.* **265**, 849-855 (1990).
30. Luiken,J.J. *et al.* Regulation of cardiac long-chain fatty acid and glucose uptake by translocation of substrate transporters. *Pflugers Arch.* **448**, 1-15 (2004).
31. Murthy,M.S. & Pande,S.V. Malonyl-CoA binding site and the overt carnitine palmitoyltransferase activity reside on the opposite sides of the outer mitochondrial membrane. *Proc. Natl. Acad. Sci. U. S. A* **84**, 378-382 (1987).
32. Murthy,M.S. & Pande,S.V. Characterization of a solubilized malonyl-CoA-sensitive carnitine palmitoyltransferase from the mitochondrial outer membrane as a protein distinct from the malonyl-CoA-insensitive carnitine palmitoyltransferase of the inner membrane. *Biochem. J.* **268**, 599-604 (1990).
33. Derrick,J.P. & Ramsay,R.R. L-carnitine acyltransferase in intact peroxisomes is inhibited by malonyl-CoA. *Biochem. J.* **262**, 801-806 (1989).
34. Mosser,J. *et al.* Putative X-linked adrenoleukodystrophy gene shares unexpected homology with ABC transporters. *Nature* **361**, 726-730 (1993).
35. van Roermund,C.W., Hetteema,E.H., van Den,B.M., Tabak,H.F., & Wanders,R.J. Molecular characterization of carnitine-dependent transport of acetyl-CoA from peroxisomes to mitochondria in *Saccharomyces cerevisiae* and identification of a plasma membrane carnitine transporter, Agp2p. *EMBO J.* **18**, 5843-5852 (1999).

36. Bian, F. *et al.* Peroxisomal and Mitochondrial Oxidation of Fatty Acids in the Heart, Assessed from the ¹³C Labeling of Malonyl-CoA and the Acetyl Moiety of Citrate. *J. Biol. Chem.* **280**, 9265-9271 (2005).
37. Vanhove, G.F. *et al.* The CoA esters of 2-methyl-branched chain fatty acids and of the bile acid intermediates di- and trihydroxycoprostanic acids are oxidized by one single peroxisomal branched chain acyl-CoA oxidase in human liver and kidney. *J. Biol. Chem.* **268**, 10335-10344 (1993).
38. Weis, B.C., Esser, V., Foster, D.W., & McGarry, J.D. Rat heart expresses two forms of mitochondrial carnitine palmitoyltransferase I. The minor component is identical to the liver enzyme. *J. Biol. Chem.* **269**, 18712-18715 (1994).
39. McGarry, J.D., Leatherman, G.F., & Foster, D.W. Carnitine palmitoyltransferase I. The site of inhibition of hepatic fatty acid oxidation by malonyl-CoA. *J. Biol. Chem.* **253**, 4128-4136 (1978).
40. McGarry, J.D., Mills, S.E., Long, C.S., & Foster, D.W. Observations on the affinity for carnitine, and malonyl-CoA sensitivity, of carnitine palmitoyltransferase I in animal and human tissues. Demonstration of the presence of malonyl-CoA in non-hepatic tissues of the rat. *Biochem. J.* **214**, 21-28 (1983).
41. Kudo, N., Barr, A.J., Barr, R.L., Desai, S., & Lopaschuk, G.D. High rates of fatty acid oxidation during reperfusion of ischemic hearts are associated with a decrease in malonyl-CoA levels due to an increase in 5'-AMP-activated protein kinase inhibition of acetyl-CoA carboxylase. *J. Biol. Chem.* **270**, 17513-17520 (1995).
42. Guzman, M. & Geelen, M.J. Activity of carnitine palmitoyltransferase in mitochondrial outer membranes and peroxisomes in digitonin-permeabilized hepatocytes. Selective modulation of mitochondrial enzyme activity by okadaic acid. *Biochem. J.* **287** (Pt 2), 487-492 (1992).
43. McGarry, J.D. & Brown, N.F. The mitochondrial carnitine palmitoyltransferase system. From concept to molecular analysis. *Eur. J. Biochem.* **244**, 1-14 (1997).
44. Kerner, J. *et al.* Phosphorylation of rat liver mitochondrial carnitine palmitoyltransferase-I: effect on the kinetic properties of the enzyme. *J. Biol. Chem.* **279**, 41104-41113 (2004).
45. Fraser, F., Corstorphine, C.G., & Zammit, V.A. Topology of carnitine palmitoyltransferase I in the mitochondrial outer membrane. *Biochem. J.* **323** (Pt 3), 711-718 (1997).

46. Shi,J., Zhu,H., Arvidson,D.N., Cregg,J.M., & Woldegiorgis,G. Deletion of the conserved first 18 N-terminal amino acid residues in rat liver carnitine palmitoyltransferase I abolishes malonyl-CoA sensitivity and binding. *Biochemistry* **37**, 11033-11038 (1998).
47. Shi,J., Zhu,H., Arvidson,D.N., & Woldegiorgis,G. A single amino acid change (substitution of glutamate 3 with alanine) in the N-terminal region of rat liver carnitine palmitoyltransferase I abolishes malonyl-CoA inhibition and high affinity binding. *J. Biol. Chem.* **274**, 9421-9426 (1999).
48. Zammit,V.A., Fraser,F., & Orstorphine,C.G. Regulation of mitochondrial outer-membrane carnitine palmitoyltransferase (CPT I): role of membrane-topology. *Adv. Enzyme Regul.* **37**, 295-317 (1997).
49. Hamilton,C. & Saggerson,E.D. Malonyl-CoA metabolism in cardiac myocytes. *Biochem. J.* **350 Pt 1**, 61-67 (2000).
50. Dyck,J.R., Barr,A.J., Barr,R.L., Kolattukudy,P.E., & Lopaschuk,G.D. Characterization of cardiac malonyl-CoA decarboxylase and its putative role in regulating fatty acid oxidation. *Am. J. Physiol.* **275**, H2122-H2129 (1998).
51. Lopaschuk,G.D. & Gamble,J. The 1993 Merck Frosst Award. Acetyl-CoA carboxylase: an important regulator of fatty acid oxidation in the heart. *Can. J. Physiol. Pharmacol.* **72**, 1101-1109 (1994).
52. Abu-Elheiga,L., Jayakumar,A., Baldini,A., Chirala,S.S., & Wakil,S.J. Human acetyl-CoA carboxylase: characterization, molecular cloning, and evidence for two isoforms. *Proc. Natl. Acad. Sci. U. S. A* **92**, 4011-4015 (1995).
53. Abu-Elheiga,L., marza-Ortega,D.B., Baldini,A., & Wakil,S.J. Human acetyl-CoA carboxylase 2. Molecular cloning, characterization, chromosomal mapping, and evidence for two isoforms. *J. Biol. Chem.* **272**, 10669-10677 (1997).
54. Bianchi,A. *et al.* Identification of an isozymic form of acetyl-CoA carboxylase. *J. Biol. Chem.* **265**, 1502-1509 (1990).
55. Thampy,K.G. Formation of malonyl coenzyme A in rat heart. Identification and purification of an isozyme of A carboxylase from rat heart. *J. Biol. Chem.* **264**, 17631-17634 (1989).
56. Abu-Elheiga,L. *et al.* The subcellular localization of acetyl-CoA carboxylase 2. *Proc. Natl. Acad. Sci. U. S. A* **97**, 1444-1449 (2000).
57. Fukao,T., Lopaschuk,G.D., & Mitchell,G.A. Pathways and control of ketone body metabolism: on the fringe of lipid biochemistry. *Prostaglandins Leukot. Essent. Fatty Acids* **70**, 243-251 (2004).

58. Kim, J.M., Yoon, M., Kang, I., Kim, S.S., & Ha, J. Evidence that acetyl-CoA carboxylase isoforms play different biological roles in H9c2 cardiomyocyte. *Biochem. Biophys. Res. Commun.* **248**, 490-496 (1998).
59. Abu-Elheiga, L., Matzuk, M.M., bo-Hashema, K.A., & Wakil, S.J. Continuous fatty acid oxidation and reduced fat storage in mice lacking acetyl-CoA carboxylase 2. *Science* **291**, 2613-2616 (2001).
60. Tipper, J.P., Bacon, G.W., & Witters, L.A. Phosphorylation of acetyl-coenzyme A carboxylase by casein kinase I and casein kinase II. *Arch. Biochem. Biophys.* **227**, 386-396 (1983).
61. Witters, L.A. & Bacon, G.W. Protein phosphatases active on acetyl-CoA carboxylase phosphorylated by casein kinase I, casein kinase II and the cAMP-dependent protein kinase. *Biochem. Biophys. Res. Commun.* **130**, 1132-1138 (1985).
62. Witters, L.A. & Watts, T.D. Yeast acetyl-CoA carboxylase: in vitro phosphorylation by mammalian and yeast protein kinases. *Biochem. Biophys. Res. Commun.* **169**, 369-376 (1990).
63. Kudo, N. *et al.* Characterization of 5'AMP-activated protein kinase activity in the heart and its role in inhibiting acetyl-CoA carboxylase during reperfusion following ischemia. *Biochim. Biophys. Acta* **1301**, 67-75 (1996).
64. Hutber, C.A., Hardie, D.G., & Winder, W.W. Electrical stimulation inactivates muscle acetyl-CoA carboxylase and increases AMP-activated protein kinase. *Am. J. Physiol.* **272**, E262-E266 (1997).
65. Vavvas, D. *et al.* Contraction-induced changes in acetyl-CoA carboxylase and 5'-AMP-activated kinase in skeletal muscle. *J. Biol. Chem.* **272**, 13255-13261 (1997).
66. Munday, M.R., Campbell, D.G., Carling, D., & Hardie, D.G. Identification by amino acid sequencing of three major regulatory phosphorylation sites on rat acetyl-CoA carboxylase. *Eur. J. Biochem.* **175**, 331-338 (1988).
67. Dyck, J.R. *et al.* Characterization of rat liver malonyl-CoA decarboxylase and the study of its role in regulating fatty acid metabolism. *Biochem. J.* **350 Pt 2**, 599-608 (2000).
68. Dyck, J.R. *et al.* Malonyl coenzyme a decarboxylase inhibition protects the ischemic heart by inhibiting fatty acid oxidation and stimulating glucose oxidation. *Circ. Res.* **94**, e78-e84 (2004).
69. Dyck, J.R.B. *et al.* Hearts from Malonyl CoA Decarboxylase Null Mice are Protected from Ischemic Damage. *Circulation* . 2004.
Ref Type: Abstract

70. Voilley,N. *et al.* Cloning and expression of rat pancreatic beta-cell malonyl-CoA decarboxylase. *Biochem. J.* **340** (Pt 1), 213-217 (1999).
71. FitzPatrick,D.R., Hill,A., Tolmie,J.L., Thorburn,D.R., & Christodoulou,J. The molecular basis of malonyl-CoA decarboxylase deficiency. *Am. J. Hum. Genet.* **65**, 318-326 (1999).
72. Kerner,J. & Hoppel,C.L. Radiochemical malonyl-CoA decarboxylase assay: activity and subcellular distribution in heart and skeletal muscle. *Anal. Biochem.* **306**, 283-289 (2002).
73. Kim,Y.S. & Kolattukudy,P.E. Malonyl-CoA decarboxylase from the mammary gland of lactating rat. Purification, properties and subcellular localization. *Biochim. Biophys. Acta* **531**, 187-196 (1978).
74. Sacksteder,K.A., Morrell,J.C., Wanders,R.J., Matalon,R., & Gould,S.J. MCD encodes peroxisomal and cytoplasmic forms of malonyl-CoA decarboxylase and is mutated in malonyl-CoA decarboxylase deficiency. *J. Biol. Chem.* **274**, 24461-24468 (1999).
75. Park,H. *et al.* Coordinate regulation of malonyl-CoA decarboxylase, sn-glycerol-3-phosphate acyltransferase, and acetyl-CoA carboxylase by AMP-activated protein kinase in rat tissues in response to exercise. *J. Biol. Chem.* **277**, 32571-32577 (2002).
76. Saha,A.K. *et al.* Activation of malonyl-CoA decarboxylase in rat skeletal muscle by contraction and the AMP-activated protein kinase activator 5-aminoimidazole-4-carboxamide-1-beta -D-ribofuranoside. *J. Biol. Chem.* **275**, 24279-24283 (2000).
77. Habinowski,S.A. *et al.* Malonyl-CoA decarboxylase is not a substrate of AMP-activated protein kinase in rat fast-twitch skeletal muscle or an islet cell line. *Arch. Biochem. Biophys.* **396**, 71-79 (2001).
78. Reszko,A.E. *et al.* Peroxisomal fatty acid oxidation is a substantial source of the acetyl moiety of malonyl-CoA in rat heart. *J. Biol. Chem.* **279**, 19574-19579 (2004).
79. Saddik,M., Gamble,J., Witters,L.A., & Lopaschuk,G.D. Acetyl-CoA carboxylase regulation of fatty acid oxidation in the heart. *J. Biol. Chem.* **268**, 25836-25845 (1993).
80. James,D.E., Brown,R., Navarro,J., & Pilch,P.F. Insulin-regulatable tissues express a unique insulin-sensitive glucose transport protein. *Nature* **333**, 183-185 (1988).

81. Slot,J.W., Geuze,H.J., Gigengack,S., James,D.E., & Lienhard,G.E. Translocation of the glucose transporter GLUT4 in cardiac myocytes of the rat. *Proc. Natl. Acad. Sci. U. S. A* **88**, 7815-7819 (1991).
82. Zaninetti,D., Greco-Perotto,R., ssimacopoulos-Jeannet,F., & Jeanrenaud,B. Effects of insulin on glucose transport and glucose transporters in rat heart. *Biochem. J.* **250**, 277-283 (1988).
83. Sun,D., Nguyen,N., DeGrado,T.R., Schwaiger,M., & Brosius,F.C., III Ischemia induces translocation of the insulin-responsive glucose transporter GLUT4 to the plasma membrane of cardiac myocytes. *Circulation* **89**, 793-798 (1994).
84. Douen,A.G. *et al.* Exercise-induced increase in glucose transporters in plasma membranes of rat skeletal muscle. *Endocrinology* **124**, 449-454 (1989).
85. Goodyear,L.J., Hirshman,M.F., & Horton,E.S. Exercise-induced translocation of skeletal muscle glucose transporters. *Am. J. Physiol.* **261**, E795-E799 (1991).
86. Kristiansen,S., Hargreaves,M., & Richter,E.A. Exercise-induced increase in glucose transport, GLUT-4, and VAMP-2 in plasma membrane from human muscle. *Am. J. Physiol.* **270**, E197-E201 (1996).
87. Thorell,A. *et al.* Exercise and insulin cause GLUT-4 translocation in human skeletal muscle. *Am. J. Physiol.* **277**, E733-E741 (1999).
88. Russell,R.R., III, Bergeron,R., Shulman,G.I., & Young,L.H. Translocation of myocardial GLUT-4 and increased glucose uptake through activation of AMPK by AICAR. *Am. J. Physiol.* **277**, H643-H649 (1999).
89. Cheatham,B. *et al.* Phosphatidylinositol 3-kinase activation is required for insulin stimulation of pp70 S6 kinase, DNA synthesis, and glucose transporter translocation. *Mol. Cell. Biol.* **14**, 4902-4911 (1994).
90. Kraegen,E.W. *et al.* Glucose transporters and in vivo glucose uptake in skeletal and cardiac muscle: fasting, insulin stimulation and immunoisolation studies of GLUT1 and GLUT4. *Biochem. J.* **295 (Pt 1)**, 287-293 (1993).
91. Marsin,A.S. *et al.* Phosphorylation and activation of heart PFK-2 by AMPK has a role in the stimulation of glycolysis during ischaemia. *Curr. Biol.* **10**, 1247-1255 (2000).
92. Marsin,A.S., Bouzin,C., Bertrand,L., & Hue,L. The stimulation of glycolysis by hypoxia in activated monocytes is mediated by AMP-activated protein kinase and inducible 6-phosphofructo-2-kinase. *J. Biol. Chem.* **277**, 30778-30783 (2002).

93. Maizels,E.Z., Ruderman,N.B., Goodman,M.N., & Lau,D. Effect of acetoacetate on glucose metabolism in the soleus and extensor digitorum longus muscles of the rat. *Biochem. J.* **162**, 557-568 (1977).
94. Randle,P.J. *et al.* Interactions of metabolism and the physiological role of insulin. *Recent Prog. Horm. Res.* **22**, 1-48 (1966).
95. Nestorescu,M.L., Siess,E.A., & Wieland,O.H. Ultrastructural localization of pyruvate dehydrogenase in rat heart muscle. *Histochemie.* **34**, 355-360 (1973).
96. Bremer,J. Pyruvate dehydrogenase, substrate specificity and product inhibition. *Eur. J. Biochem.* **8**, 535-540 (1969).
97. Kerbey,A.L. *et al.* Regulation of pyruvate dehydrogenase in rat heart. Mechanism of regulation of proportions of dephosphorylated and phosphorylated enzyme by oxidation of fatty acids and ketone bodies and of effects of diabetes: role of coenzyme A, acetyl-coenzyme A and reduced and oxidized nicotinamide-adenine dinucleotide. *Biochem. J.* **154**, 327-348 (1976).
98. Randle,P.J., Garland,P.B., Hales,C.N., & Newsholme,E.A. The glucose fatty-acid cycle. Its role in insulin sensitivity and the metabolic disturbances of diabetes mellitus. *Lancet* **1**, 785-789 (1963).
99. Linn,T.C., Pettit,F.H., Hucho,F., & Reed,L.J. Alpha-keto acid dehydrogenase complexes. XI. Comparative studies of regulatory properties of the pyruvate dehydrogenase complexes from kidney, heart, and liver mitochondria. *Proc. Natl. Acad. Sci. U. S. A* **64**, 227-234 (1969).
100. Linn,T.C., Pettit,F.H., & Reed,L.J. Alpha-keto acid dehydrogenase complexes. X. Regulation of the activity of the pyruvate dehydrogenase complex from beef kidney mitochondria by phosphorylation and dephosphorylation. *Proc. Natl. Acad. Sci. U. S. A* **62**, 234-241 (1969).
101. Cooper,R.H., Randle,P.J., & Denton,R.M. Regulation of heart muscle pyruvate dehydrogenase kinase. *Biochem. J.* **143**, 625-641 (1974).
102. Bowker-Kinley,M.M., Davis,W.I., Wu,P., Harris,R.A., & Popov,K.M. Evidence for existence of tissue-specific regulation of the mammalian pyruvate dehydrogenase complex. *Biochem. J.* **329** (Pt 1), 191-196 (1998).
103. Gudi,R., Bowker-Kinley,M.M., Kedishvili,N.Y., Zhao,Y., & Popov,K.M. Diversity of the pyruvate dehydrogenase kinase gene family in humans. *J. Biol. Chem.* **270**, 28989-28994 (1995).
104. Wu,P. *et al.* Starvation and diabetes increase the amount of pyruvate dehydrogenase kinase isoenzyme 4 in rat heart. *Biochem. J.* **329** (Pt 1), 197-201 (1998).

105. Wu,P., Inskeep,K., Bowker-Kinley,M.M., Popov,K.M., & Harris,R.A. Mechanism responsible for inactivation of skeletal muscle pyruvate dehydrogenase complex in starvation and diabetes. *Diabetes* **48**, 1593-1599 (1999).
106. Wu,P. *et al.* Starvation increases the amount of pyruvate dehydrogenase kinase in several mammalian tissues. *Arch. Biochem. Biophys.* **381**, 1-7 (2000).
107. Wu,P., Peters,J.M., & Harris,R.A. Adaptive increase in pyruvate dehydrogenase kinase 4 during starvation is mediated by peroxisome proliferator-activated receptor alpha. *Biochem. Biophys. Res. Commun.* **287**, 391-396 (2001).
108. Cooper,R.H., Randle,P.J., & Denton,R.M. Stimulation of phosphorylation and inactivation of pyruvate dehydrogenase by physiological inhibitors of the pyruvate dehydrogenase reaction. *Nature* **257**, 808-809 (1975).
109. McVeigh,J.J. & Lopaschuk,G.D. Dichloroacetate stimulation of glucose oxidation improves recovery of ischemic rat hearts. *Am. J. Physiol.* **259**, H1079-H1085 (1990).
110. Korotchkina,L.G. & Patel,M.S. Probing the mechanism of inactivation of human pyruvate dehydrogenase by phosphorylation of three sites. *J. Biol. Chem.* **276**, 5731-5738 (2001).
111. Korotchkina,L.G. & Patel,M.S. Site specificity of four pyruvate dehydrogenase kinase isoenzymes toward the three phosphorylation sites of human pyruvate dehydrogenase. *J. Biol. Chem.* **276**, 37223-37229 (2001).
112. Karpova,T., Danchuk,S., Kolobova,E., & Popov,K.M. Characterization of the isozymes of pyruvate dehydrogenase phosphatase: implications for the regulation of pyruvate dehydrogenase activity. *Biochim. Biophys. Acta* **1652**, 126-135 (2003).
113. Denton,R.M., Randle,P.J., & Martin,B.R. Stimulation by calcium ions of pyruvate dehydrogenase phosphate phosphatase. *Biochem. J.* **128**, 161-163 (1972).
114. Severson,D.L., Denton,R.M., Pask,H.T., & Randle,P.J. Calcium and magnesium ions as effectors of adipose-tissue pyruvate dehydrogenase phosphate phosphatase. *Biochem. J.* **140**, 225-237 (1974).
115. Schoder,H., Knight,R.J., Kofoed,K.F., Schelbert,H.R., & Buxton,D.B. Regulation of pyruvate dehydrogenase activity and glucose metabolism in post-ischaemic myocardium. *Biochim. Biophys. Acta* **1406**, 62-72 (1998).

116. Stanley, W.C. *et al.* Pyruvate dehydrogenase activity and malonyl CoA levels in normal and ischemic swine myocardium: effects of dichloroacetate. *J. Mol. Cell. Cardiol.* **28**, 905-914 (1996).
117. Dreyer, C. *et al.* Control of the peroxisomal beta-oxidation pathway by a novel family of nuclear hormone receptors. *Cell* **68**, 879-887 (1992).
118. Issemann, I., Prince, R.A., Tugwood, J.D., & Green, S. The peroxisome proliferator-activated receptor:retinoid X receptor heterodimer is activated by fatty acids and fibrate hypolipidaemic drugs. *J. Mol. Endocrinol.* **11**, 37-47 (1993).
119. Gottlicher, M., Widmark, E., Li, Q., & Gustafsson, J.A. Fatty acids activate a chimera of the clofibric acid-activated receptor and the glucocorticoid receptor. *Proc. Natl. Acad. Sci. U. S. A* **89**, 4653-4657 (1992).
120. Keller, H. *et al.* Fatty acids and retinoids control lipid metabolism through activation of peroxisome proliferator-activated receptor-retinoid X receptor heterodimers. *Proc. Natl. Acad. Sci. U. S. A* **90**, 2160-2164 (1993).
121. Krey, G. *et al.* Fatty acids, eicosanoids, and hypolipidemic agents identified as ligands of peroxisome proliferator-activated receptors by coactivator-dependent receptor ligand assay. *Mol. Endocrinol.* **11**, 779-791 (1997).
122. Issemann, I. & Green, S. Activation of a member of the steroid hormone receptor superfamily by peroxisome proliferators. *Nature* **347**, 645-650 (1990).
123. Berger, J. *et al.* Thiazolidinediones produce a conformational change in peroxisomal proliferator-activated receptor-gamma: binding and activation correlate with antidiabetic actions in db/db mice. *Endocrinology* **137**, 4189-4195 (1996).
124. Lambe, K.G. & Tugwood, J.D. A human peroxisome-proliferator-activated receptor-gamma is activated by inducers of adipogenesis, including thiazolidinedione drugs. *Eur. J. Biochem.* **239**, 1-7 (1996).
125. Gearing, K.L., Gottlicher, M., Teboul, M., Widmark, E., & Gustafsson, J.A. Interaction of the peroxisome-proliferator-activated receptor and retinoid X receptor. *Proc. Natl. Acad. Sci. U. S. A* **90**, 1440-1444 (1993).
126. Tugwood, J.D. *et al.* The mouse peroxisome proliferator activated receptor recognizes a response element in the 5' flanking sequence of the rat acyl CoA oxidase gene. *EMBO J.* **11**, 433-439 (1992).

127. Kliewer, S.A. *et al.* Differential expression and activation of a family of murine peroxisome proliferator-activated receptors. *Proc. Natl. Acad. Sci. U. S. A* **91**, 7355-7359 (1994).
128. Planavila, A. *et al.* Peroxisome proliferator-activated receptor beta/delta activation inhibits hypertrophy in neonatal rat cardiomyocytes. *Cardiovasc. Res.* **65**, 832-841 (2005).
129. Cheng, L. *et al.* Cardiomyocyte-restricted peroxisome proliferator-activated receptor-delta deletion perturbs myocardial fatty acid oxidation and leads to cardiomyopathy. *Nat. Med.* **10**, 1245-1250 (2004).
130. Motojima, K., Passilly, P., Peters, J.M., Gonzalez, F.J., & Latruffe, N. Expression of putative fatty acid transporter genes are regulated by peroxisome proliferator-activated receptor alpha and gamma activators in a tissue- and inducer-specific manner. *J. Biol. Chem.* **273**, 16710-16714 (1998).
131. Sato, O., Kuriki, C., Fukui, Y., & Motojima, K. Dual promoter structure of mouse and human fatty acid translocase/CD36 genes and unique transcriptional activation by peroxisome proliferator-activated receptor alpha and gamma ligands. *J. Biol. Chem.* **277**, 15703-15711 (2002).
132. Mallordy, A., Poirier, H., Besnard, P., Niot, I., & Carlier, H. Evidence for transcriptional induction of the liver fatty-acid-binding-protein gene by bezafibrate in the small intestine. *Eur. J. Biochem.* **227**, 801-807 (1995).
133. Niot, I., Poirier, H., & Besnard, P. Regulation of gene expression by fatty acids: special reference to fatty acid-binding protein (FABP). *Biochimie* **79**, 129-133 (1997).
134. Schoonjans, K., Staels, B., Grimaldi, P., & Auwerx, J. Acyl-CoA synthetase mRNA expression is controlled by fibric-acid derivatives, feeding and liver proliferation. *Eur. J. Biochem.* **216**, 615-622 (1993).
135. Schoonjans, K. *et al.* Induction of the acyl-coenzyme A synthetase gene by fibrates and fatty acids is mediated by a peroxisome proliferator response element in the C promoter. *J. Biol. Chem.* **270**, 19269-19276 (1995).
136. Mascaro, C. *et al.* Control of human muscle-type carnitine palmitoyltransferase I gene transcription by peroxisome proliferator-activated receptor. *J. Biol. Chem.* **273**, 8560-8563 (1998).
137. Reddy, J.K. *et al.* Transcription regulation of peroxisomal fatty acyl-CoA oxidase and enoyl-CoA hydratase/3-hydroxyacyl-CoA dehydrogenase in rat liver by peroxisome proliferators. *Proc. Natl. Acad. Sci. U. S. A* **83**, 1747-1751 (1986).

138. Auwerx,J., Schoonjans,K., Fruchart,J.C., & Staels,B. Transcriptional control of triglyceride metabolism: fibrates and fatty acids change the expression of the LPL and apo C-III genes by activating the nuclear receptor PPAR. *Atherosclerosis* **124 Suppl**, S29-S37 (1996).
139. Schoonjans,K. *et al.* PPARalpha and PPARgamma activators direct a distinct tissue-specific transcriptional response via a PPRE in the lipoprotein lipase gene. *EMBO J.* **15**, 5336-5348 (1996).
140. Lee,G.Y., Kim,N.H., Zhao,Z.S., Cha,B.S., & Kim,Y.S. Peroxisomal-proliferator-activated receptor alpha activates transcription of the rat hepatic malonyl-CoA decarboxylase gene: a key regulation of malonyl-CoA level. *Biochem. J.* **378**, 983-990 (2004).
141. Acin,A. *et al.* Cloning and characterization of the 5' flanking region of the human uncoupling protein 3 (UCP3) gene. *Biochem. Biophys. Res. Commun.* **258**, 278-283 (1999).
142. Aubert,J. *et al.* Up-regulation of UCP-2 gene expression by PPAR agonists in preadipose and adipose cells. *Biochem. Biophys. Res. Commun.* **238**, 606-611 (1997).
143. Brun,S. *et al.* Activators of peroxisome proliferator-activated receptor-alpha induce the expression of the uncoupling protein-3 gene in skeletal muscle: a potential mechanism for the lipid intake-dependent activation of uncoupling protein-3 gene expression at birth. *Diabetes* **48**, 1217-1222 (1999).
144. Kelly,L.J. *et al.* Peroxisome proliferator-activated receptors gamma and alpha mediate in vivo regulation of uncoupling protein (UCP-1, UCP-2, UCP-3) gene expression. *Endocrinology* **139**, 4920-4927 (1998).
145. Nagase,I. *et al.* Up-regulation of uncoupling protein 3 by thyroid hormone, peroxisome proliferator-activated receptor ligands and 9-cis retinoic acid in L6 myotubes. *FEBS Lett.* **461**, 319-322 (1999).
146. Teruel,T., Smith,S.A., Peterson,J., & Clapham,J.C. Synergistic activation of UCP-3 expression in cultured fetal rat brown adipocytes by PPARalpha and PPARgamma ligands. *Biochem. Biophys. Res. Commun.* **273**, 560-564 (2000).
147. Evans,R.M., Barish,G.D., & Wang,Y.X. PPARs and the complex journey to obesity. *Nat. Med.* **10**, 355-361 (2004).
148. Lerch,R., Tamm,C., Papageorgiou,I., & Benzi,R.H. Myocardial fatty acid oxidation during ischemia and reperfusion. *Mol. Cell. Biochem.* **116**, 103-109 (1992).

149. Liedtke,A.J., Demaison,L., Eggleston,A.M., Cohen,L.M., & Nellis,S.H. Changes in substrate metabolism and effects of excess fatty acids in reperfused myocardium. *Circ. Res.* **62**, 535-542 (1988).
150. Lopaschuk,G.D., Spafford,M.A., Davies,N.J., & Wall,S.R. Glucose and palmitate oxidation in isolated working rat hearts reperfused after a period of transient global ischemia. *Circ. Res.* **66**, 546-553 (1990).
151. Kurien,V.A. & Oliver,M.F. Free fatty acids during acute myocardial infarction. *Prog. Cardiovasc. Dis.* **13**, 361-373 (1971).
152. Lopaschuk,G.D. *et al.* Plasma fatty acid levels in infants and adults after myocardial ischemia. *Am. Heart J.* **128**, 61-67 (1994).
153. Mueller,H.S. & Ayres,S.M. Metabolic response of the heart in acute myocardial infarction in man. *Am. J. Cardiol.* **42**, 363-371 (1978).
154. Dyck,J.R., Barr,A.J., Barr,R.L., Kolattukudy,P.E., & Lopaschuk,G.D. Characterization of cardiac malonyl-CoA decarboxylase and its putative role in regulating fatty acid oxidation. *Am. J. Physiol. Heart Circ. Physiol.* **275**, H2122-H2129 (1998).
155. Beauloye,C. *et al.* Insulin antagonizes AMP-activated protein kinase activation by ischemia or anoxia in rat hearts, without affecting total adenine nucleotides. *FEBS Lett.* **505**, 348-352 (2001).
156. Bricknell,O.L. & Opie,L.H. Effects of substrates on tissue metabolic changes in the isolated rat heart during underperfusion and on release of lactate dehydrogenase and arrhythmias during reperfusion. *Circ. Res.* **43**, 102-115 (1978).
157. Neely,J.R., Rovetto,M.J., Whitmer,J.T., & MORGAN,H.E. Effects of ischemia on function and metabolism of the isolated working rat heart. *Am. J. Physiol.* **225**, 651-658 (1973).
158. Vary,T.C. & Randle,P.J. The effect of ischaemia on the activity of pyruvate dehydrogenase complex in rat heart. *J. Mol. Cell. Cardiol.* **16**, 723-733 (1984).
159. Lopaschuk,G.D., Wambolt,R.B., & Barr,R.L. An imbalance between glycolysis and glucose oxidation is a possible explanation for the detrimental effects of high levels of fatty acids during aerobic reperfusion of ischemic hearts. *J. Pharmacol. Exp. Ther.* **264**, 135-144 (1993).
160. Liu,Q., Docherty,J.C., Rendell,J.C., Clanachan,A.S., & Lopaschuk,G.D. High levels of fatty acids delay the recovery of intracellular pH and cardiac efficiency in post-ischemic hearts by inhibiting glucose oxidation. *J. Am. Coll. Cardiol.* **39**, 718-725 (2002).

161. Karmazyn, M. & Moffat, M.P. Role of Na⁺/H⁺ exchange in cardiac physiology and pathophysiology: mediation of myocardial reperfusion injury by the pH paradox. *Cardiovasc. Res.* **27**, 915-924 (1993).
162. Liu, B., el Alaoui-Talibi, Z., Clanachan, A.S., Schulz, R., & Lopaschuk, G.D. Uncoupling of contractile function from mitochondrial TCA cycle activity and MVO₂ during reperfusion of ischemic hearts. *Am. J. Physiol.* **270**, H72-H80 (1996).
163. Lopaschuk, G.D., Wall, S.R., Olley, P.M., & Davies, N.J. Etomoxir, a carnitine palmitoyltransferase I inhibitor, protects hearts from fatty acid-induced ischemic injury independent of changes in long chain acylcarnitine. *Circ. Res.* **63**, 1036-1043 (1988).
164. Lopaschuk, G.D., McNeil, G.F., & McVeigh, J.J. Glucose oxidation is stimulated in reperfused ischemic hearts with the carnitine palmitoyltransferase 1 inhibitor, Etomoxir. *Mol. Cell. Biochem.* **88**, 175-179 (1989).
165. Lopaschuk, G.D. Trimetazidine in AMI. *Eur. Heart J.* **22**, 977-978 (2001).
166. McCormack, J.G., Barr, R.L., Wolff, A.A., & Lopaschuk, G.D. Ranolazine stimulates glucose oxidation in normoxic, ischemic, and reperfused ischemic rat hearts. *Circulation* **93**, 135-142 (1996).
167. Liu, B., Clanachan, A.S., Schulz, R., & Lopaschuk, G.D. Cardiac efficiency is improved after ischemia by altering both the source and fate of protons. *Circ. Res.* **79**, 940-948 (1996).
168. Bavenholm, P.N. *et al.* Insulin resistance in type 2 diabetes: association with truncal obesity, impaired fitness, and atypical malonyl coenzyme A regulation. *J. Clin. Endocrinol. Metab.* **88**, 82-87 (2003).
169. Zhou, G. *et al.* Role of AMP-activated protein kinase in mechanism of metformin action. *J. Clin. Invest.* **108**, 1167-1174 (2001).
170. Sambandam, N. & Lopaschuk, G.D. AMP-activated protein kinase (AMPK) control of fatty acid and glucose metabolism in the ischemic heart. *Prog. Lipid Res.* **42**, 238-256 (2003).
171. Baker, J.C., Yan, X., Peng, T., Kasten, S., & Roche, T.E. Marked differences between two isoforms of human pyruvate dehydrogenase kinase. *J. Biol. Chem.* **275**, 15773-15781 (2000).
172. Peters, S.J., Harris, R.A., Heigenhauser, G.J., & Spriet, L.L. Muscle fiber type comparison of PDH kinase activity and isoform expression in fed and fasted rats. *Am. J. Physiol Regul. Integr. Comp. Physiol.* **280**, R661-R668 (2001).

173. Holness,M.J., Kraus,A., Harris,R.A., & Sugden,M.C. Targeted upregulation of pyruvate dehydrogenase kinase (PDK)-4 in slow-twitch skeletal muscle underlies the stable modification of the regulatory characteristics of PDK induced by high-fat feeding. *Diabetes* **49**, 775-781 (2000).
174. Sugden,M.C., Orfali,K.A., Fryer,L.G., Holness,M.J., & Priestman,D.A. Molecular mechanisms underlying the long-term impact of dietary fat to increase cardiac pyruvate dehydrogenase kinase: regulation by insulin, cyclic AMP and pyruvate. *J. Mol. Cell. Cardiol.* **29**, 1867-1875 (1997).
175. Sugden,M.C., Langdown,M.L., Harris,R.A., & Holness,M.J. Expression and regulation of pyruvate dehydrogenase kinase isoforms in the developing rat heart and in adulthood: role of thyroid hormone status and lipid supply. *Biochem. J.* **352 Pt 3**, 731-738 (2000).
176. Brown,G.K., Scholem,R.D., Bankier,A., & Danks,D.M. Malonyl coenzyme A decarboxylase deficiency. *J. Inherit. Metab. Dis.* **7**, 21-26 (1984).
177. Gao,J., Waber,L., Bennett,M.J., Gibson,K.M., & Cohen,J.C. Cloning and mutational analysis of human malonyl-coenzyme A decarboxylase. *J. Lipid Res.* **40**, 178-182 (1999).
178. Haan,E.A., Scholem,R.D., Croll,H.B., & Brown,G.K. Malonyl coenzyme A decarboxylase deficiency. Clinical and biochemical findings in a second child with a more severe enzyme defect. *Eur. J. Pediatr.* **144**, 567-570 (1986).
179. Krawinkel,M.B. *et al.* Association of malonyl-CoA decarboxylase deficiency and heterozygote state for haemoglobin C disease. *J. Inherit. Metab. Dis.* **17**, 636-637 (1994).
180. MacPhee,G.B. *et al.* Malonyl coenzyme A decarboxylase deficiency. *Arch. Dis. Child* **69**, 433-436 (1993).
181. Matalon,R. *et al.* Malonic aciduria and cardiomyopathy. *J. Inherit. Metab. Dis.* **16**, 571-573 (1993).
182. Yano,S., Sweetman,L., Thorburn,D.R., Mofidi,S., & Williams,J.C. A new case of malonyl coenzyme A decarboxylase deficiency presenting with cardiomyopathy. *Eur. J. Pediatr.* **156**, 382-383 (1997).
183. Wightman,P.J. *et al.* MLYCD mutation analysis: evidence for protein mistargeting as a cause of MLYCD deficiency. *Hum. Mutat.* **22**, 288-300 (2003).

184. Buckner, J.S., Kolattukudy, P.E., & Poulou, A.J. Purification and properties of malonyl-coenzyme A decarboxylase, a regulatory enzyme from the uropygial gland of goose. *Arch. Biochem. Biophys.* **177**, 539-551 (1976).
185. Buckner, J.S., Kolattukudy, P.E., & Rogers, L. Synthesis of multimethyl-branched fatty acids by avian and mammalian fatty acid synthetase and its regulation by malonyl-CoA decarboxylase in the uropygial gland. *Arch. Biochem. Biophys.* **186**, 152-163 (1978).
186. Courchesne-Smith, C. *et al.* Cytoplasmic accumulation of a normally mitochondrial malonyl-CoA decarboxylase by the use of an alternate transcription start site. *Arch. Biochem. Biophys.* **298**, 576-586 (1992).
187. Flurkey, W., Kim, Y.S., & Kolattukudy, P.E. Precursor of a mitochondrial enzyme accumulates in the cytoplasm of preen glands for a specialized function. *Biochem. Biophys. Res. Commun.* **106**, 1346-1352 (1982).
188. Kim, Y.S., Kolattukudy, P.E., & Boos, A. Dual sites of occurrence of malonyl-CoA decarboxylase and their possible functional significance in avian tissues. *Comp. Biochem. Physiol B* **62**, 443-447 (1979).
189. An, J. *et al.* Hepatic expression of malonyl-CoA decarboxylase reverses muscle, liver and whole-animal insulin resistance. *Nat. Med.* **10**, 268-274 (2004).

Chapter 2

Control of Cardiac Pyruvate Dehydrogenase Activity in PPAR α Transgenic Mice

Isolated working mouse heart perfusions were performed by Ray Kozak

Immunoblots of PDK and PDC E1- α were performed by Karen Bulmer,
in collaboration with Dr. Mary C. Sugden

A portion of this work has been published in the American Journal of
Physiology (Heart and Circulatory Physiology)
Hopkins TA, Sugden MC, Holness MJ, Kozak R, Dyck JRB,
and GD Lopaschuk. 285: H270-276, 2003.

2.1 Introduction

The heart primarily uses fatty acids and glucose as energy substrates, at rates determined by both the substrate availability and oxygen supply. In the aerobic setting fatty acid oxidation is the predominant source of energy, while during ischemia the absence of oxygen prevents the oxidative catabolism of both fatty acids and glucose. Glycolysis is activated and is responsible for the majority of ATP production during severe ischemia. The post-ischemic heart utilizes mainly fatty acids, which is associated with a decrease in cardiac functional recovery that can be improved by enhancing glucose oxidation rates. One important mechanism controlling the switch to the use of fatty acids over glucose is mediated by the activity of the pyruvate dehydrogenase complex.

PDC catalyzes the conversion of pyruvate to acetyl CoA and is the rate-limiting step of the glucose oxidation pathway. The activity of PDC is controlled both by allosteric regulation and phosphorylation, which are each sensitive to the acetyl CoA/CoA ratio and NADH/NAD⁺ ratio. High concentrations of acetyl CoA/CoA allosterically inhibit the PDC complex^{1,2}. Similarly, high ratios of acetyl CoA/CoA and NADH/NAD⁺ activate the PDC associated kinase, which phosphorylates and inhibits the complex^{3,4}. Since high fatty acid oxidation rates produce increased ratios of acetyl CoA/CoA and NADH/NAD⁺, high fatty acid rates control PDC activity by both feedback inhibition of PDC and enhanced phosphorylation by PDK. Therefore, the inhibition of PDC activity and glucose oxidation rates represents a level of substrate preference control.

Despite considerable data showing a correlation between PDC activity and glucose oxidation rates, the inactivation of PDC and a reduction in glucose oxidation

rates does not correlate in some studies ^{5, 6}. Therefore it is currently not known whether the most important regulator of PDC activity in the heart is due to phosphorylation of the enzyme complex or allosteric control by end-product inhibition. PDC activity is controlled not only by this acute allosteric and phosphorylation status but also by the chronic induction of PDK expression by PPAR α during fasting and diabetes, suggesting PPAR α may mediate control of glucose oxidation rates at the level of PDC.

PPAR α is a nuclear receptor shown to alter the transcription of several enzymes involved in fatty acid oxidation including CPT-1 ⁷ and FAT/CD36 ^{8, 9}. Activation of PPAR α by WY 14,643 is one effective approach to increase the expression of PPAR α -controlled genes involved in fatty acid oxidation and promote a switch in substrate preference towards the use of fatty acids. PPAR α transgenic mice are another important tool for cardiac specific activation of PPAR α . Transgenic mice over-expressing PPAR α in the heart (under the control of the myosin heavy chain (MHC) promoter (MHC-PPAR α)) exhibit many characteristics of diabetic cardiomyopathy and increased reliance on fatty acid utilization ¹⁰, suggesting that PPAR α is an important mediator of cardiac substrate preference. Since PPAR α enhances fatty acid oxidation rates and increases PDK expression, the use of mice over-expressing PPAR α may delineate which of these major factors is more important for the inhibition of glucose oxidation rates in the heart.

The **specific hypothesis** of this chapter is that PPAR α activation increases expression of PDK4 and inhibits glucose oxidation rates. The relative importance of phosphorylation control versus end-product inhibition of pyruvate dehydrogenase was investigated using mice with cardiac-specific over-expression of PPAR α . The **objective** of this chapter was to determine whether PDC phosphorylation can be equated to rates of

cardiac glucose oxidation. We sought to analyze the impact of PPAR α over-expression on cardiac fuel selection and furthermore we evaluated the response of cardiac glucose oxidation to fasting in relationship to cardiac PDC activity and PDK protein expression. We also determined whether PPAR α controls glucose oxidation rates in the heart primarily by regulation of PDK expression or through its effects on fatty acid oxidation.

2.2 Methods

2.2.1: Transgenic animals

Mice over-expressing PPAR α (of the 402-2 line) were produced as previously described ¹⁰ and wild-type littermates were used as controls. The 402-2 line of PPAR α transgenic mice provided by Dr. Daniel P. Kelly, exhibited cardiac-restricted transgene expression that was approximately 80-fold higher than that of wild-type littermates ¹⁰.

In the second portion of the study, animals were either fasted for 48 hours or provided with 0.1 % w/w WY 14,643 in standard rodent chow *ad libitum* for one week. Male animals (age 12 weeks) were used in both wild-type and PPAR α transgenic groups.

2.2.2: Isolated working mouse heart model

Hearts from male mice (10-12 weeks) were perfused as described by Belke *et al* ¹¹. Briefly, hearts were aerobically perfused at a preload of 7 mmHg and an aortic afterload of 50 mmHg for 30 minutes with Krebs-Henseleit solution containing 0.4 mM palmitate, 3% BSA, 5 mM glucose, 2.5 mM calcium, and 100 μ U/mL insulin. Fatty acid oxidation and glucose oxidation rates were measured as previously described by Saddik and Lopaschuk ¹². Glucose oxidation rates were determined by measuring ¹⁴CO₂ release from the metabolism of U-¹⁴C glucose. Palmitate oxidation rates were measured either by measuring ¹⁴CO₂ production from hearts perfused with 1-¹⁴C palmitate or when hearts were simultaneously perfused with U-¹⁴C glucose through ³H₂O released from hearts perfused with 9,10-³H palmitate. Glycolytic flux was measured as previously described ¹¹

by measuring the amount of $^3\text{H}_2\text{O}$ released from the metabolism of $5\text{-}^3\text{H}$ glucose by the triosephosphate isomerase and enolase steps of the glycolytic pathway ¹².

2.2.3: PDC activity measurements

PDC activities were measured using a revised protocol based on the radiometric assay described by Constantin-Teodosiu *et al* ¹³. Briefly, for measurement of 'active' PDC, frozen mouse heart tissue was homogenized in buffer containing 200 mM sucrose, 50 mM KCl, 5 mM ethylene glycol-bis(β -aminoethyl ether)-N,N,N',N'-tetraacetic acid (EGTA), 50 mM tris(hydroxymethyl)aminomethane (Tris)-HCl, 50 mM sodium fluoride (NaF), 50 mM sodium pyrophosphate (NaPPi), 5 mM dichloroacetate and 0.1% Triton X-100, pH 7.8.

For assay of 'total' PDC activity (dephosphorylated form of PDC), frozen tissue was homogenized in buffer containing 1 mM calcium chloride (CaCl_2), but in the absence of NaF, NaPPi, and EGTA. The 'total' PDC samples were incubated in 0.8 mM magnesium chloride (MgCl_2) at 37 °C for 20 minutes.

Both 'active' and 'total' samples were then incubated in assay buffer (150 mM Tris-HCl, 0.75 mM EDTA, 0.75 mM nicotinamide adenine dinucleotide (NAD), 1.5 mM thiamine pyrophosphate (TPP), 5 mM EGTA, 5 mM dichloroacetate, and 0.75 mM coenzyme-A (CoA) and the reaction initiated by the addition of pyruvate. The reaction was terminated after 10 minutes by 40 μL of 0.5 M perchloric acid. Samples were neutralized, centrifuged, and the resulting supernatant was used to determine acetyl-CoA content. Acetyl CoA was converted to ^{14}C citrate, and separated from unreacted ^{14}C oxaloacetate radioactivity using Dowex resin (50WX8, 100-200 mesh; Sigma). The

amount of acetyl CoA was determined by comparison of acetyl CoA standard curves run in parallel in each experiment.

2.2.4: Immunoblotting

Samples were prepared as previously described by Holness, MJ *et al* ¹⁴. Cardiac samples were homogenized in ice-cold buffer containing 10 mM Tris-HCl, 150 mM NaCl, 1% Igepal[®], 0.4% sodium deoxycholate, 0.1% sodium dodecyl sulfate (SDS), 45 mM sodium orthovanadate, 0.2 mM PMSF, 10 µg/ml leupeptin, 1.5 mg/ml benzamidine, 50 µg/ml aprotinin, 50 µg/ml pepstatin A (in dimethylsulfoxide), pH 8.0. Samples (25 µg total protein) were subjected to SDS-PAGE and subsequently transferred electrophoretically to nitrocellulose membranes. Membranes were blocked with Tris-buffered saline supplemented with 0.05% Tween (TBS-T) and 5% (w/v) non-fat powdered milk. The nitrocellulose blots were incubated overnight with polyclonal antisera raised against specific recombinant PDK isoforms, washed in TBS-T (3 x 10 min) and incubated with the horseradish peroxidase-linked secondary antibody IgG anti-rabbit (1:5000, in 1% (w/v) non-fat milk in TBS-T). Bound antibody was visualized using ECL[®] according to the manufacturer's instructions. The blots were exposed to Hyperfilm[®], signals quantified by scanning densitometry and analyzed with Molecular Analyst software (Bio-Rad[®]).

2.2.5: Statistics

Values are expressed as mean \pm S.E.M. The Student's unpaired t-test was used to evaluate significance between two groups, however groups with unequal standard

deviations were evaluated using the non-parametric Alternate Welch t-test. A value of $p < 0.05$ was judged as significant.

2.3 Results

2.3.1: Contractile function of isolated perfused mouse hearts

The contractile function of isolated perfused working hearts from fed MHC-PPAR α mice and control animals is shown in Table 2-1. There were no differences in heart rate, peak systolic pressure, coronary flow, cardiac output or cardiac work in mice over-expressing PPAR α and their respective controls over the 30 minute aerobic perfusion period. Therefore, metabolic measurements in these hearts were not confounded by differences in metabolic demand. Although heart rates in the isolated hearts were lower than rates seen *in vivo*, cardiac function in these hearts was comparable to isolated working heart function observed in other published studies^{15, 16} and function was maintained throughout the entire perfusion period.

	Heart Rate (beats/min)	Peak Systolic Pressure (mmHg)	Pulse Pressure (mmHg)	Coronary flow (mL/min)	Cardiac Output (mL/min)	Cardiac Work (ml·mmHg· min ⁻¹)
Wild-type	273.8 \pm 8.0	78.0 \pm 8.0	49.0 \pm 6.0	4.1 \pm 0.4	8.2 \pm 0.8	6.5 \pm 0.8
MHC-PPAR α	238.0 \pm 22.0	79.0 \pm 2.0	45.0 \pm 3.0	4.1 \pm 0.6	8.3 \pm 0.7	6.6 \pm 0.8

Table 2-1: Contractile parameters of isolated working hearts from wild-type and MHC-PPAR α transgenic mice

2.3.2: Metabolism and PDC activity measurements

MHC-PPAR α hearts exposed to 0.4 mM palmitate had significantly higher palmitate oxidation rates than the rates measured from hearts of wild-type animals, as shown in Figure 2-1a. This increase in palmitate oxidation rates was paralleled by a

significant decrease in glucose oxidation rates of MHC-PPAR α mice compared to wild-type animals (Figure 2-1b). The relative contribution of palmitate and glucose to the production of acetyl CoA are shown in Figure 2-1c and indicates that mice over-expressing PPAR α derive more acetyl CoA from palmitate oxidation compared to control animals (71.5% vs. 47.2%, respectively). Despite this decrease in glucose oxidation rates, the activity of pyruvate dehydrogenase in the active form was not different in MHC-PPAR α heart extracts compared to wild-type heart extracts (Figure 2-1d). Figure 2-1d also shows that total PDC activity was similar in both animal groups, suggesting that there were no changes in PDC protein expression in MHC-PPAR α mice. Interestingly, we also found that cardiac PDC activity of mice lacking the PPAR α gene was $2.4 \pm 0.6 \mu\text{mol}\cdot\text{g dry weight}^{-1}\cdot\text{min}^{-1}$, which is not different from mice over-expressing PPAR α (Figure 2-1d), even though previous studies have shown that glucose oxidation rates are significantly increased in animals lacking PPAR α ¹⁷. Taken together, these data show that although glucose oxidation rates are widely varied, the activity of PDC is unchanged.

2.3.3: Expression levels of PDK and PDH E1- α

To determine if the low glucose oxidation rates of the PPAR α transgenic mice are due to increases in protein expression of PDK, western blot analysis was performed for all three PDK isoforms present in the heart (PDK1, 2, and 4). Figure 2-2a,b,c shows that cardiac expression levels of PDK1 were significantly increased in MHC-PPAR α hearts while levels of PDK2 and PDK4 were unchanged. Therefore, contrary to our expectation protein expression of PDK4 was only marginally influenced by PPAR α over-expression.

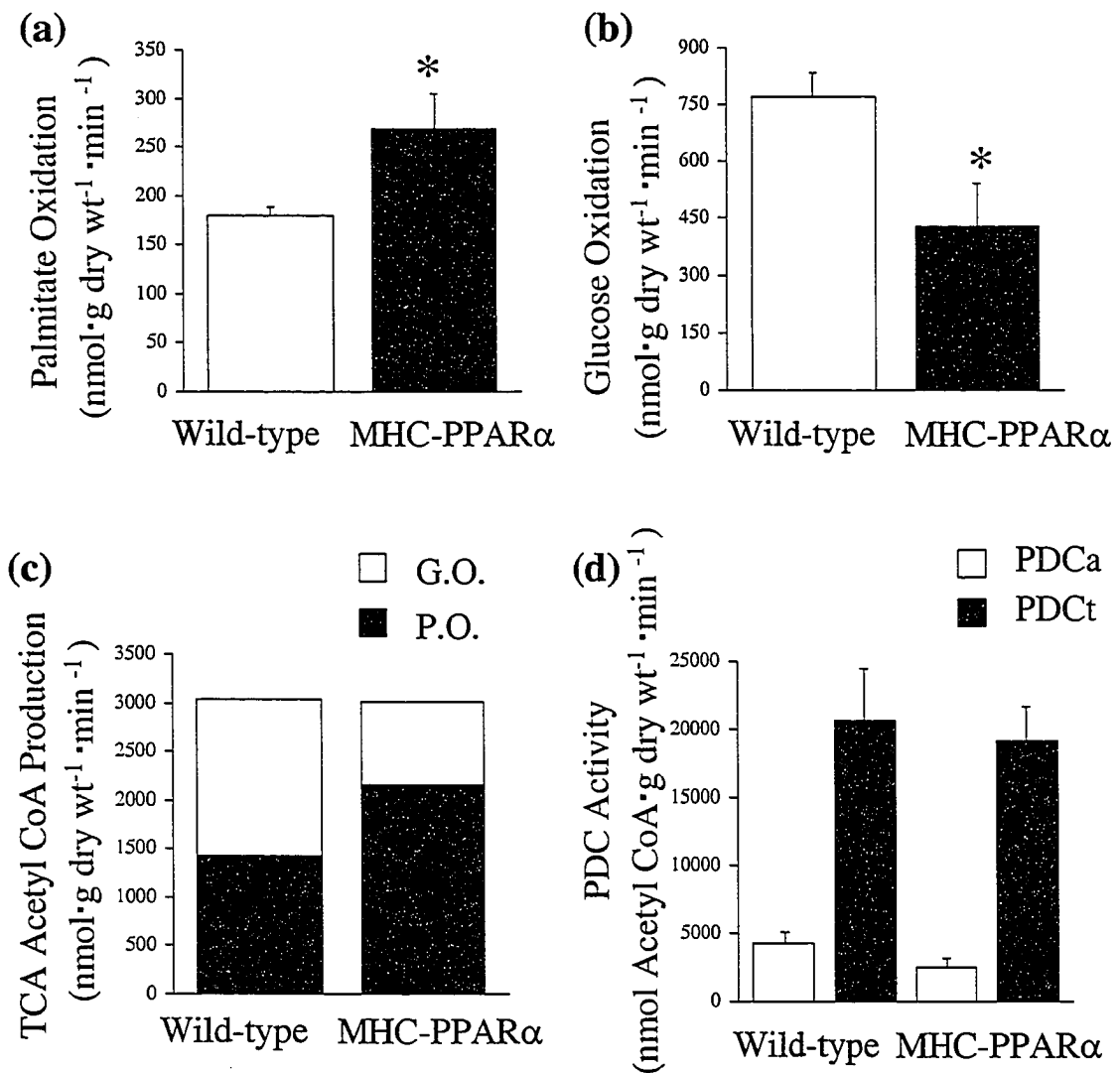


Figure 2-1: Palmitate oxidation, glucose oxidation, tricarboxylic acid cycle production and PDC activity of isolated working hearts from wild-type and MHC-PPAR α mice. Steady-state rates of palmitate oxidation (a), and glucose oxidation (b) were measured as described in the Section 2.2.2. TCA cycle production of acetyl CoA (c) was calculated from the palmitate and glucose oxidation rates using a value of 8mol acetyl CoA per 1mol palmitate oxidized and 2mol acetyl CoA per 1mol glucose oxidized. PDC activity was measured in the ‘active form’ (PDCa) and in the dephosphorylated ‘total’ form (PDCt) (d). Values are means \pm SEM of 5 control hearts and 7 MHC-PPAR α hearts for palmitate oxidation, glucose oxidation and TCA cycle activity; 5 control hearts and 8 MHC-PPAR α hearts for PDC activity. *Significantly different from control hearts, $p < 0.05$.

We also measured the expression of PDH E1- α (the subunit of PDC that is phosphorylated by PDK) in wild-type and MHC-PPAR α mouse hearts (Figure 2-2d). Similar to the PDK isoforms, no difference in PDH E1- α was observed between wild-type and MHC-PPAR α mouse hearts.

2.3.4: Metabolism and PDC activity measurements of WY 14,643 treated animals

In order to amplify differences among the groups in terms of PDC activity, wild-type and MHC-PPAR α mice were also treated with the PPAR α agonist WY 14,643 for one week or were fasted for 48 hours prior to study. There were no differences between pre-perfusion body weight of fed and fasted wild-type animals and only a minor drop in pre-perfusion weight (~10%) of the fasted MHC-PPAR α mice compared to their fed counterparts (data not shown). However, weights prior to fasting were not recorded and thus may underestimate the weight loss and level of starvation observed in each group. The level of fasting was assumed to be appropriate for PPAR α activation. Cardiac function as assessed by cardiac work was depressed in fasted mice, however there was no difference between fasted wild-type and fasted MHC-PPAR α heart function (3.4 ± 0.6 vs. 3.6 ± 0.9 ml \cdot mmHg \cdot min⁻¹, respectively). Similarly, cardiac work was not changed following treatment with WY 14, 643 (6.5 ± 3.5 vs. 6.1 ± 0.6 ml \cdot mmHg \cdot min⁻¹ in control and MHC-PPAR α treated groups, respectively).

Fatty acid oxidation rates were similar in wild-type fasted and MHC-PPAR α hearts (168 ± 36 vs. 162 ± 13 nmol \cdot g dry weight⁻¹ \cdot min⁻¹, respectively), however fatty acid

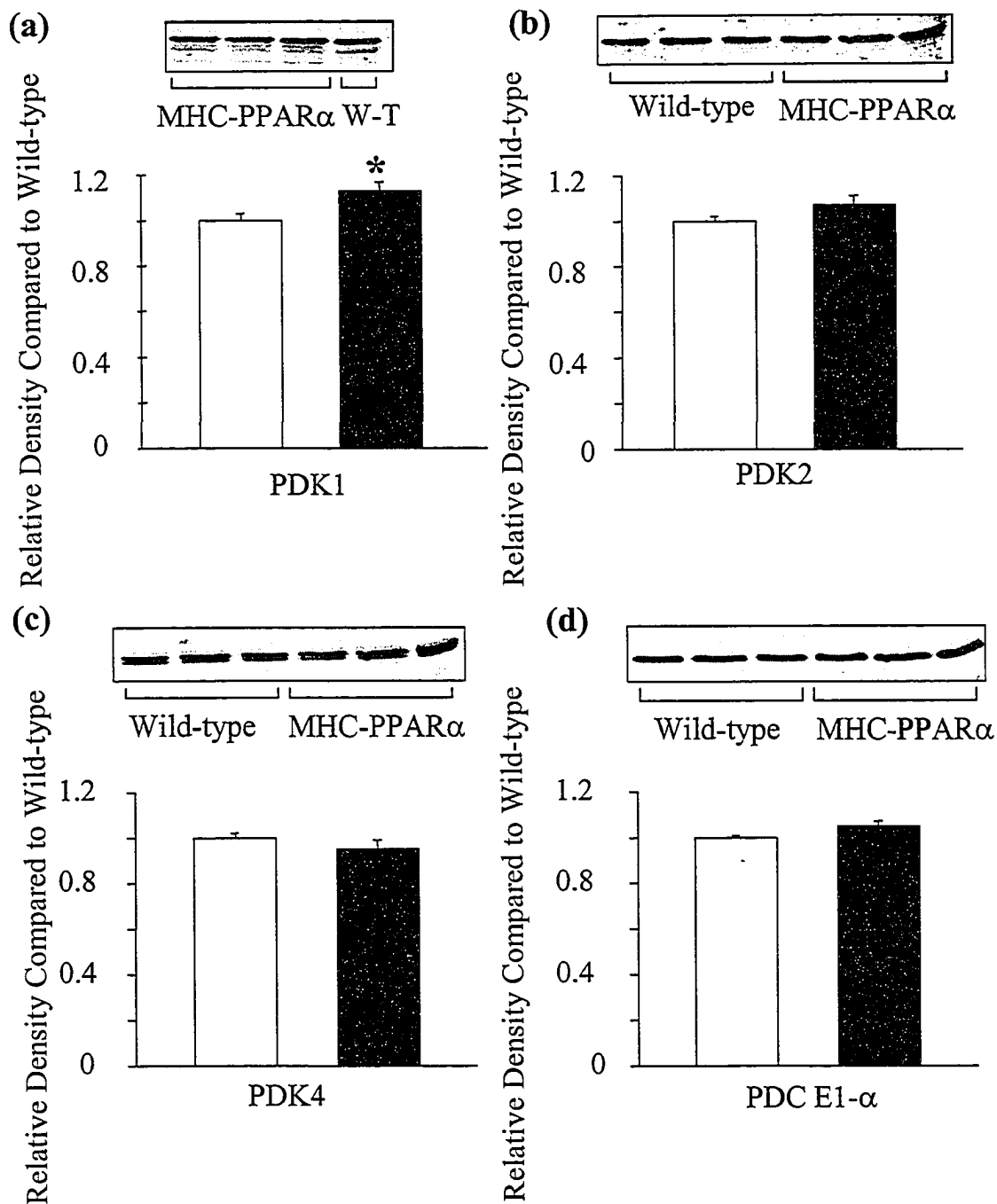


Figure 2-2: Expression levels of the cardiac pyruvate dehydrogenase kinase (PDK) isoforms and PDC E1- α . Densitometric analysis was performed on Western blots as described in Section 2.2.4. Representative blots of PDK1 (a), PDK2 (b), PDK4 (c) and PDC E1- α (d) expression in wild-type mice (white bars) and MHC-PPAR α mice (black bars). Values are means \pm SEM of 6 control hearts and 3 MHC-PPAR α hearts. *Significantly different from control hearts, $p < 0.05$.

oxidation rates were significantly increased in MHC-PPAR α hearts treated with WY 14,643 compared to wild-type WY 14,643 treated hearts (351 ± 27 vs. 126 ± 23 nmol·g dry weight⁻¹·min⁻¹, respectively).

Treatment with WY 14,643 resulted in significantly lower glucose oxidation rates in MHC-PPAR α mice than in wild-type animals, as shown in Figure 2-3a. Figure 2-3b indicates that fasting of animals for 48 hours resulted in a severe drop in glucose oxidation rates in both animal groups although no difference was observed between control and MHC-PPAR α mice. Even with these drastic changes in glucose oxidation rates no change in PDC activity occurred with WY 14,643 treatment (Figure 2-3c) or fasting (Figure 2-3d). These data suggest that the rates of glucose oxidation are not closely correlated with rates of PDC activity. However, fasting of wild-type animals, a condition known to increase PDK expression¹⁸ did cause a decrease in PDC in the active form compared to the fed wild-type animals (2.4 ± 0.7 vs. 4.3 ± 0.8 μ mol·g dry weight⁻¹·min⁻¹ for fasted and fed respectively). This result confirms previous studies that show fasting can alter PDC activity. However, these changes in PDC can be dissociated from changes in glucose oxidation. For ease of comparison, PDC activity (in the active form) among all of the treated groups is summarized in Table 2-2.

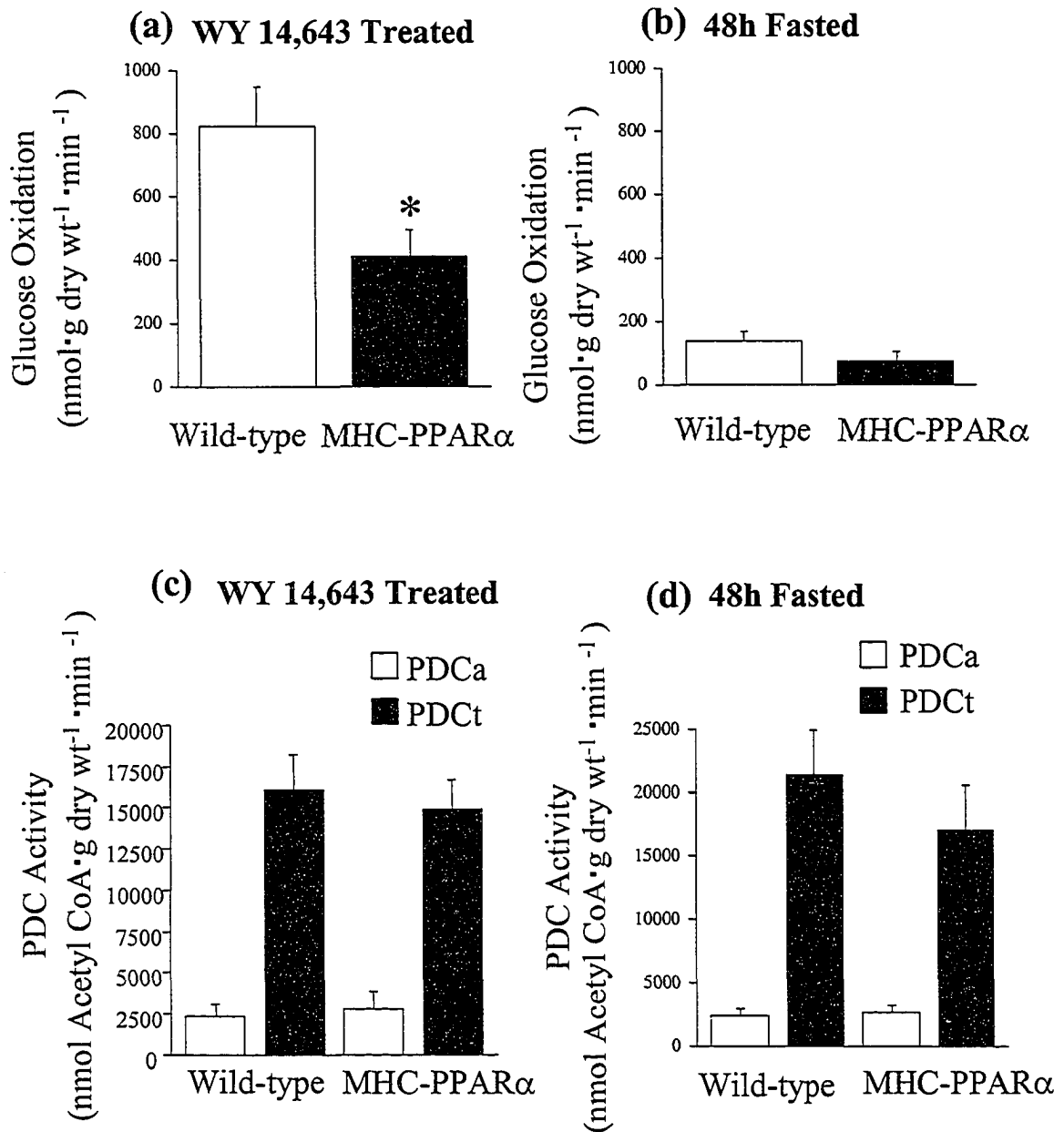


Figure 2-3: Glucose oxidation and PDC activity of fasted wild-type and MHC-PPAR α mouse hearts. Steady state rates of glucose oxidation were measured as described in Section 2.2.2. Glucose oxidation rates of WY 14,643 treated animals (a) and fasted animals (b) are shown with the corresponding PDC activity in WY 14,643 treated animals (c) and fasted animals (d). Values are means \pm SEM of 5 fasted control hearts, 4 MHC-PPAR α hearts, 3 WY 14,643 treated controls and 7 WY 14,643 treated MHC-PPAR α mice for glucose oxidation and 10 fasted controls, 8 fasted MHC-PPAR α mice, 3 WY 14,643 treated controls and 7 WY 14,643 treated MHC-PPAR α hearts for PDC activity. *Significantly different from control hearts, $p < 0.05$.

	Control	MHC-PPAR α	Control Fasted	MHC-PPAR α Fasted	Control + WY 14,643	MHC-PPAR α + WY 14,643
PDCa Activity (nmol·g dry weight ⁻¹ ·min ⁻¹)	4268 ± 851	2533 ± 577	2386 ± 706	2798 ± 1038	2364 ± 592	2711 ± 530

Table 2-2: Activity of PDC in the active form (PDCa) in untreated, fasted and WY 14, 643 treated wild-type and MHC-PPAR α hearts (values \pm SEM).

To determine if pyruvate supply from glycolysis was responsible for altering glucose oxidation rates in fasted hearts, we measured glycolytic flux in these animals. Glycolytic rates after 30 minutes aerobic perfusion were 5.3 ± 0.1 and 5.1 ± 0.5 $\mu\text{mol } ^3\text{H}$ glucose g dry/min in fasted wild-type and PPAR α transgenic mice, respectively. To determine the relationship between PDC activity and glucose oxidation rates a correlation curve was plotted for both animal groups and is shown in Figure 2-4. There was no correlation between PDC activity and rates of glucose oxidation in hearts perfused under our conditions ($R=0.181$, $r^2=0.033$). Similarly, palmitate oxidation and PDC activity have no correlation in these perfused hearts ($R=0.022$, $r^2=0.000$).

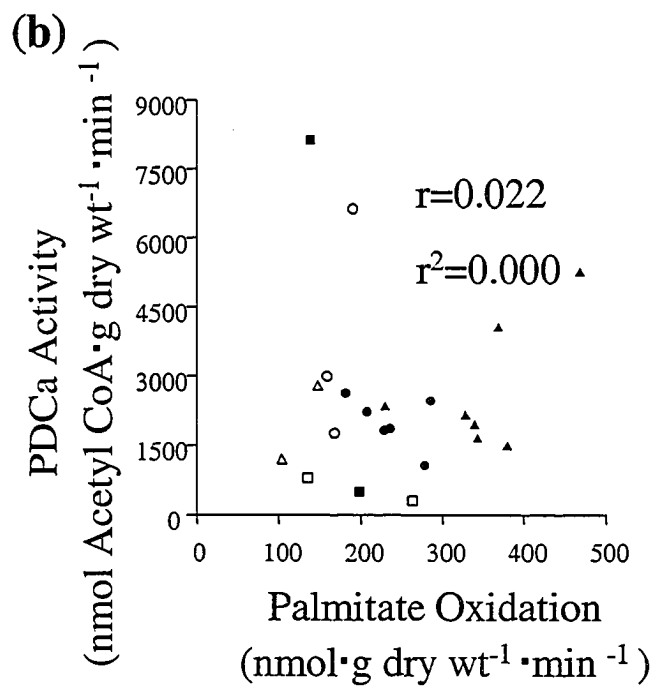
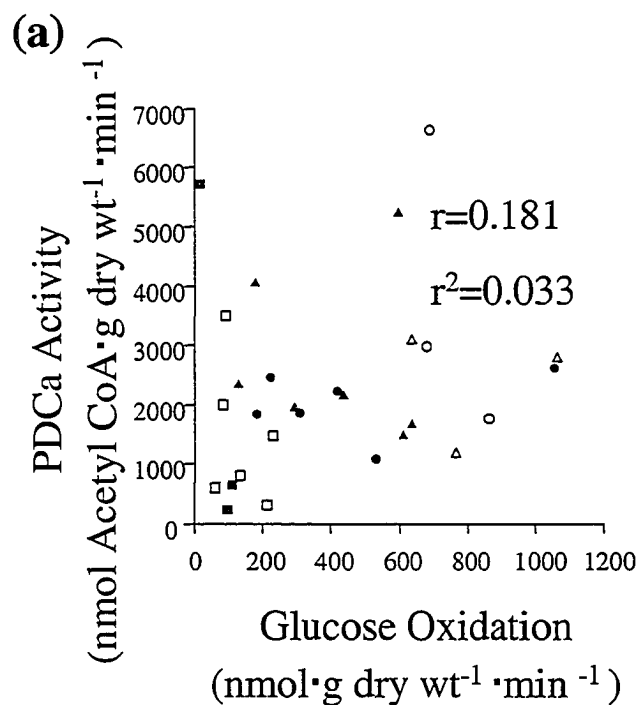


Figure 2-4: Correlation curves of (a) PDCa activity compared with glucose oxidation rates, (b) PDCa activity compared with fatty acid oxidation rates. Data for control mice (open circles), MHC-PPAR mice (closed circles), fasted control mice (open squares), fasted MHC-PPAR mice (closed squares), WY 14,643 treated controls (open triangles), and WY 14,643 treated MHC-PPAR mice (closed triangles) is represented.

2.4 Discussion

2.4.1: Diabetic phenotype of MHC-PPAR α transgenic mice and metabolic control by PPAR α

Under resting conditions *in vivo*, the mouse heart derives approximately 40-60% of its energy from the oxidation of fatty acids, while the remainder originates primarily from glycolysis and glucose oxidation¹². However, the relative contribution of fatty acid oxidation to energy production increases in fasting and diabetes. It has been recently reported that the cardiac metabolic phenotype induced by PPAR α over-expression, in particular enhanced expression of genes involved in myocardial fatty acid utilization and evidence of altered lipid balance, mimics that found in uncontrolled or poorly controlled diabetes¹⁰. Perfusions of hearts from mice with a cardiac-specific over-expression of PPAR α , allows analysis of a switch in cardiac substrate preference that are retained *ex vivo* under controlled conditions of substrate delivery. These perturbations include enhanced reliance of the heart on fatty acids and a reduction in glucose oxidation rates.

2.4.2: PPAR α increases PDK4 expression and decreases glucose oxidation rates in the absence of depressed PDC activity

Data from other laboratories have clearly shown that PPAR α activation^{10, 19} and over-expression¹⁰ causes an increase in PDK4 expression suggesting a direct role of PPAR α in the control of glucose oxidation. However, although we show that mice over-expressing the PPAR α gene have significantly decreased glucose oxidation rates¹⁰, we found that PDC activity was not different between wild-type and MHC-PPAR α mice under a variety of conditions in which the glucose oxidation rates were varied. In a

previous study, hearts from PPAR α knockout mice ¹⁷ showed a decrease in fatty acid oxidation and an increase in glucose oxidation ¹⁷, the opposite metabolic phenotype of the MHC-PPAR α mice. These dramatic changes in glucose oxidation were also not evidenced by changes in PDC activity, as the PPAR α knockout mice and the MHC-PPAR α animals exhibit similar PDC activities. This suggests that PPAR α does not alter glucose oxidation at the level of PDK or PDC, but most likely secondary to changes in fatty acid oxidation.

2.4.3: In vitro assay conditions do not measure PDC flux

The PDC assay utilizes excess pyruvate to form acetyl CoA and careful procedures prevent the phosphorylated state of PDC from being altered during the experiment. In this manner, the PDC assay reflects the amount of PDC in the phosphorylated state, but not physiological PDC flux. A second determinant of flux through PDC is the concentration of substrates and products of the reaction ²⁰, including pyruvate, acetyl CoA and NADH. Increasing levels of acetyl CoA and NADH will feedback and inhibit the PDC complex in two ways: 1) by activation of PDK ²¹, which is likely not the mechanism active in these hearts as evidenced by our measurements of PDC activity and 2) acetyl CoA and NADH can inhibit the PDC complex directly to decrease flux through the complex ²⁰. This action is through negative feedback regulation, where fatty acid oxidation can inhibit glucose oxidation at the level of PDC. We are unable to measure the changes due to negative feedback as our *in vitro* assay cannot reflect limiting substrate or product levels within the mitochondrial matrix. However, our data suggest that the main determinant of flux through PDC of these hearts

is the substrate/product concentration, as we observe no changes in PDC activity in the unphosphorylated form. In this study we used a physiological level of palmitate (0.4 mM) to measure negative feedback of the PDC enzyme complex. Future studies using a higher concentration of palmitate may provide further insight into the PPAR α regulation of glucose oxidation through feedback inhibition of PDC.

2.4.4: Fasting and WY 14,643 alter glucose oxidation rates with only minor changes in PDC activity

It is possible that the expressional level of PDK4 was not high enough in the MHC-PPAR α mouse hearts to reflect a change in the active form of PDC. Previous studies¹⁰ have shown a dramatic increase in PDK4 mRNA expression in these mice, however protein content was not determined. In addition, the role of PPAR β/δ in these hearts has not been determined and down-regulation of PPAR β/δ (which also controls PDK4 expression) may negate the effects of PPAR α over-expression. Therefore, we may speculate that PDK4 protein levels are not altered due to this down-regulation of PPAR β/δ , which warrants further study in MHC-PPAR α mouse hearts.

Expression of several PPAR α regulated genes is further increased in MHC-PPAR α mice upon treatment with the PPAR α ligand WY 14,643, suggesting that the ligand may be limiting for PPAR α activation in these mice¹⁰. Similarly, Wu *et al* demonstrated an increase in PDK4 expression with both starvation and treatment with WY 14,643¹⁹, therefore in order to amplify these changes we treated animals with WY 14,643 or by fasting. Under these conditions PDK expression should have been sufficient to cause changes in the phosphorylated state of the PDC complex. In wild-type hearts we

did observe a decrease in PDC activity in both fasted and WY 14,643 treated mice. This indicates an increase in phosphorylated PDC and suggests PDK involvement. These data also support previous studies, which demonstrate that the levels of PDK are indeed altered during both fasting and treatment with WY 14, 643. However, we were unable to demonstrate any changes in PDC activity in the fed, fasted or WY 14,643 treated MHC-PPAR α mice compared to wild-type control. Taken together, the data can be interpreted that PDK expression in the MHC-PPAR α mice (regardless of treatment) is not the main determinant of the decreased flux through pyruvate dehydrogenase.

2.4.5: Diminished pyruvate supply and effect on glucose oxidation rates

In addition to feedback inhibition, diminished pyruvate supply may also play a role in the decreased glucose oxidation rates observed in the MHC-PPAR α mice. Both GLUT-4 and phosphofructokinase expression is decreased in MHC-PPAR α mice compared to control¹⁰. This reduction in pyruvate supply from glucose uptake and glycolysis could contribute to the reduced glucose oxidation rates in the heart. Reduced pyruvate levels *in vivo* may inhibit flux through the PDC complex. This inhibition by decreased pyruvate supply would not be detected in our *in vitro* assay. However, our measurements of glycolytic flux in fasted wild-type and PPAR α transgenic animals suggest that pyruvate supply is not limiting in these hearts.

2.4.6: WY 14,643 treatment of MHC-PPAR α mice

A previous study has suggested that PPAR α expression is reduced under conditions where fatty acid utilization is high and thus providing the synthetic PPAR α

activator WY 14,643 can further activate PPAR α ²². Treatment with WY 14,643 would ensure complete activation of the PPAR α protein however it has not been proven that pharmacological treatment by WY 14,643 is required to observe changes in metabolism of these transgenic mice. A diet of WY 14,643 for 7 days has been shown to moderately activate PPAR α ²³. Using a similar protocol, we found that mean steady-state rates of palmitate oxidation were significantly increased in hearts of MHC-PPAR α animals administered WY 14,643 compared with MHC-PPAR α animals maintained on standard high-carbohydrate/low fat diet (data not shown). By contrast, dietary WY 14,643 administration did not increase exogenous palmitate oxidation rates in perfused hearts from wild-type mice. The latter findings suggest that PPAR α may be saturated with its physiological ligand in fed wild-type mice, whereas PPAR α ligand may be limiting for full activation of fatty acid oxidation in fed MHC-PPAR α mice. Overall, our data suggest that PPAR α activity may be relatively suppressed in the fed state, such that myocardial fatty acid oxidation increases with increased PPAR α expression levels. However, ligand activation by fatty acids may become limiting when the expression level of PPAR α is increased by overexpression.

2.4.7: Contribution of PDC phosphatase in hearts of MHC-PPAR α mice is unknown

An alternative explanation to the discrepancy between PDK expression and glucose oxidation in MHC-PPAR α and control mice, are that differences in expression or activity of the intrinsically linked PDH phosphatase may compensate for the increased PDK expression in hearts from MHC-PPAR α mice. Thus, the net phosphorylated state of

the PDC complex would not be altered and the feedback inhibition would be the main determinant of flux in these hearts. Whether the phosphatase is increased in a compensatory mechanism in these transgenic mice in order to maintain total energy production is not clear. Further studies are required to determine the role, if any, of the phosphatase. However, alterations in PDC phosphorylation would be expected to alter the ratio of PDC active to PDC total in these hearts, which did not occur.

2.4.8: Limitations

Although our interpretation of this study indicates that flux through the PDC complex in MHC-PPAR α hearts is controlled mainly by feedback regulation, there are limitations to the study that may affect this interpretation. The number of hearts used for the WY 14,643 treated and fasted animal groups was small due to the availability of animals. Therefore, increasing the number of animals in these groups may provide more insight into the control of PDC activity. As well, an analysis of statistical power would determine the number of animals required to have an accurate statistical assessment of our hypothesis. Similarly, the availability of the PDK antibodies made it difficult to measure protein levels of PDK in the treated animal groups and therefore an assumption was made that PDK4 is upregulated by fasting/ WY 14,643 treatment. This assumption may be incorrect and expression levels of PDK could be assessed by Northern blot analysis of mRNA. Analysis of mRNA levels of PDK would also indicate whether there is a change in mRNA that may preclude protein level changes in these hearts. As well, the use of transgenic animals has several limitations including compensation mechanisms due to alterations in gene expression. For example, over-expression of PPAR α in these

animals may have an effect on other PPAR isoforms or cause compensational changes in metabolism that are not due to the transgene expression. The interpretation of data in this chapter is based on several assumptions and therefore limited by the data currently available.

2.4.9: Summary

In conclusion, the data from this study suggest that flux through the PDC complex in MHC-PPAR α hearts is dependent mainly on the substrates and products of the reaction, rather than by alterations in PDC phosphorylation by PDK. Although the exact mechanism remains to be determined, we have demonstrated that a disconnect exists between PDC phosphorylation and glucose oxidation rates such that PDC phosphorylation cannot be equated directly to glucose oxidation rates in the heart.

Therefore, the control of PDC activity by phosphorylation status of the enzyme is secondary to feedback inhibition, suggesting that PDK is not an ideal pharmacological target to switch substrate preference in the heart.

Literature Cited

1. Bremer, J. Pyruvate dehydrogenase, substrate specificity and product inhibition. *Eur. J. Biochem.* **8**, 535-540 (1969).
2. Kerbey, A.L. *et al.* Regulation of pyruvate dehydrogenase in rat heart. Mechanism of regulation of proportions of dephosphorylated and phosphorylated enzyme by oxidation of fatty acids and ketone bodies and of effects of diabetes: role of coenzyme A, acetyl-coenzyme A and reduced and oxidized nicotinamide-adenine dinucleotide. *Biochem. J.* **154**, 327-348 (1976).
3. Cooper, R.H., Randle, P.J., & Denton, R.M. Regulation of heart muscle pyruvate dehydrogenase kinase. *Biochem. J.* **143**, 625-641 (1974).
4. Cooper, R.H., Randle, P.J., & Denton, R.M. Stimulation of phosphorylation and inactivation of pyruvate dehydrogenase by physiological inhibitors of the pyruvate dehydrogenase reaction. *Nature* **257**, 808-809 (1975).
5. Schoder, H., Knight, R.J., Kofoed, K.F., Schelbert, H.R., & Buxton, D.B. Regulation of pyruvate dehydrogenase activity and glucose metabolism in post-ischaemic myocardium. *Biochim. Biophys. Acta* **1406**, 62-72 (1998).
6. Stanley, W.C. *et al.* Pyruvate dehydrogenase activity and malonyl CoA levels in normal and ischemic swine myocardium: effects of dichloroacetate. *J. Mol. Cell. Cardiol.* **28**, 905-914 (1996).
7. Mascaro, C. *et al.* Control of human muscle-type carnitine palmitoyltransferase I gene transcription by peroxisome proliferator-activated receptor. *J. Biol. Chem.* **273**, 8560-8563 (1998).
8. Motojima, K., Passilly, P., Peters, J.M., Gonzalez, F.J., & Latruffe, N. Expression of putative fatty acid transporter genes are regulated by peroxisome proliferator-activated receptor alpha and gamma activators in a tissue- and inducer-specific manner. *J. Biol. Chem.* **273**, 16710-16714 (1998).
9. Sato, O., Kuriki, C., Fukui, Y., & Motojima, K. Dual promoter structure of mouse and human fatty acid translocase/CD36 genes and unique transcriptional activation by peroxisome proliferator-activated receptor alpha and gamma ligands. *J. Biol. Chem.* **277**, 15703-15711 (2002).
10. Finck, B.N. *et al.* The cardiac phenotype induced by PPARalpha overexpression mimics that caused by diabetes mellitus. *J. Clin. Invest.* **109**, 121-130 (2002).

11. Belke,D.D., Larsen,T.S., Lopaschuk,G.D., & Severson,D.L. Glucose and fatty acid metabolism in the isolated working mouse heart. *Am. J. Physiol.* **277**, R1210-R1217 (1999).
12. Saddik,M. & Lopaschuk,G.D. Myocardial triglyceride turnover and contribution to energy substrate utilization in isolated working rat hearts. *J. Biol. Chem.* **266**, 8162-8170 (1991).
13. Constantin-Teodosiu,D., Cederblad,G., & Hultman,E. A sensitive radioisotopic assay of pyruvate dehydrogenase complex in human muscle tissue. *Anal. Biochem.* **198**, 347-351 (1991).
14. Holness,M.J. *et al.* Evaluation of the role of peroxisome-proliferator-activated receptor alpha in the regulation of cardiac pyruvate dehydrogenase kinase 4 protein expression in response to starvation, high-fat feeding and hyperthyroidism. *Biochem. J.* **364**, 687-694 (2002).
15. Aasum,E. *et al.* Cardiac function and metabolism in Type 2 diabetic mice after treatment with BM 17.0744, a novel PPAR-alpha activator. *Am. J. Physiol. Heart Circ. Physiol.* **283**, H949-H957 (2002).
16. Atkinson,L.L., Fischer,M.A., & Lopaschuk,G.D. Leptin activates cardiac fatty acid oxidation independent of changes in the AMP-activated protein kinase-acetyl-CoA carboxylase-malonyl-CoA axis. *J. Biol. Chem.* **277**, 29424-29430 (2002).
17. Campbell,F.M. *et al.* A role for peroxisome proliferator-activated receptor alpha (PPARalpha) in the control of cardiac malonyl-CoA levels: reduced fatty acid oxidation rates and increased glucose oxidation rates in the hearts of mice lacking PPARalpha are associated with higher concentrations of malonyl-CoA and reduced expression of malonyl-CoA decarboxylase. *J. Biol. Chem.* **277**, 4098-4103 (2002).
18. Wu,P. *et al.* Starvation and diabetes increase the amount of pyruvate dehydrogenase kinase isoenzyme 4 in rat heart. *Biochem. J.* **329 (Pt 1)**, 197-201 (1998).
19. Wu,P., Inskeep,K., Bowker-Kinley,M.M., Popov,K.M., & Harris,R.A. Mechanism responsible for inactivation of skeletal muscle pyruvate dehydrogenase complex in starvation and diabetes. *Diabetes* **48**, 1593-1599 (1999).
20. Randle,P.J. *et al.* Interactions of metabolism and the physiological role of insulin. *Recent Prog. Horm. Res.* **22**, 1-48 (1966).
21. Randle,P.J. Fuel selection in animals. *Biochem. Soc. Trans.* **14**, 799-806 (1986).

22. Young, M.E. *et al.* Uncoupling protein 3 transcription is regulated by peroxisome proliferator-activated receptor (alpha) in the adult rodent heart. *FASEB J.* **15**, 833-845 (2001).
23. Lock, E.A., Mitchell, A.M., & Elcombe, C.R. Biochemical mechanisms of induction of hepatic peroxisome proliferation. *Annu. Rev. Pharmacol. Toxicol.* **29**, 145-163 (1989).

Chapter 3

Subcellular Localization of Cardiac Malonyl CoA Decarboxylase

Rat heart perfusions were performed by Grant Masson

Neonatal rat cardiac myocytes were isolated by Suzanne Kovacic

3.1 Introduction

Although the role of MCD in the regulation of fatty acid oxidation in the heart is becoming clearer, the subcellular localization of cardiac MCD is still unknown. The confusion regarding subcellular localization of MCD is due in part to the presence of two putative targeting sequences on the MCD protein: (1) an N-terminal positively charged sequence for targeting to the mitochondria and (2) a C-terminal serine-lysine-leucine (SKL) motif or peroxisomal targeting sequence type 1 (PTS-1) for targeting to the peroxisomes ¹.

Another source of controversy exists as to whether two potential translational start sites of MCD encode for two isoforms of MCD with molecular weights of 54.7 kDa and 50.7 kDa. Following translation from the first start site, the 54.7 kDa isoform of MCD may produce a protein which contains both a mitochondrial targeting sequence and a peroxisomal targeting sequence. Whether both sequences are functional and/or competitive, or whether one of the two targeting sequences is removed by a post-translational cleavage event remains unclear. The smaller isoform has been suggested to be either the result of translation from the second internal translational start site or a result of a post-translational cleavage event ². It is unclear if the small isoform of MCD is a result of transport into the mitochondria and cleavage of the N-terminal targeting sequence, as was shown in the goose liver ¹, or whether the 50.7 kDa form is a result of the alternate translational start site that omits the mitochondrial targeting sequence. These scenarios are favored by me over use of the first translational start site with no post-translational modification, since the smaller isoform is the predominant form of MCD in the heart.

The localization of MCD in different organelles in the myocyte may regulate the levels of separate malonyl CoA pools. It has been suggested that malonyl CoA resides in several different cellular compartments, since the concentration of total malonyl CoA in the heart exists at a level that should normally completely inhibit CPT-1 activity³ if the malonyl CoA was entirely cytosolic. Since only cytosolic malonyl CoA inhibits CPT-1⁴⁻⁷ the compartmentalization of malonyl CoA would allow the level of cytosolic malonyl CoA to remain low enough to allow CPT-1 mediated mitochondrial uptake of fatty acids. Therefore, to explain the role of MCD in the regulation of fatty acid oxidation in the heart, MCD must have access to cytosolic malonyl CoA. In addition, no shuttle system for malonyl CoA has been described and the localization of MCD in specific compartments could represent a mechanism for the subcellular control of malonyl CoA and fatty acid oxidation rates.

To study the subcellular mechanism of MCD in the regulation of malonyl CoA, we sought to investigate the localization of MCD in the rat heart by subcellular fractionation of ventricle tissue and in rat neonatal cardiac myocytes using immunocytochemistry and confocal microscopy.

We sought to investigate the **hypothesis** that rat cardiac MCD is a 50.7 kDa mitochondrial enzyme, resulting from translation initiating from the first methionine start site to produce a 54.7 kDa protein imported into the mitochondria and cleaved to the smaller molecular weight form. The **objectives** of this study were therefore three-fold: (i) to determine the localization of MCD in the normal rat heart, (ii) to determine if both putative targeting sequences (mitochondrial and peroxisomal) are capable of controlling

MCD localization, and (iii) to propose a role for MCD in the control of mitochondrial fatty acid oxidation.

3.2 Methods

3.2.1: Subcellular fractionation using an Optiprep™ gradient

Subcellular fractionation of rat hearts was performed using a protocol adapted from Singh and Polous⁸ and Van Veldhoven *et al*⁹. Male Sprague-Dawley rats were sacrificed by sodium pentobarbital injection and the ventricles were rinsed in ice-cold phosphate buffered saline (PBS). The tissue was minced into very small pieces (~1 mm) using a razor blade and homogenized by hand 20-30 times with a glass-teflon homogenizer in 9 mL of homogenization buffer (0.25 M sucrose, 10 mM Tris-HCL and 1 mM EDTA, pH 8.0). Homogenate was spun at 200 x g in a Beckman-Coulter TJ-25 centrifuge for 5 minutes to remove cell debris. The resulting supernatant was then centrifuged at 600 x g for 10 minutes and the pellet ('nuclear fraction') was resuspended in 1 mL of homogenization buffer for analysis. The supernatant was further centrifuged for 10 minutes at 20,500 x g. The pellet ('mixed fraction') was resuspended in 1 mL of buffer for immunoblotting. The supernatant was centrifuged using a Ti60 fixed angle rotor in a Beckman L8-60M ultracentrifuge at 27,000 x g for 60 minutes. The resulting pellet ('microsomal fraction 1') was resuspended as above. The 27,800 x g supernatant was further centrifuged at 110,000 x g for 60 minutes. The resulting supernatant ('cytosolic fraction') and pellet ('microsomal fraction 2') were kept for analysis.

The 'mixed fraction' collected above was layered onto a 15 mL Optiprep™ gradient (20-40%) and centrifuged at 62,000 x g for 40 minutes. Fractions (1.5 mL each) were removed from the top of the gradient to the bottom and kept for analysis. All fractions were sonicated for 10 seconds using a microtip level 3 (Sonifier, Model W185D,

Heat Systems-Ultrasonics, Inc., NY, USA) to lyse the organelles prior to immunoblotting.

3.2.2: Immunoblot analysis of fractions

Protein content of each fraction was assayed using Biorad™ Reagent and 15 µg of protein was loaded onto a 10% SDS polyacrylamide gel. Following electrophoresis at 120 V, samples were transferred to nitrocellulose membrane (2 hours at 100 V) and then blocked overnight in 10% (w/v) milk. Membranes were incubated in primary antibody (in 1% (w/v) milk) for a minimum of 2 hours at room temperature and then washed once (5 minutes) in phosphate buffered saline (PBS) containing 0.05% Tween-20 (PBS-T). Nitrocellulose was washed twice more in PBS (5 minutes each) and then incubated in the appropriate secondary antibody (in 1% (w/v) milk) for 1 hour at room temperature. Membranes were washed twice in PBS-T and then three times in PBS for 5 minutes each.

Application	Primary Antibody or Stain	Duration	Secondary Antibody	Duration
IB	LDH; 1/2000	2h	Donkey Anti-Goat; 1/2000	1h
IB	VDAC-1; 1/500	Overnight	Donkey Anti-Goat; 1/2000	1h
IB	Catalase; 1/1000	Overnight	Goat Anti-Rabbit; 1/2000	1h
IB	H240; 1/1000	Overnight	Goat Anti-Rabbit; 1/2000	1h
IB	Rb Anti-SKL; 1/1000	Overnight	Goat Anti-Rabbit; 1/2000	1h
IB	c-myc; 1/250	Overnight	Goat Anti-Mouse; 1/2000	1h
ICC	H240 Anti-MCD; 1/100	2h	GAR-FITC; 1/400 GAR-TRITC; 1/200	20min 1h
ICC	Gp Anti-SKL; 1/100	2h	DAGp; 1/200	1h
ICC	Rb Anti-SKL; 1/100	2h	GAR-TRITC; 1/200	1h
ICC	Mitotracker Red; 100nM	30min	None	n/a
ICC	Nile Red; 1/1500	10min	None	n/a
ICC	c-myc-FITC; 1/100	2h	None	n/a

Table 3-1: Antibody dilutions and protocols for immunoblotting (IB) and immunocytochemistry (ICC) discussed in this chapter.

Bound antibody was visualized using ECL[®] according to the manufacturer's instructions. Antibody dilutions for immunoblotting and immunocytochemistry (Section 3.2.13) are summarized in Table 3-1.

3.2.3: Isolated working rat heart model for subcellular fractionation

Isolated working male Sprague-Dawley rat hearts were subjected to perfusion as previously described ¹⁰, with a modified Krebs-Henseleit solution containing 5.5 mM glucose, 1.2 mM palmitate, 3% bovine serum albumin, and 100 μ U/mL insulin. The ischemia/reperfusion group was aerobically perfused for 30 minutes, subjected to 30 minutes global ischemia, and re-perfused for a 60 minute period, while control hearts were perfused for a 120 minute time-matched protocol. The spontaneously beating hearts were perfused at an 11.5 mm Hg left atrial preload and an 80 mm Hg aortic afterload. Following the reperfusion period, ventricles were removed from the cannula and placed immediately in ice-cold PBS. Subcellular fractionation was performed as described in Section 3.2.1.

3.2.4: Isolation of pure peroxisomes using a vertical rotor

Peroxisomes were isolated from an adapted protocol originally described by Leighton *et al* ¹¹ and Alexson *et al* ¹². Five male Sprague-Dawley rats (300 to 350 g) were anesthetized with sodium pentobarbital (60 mg·kg⁻¹) and hearts excised. Hearts were perfused with Krebs-Henseleit solution in Langendorff mode for 5 minutes to remove blood from the coronary arteries. Ventricles were immersed in ice-cold sucrose-imidazole buffer (0.25 M sucrose, 3 mM imidazole-HCl pH 7.2, 0.1% v/v ethanol, 1 mM

EDTA) and minced with scissors. Tissue was homogenized for 1-5 strokes (1000 rpm/stroke) in sucrose-imidazole buffer (20% w/v ratio) using a Potter's homogenizer equipped with a serrated Teflon pestle. The homogenate was centrifuged at 2440 x g for 10 minutes at 4 °C and the resulting pellet containing heavy mitochondria was kept for immunoblot analysis. The supernatant was re-centrifuged at 17,100 x g for 20 minutes at 4 °C. The resulting supernatant containing crude microsomes was saved for immunoblot analysis. The 17,100 x g pellet ('light mitochondrial fraction') was worked into a paste with a glass rod and re-suspended in 1.5 mL sucrose imidazole buffer. The entire light mitochondrial fraction was layered gently onto a linear sucrose gradient from 1.15 g/cm³ to 1.27 g/cm³, with a sucrose cushion of 1.32 g/cm³. Isopycnic centrifugation of the light mitochondrial fraction was performed in a VTi50 rotor at $\int \omega^2 dt$ of 6.66x10¹⁰ s⁻¹. A peristaltic pump was used to remove 2 mL fractions from the bottom of the gradient to the top. The resulting fractions were analyzed by Western blotting for MCD, the peroxisomal marker catalase, and the mitochondrial marker VDAC-1. Fractions were analyzed by immunoblotting as described in Section 3.2.2 and Table 3-1.

3.2.5: Production of MYC-labelled MCD constructs by PCR

MCD cDNA constructs were made by PCR using gene-specific MCD primers derived from the rat cDNA sequence. Some of the PCR primers also included nucleotides that encode for 10 amino acids of the MYC tag. Table 3-2 provides the sequence of the primers used for each specific construct in 5'→3' order with the MYC tag in bold text. Constructs were produced by PCR with Platinum Pfx DNA Polymerase (Invitrogen) using the following PCR program:

94 °C 2 min
x 1 cycle

94 °C 30 sec
60 °C 1 min
68 °C 1 min 30 sec
x 35-40 cycles

Construct	Forward Strand Primer	Reverse Strand Primer
MYC-MCD _{fl}	GGA TCC ACC ATG GAA CAA AAA CTC ATC TCA GAA GAG GAT CTG AAT AGA GGC TTG	TCC CTA GAG TTT GCT GTT GCT CTG
MCD _{fl} -MYC	GAC ATG AGA GGC TTG GGG CCA AGC TTG	GGA ATT CTA ATT CAG ATC CTC TTC TGA GAT GAG TTT TTG TTC GAG TTT GCT GTT GCT
MYC-MCD _{tr}	GGA TCC ACC ATG GAA CAA AAA CTC ATC TCA GAA GAG GAT CTG AAT CAC GAG CTG CTA CGG	TCC CTA GAG TTT GCT GTT GCT CTG
MCD _{tr} -MYC	ATG CAC GAG CTG CTA CGG CGA GCC	GGA ATT CTA ATT CAG ATC CTC TTC TGA GAT GAG TTT TTG TTC GAG TTT GCT GTT GCT

Table 3-2: PCR primer sequences for the development of MYC-tagged MCD constructs.

The expression vector constructs and MCD fusion proteins were named according to the following scheme: MCD_{fl} denotes full-length MCD of 54.7 kDa; MCD_{tr} denotes the truncated forms of MCD using the second translational start site; MYC-MCD_x denotes an N-terminal MYC tag, while MCD_x-MYC denotes a C-terminal MYC tag.

3.2.6 Preparation of MYC-tagged constructs for sub-cloning into the mammalian expression vector pcDNA 3.1(+)

Constructs were sub-cloned into a TOPO vector using either the TA-Cloning Kit (Invitrogen) or the pZero-Blunt Cloning Kit (Invitrogen) and transformed into One-shot TOP10 cells (Invitrogen), as described in the manufacturer's instruction manual. MYC-tagged MCD fragments were excised from the TOPO vector using the BamH1/EcoR1 restriction enzyme sites for MYC-MCD_{tr}, MYC-MCD_{fl}, MCD_{tr}-MYC, and with EcoR1 alone for MCD_{fl}-MYC. Plasmids were gel-purified with the QIAEX II gel extraction kit using the manufacturer's instructions. The mammalian expression vector pcDNA3.1(+) was also digested with BamH1/EcoR1 (or EcoR1 only) followed by a dephosphorylation step for one hour with alkaline phosphatase (Roche). The plasmid was gel-purified using the QIAEX II system as per manufacturer's instructions.

3.2.7: Ligation and transformation of MYC-tagged constructs in pcDNA3.1(+)

The purified vector and insert were ligated together as follows: 50 ng pcDNA3.1(+), 150 ng MYC-MCD insert, 2 μ L 10 x ligation buffer, 1 μ L T4 ligase and sterile water to a final volume of 20 μ L. Ligation mix was incubated for 1 hour at room temp and then transformed into XL-1 Blue super-competent cells (Stratagene) as follows:

20 μL of cells were thawed and transferred to 15 mL Falcon polypropylene tubes and 2 μL of ligated DNA was added. The mixture was stirred gently with a pipette tip and incubated on ice for 20 minutes. Cells were subjected to heat shock for 30 seconds at 42 $^{\circ}\text{C}$ and placed on ice for 2 minutes. Following heat shock, the cells were grown for one hour at 37 $^{\circ}\text{C}$ in 250 μL of SOC media and shaken gently in a dry shaking incubator at 80 rpm. Transformants were plated onto LB-Agar plates containing 50 $\mu\text{g}/\text{mL}$ Ampicillin (for TA-cloning kit) or 40 $\mu\text{g}/\text{mL}$ Kanamycin (pZero Blunt Kit) and grown overnight at 37 $^{\circ}\text{C}$ in a shaking incubator (250 rpm). Isolated colonies were chosen at random and grown in 3.5 mL cultures overnight. Approximately 1.5 mL of the culture was used for plasmid isolation using the Qiaprep Mini Spin Kit as suggested by the manufacturer's protocol. Plasmids were digested with BamH1/EcoR1 to determine insert size and SacI to determine orientation of the insert. Plasmids containing the correct insert were sequenced by the Biochemistry DNA Core Lab Facility and stocks were frozen down at -80 $^{\circ}\text{C}$ in 15% glycerol. Large scale plasmid preps were used to isolate large amounts of each plasmid for transfections. 150 mL cultures were grown overnight at 37 $^{\circ}\text{C}$; 250 rpm and plasmid was isolated using the Qiagen Plasmid Maxi kit as per the manufacturer's instructions.

3.2.8: Transfection of MYC-tagged MCD constructs into CHO cells and analysis by immunoblotting

Mutant MCD constructs were transfected into CHO cells (90% confluent) using Fugene-6 transfection reagent (Roche). Fugene-6 reagent (6 μL) was pre-incubated in 94 μL serum-free OptiMEM media for 5 minutes at room temperature. The

OptiMEM/Fugene-6 mixture was added dropwise to approximately 1 μg of plasmid DNA and incubated at room temperature for 15 minutes. During this period, cells were washed three times with Hank's Balanced Salt Solution and given fresh Hams-F12 media supplemented with 10% serum. The transfection mixture was added dropwise to cells and incubated for 48 hours at 37 °C in a 95% air/5% CO₂ incubator. After 48 hours, cells were prepared for immunoblotting as follows: cells were washed three times with 2 mL PBS and then scraped in 150 μL PBS. The cells were sonicated for 10 seconds at microtip level 3 of a probe sonicator (Sonifier, Model W185D, Heat Systems-Ultrasonics, Inc., NY, USA). Samples (20 μL) were boiled and run on 10% SDS polyacrylamide gels for immunoblotting, as described in Section 3.1.2. Antibody dilutions for immunoblotting are shown in Table 3-1.

3.2.9: Determination of MCD construct activity in CHO Cells

MCD activity was measured using a fluorometric assay, which determines the production of acetyl CoA by coupling it to the malate dehydrogenase and citrate synthase reactions^{2, 13}. The production of acetyl CoA by MCD removes oxaloacetate to form citrate, thus allowing the malate dehydrogenase reaction to proceed. The malate dehydrogenase reaction produces NADH, which is measured by excitation at 340 nm and emission at a wavelength of 460 nm.

The assay buffer was made as a 1.5 mL stock and contained 0.02 M Tris-base (pH 8.0), 0.2 mM dithioerythritol, 2 mM L-malic acid, 0.17 mM NAD⁺, 0.136 mM malonyl CoA, 11 U malate dehydrogenase, 0.44 U citrate synthase. For the assay 245 μL of assay buffer was added to each well and the baseline production of NADH was sampled for 5

minutes to ensure a stable, equilibrium level of NADH fluorescence in the assay. Cells were scraped as described in Section 3.2.8 and 25 μ L samples were added to the appropriate wells in duplicate. The plate was mixed briefly and the fluorescence read for 5 minutes using a Shimadzu RF-5000 spectrofluorimeter. Typically the reaction reached a plateau at approximately 2 minutes; therefore measurements were taken at the 2 minute time point. Statistical analysis was performed using a one-way ANOVA with a Tukey post-hoc test.

3.2.10: Isolation of neonatal rat cardiac myocytes

Hearts from 1 to 2-day-old neonatal Sprague-Dawley rat pups were isolated and placed in ice-cold phosphate buffered saline (PBS). After repeated rinsing with PBS, the atria were removed and the ventricles were minced with scissors. The minced tissue was washed three times in ice-cold PBS and then placed in a T-25-cm² tissue culture flask containing 19.5 ml of ice-cold PBS, 0.025% DNase (w/v), 0.10% collagenase (w/v), and 0.05% trypsin (w/v). The tissue was digested on a rotary shaker at 37 °C for 20 minutes. After digestion the tissue was centrifuged at 114 x g for one minute at 4 °C in 20 ml of DF20 media, 20% fetal bovine serum, and 50 μ g/ml gentamycin. The supernatant was discarded and the pellet was subsequently added to DNase/collagenase/trypsin buffer for further digestion at 37 °C for 20 minutes. After a second digestion the tissue was again transferred into a 50 ml falcon tube with 20 ml of DF20 media and centrifuged at 114 x g for one minute at 4 °C. This step was repeated twice. After the final digestion the supernatant fractions were pooled and centrifuged at 300 x g for 7 minutes at 4 °C. The resulting pellet was resuspended in 10 ml of plating media (DF20 media, 5% fetal bovine

serum, 10% horse serum, 50 µg/ml gentamycin) and incubated at 37 °C in a T-25-cm² tissue culture flask for 60 minutes. The supernatant was removed and placed in a fresh T-25-cm² tissue culture flask for an additional 60 minutes. This step was repeated twice. After serial plating, the resulting pellet was resuspended in plating media and cultured as described in Section 3.2.11.

3.2.11: Culture of neonatal rat cardiac myocytes

For Immunoblotting: Cells were plated on 6-well Primaria dishes (Falcon) at a density of $1.8\text{--}2.0 \times 10^6$ cells/well and incubated overnight at 37 °C to allow cells to adhere to the dish. Myocytes were washed three times in Hank's Balanced Salt Solution and cultured in 2 mL DMEM-F12 media (Invitrogen) containing 50 µmol/mL gentamycin and 1 x ITS (insulin, transferrin and selenium) buffer or 10% fetal bovine serum.

For Immunocytochemistry: 1 mm thick glass coverslips (22 mm x 22 mm square) were rinsed in 95% ethanol and sterilized by passage through a Bunsen burner flame. Sterile coverslips were laid gently into each well of a 6-well dish (1 coverslip/well). Wells (including coverslips) were coated with 1 mL Fibronectin (1 mg Fibronectin (Sigma) in 80 mL 0.02% gelatin; autoclaved) overnight at 37 °C. Neonatal rat cardiac myocytes were plated at $0.9\text{--}1.0 \times 10^6$ cells/well (half-density) and cultured in DMEM-F12 supplemented with gentamycin and ITS buffer or 10% fetal bovine serum.

3.2.12: Transfection of MYC-tagged MCD constructs into neonatal rat cardiac myocytes

Tagged MCD constructs were transfected into cultured neonatal rat cardiac myocytes using Fugene-6 (Roche) reagent. Fugene-6 reagent (6 μ L) was pre-incubated in 94 μ L serum-free DMEM media for 5 minutes at room temperature. The DMEM/Fugene-6 mixture was added dropwise to approximately 1-2 μ g of plasmid DNA and incubated at room temperature for 15 minutes. During this period, cells were washed three times with Hank's Balanced Salt Solution and given 2 mL of fresh DMEM-F12 media supplemented with ITS buffer. The transfection mixture was added dropwise to cells and incubated for 48 hours at 37°C in a 95% air/5% CO₂ incubator.

3.2.13: Immunocytochemistry of neonatal rat cardiac myocytes

After a 48 hour transfection period, live cells were stained with 100 nM Mitotracker Red for 30 minutes at 37 °C. Cells were washed three times in PBS and fixed with ice-cold (-20 °C) methanol for 5 minutes on ice. Cells were then permeabilized with 1 x TA-PBS (0.05% Triton X-100, 0.05% BSA in 1x PBS) for one minute and washed three times in PBS. The coverslips were blocked with 5% FBS for 20 minutes at room temperature and washed once in PBS. Myocytes were further incubated in H240 MCD antibody for 2 hours, Anti-SKL antibody (against the peroxisomal targeting sequence type 1 (PTS-1)) for 2 hours (for select experiments) and the corresponding fluorescent secondary antibodies for 1 hour each. Nile Red was applied for 10 minutes as required. Cells were rinsed three times in PBS and coverslips were mounted onto slides using Prolong Anti-Fade reagent (Molecular Probes) as per manufacturer's instructions. Slides

were placed in a dark drawer overnight and excess Prolong mounting media was removed using 70% ethanol. Clear nail-polish was applied around the edges of the slide to prevent shrinking of the mounting media and slides were stored at room temperature for short periods (<3 weeks) or at -20 °C for long-term storage.

3.2.14: Visualization of MCD localization using confocal microscopy

Fluorescence was visualized with a Zeiss 510 confocal microscope system available in the Department of Cell Biology (Room 5-05 Medical Sciences Building). This system uses a Zeiss inverted microscope coupled to three one-photon lasers. Green fluorescence was excited using an Argon laser at a wavelength of 488 nm, while red fluorescence was excited using a Helium-Neon laser at a wavelength of 543 nm. A Plan-Neofluar 40x/1.3 oil objective was used for every experiment. Zeiss LSM Image Software was used to store pictures, add scale-bars and maintain databases of each experiment.

3.3 Results

3.3.1: MCD protein localization by subcellular fractionation of rat heart tissue

Rat ventricles were fractionated into nuclear, microsomal, cytosolic and mixed fractions as described in Section 3.2.1 and Figure 3-1. The mixed fraction was centrifuged through an Optiprep™ gradient in order to separate mitochondria from peroxisomes by the mass of the organelle. Immunoblots of lactate dehydrogenase (LDH), catalase, and the voltage dependent anion channel (VDAC-1) were used as markers for the cytosolic, peroxisomal and mitochondrial fractions, respectively. Figure 3-2 shows the purity of the fractions as assessed by these markers and the localization of MCD. Although this fractionation method allowed a good separation of cytosol from the organelles, the presence of both catalase and VDAC-1 in the same fractions indicated some contamination occurred between the mitochondrial and peroxisomal fractions. The majority of the MCD protein was in the microsomal and mixed fractions. However, we were unable to separate mitochondria from peroxisomes effectively. Therefore, this method does not allow for absolute confirmation of MCD localization in the heart.

Due to the adequate separation of the cytosolic and mitochondrial-enriched fractions we could use these fractions to investigate the translocation of MCD from the large organelles to the cytosol. Preliminary results from our laboratory suggested that AMPK activation caused a translocation of MCD from the mitochondria to the cytosol. Therefore using these fractionation methods we sought to investigate the localization of MCD in response to ischemia/reperfusion when AMPK activity is high. Rat hearts were subjected to a 30 minute aerobic period, 30 minutes ischemia followed by a 60 minute reperfusion period using the isolated working heart model (Figure 3-3). The perfusate

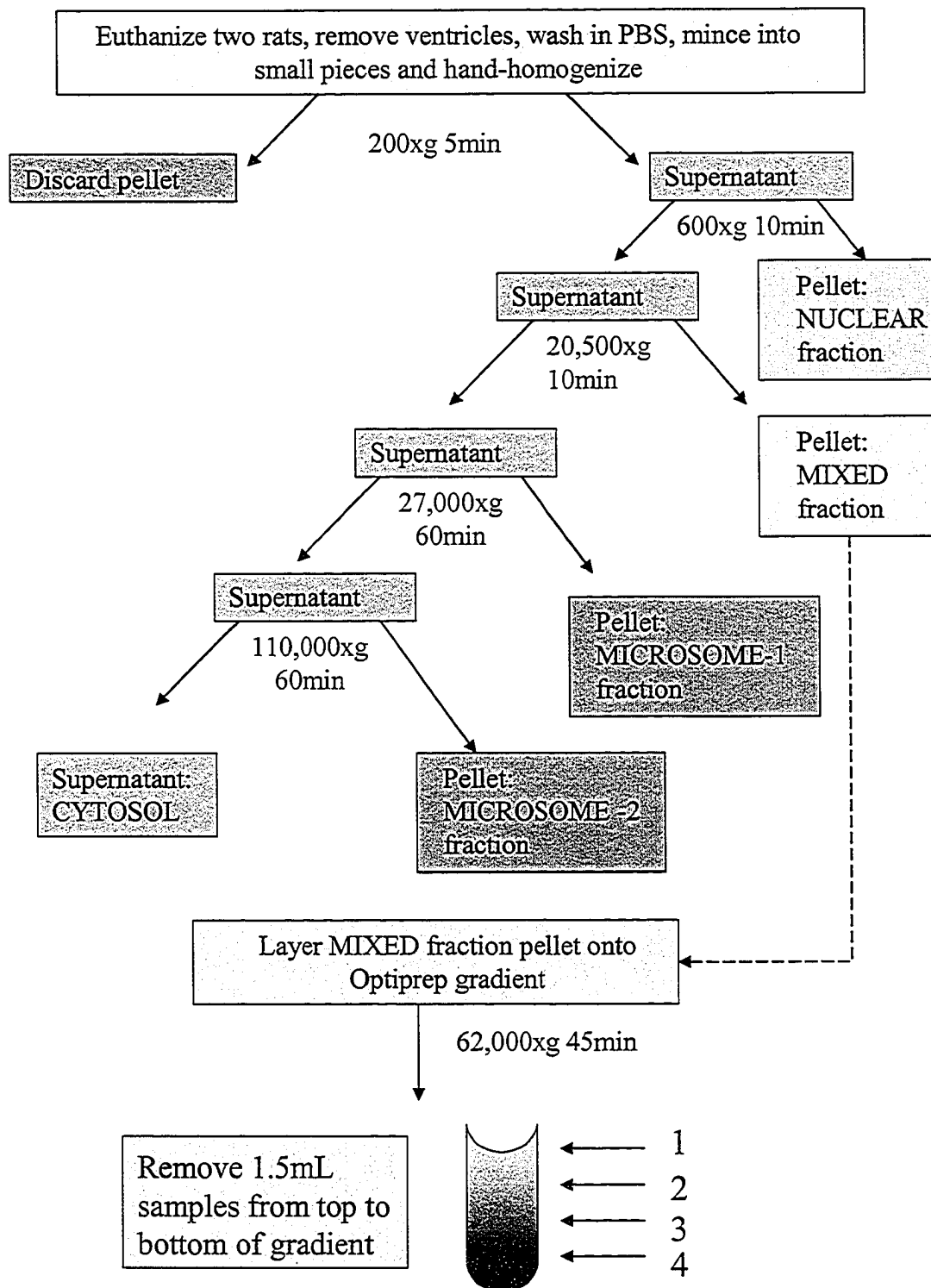


Figure 3-1: Subcellular fractionation protocol to isolate nuclear, microsomal, cytosolic, mitochondrial and peroxisomal fractions for the purpose of determining MCD localization.

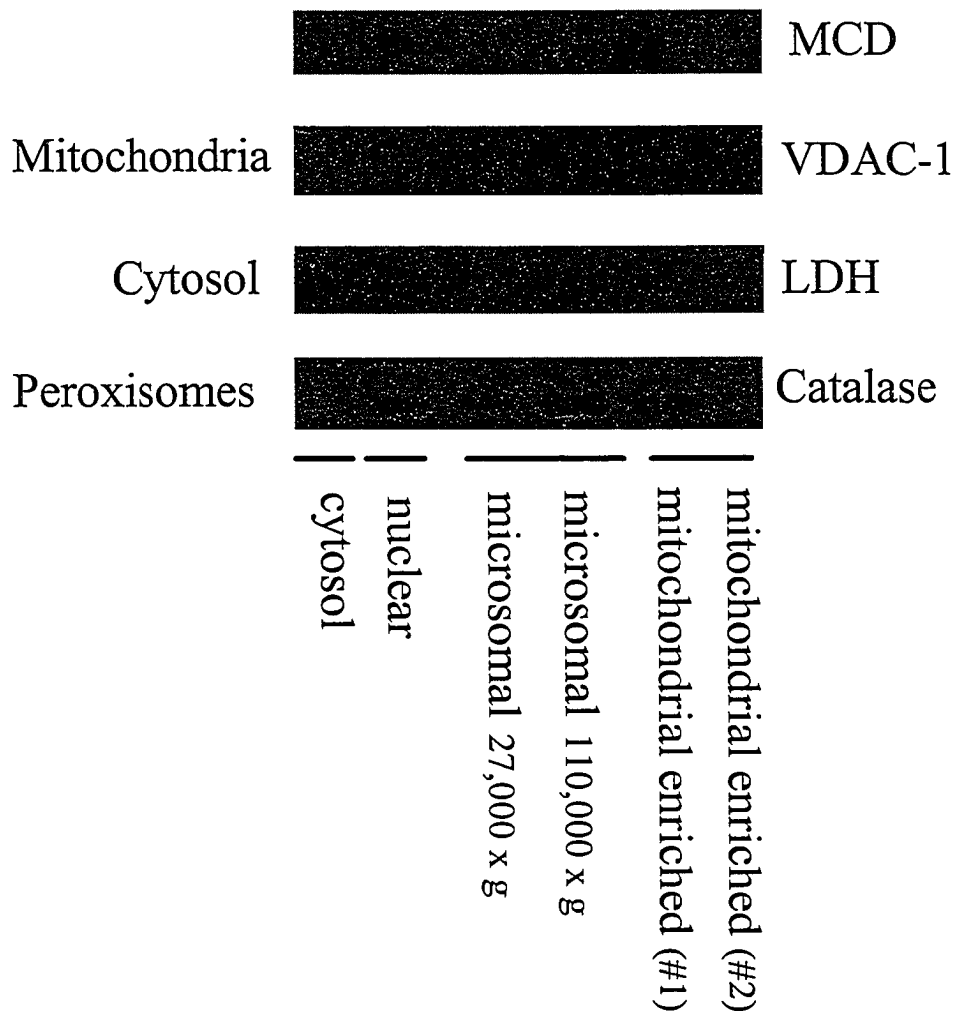
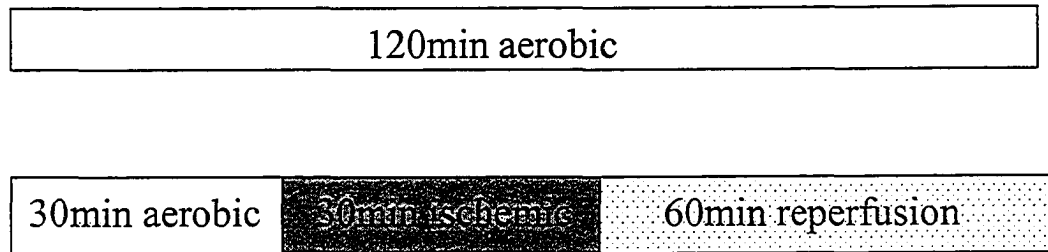


Figure 3-2: Immunoblots of the cytosol, nuclear, microsomal, and mitochondrial-enriched fractions. Lactate dehydrogenase (LDH) was used to assess purity of the cytosolic fraction; Voltage-dependent anion channel (VDAC-1) was used for mitochondrial purity and Catalase was used for peroxisomal purity. The localization of MCD was assessed by immunoblotting and was detected in both the nuclear and mitochondrial-enriched fraction.

(a)



(b)

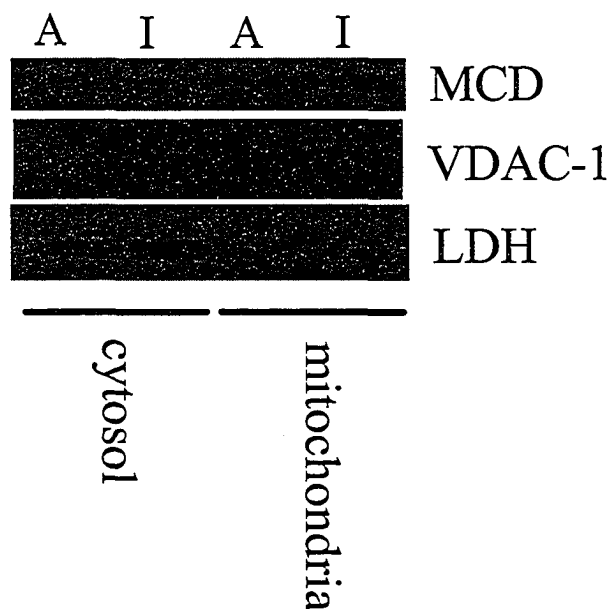


Figure 3-3: Lack of translocation of MCD in response to ischemia/reperfusion. (a) Perfusion protocol for Ischemia/Reperfused rat hearts and time-matched aerobic control hearts, (b) Immunoblots of the cytosolic and mitochondrial fractions for VDAC-1 (mitochondrial marker), LDH (cytosolic marker) and MCD in both aerobic (A) and ischemia/reperfusion (I) rat hearts.

contained 1.2 mM palmitate (high fat) and 5.5 mM glucose. Fractionation of the ventricles was performed following perfusion and samples were assessed by immunoblotting. Fractional purity of the cytosol was determined by the presence of LDH in the fraction and the absence of VDAC-1 (mitochondrial marker). Similarly, the mitochondrial fractional purity was determined by the presence of VDAC-1 but the absence of LDH. MCD was present in the mitochondrial-enriched fraction, but was not abundant in the cytosolic fraction. In addition, there was no difference in localization between these two compartments in response to ischemia/reperfusion. Therefore in this model of ischemia/reperfusion, MCD does not translocate from the mitochondria to the cytosol or vice versa.

In order to address the possibility of MCD localization to peroxisomes we attempted to isolate pure peroxisomes by adapting a protocol used for liver tissue ¹¹. The protocol is described in Section 3.2.4 and Figure 3-4. The major difference between the isolation of pure peroxisomes and the previous subcellular fractionation technique was that the peroxisomes are purified by density rather than by mass of the organelle. Using this isopycnic centrifugation technique we were able to isolate a pure peroxisomal fraction as indicated in Figure 3-5. However, there may be a small amount of contaminating VDAC-1 and therefore mitochondria in our peroxisomal preparation. This contamination was attributed to the difficulty in isolating peroxisomes from mitochondria in heart tissue and suggests that in the normal rat heart there is little difference in the size of mitochondria and peroxisomes. However, this protocol was an improvement over the previous subcellular fractionation protocol and suggests that a large amount of MCD is

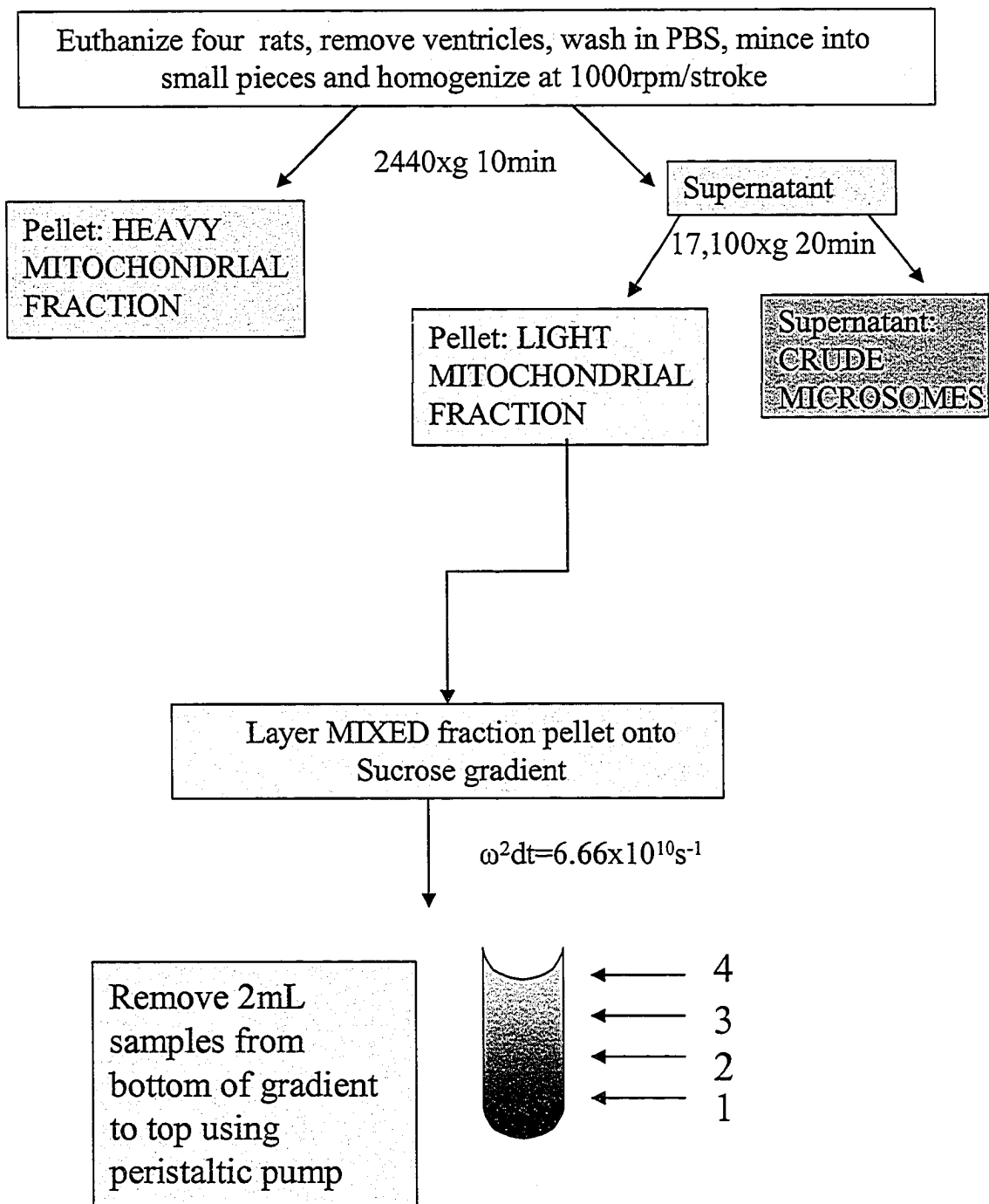


Figure 3-4: Subcellular fractionation for isolation of pure peroxisomes using a vertical rotor and a linear sucrose gradient.

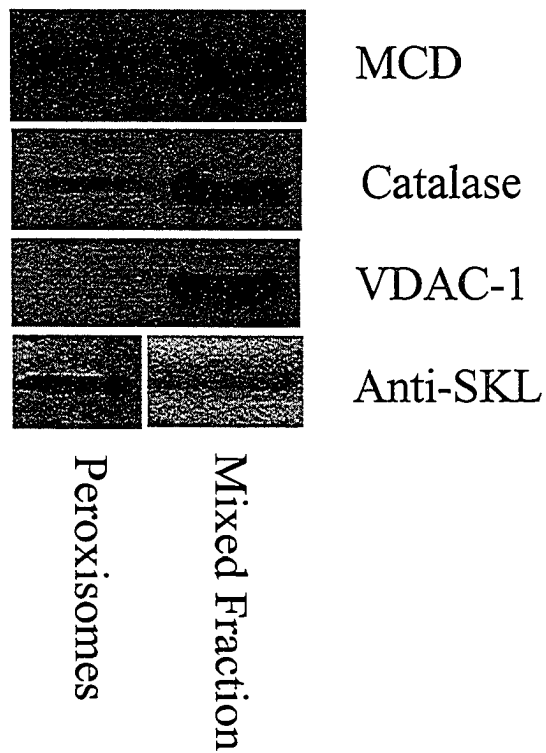


Figure 3-5: (a) Immunoblots of peroxisomal markers (catalase, anti-SKL) and mitochondrial markers (VDAC-1) to assess fractional purity of peroxisomal fraction in order to determine localization of MCD

present in the peroxisomal fraction that cannot be attributed to possible contamination between fractions.

In order to further confirm this peroxisomal localization of MCD immunocytochemistry was performed on isolated neonatal rat cardiac myocytes to determine the localization of MCD.

3.3.2: Localization of endogenous MCD in isolated neonatal rat cardiac myocytes

Cells were transfected and treated as described in Sections 3.2.11 to 3.2.13. The confocal set-up for fluorescence detection is depicted in Figure 3-6. A band pass filter between 500-530 nm was used to detect emission of the fluorescein (green) fluorescence, while a long pass filter was used to detect red fluorescence from emission beyond a wavelength of 560 nm. The third channel was not used, nor was transmitted light measured in these samples. The samples were scanned with an optimal pinhole size of 1, which allowed an optical slice of approximately 0.9-1.0 μm thickness. The background level of fluorescence was determined by incubation of a control group of cells with the antibody pre-serum and the appropriate fluorescent secondary antibody. The confocal detector gain was not set within this range of fluorescence to avoid detection of background fluorescence.

The co-localization of the MCD antibody with fluorescent markers in untransfected myocytes treated with ITS buffer is shown in Figure 3-7. The top panel represents co-localization of the green MCD fluorescence with the mitochondrial marker Mitotracker Red, while the bottom panel shows co-localization of the red MCD

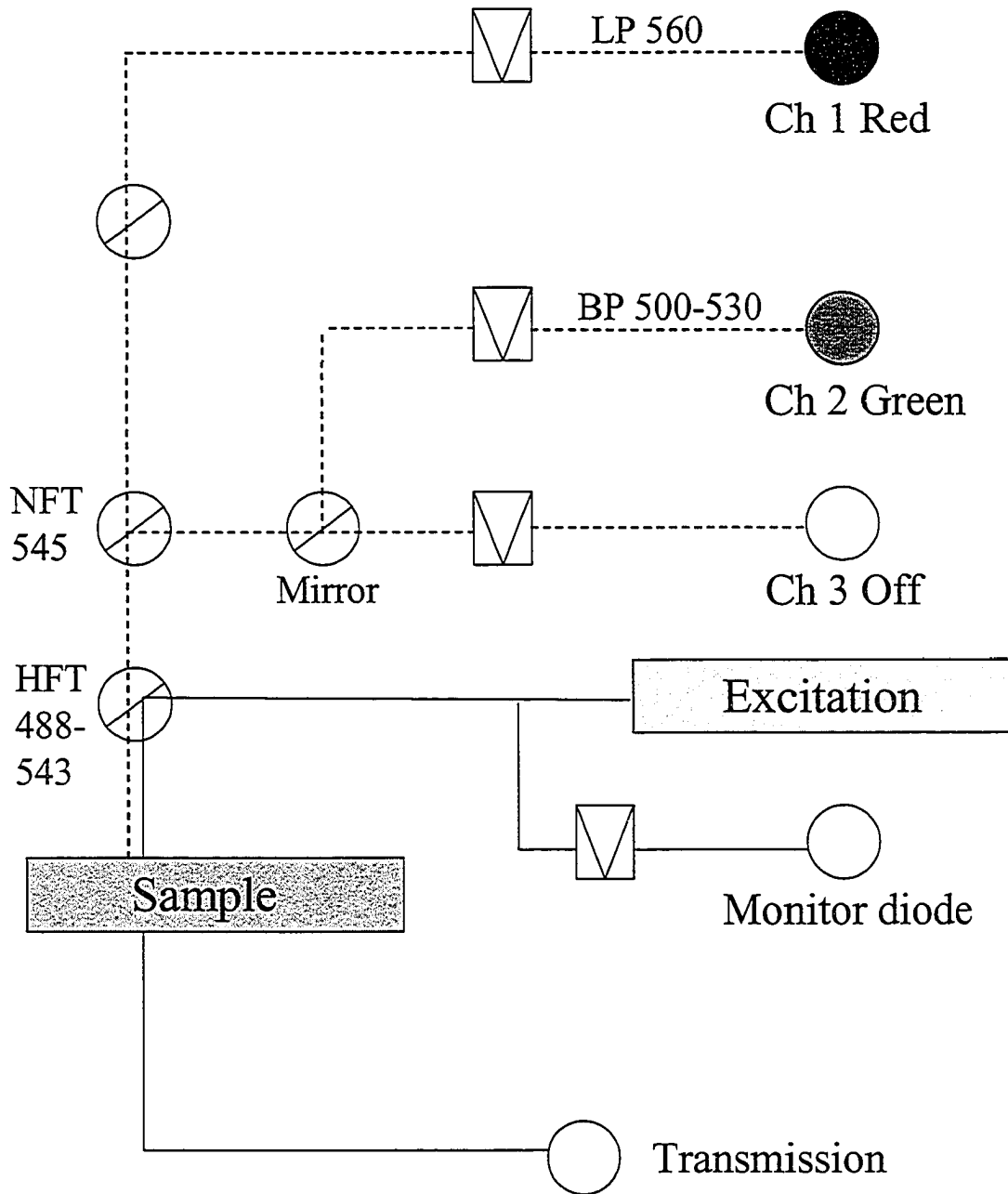


Figure 3-6: Confocal configuration of Zeiss 510 confocal microscope system for immunocytochemistry of endogenous MCD and transfected MCD constructs.

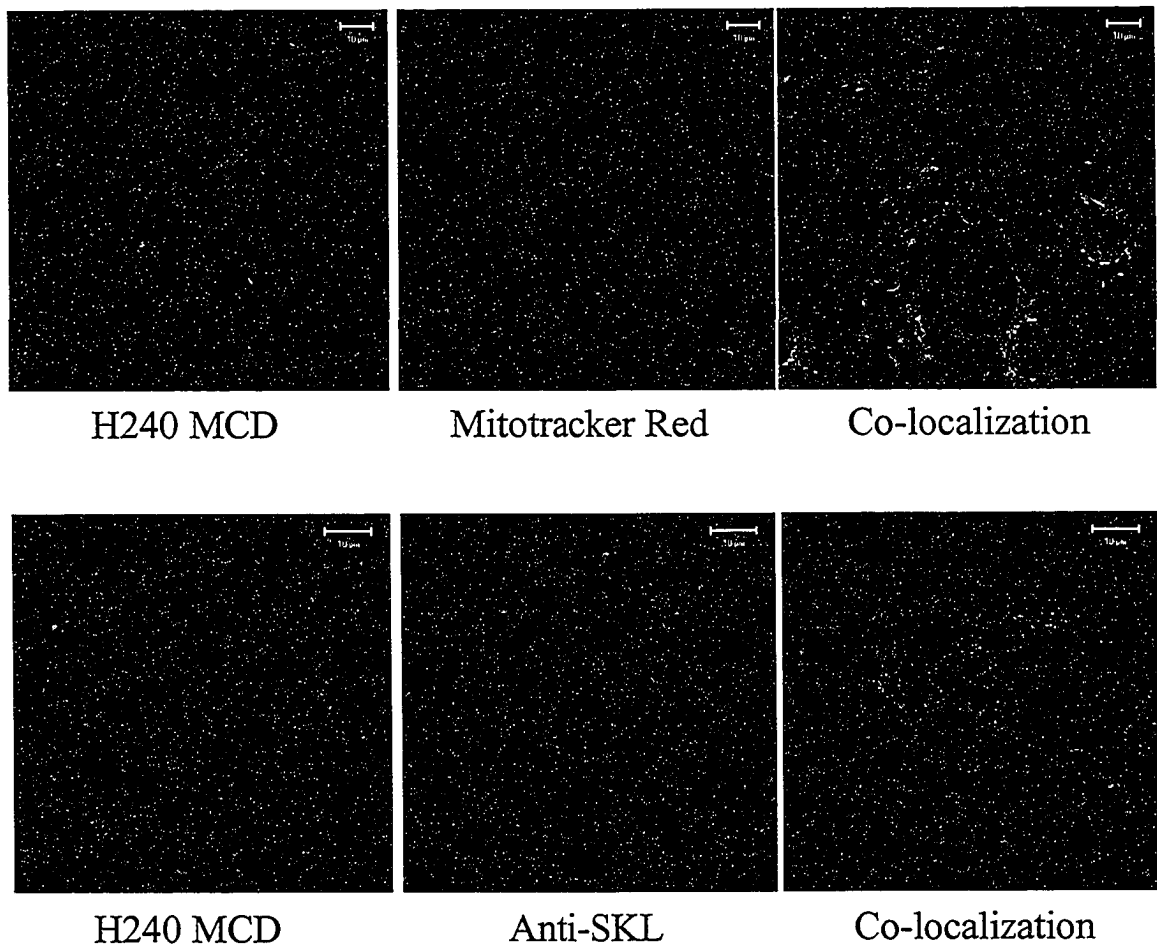


Figure 3-7: Immunocytochemistry of endogenous MCD in neonatal rat cardiac myocytes grown in ITS buffer, showing co-localization with mitochondria (upper panel) and peroxisomes (lower panel). Scale bars shown on each picture are 10µm in length. Representative pictures are shown of n=6 separate neonatal myocyte isolations for both mitochondrial and peroxisomal co-localization.

fluorescence with the green peroxisomal antibody. Although MCD appeared to co-localize with both mitochondria and peroxisomes, the fluorescence of the MCD signal was hardly above the background fluorescence. Therefore in an attempt to heighten the MCD fluorescent signal, cells were further permeabilized with varying concentrations of digitonin after fixation. Treatment with digitonin had no effect on the signal strength of MCD (data not shown). Similarly, a group of cells was treated with 100 μ M WY 14,643 (PPAR α agonist) to increase MCD expression in the myocyte, but this treatment had no effect on MCD protein expression or signal strength with immunocytochemistry (data not shown). A group of cells were then treated with 10% fetal bovine serum, which contains several non-specific growth factors. The signal strength of MCD was much stronger when cells were incubated in serum for 48 hours as depicted in Figure 3-8.

The top panel of Figure 3-8 shows the localization of MCD in punctates within the myocyte (green fluorescence) that do not co-localize with Mitotracker Red staining of mitochondria. This suggests that there is very little mitochondrial MCD in these myocytes. The bottom panel of Figure 3-8 shows the co-localization of MCD with a peroxisomal marker and indicates that the majority of the MCD in these cells is present in the peroxisomes.

Due to this large increase in MCD signal strength in myocytes growing in 10% fetal bovine serum, MCD expression was determined by immunoblotting. When equal protein was loaded onto the gel, there was no difference in MCD expression compared to actin, as shown in Figure 3-9. However, the total protein content (measured using a BioRad™ protein assay) of serum-treated neonatal rat cardiac myocytes was much higher than cells incubated in ITS buffer. This suggests that an overall increase in protein

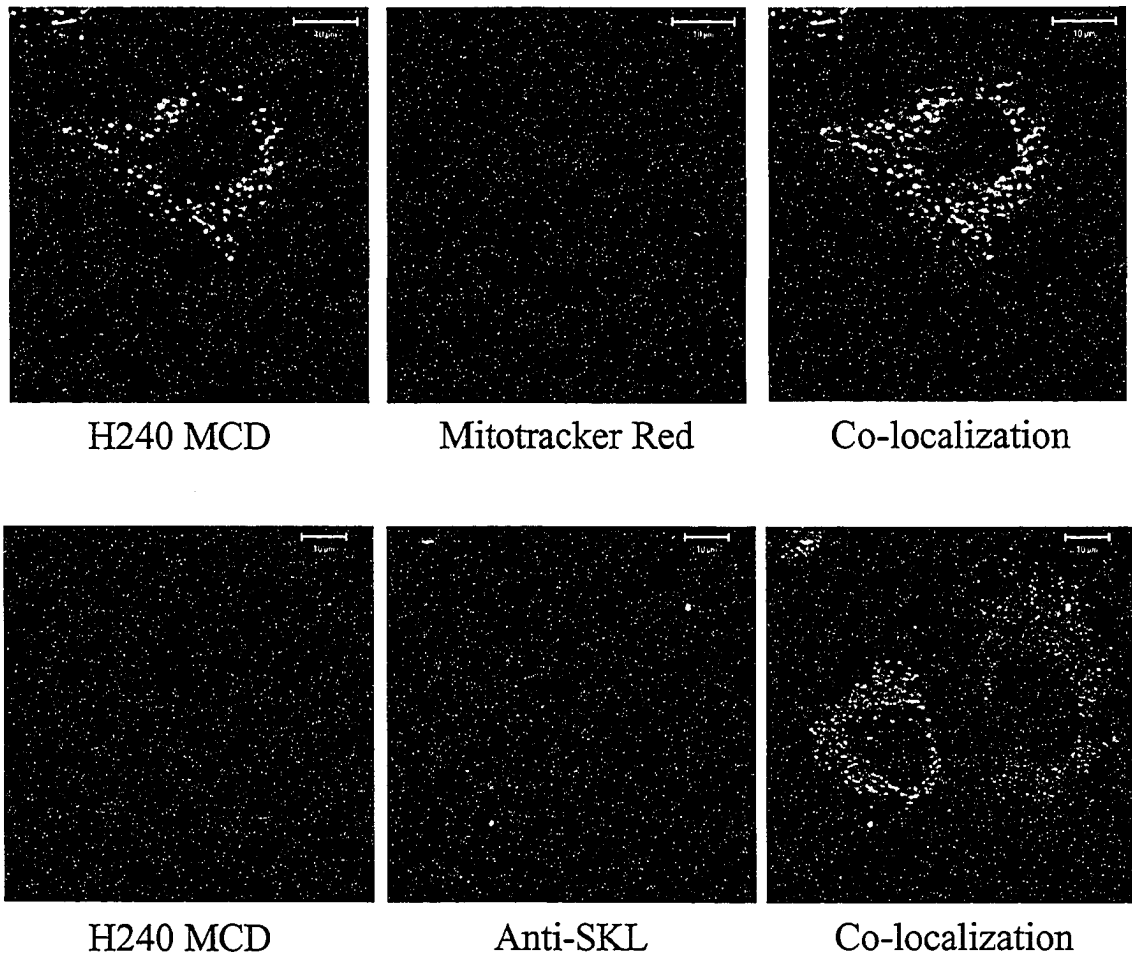


Figure 3-8: Immunocytochemistry of endogenous MCD in neonatal rat cardiac myocytes grown in 10% fetal bovine serum, showing co-localization with mitochondria (upper panel) and peroxisomes (lower panel). Scale bars shown on each picture are 10µm in length. Representative pictures are shown of n=6 and n=8 separate neonatal myocyte isolations for mitochondrial and peroxisomal co-localization, respectively.

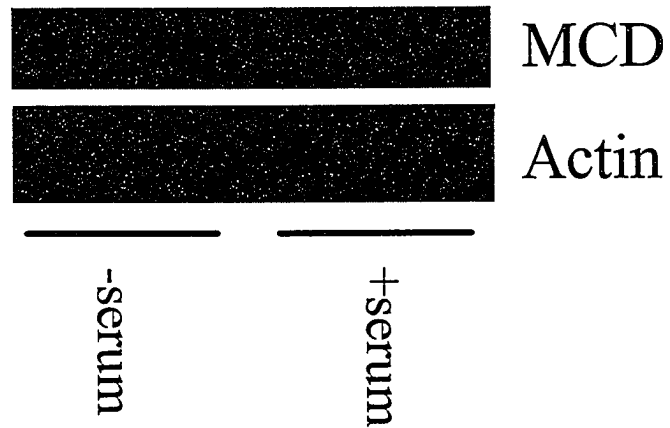


Figure 3-9: Growth of neonatal cardiac myocytes in ITS buffer (-serum) or in 10% fetal bovine serum (+serum) had no effect on MCD expression when compared to actin. Representative blot is shown for n=3 separate neonatal myocyte isolations.

synthesis may contribute to the signal strength rather than a change in MCD expression alone.

MCD was localized to distinct punctates and in order to rule out these punctates as lipid droplet accumulation, myocytes were treated with Nile Red (a neutral lipid and cholesteryl ester marker). Figure 3-10 (bottom panel) indicates that there are a few lipid droplets present in the serum-treated myocytes but the droplets did not co-localize with green MCD fluorescence. The top panel of cells treated in ITS buffer show only background red fluorescence and no lipid droplets were observed using microscopy. This suggests that the punctates observed with the MCD antibody are indeed peroxisomal.

Taken together, the strong co-localization of MCD fluorescence with the peroxisomal marker suggests that endogenous MCD of cultured neonatal rat cardiac myocytes is present mainly in the peroxisomes. MCD was not detected in the mitochondria of neonatal rat cardiac myocytes.

3.3.3: Transfection, intracellular processing and activity measurements of MYC-tagged MCD constructs in CHO cells

The peroxisomal distribution of MCD was unexpected since MCD has previously been suggested to be a mitochondrial protein^{14, 15}. Therefore, we sought to investigate if the mitochondrial targeting sequence of MCD is functional. Similarly, we investigated the control of MCD localization by the peroxisomal targeting sequence.

The localization of MCD was explored using MYC-MCD fusion proteins designed to alter MCD localization. The MCD protein was tagged with a 10 amino acid MYC tag at the N-terminus to mask the mitochondrial targeting sequence. The MYC tag

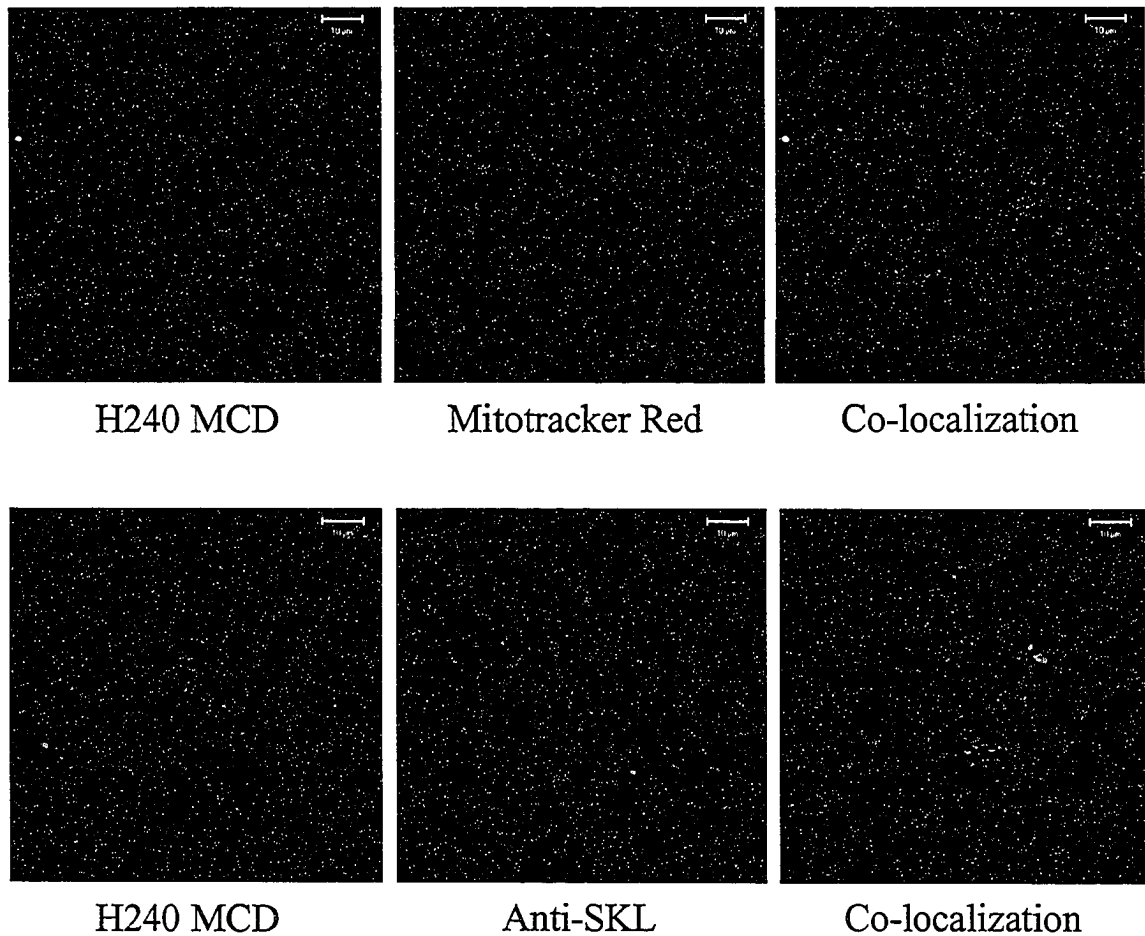


Figure 3-10: Nile Red analysis of lipid accumulation in cells treated with or without serum. Growth of neonatal cardiac myocytes in 10% fetal bovine serum (lower panel) caused accumulation of lipid in the cytosol as evidenced by Nile Red staining, while growth of myocytes in ITS buffer (upper panel) did not produce cytosolic lipid droplets. Representative pictures are shown of n=4 and n=6 separate neonatal myocyte isolations for treatment with ITS buffer or serum, respectively.

was also placed at the C-terminus of another MYC-MCD fusion protein to mask the peroxisomal targeting sequence. These MYC tags were placed on the long form of MCD (54.7 kDa), as well as the short form of MCD (50.7 kDa) to investigate localization. Production of the long and short isoform of MCD was achieved by use of the first and second translational start sites of MCD respectively. Figure 3-11a shows the putative targeting sequences and translational start sites of MCD. The four MCD constructs developed by PCR and the location of the MYC tags are shown in Figure 3-11b.

Following construction, each of the MCD expression vectors were transfected separately into Chinese hamster ovary (CHO) cells to determine intracellular processing of the protein produced. The two smaller MCD constructs (MYC-MCD_{tr} and MCD_{tr}-MYC) produce a 50.7 kDa protein, as expected. The MYC tags on both of these constructs are not removed by a cleavage event and as evidenced by the Anti-SKL antibody only the MYC-MCD_{tr} construct has an open SKL sequence. Therefore, the MYC tag is effective in masking the peroxisomal targeting sequence.

The larger two constructs produced the expected 54.7 kDa protein. However the MYC-MCD_n construct also produced a smaller protein less than 50 kDa. This smaller protein did not contain a MYC tag suggesting that the protein was either cleaved or produced using the second ATG start site. The 54.7 kDa MYC-MCD_n protein retained the exposed SKL sequence, while the smaller protein retained only a portion suggesting that a partial cleavage event may play a role in processing of this construct.

The MCD_n-MYC construct produced the two isoforms of MCD observed in rat islet cells (54.7 kDa and 50.7 kDa). Both proteins retained the MYC tag but have no exposed SKL sequence, suggesting that a cleavage event did not occur to remove the

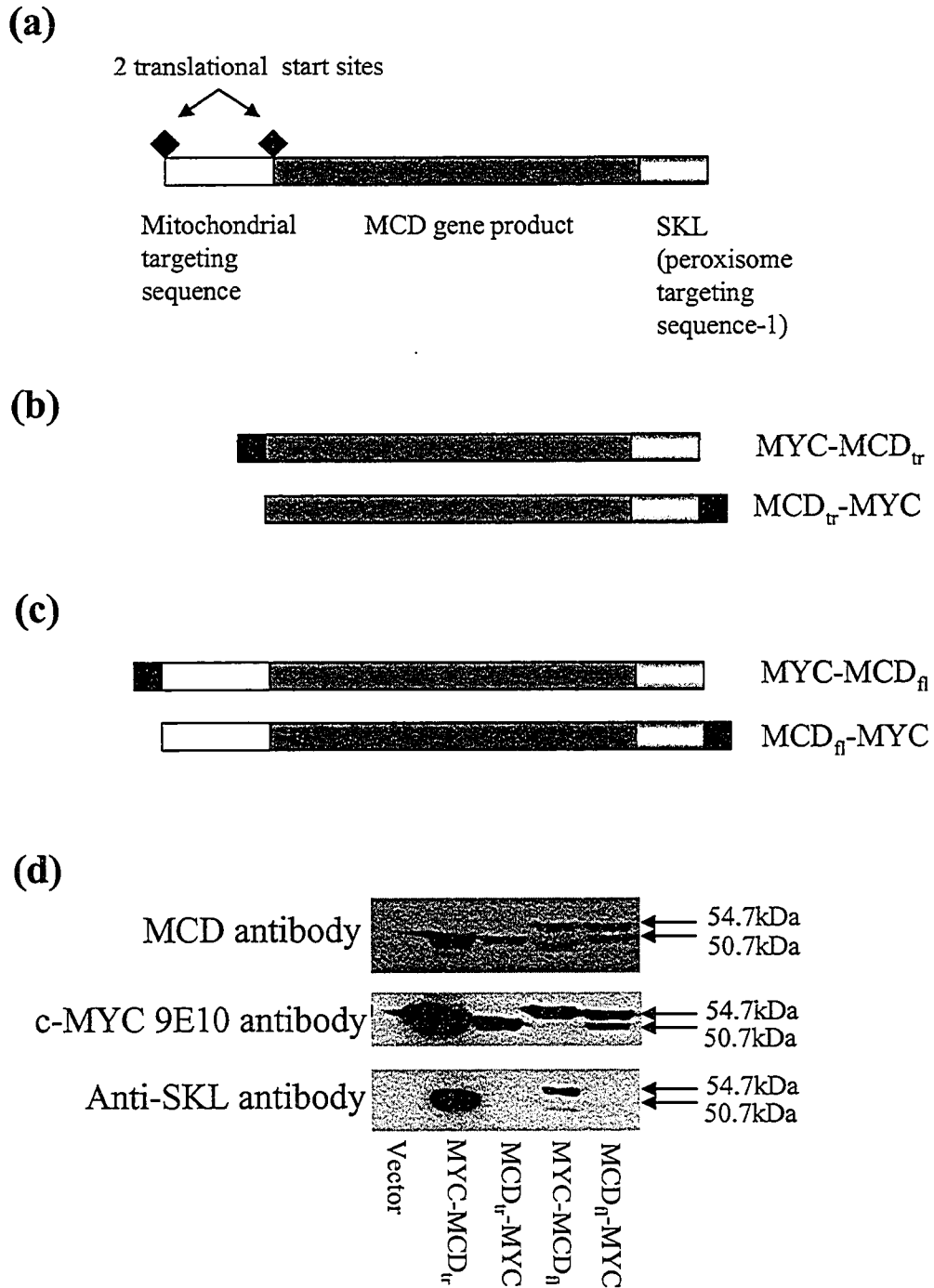


Figure 3-11: Design and transfection of MYC tagged MCD constructs in CHO cells. (a) Putative targeting sequences and transcriptional start sites of MCD, (b) constructs of MCD produced using the second ATG start site, (c) or the first ATG start site; (d) Transfection of constructs into CHO cells and immunoblotting for MCD, the MYC tag (to determine if cleavage occurs), and the anti-SKL antibody (to determine if the peroxisomal sequence is masked)

MYC tag. Therefore, import of the MCD_{fl}-MYC construct into mitochondria and cleavage of the C-terminal targeting sequence did not likely occur in these cells.

In order to determine if the MYC tags interfere with normal MCD function, transfected CHO cells were assayed for MCD activity. The activity of MCD was indirectly measured by acetyl CoA production coupled to the malate dehydrogenase reaction, which produces NADH. Figure 3-12 shows the activity measurements of untransfected control cells, vector transfected control cells, untagged MCD transfected cells and MYC construct transfected cells. The top panel shows the MCD activity normalized to total cellular protein content. All of the constructs were active above control levels however the MCD_{fl}-MYC construct had much lower activity. Immunoblotting of the transfected cells, shown in Figure 3-12 (middle panel), indicates a difference in MCD expression level among the constructs. Western blots were run on every experiment and the activity normalized to unit MCD protein using densitometry measurements with Quantity One software. The results are shown in Figure 3-12 (bottom panel), which show that all of the constructs have either equal or higher activity than the transfected untagged MCD protein. This suggests that the MYC tags affect intracellular processing and localization, but do not alter the MCD fusion protein sufficiently to remove MCD activity. Statistical analysis of the MCD fusion protein activity (Figure 3-12; bottom panel) using ANOVA indicates that there is no statistical difference among the activity of the fusion proteins when compared to the overexpressed, untagged MCD. We are currently unable to rule out the possibility that a certain subcellular domain may be required for maximal activity or that there may be differential control/regulation of MCD activity in each subcellular compartment.

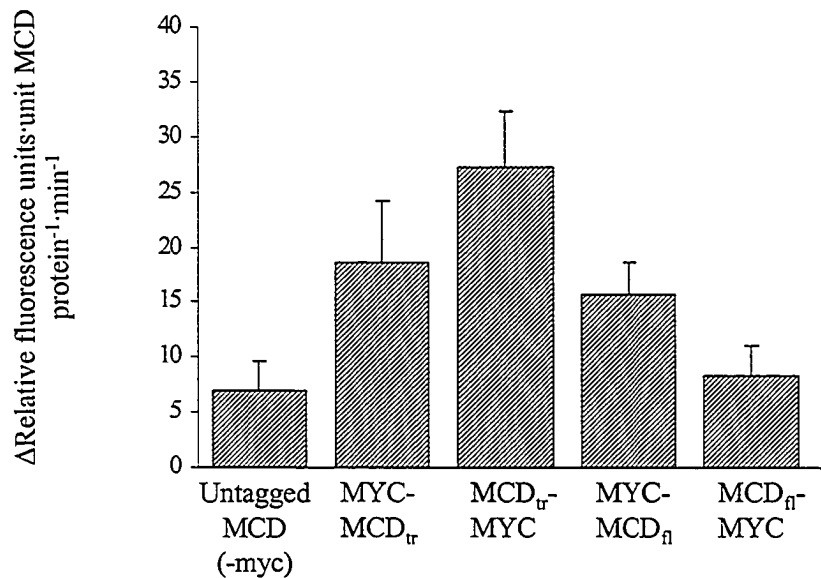
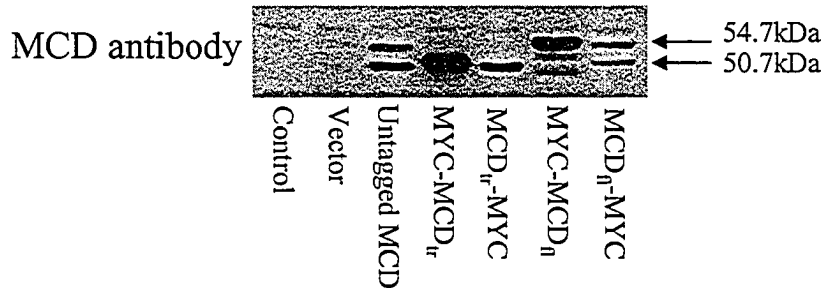
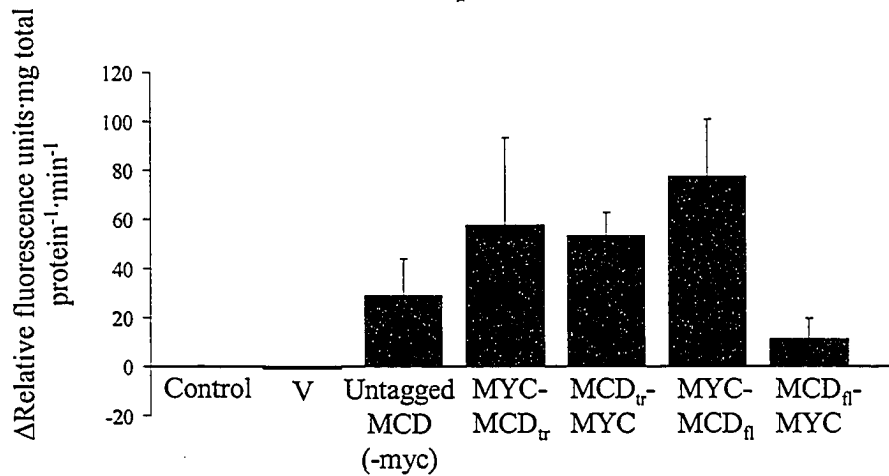


Figure 3-12: MCD activity of MCD fusion proteins in CHO cells. (a) MCD activity of transfected CHO cells expressed per milligram total protein, (b) Immunoblots showing different levels of MCD expression in transfected cells, (c) MCD activity adjusted to the unit of MCD protein expressed. A representative immunoblot is shown of n=5 separate CHO cell passages.

3.3.4: Immunocytochemistry and localization of MCD fusion proteins in neonatal rat cardiac myocytes

To determine the effect of the MYC tags on MCD localization in the heart, constructs were transfected into neonatal rat cardiac myocytes and immunocytochemistry was performed as described in Section 3.2.13. Figure 3-13 shows co-localization of the MYC-MCD_{tr} fusion protein with Mitotracker Red (upper panel) and Anti-SKL (bottom panel). The MYC-MCD_{tr} fusion protein was apparent in distinct punctates that appeared to co-localize with peroxisomes but not with mitochondria. Therefore, the MYC-MCD_{tr} construct produces a peroxisomal protein.

The MCD_{tr}-MYC fusion protein displayed a more diffuse pattern of expression than the MYC-MCD_{tr} fusion protein. The co-localization of MCD_{tr}-MYC is shown in Figure 3-14. This construct does not appear to co-localize to either mitochondria or peroxisomes, suggesting that this construct produces a cytosolic protein.

The longer protein tagged at the N-terminus (MYC-MCD_{fl}) has a distribution very similar to the other N-terminal tagged protein (MYC-MCD_{tr}). The MYC-MCD_{fl} localization is shown in Figure 3-15 and indicates a peroxisomal co-localization. There does not appear to be any co-localization of the MYC-MCD_{fl} protein with mitochondria, however since this construct produced a mature MCD protein devoid of a MYC tag we cannot rule out the possibility of MYC-MCD_{fl} MCD in the mitochondria.

Finally, the MCD_{fl}-MYC construct localization is shown in Figure 3-16. Unlike all of the other constructs, the MCD protein produced by the MCD_{fl}-MYC construct displayed a mitochondrial distribution. There was no evidence of a peroxisomal form of MCD produced.

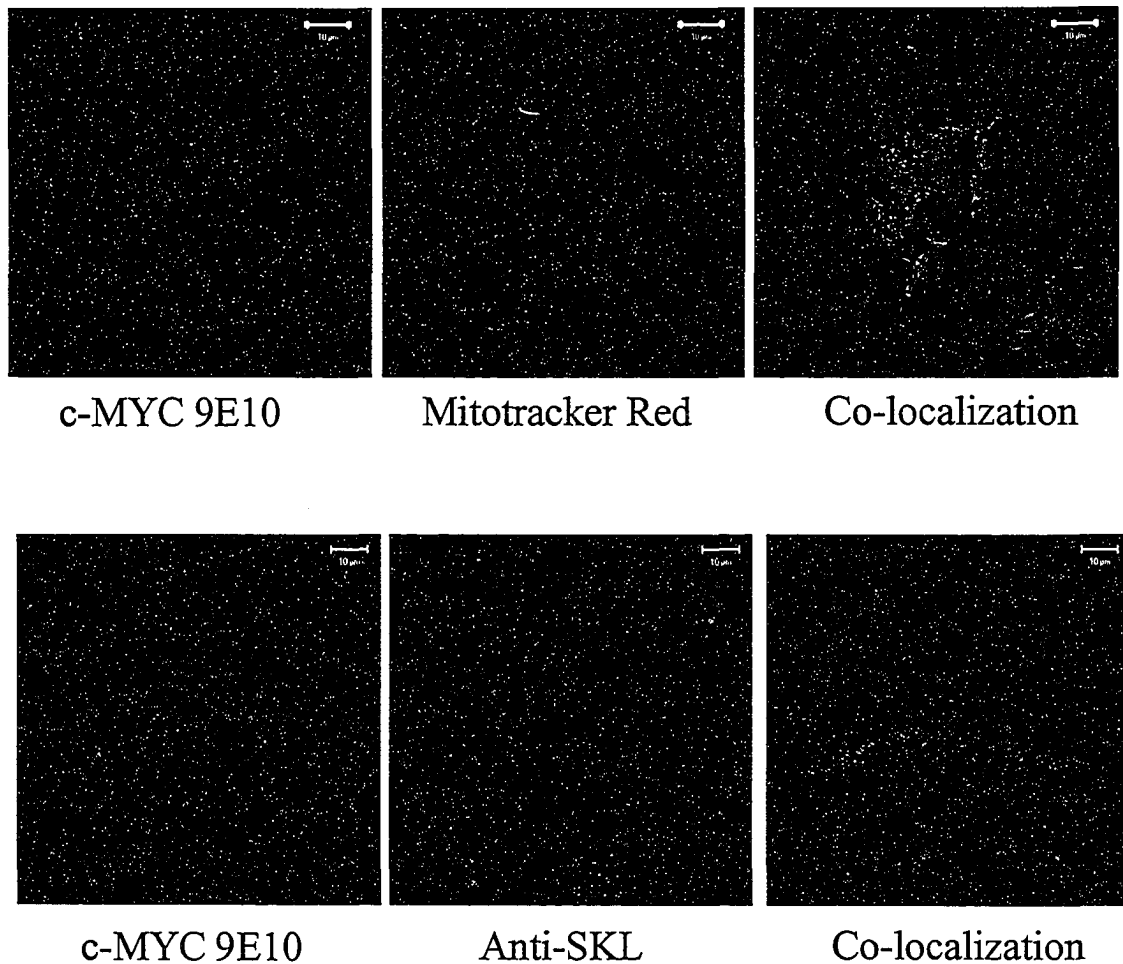


Figure 3-13: Co-localization of the MYC-MCD_{tr} construct using the c-myc 9E10 antibody. MYC-MCD_{tr} does not co-localize with the mitochondrial marker Mitotracker Red (upper panel) but is predominantly co-localized to the peroxisomal marker Anti-SKL (lower panel). MCD localization is shown in green, while the markers are red. Representative pictures are shown of n=5 separate neonatal myocyte isolations for both mitochondrial and peroxisomal co-localization.

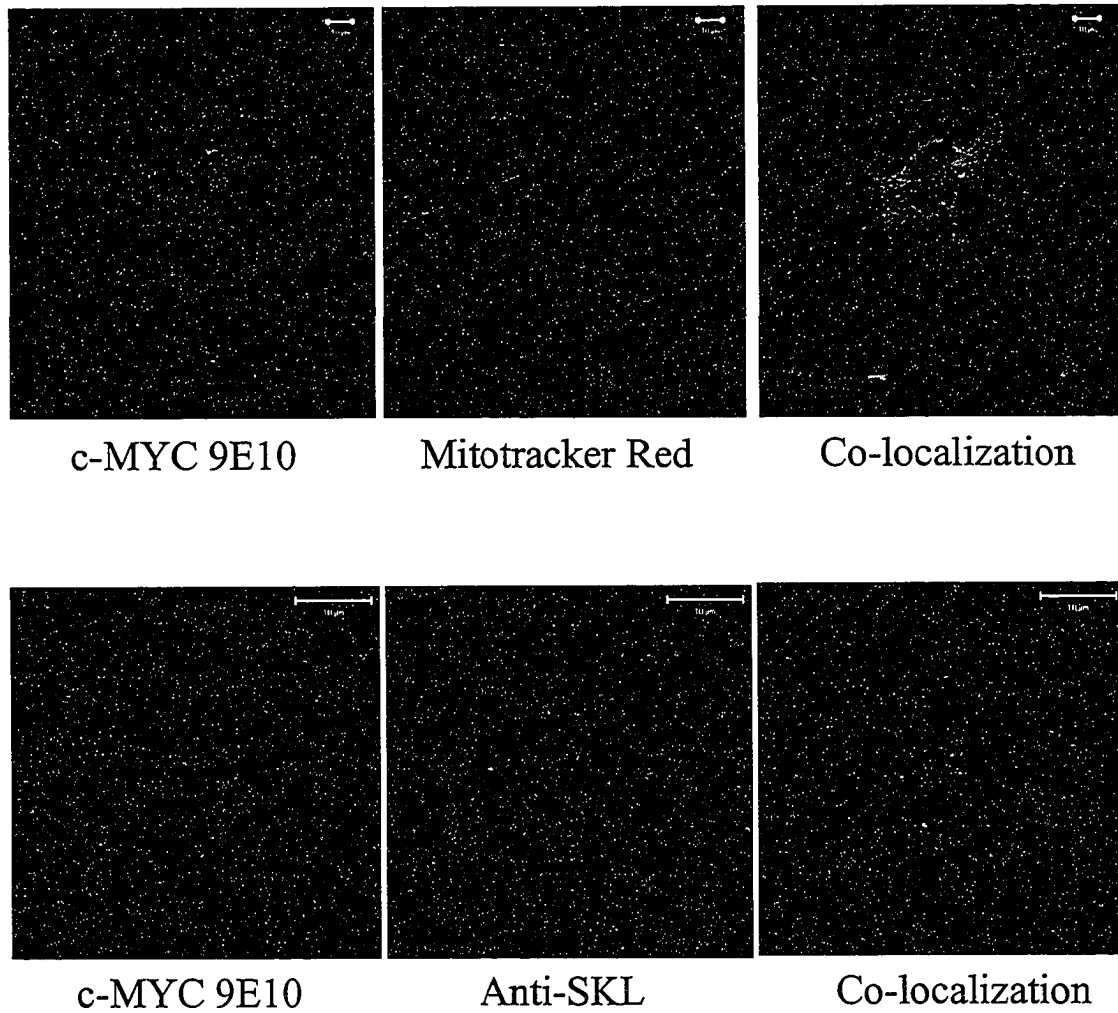


Figure 3-14: Co-localization of the MCD_{tr}-MYC construct using the c-myc 9E10 antibody. MCD_{tr}-MYC does not co-localize with either the mitochondrial marker Mitotracker Red (upper panel) or the peroxisomal marker Anti-SKL (lower panel). MCD localization is shown in green, while the markers are red. Representative pictures are shown of n=5 and n=4 separate neonatal myocyte isolations for mitochondrial and peroxisomal co-localization, respectively.

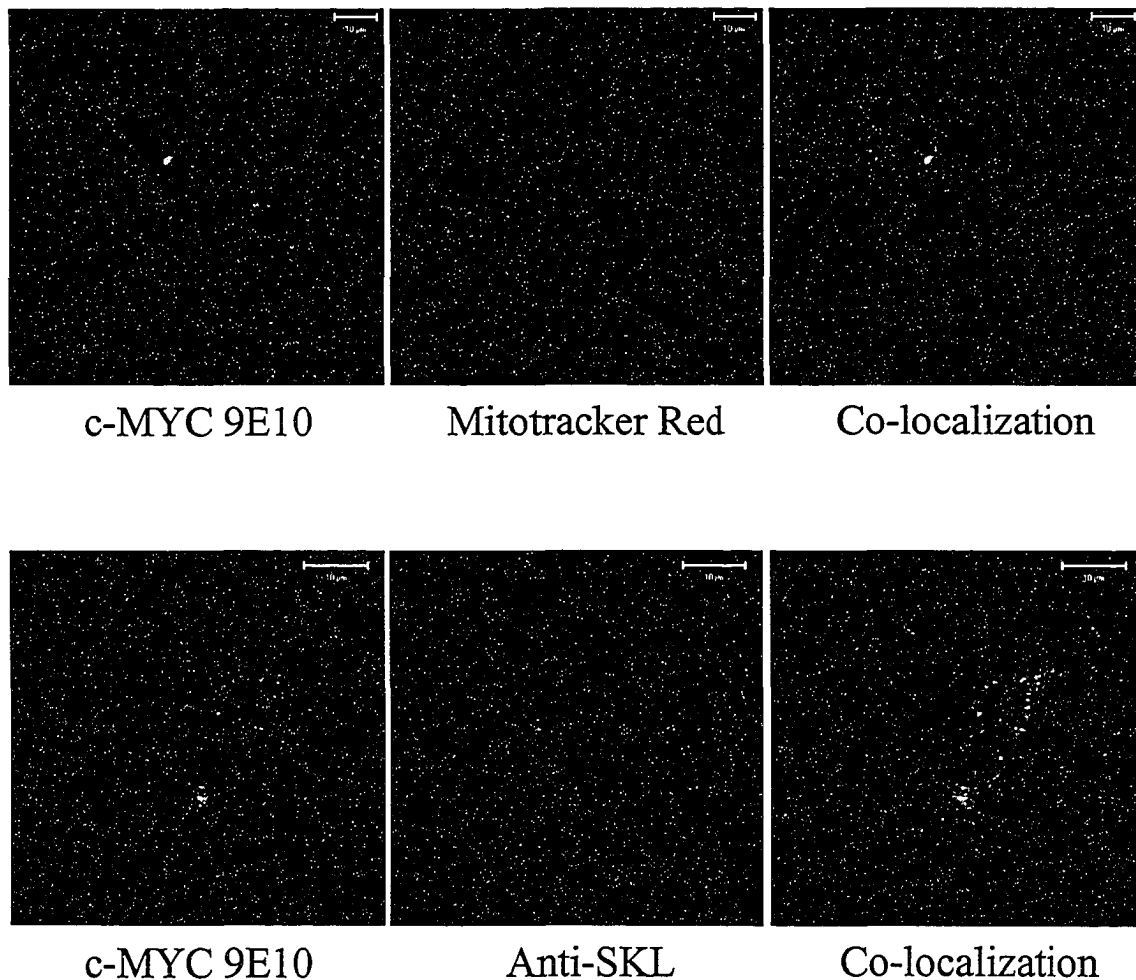


Figure 3-15: Co-localization of the MYC-MCD_n construct using the c-myc 9E10 antibody. MYC-MCD_n does not co-localize with the mitochondrial marker Mitotracker Red (upper panel) but does co-localize with the peroxisomal marker Anti-SKL (lower panel). MCD localization is shown in green, while the markers are red. Representative pictures are shown of n=5 and n=7 separate neonatal myocyte isolations for mitochondrial and peroxisomal co-localization, respectively.

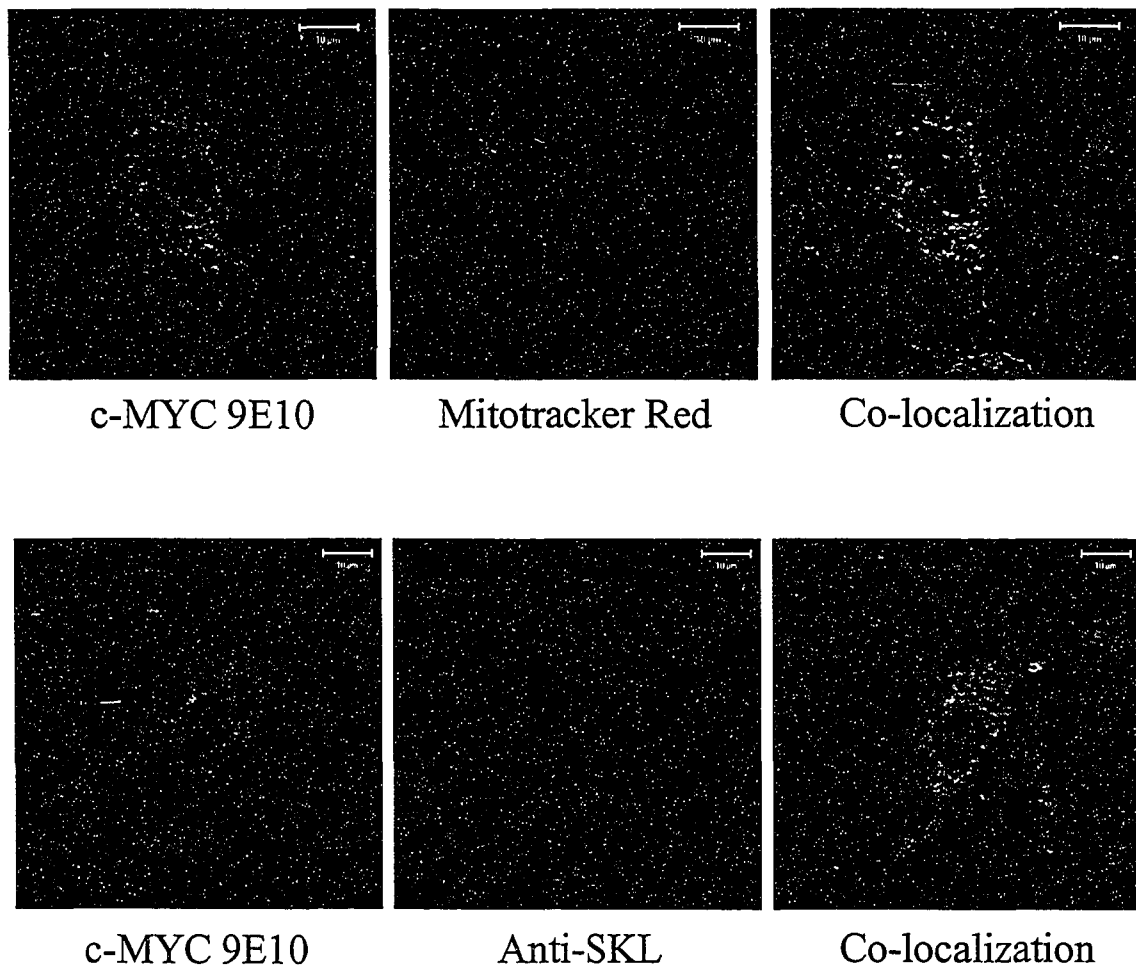


Figure 3-16: Co-localization of the MCD_n -MYC construct using the c-myc 9E10 antibody. MCD_n -MYC co-localizes with the mitochondrial marker Mitotracker Red (upper panel) but does not co-localize with the peroxisomal marker Anti-SKL (lower panel). MCD localization is shown in green, while the markers are red. Representative pictures are shown of n=6 and n=4 separate neonatal myocyte isolations for mitochondrial and peroxisomal co-localization, respectively.

3.3.5: Summary of MCD localization using MCD-MYC fusion proteins

To summarize these localization experiments, the constructs which contain an unmasked peroxisomal targeting sequence are localized to the peroxisomes, while the construct with an unmasked mitochondrial targeting sequence produces a mitochondrial protein. If both sequences are unavailable as in the shorter MCD which lacks both the N-terminal mitochondrial targeting sequence and has a masked peroxisomal targeting sequence, the protein produced remains in the cytosol. This suggests that there is very little endogenous MCD in the cytosol of cardiac myocytes since either the mitochondrial targeting sequence or peroxisomal targeting sequence is sufficient to target MCD to those organelles.

3.4 Discussion

3.4.1: Subcellular fractionation of MCD

Using two different subcellular fractionation techniques we were unable to unequivocally determine the exact localization of MCD in rat ventricle tissue. The results presented suggest that peroxisomes and mitochondria in the heart are very similar in both density and mass. It is therefore difficult to isolate each organelle and provide conclusive evidence of MCD localization to either mitochondria or peroxisomes. Isolation of peroxisomes can be very difficult since mammalian peroxisomes are osmotically sensitive upon isolation¹⁶. It has recently been suggested that peroxisomes absorb water causing a small rupture of the peroxisomal membrane, which may lead to a release of intra-peroxisomal proteins during isolation procedures¹⁶. However, despite these difficulties the subcellular fractionation data are complementary to further immunocytochemistry studies suggesting that there is a large proportion of MCD in the peroxisomes. While these subcellular fractionation techniques do not conclusively localize MCD in the rat heart, the data allow further corroborative proof that MCD is localized to peroxisomes in the heart.

3.4.2: Translocation of MCD

Preliminary results from our laboratory had previously suggested that MCD localization is altered by over-expression of AMPK. Therefore, an ischemia/reperfusion protocol was utilized, which was originally designed to activate AMPK¹⁷. Subcellular fractionation was performed on the ischemia/reperfused rat hearts to isolate both cytosolic and mitochondrial-enriched fractions. However, there was no difference in

localization of MCD in aerobic vs. ischemia/reperfused rat hearts. These data combined with work performed in our lab by Nanda Sambandam¹⁸ suggest that AMPK does not alter localization of MCD. However, these studies did suggest that AMPK may alter MCD expression and activity¹⁸. Taken together, MCD does not translocate between the cytosolic and mixed organelle fractions in response to ischemia/reperfusion under conditions shown previously to activate AMPK.

3.4.3: Putative targeting sequences of MCD

The systematic investigation of MCD subcellular localization described in this chapter produced some novel results. This work shows for the first time that both the mitochondrial and peroxisomal targeting sequences of rat heart MCD are functional. Therefore, there are two possible distributions for the MCD protein: peroxisomal and mitochondrial. Since either targeting sequence is sufficient to target MCD to the mitochondria and peroxisomes, it is unlikely that a significant amount of MCD exists in the cytosol of the myocyte. Therefore the role of MCD in subcellular malonyl CoA control is likely not through a cytosolic form of MCD.

3.4.4: Peroxisomal localization of MCD in the heart

The data described in this chapter suggest a peroxisomal localization of MCD in neonatal rat cardiac myocytes, which is due to translation from the second ATG start site. This is supported by the punctated distribution observed upon immunocytochemistry with the MCD antibody in neonatal rat cardiac myocytes. As well, MCD has been shown to

co-purify with catalase ² suggesting that these proteins reside in a similar intracellular compartment.

Further insight into MCD localization was provided by immunocytochemistry of the MYC tagged MCD constructs. The full-length construct masked at the mitochondrial targeting sequence (MYC-MCD_n) produced a protein of 54.7 kDa that was localized to peroxisomes, suggesting that peroxisomal localization does not involve a cleavage event to produce the small isoform of MCD.

The shorter construct of MCD tagged at the N-terminal end (MYC-MCD_{tr}) was also localized to peroxisomes and supports the proposed peroxisomal localization of MCD in the heart. Blockade of the peroxisomal targeting sequence in the MCD_{tr}-MYC construct disrupts this peroxisomal targeting of the protein. Since both of these constructs produced only one protein and neither MYC tag was cleaved off, the results suggest that MCD is targeted to the peroxisomes and is not cleaved upon import. The shorter constructs maintained their MCD activity and thus represents a functional MCD that is localized to the peroxisomes.

The full-length form of MCD tagged at the C-terminus (MCD_n-MYC) was localized only to the mitochondria, yet yielded both a 54.7 and a 50.7 kDa protein. The MCD_n-MYC construct was very similar in activity and protein molecular weight to the untagged rat heart MCD construct, which may suggest that this is the main localization of MCD. However, endogenous expression of MCD is not observed in the mitochondria of neonatal rat cardiac myocytes, nor is the larger isoform detected in these cells. This result may therefore be an artifact due to the use of a PCR produced Kozak sequence provided upstream of the first ATG start site, which may allow the first ATG start site to produce

the 54.7kDa protein, while the endogenous Kozak sequence for MCD may preferentially use the second ATG start site. In support of this result is work by Gould and colleagues who suggest that the first translational start site of MCD is followed immediately by a pyrimidine within the Kozak sequence, which may make it an inefficient initiator of translation¹⁹.

Taken together these data suggest that endogenous MCD is localized to the peroxisomes in neonatal rat cardiac myocytes and is likely a result of translation from the second methionine start site. Unfortunately, the experiments presented are not sufficient to determine which translational start site is utilized. Further experiments involving isolation of mRNA, reverse-transcription of cDNA, and sequencing may identify the mRNA species present in the heart and thus the translational start site utilized.

3.4.5: Mitochondrial localization of MCD in the heart

The distribution of endogenous MCD primarily to peroxisomes was unexpected since previous work had suggested a mitochondrial localization of MCD^{14, 15}. However, the reasons why mitochondrial MCD was not detected are discussed below.

It is possible that mitochondrial MCD could not be detected due to incomplete permeabilization of the mitochondrial membrane. Unlike the plasma membrane and the peroxisomal membrane, there are two distinct lipid bilayers in the mitochondria. The level of permeabilization may therefore allow antibody entry into the myocyte and peroxisomes but not into the mitochondria. However, investigation of the MCD_n-MYC construct shows mitochondrial localization using the same permeabilization techniques,

although a different antibody was used. This suggests that the lack of mitochondrial MCD is not due to restriction of antibody entry into the mitochondria.

Secondly, the presence of MCD in cardiac mitochondria has only been explored through the use of activity measurements on subcellular fractions ¹⁵. The inherent problems of contamination among fractions using these techniques may inappropriately localize MCD to the mitochondria. Peroxisomes are not easily separated from mitochondria in the heart due to similar densities and masses of the organelles, as evidenced by this study. As well, it has been shown that peroxisomes are very osmotically sensitive and using *in vitro* techniques often release intra-peroxisomal proteins ¹⁶. This could account for the difficulties in determination of MCD localization using subcellular fractionation techniques.

A final possibility is that mitochondrial MCD is in a conformation which does not allow the epitope to bind the antibody. Therefore, the folding of mitochondrial MCD or the formation of MCD complexes may be responsible for this lack of mitochondrial MCD visualization. In support of this proposal, MCD has previously been shown to exist as a tetramer ^{20, 21} and this complex formation may inhibit antibody binding. Similarly, the interaction of another protein with MCD may also inhibit the antibody binding to the epitope and further studies may determine potential interacting proteins. Since the antibody was made against a denatured MCD protein it is possible that when folded into the correct conformation the antibody is unable to recognize the epitope. However, activity assays performed on each of the constructs shows that all of the MCD-MYC fusion proteins maintain MCD activity, suggesting that each protein is properly folded.

The localization of MCD to mitochondria and formation of complexes cannot be ruled out by the data presented.

Although the techniques utilized in this project are unable to rule out the presence of MCD in the mitochondria, the data presented indicate that a large proportion of MCD is localized mainly to the peroxisomes in the heart.

3.4.6: What is the role of peroxisomal MCD?

Although there is a role for MCD in the control of fatty acid oxidation rates, the exact cellular mechanism remains unclear. Since peroxisomal oxidative enzymes have very low affinity for chain lengths shorter than butyryl CoA ²², it is unclear where peroxisomal malonyl CoA would be derived from. However, these chain length studies were performed in liver and kidney, suggesting that cardiac peroxisomes may contain different oxidative enzymes in the peroxisomes that may produce malonyl CoA. Another possible source of malonyl CoA in peroxisomes occurs from the oxidation of odd-chain dicarboxylic acids.

It has been previously suggested that MCD is important for the degradation of malonyl CoA produced from these odd-chain dicarboxylic fatty acids in peroxisomes ¹⁹. However, this is a very specialized role and may not be able to account for the regulation of fatty acid oxidation by MCD observed under various conditions in the heart. In fact, in hearts perfused with palmitate (not a dicarboxylic fatty acid) alone inhibition of MCD still produced a reduction in malonyl CoA levels ²³. The role of MCD in regulating malonyl CoA likely extends beyond degradation of malonyl CoA from odd-chain

dicarboxylic fatty acids. Another role for MCD may exist in the local reduction of malonyl CoA levels inside the peroxisomes.

MCD has been suggested to protect mitochondrial enzymes from inhibition by malonyl CoA ²⁴. Propionyl CoA carboxylase, which catalyses the conversion of propionyl CoA to methmalonyl CoA during odd-chain fatty acid oxidation, is also capable of generating malonyl CoA from acetyl CoA ²⁵. This malonyl CoA may inhibit methmalonyl CoA mutase and other enzymes ²⁵, suggesting that the role of MCD is to protect these enzymes from inhibition. The role of peroxisomal MCD may be very similar such that it may protect peroxisomal enzymes from inhibition. However, the differences between the metabolic enzymes located in the mitochondria and those of the peroxisome are not yet fully delineated.

Peroxisomes are also important for fatty acid synthesis in the liver and provide lipids for post-translational modification of proteins. Although the presence of a peroxisomal ACC isoform has not been shown, the production of malonyl CoA for synthesis of these lipids may occur in peroxisomes. Therefore, MCD may regulate the level of lipid synthesis versus acetyl CoA release from the peroxisome. Unfortunately, since fatty acid synthase expression is extremely low in the heart it is unlikely that this is the primary role of MCD in the peroxisome.

Another role of MCD may be to control malonyl CoA sensitive efflux of medium to long chain fatty acids from the peroxisome. Since an ABC transporter exists to move very long chain fatty acids into the peroxisome, it is possible that the malonyl CoA sensitive fatty acid transporter in the peroxisome is responsible for efflux of fatty acids into the cytosol. In this orientation the transporter may have an internal malonyl CoA

binding site and MCD may therefore regulate efflux of partially oxidized fatty acids for further metabolism in mitochondria.

Whatever its localization is, MCD has been shown to dramatically alter malonyl CoA tissue content and presumably cytosolic malonyl CoA levels, which alters cardiac fatty acid oxidation rates. The lack of MCD translocation and mitochondrial localization observed in this study suggests a malonyl CoA shuttle may exist to move malonyl CoA between subcellular compartments. Since there has been no malonyl CoA shuttle system described in the heart the mechanism behind the possible movement of cytosolic malonyl CoA into the peroxisome is not known. However, it is still possible that a mechanism exists to move malonyl CoA from one compartment to another. In the absence of a cytosolic form of MCD in the heart, malonyl CoA may be moved from the cytosol into organelles for degradation and control of local malonyl CoA concentrations in tissue compartments.

The data generated in this study are unable to suggest a role for MCD localized to the peroxisome in light of the current knowledge of peroxisomal oxidation and function. Future studies may delineate the role of peroxisomal MCD in the control of mitochondrial fatty acid oxidation rates.

3.4.7: Signaling events and MCD localization

Although MCD appears to be peroxisomal in the neonatal rat cardiac myocytes, there may be a signaling mechanism that could target MCD to different cellular compartments. MCD expression can be increased by the activation of PPAR α ²⁶, suggesting that there is control of MCD at the transcriptional level. However, PPAR α

may not be the only nuclear receptor that exerts control on the MCD promoter. Previous work from our laboratory suggests that AMPK may somehow regulate the transcription of MCD in H9c2 myoblasts¹⁸. Other metabolic nuclear receptors such as FOXO1 or the farnesoid X receptor may also play a role.

It is unknown if a second mRNA transcript could be produced by the differential activation of nuclear receptors that would affect the isoform of MCD expressed and thus localization. Different cellular signals such as alterations in lipid profiles may activate the transcription of an mRNA that would result in expression of the full-length isoform that is most likely localized to the mitochondria. Since only the full-length isoform of MCD contains the mitochondrial targeting sequence, this could represent a control of MCD localization. Further studies into the transcriptional control of MCD may provide insight into how it regulates fatty acid oxidation rates under various conditions.

3.4.8: Initiation of MCD translation

The choice of methionine used for translation is generally due to the presence of a Kozak sequence (ACCATGG) surrounding the initiating methionine. In the rat heart the Kozak sequence for the second translational start site deviates from the Kozak sequence shown above by only one base pair. The first translational start site is much less defined and has only four of the seven base pairs for a Kozak sequence. This suggests that translation in the rat heart likely initiates from the second translational start site and produces only the shorter isoform of MCD.

3.4.9: Neonatal rat cardiac myocytes as a model

The use of neonatal rat cardiac myocytes as a model for cardiac energy metabolism is controversial for several reasons, including a lack of cardiac work performed and a neonatal phenotype of metabolic gene expression. Although neonatal myocytes contract spontaneously, there is a limited demand for cardiac work and therefore the energy production resembles that of a semi-quiescent cell. This state of quiescence is not indicative of the state of the normal heart and results should be interpreted with care. In addition, the neonatal heart relies more on glucose than the adult heart and a switch to the use of fatty acids in rabbits does not fully occur until approximately 7-days post-birth^{27,28}. Since this project is designed to look at an enzyme with an important role in cardiac fatty acid oxidation rates, the use of neonatal rat cardiac myocytes is not ideal. However there are several advantages of using these cells including the following: (i) they are easily isolated; (ii) they can be transfected, and (iii) using confocal immunocytochemistry we can observe subcellular protein expression. Although results from neonatal myocytes cannot be directly translated to the intact heart, these isolated myocytes are still an important molecular tool to test for MCD localization.

3.4.10: Limitations

While the localization of MCD was interpreted to be predominantly peroxisomal and expressed from the second translational start site, there are several limitations that may affect this interpretation. The translation of MCD from the second start site is assumed and is not rigorously proven. Reverse-transcription of mRNA would provide insight into the mRNA species present in the heart. As well, the H240 MCD antibody

also recognizes catalase and an assumption exists that the peroxisomal distribution is assumed to be due to MCD localization alone. The MCD activity assays in Figure 3-12 (normalized to MCD protein) are not statistically significant, however this may be due to a low sample number and may benefit from a calculation of statistical power. The localization of MCD to the outer surface of the peroxisome was also not rigorously proven. Isolation of peroxisomes followed by limited proteolysis with trypsin would indicate whether MCD is intra-peroxisomal or associated with the external surface of the peroxisome. While there are several limitations to our study, the interpretation based on the available data remains valid.

3.4.11: Summary

The data presented in this chapter suggest that a large proportion of MCD in the heart is peroxisomal. This peroxisomal MCD protein occurs due to translation from the second translational start site to produce the 50.7 kDa MCD protein typically observed in the heart. The role of peroxisomal MCD in the regulation of fatty acid oxidation rates, however, still remains unclear. As well, the observation that both putative targeting sequences are functional suggests that there may be a translational signal to dictate the isoform of MCD produced and therefore the localization of MCD in the myocyte.

Literature Cited

1. Courchesne-Smith, C. *et al.* Cytoplasmic accumulation of a normally mitochondrial malonyl-CoA decarboxylase by the use of an alternate transcription start site. *Arch. Biochem. Biophys.* **298**, 576-586 (1992).
2. Dyck, J.R. *et al.* Characterization of rat liver malonyl-CoA decarboxylase and the study of its role in regulating fatty acid metabolism. *Biochem. J.* **350 Pt 2**, 599-608 (2000).
3. McGarry, J.D. & Brown, N.F. The mitochondrial carnitine palmitoyltransferase system. From concept to molecular analysis. *Eur. J. Biochem.* **244**, 1-14 (1997).
4. Fraser, F., Corstorphine, C.G., & Zammit, V.A. Topology of carnitine palmitoyltransferase I in the mitochondrial outer membrane. *Biochem. J.* **323 (Pt 3)**, 711-718 (1997).
5. Shi, J., Zhu, H., Arvidson, D.N., Cregg, J.M., & Woldegiorgis, G. Deletion of the conserved first 18 N-terminal amino acid residues in rat liver carnitine palmitoyltransferase I abolishes malonyl-CoA sensitivity and binding. *Biochemistry* **37**, 11033-11038 (1998).
6. Shi, J., Zhu, H., Arvidson, D.N., & Woldegiorgis, G. A single amino acid change (substitution of glutamate 3 with alanine) in the N-terminal region of rat liver carnitine palmitoyltransferase I abolishes malonyl-CoA inhibition and high affinity binding. *J. Biol. Chem.* **274**, 9421-9426 (1999).
7. Zammit, V.A., Fraser, F., & Orstorphine, C.G. Regulation of mitochondrial outer-membrane carnitine palmitoyltransferase (CPT I): role of membrane-topology. *Adv. Enzyme Regul.* **37**, 295-317 (1997).
8. Singh, H. & Poulos, A. Distinct long chain and very long chain fatty acyl CoA synthetases in rat liver peroxisomes and microsomes. *Arch. Biochem. Biophys.* **266**, 486-495 (1988).
9. Van Veldhoven, P.P., Baumgart, E., & Mannaerts, G.P. Iodixanol (Optiprep), an improved density gradient medium for the iso-osmotic isolation of rat liver peroxisomes. *Anal. Biochem.* **237**, 17-23 (1996).
10. Lopaschuk, G.D. & Barr, R.L. Measurements of fatty acid and carbohydrate metabolism in the isolated working rat heart. *Mol. Cell. Biochem.* **172**, 137-147 (1997).
11. Leighton, F. *et al.* The large-scale separation of peroxisomes, mitochondria, and lysosomes from the livers of rats injected with triton WR-1339. Improved isolation procedures, automated analysis, biochemical and morphological properties of fractions. *J. Cell Biol.* **37**, 482-513 (1968).

12. Alexson, S.E., Fujiki, Y., Shio, H., & Lazarow, P.B. Partial disassembly of peroxisomes. *J. Cell Biol.* **101**, 294-304 (1985).
13. Sherwin, J.E. & Natelson, S. Serum and erythrocyte argininosuccinate lyase assay by NADH fluorescence generated from formed fumarate. *Clin. Chem.* **21**, 230-234 (1975).
14. FitzPatrick, D.R., Hill, A., Tolmie, J.L., Thorburn, D.R., & Christodoulou, J. The molecular basis of malonyl-CoA decarboxylase deficiency. *Am. J. Hum. Genet.* **65**, 318-326 (1999).
15. Kerner, J. & Hoppel, C.L. Radiochemical malonyl-CoA decarboxylase assay: activity and subcellular distribution in heart and skeletal muscle. *Anal. Biochem.* **306**, 283-289 (2002).
16. Antonenkov, V.D., Sormunen, R.T., & Hiltunen, J.K. The behavior of peroxisomes in vitro: mammalian peroxisomes are osmotically sensitive particles. *Am. J. Physiol. Cell. Physiol.* **287**, C1623-C1635 (2004).
17. Kudo, N. *et al.* Characterization of 5'AMP-activated protein kinase activity in the heart and its role in inhibiting acetyl-CoA carboxylase during reperfusion following ischemia. *Biochim. Biophys. Acta* **1301**, 67-75 (1996).
18. Sambandam, N. *et al.* Malonyl-CoA decarboxylase (MCD) is differentially regulated in subcellular compartments by 5'AMP-activated protein kinase (AMPK). Studies using H9c2 cells overexpressing MCD and AMPK by adenoviral gene transfer technique. *Eur. J. Biochem.* **271**, 2831-2840 (2004).
19. Sacksteder, K.A., Morrell, J.C., Wanders, R.J., Matalon, R., & Gould, S.J. MCD encodes peroxisomal and cytoplasmic forms of malonyl-CoA decarboxylase and is mutated in malonyl-CoA decarboxylase deficiency. *J. Biol. Chem.* **274**, 24461-24468 (1999).
20. Buckner, J.S., Kolattukudy, P.E., & Poulou, A.J. Purification and properties of malonyl-coenzyme A decarboxylase, a regulatory enzyme from the uropygial gland of goose. *Arch. Biochem. Biophys.* **177**, 539-551 (1976).
21. Kim, Y.S. & Kolattukudy, P.E. Malonyl-CoA decarboxylase from the uropygial gland of waterfowl: purification, properties, immunological comparison, and role in regulating the synthesis of multimethyl-branched fatty acids. *Arch. Biochem. Biophys.* **190**, 585-597 (1978).
22. Vanhove, G.F. *et al.* The CoA esters of 2-methyl-branched chain fatty acids and of the bile acid intermediates di- and trihydroxycoprostanic acids are oxidized by one single peroxisomal branched chain acyl-CoA oxidase in human liver and kidney. *J. Biol. Chem.* **268**, 10335-10344 (1993).

23. Dyck, J.R. *et al.* Malonyl coenzyme a decarboxylase inhibition protects the ischemic heart by inhibiting fatty acid oxidation and stimulating glucose oxidation. *Circ. Res.* **94**, e78-e84 (2004).
24. Kim, Y.S. & Kolattukudy, P.E. Purification and properties of malonyl-CoA decarboxylase from rat liver mitochondria and its immunological comparison with the enzymes from rat brain, heart, and mammary gland. *Arch. Biochem. Biophys.* **190**, 234-246 (1978).
25. Scrutton, M.C. & Utter, M.F. Pyruvate carboxylase. IX. Some properties of the activation by certain acyl derivatives of coenzyme A. *J. Biol. Chem.* **242**, 1723-1735 (1967).
26. Lee, G.Y., Kim, N.H., Zhao, Z.S., Cha, B.S., & Kim, Y.S. Peroxisomal-proliferator-activated receptor alpha activates transcription of the rat hepatic malonyl-CoA decarboxylase gene: a key regulation of malonyl-CoA level. *Biochem. J.* **378**, 983-990 (2004).
27. Lopaschuk, G.D. & Spafford, M.A. Energy substrate utilization by isolated working hearts from newborn rabbits. *Am. J. Physiol.* **258**, H1274-H1280 (1990).
28. Lopaschuk, G.D., Spafford, M.A., & Marsh, D.R. Glycolysis is predominant source of myocardial ATP production immediately after birth. *Am. J. Physiol.* **261**, H1698-H1705 (1991).

Chapter 4

Malonyl CoA Decarboxylase Knockout Mice: Genotyping and Gene Expression

Isolated working mouse heart perfusions were performed by Melanie A. Fischer

CoA esters were isolated by Rick Barr and analyzed by Ken Strynadka

RT-PCR was performed in collaboration with Dr. Martin E. Young

4.1 Introduction

The substrate preference of the heart following an ischemic episode determines the level of functional recovery, such that high rates of fatty acid oxidation coupled with low glucose oxidation rates impair cardiac recovery. Rates of fatty acid oxidation are markedly influenced by intracellular malonyl CoA levels, which inhibit long chain fatty acid uptake into the mitochondria via CPT-1¹. During ischemia/reperfusion malonyl CoA levels are reduced²⁻⁵, resulting in both an increased reliance of the heart on fatty acids as a source of energy and an impaired cardiac recovery. An important determinant of the steady state levels of malonyl CoA is the rate of production by ACC and the rate of degradation by MCD, which influences the substrate preference of the heart. The activity of ACC is depressed during ischemia/reperfusion due to phosphorylation by AMPK and the activity of MCD is unchanged during ischemia/reperfusion. This maintenance of MCD activity when coupled with a reduced malonyl CoA production by ACC, results in a net reduction of malonyl CoA levels. In order to maintain malonyl CoA levels, reduce fatty acid oxidation rates and improve recovery following ischemia, MCD inhibition has been suggested to be a novel treatment for ischemia/reperfusion injury.

Previous work from our laboratory has indeed shown that MCD inhibition may be a good therapy for improving cardiac recovery following ischemia/reperfusion⁶. Hearts of animals (rats and pigs) treated with MCD inhibitors have higher malonyl CoA levels than untreated animals, which is accompanied by a decreased reliance of the heart on fatty acid oxidation and an increased contribution of glucose utilization⁶. The improvement in cardiac function following treatment with MCD inhibitors is attributed to this switch in substrate preference of the heart⁶.

While the acute regulation of MCD using these MCD inhibitors has shown promise for preventing ischemia/reperfusion injury, the effects of chronic inhibition of MCD are unknown. Similarly, the effect of systemic *in vivo* inhibition of MCD is also unknown. Since MCD deficiency in humans is associated with a metabolic disorder known as malonic aciduria with symptoms that include cardiomyopathy ⁷, it is possible that chronic, systemic inhibition of MCD may be associated with severe side effects. As well, MCD activation has been suggested as a therapy to improve insulin sensitivity ⁸, suggesting that MCD inhibition may contribute to the pathogenesis of diabetes. Therefore, in order to address these issues, MCD knockout mice were generated to study the effect of long-term MCD deficiency on whole body and cardiac metabolism.

Since MCD knockout mice would be expected to have elevated cardiac malonyl CoA levels, we would also expect these mice to have decreased fatty acid oxidation rates. Since the heart may continue to import fatty acids but not oxidize them, this may result in a build-up of fatty acids within the cardiac myocyte resulting in activation of PPAR α . Therefore, we **hypothesize** that MCD knockout hearts have elevated PPAR α activity and thus the hearts from these mice will have an increased expression of fatty acid oxidizing enzymes. However, prior to testing this hypothesis an accurate and reproducible genotyping protocol needs to be established. The **objective** of this research is to perform an initial set-up and basic characterization of the MCD knockout mouse including genotyping, back-crosses and set-up of breeding colonies, as well as the analysis of mRNA and protein levels of PPAR α responsive genes in the MCD knockout mice. We will also characterize the metabolic profile of hearts from MCD knockout mice.

4.2 Methods

4.2.1: Production of MCD knockout mice

The MCD knockout mice were produced via homologous recombination by Chugai Biopharmaceuticals (Japan) as shown in Figure 4-1. A 12 Kb fragment (pKE003) was isolated from a bacterial artificial chromosome (BAC) library, digested with EcoRI and inserted into a pBluescript vector for sequencing. The neomycin cassette was inserted into this EcoRI DNA fragment between the PvuII and EcoRV restriction sites, which flanked exon 1 of the MCD gene and inserted into a targeting expression vector. AB2.2-Prime embryonic stem (ES) cells (Lexicon Genetics, The Woodlands, TX) were transfected by electroporation with a linearized targeting vector, which allowed a homologous recombination event to occur within the regions of DNA marked with a red X in Figure 4.1. ES cells were then cultured in a medium supplemented with 300 µg/ml G418 (GIBCO/BRL) and G418-resistant clones were screened by Southern blot analysis to select cells missing the MCD gene. These selected stem cells were injected into C57 Black 6 (C57 BL6) blastocysts to produce offspring missing exon 1 (which includes both potential translational start sites) of the MCD gene and the resulting heterozygous mice were crossed with heterozygous littermates to produce mice homozygous for the insert. These mice have no overt metabolic disorder and are capable of reproduction.

4.2.2: MCD activity measurements

MCD activities were measured using a radiometric assay previously described by Dyck *et al*². Briefly, frozen mouse heart tissue was homogenized in buffer containing 20 mM sucrose, 750 mM KCl, 1 mM ethylene glycol-bis(β-aminoethyl ether)-N,N,N',N'-

tetraacetic acid (EGTA), 50 mM sodium fluoride (NaF), 5 mM sodium pyrophosphate (NaPPi), and 10mM HEPES, pH 7.4.

Samples were incubated in assay buffer (100 mM Tris-HCl pH 7.8, 1 mM dithiothreitol, 50 mM NaF, and 5 mM NaPPi) and the reaction initiated by the addition of malonyl CoA. The reaction was terminated after 10 minutes by 40 μ L of 0.5 M perchloric acid. Samples were neutralized, centrifuged, and the resulting supernatant was used to determine acetyl-CoA content. Following the conversion of acetyl CoA to 14 C citrate, the unreacted 14 C oxaloacetate was converted back to 14 C aspartic acid. The aspartate and citrate radioactivity were separated using Dowex resin (50WX8, 100-200 mesh; Sigma). The amount of acetyl CoA was determined by comparison of acetyl CoA standard curves run in parallel in each experiment.

4.2.3: Measurements of malonyl CoA levels

Extraction of malonyl CoA and the measurement of malonyl CoA levels were performed as previously described ^{2, 5, 9, 10}. Briefly, frozen ventricular tissue from perfused hearts was powdered using a mortar and pestle cooled to the temperature of liquid N₂. Malonyl CoA was extracted from the powdered tissue using a 6 % perchloric acid extract solution (pH 2-3) and measured using a modified HPLC procedure described by King et al ⁹. Separation was performed on a Beckman System Gold with a UV detector 167. Each sample (100 μ l each) was run through a pre-column cartridge ((218, size 3 cm, 7 μ m) and a Microsorb short-one column (type C18, particle size 3 μ m, size 4.6 x 100 mm). Absorbance was set at 254 nm and a flow rate of 1 ml/minute. A gradient was initiated using two buffers: buffer A consisted of 0.2 M NaH₂PO₄ pH 5.0, and buffer B

was a mixture of 0.25 M NaH₂PO₄, and acetonitrile pH 5.0, at a ratio of 80:20 (v/v). Buffers were filtered using pure Nylon-66 filter membrane (Pierce). Initial conditions (97% A and 3% B) were maintained for 2.5 minutes and were changed thereafter to 18% B over 5 min using Beckman's curve 3. At 15 minutes the gradient was changed linearly to 37% B over 3 minutes and subsequently to 90% B over 17 minutes. At 42 minutes the composition was returned linearly back to 3% B over 0.5 minutes, and at 50 minutes column equilibration was complete. Peaks were integrated by Beckman System Gold software package.

4.2.3: Isolation of genomic DNA from ear notches

Ear tissue was collected when animals were notched for identification purposes and frozen at -20°C. Animal numbers, sex, and parentage were recorded. Prior to isolation of genomic DNA the ear notches were removed from the freezer and thawed to room temperature. Genomic DNA isolation was performed using the Qiagen DNeasy kit as per the manufacturer's instructions and eluted into 2 mL microcentrifuge tubes. The volume used for DNA elution from the column was 200 µL and the elution step was performed twice for a total elution volume of 400 µL.

4.2.4: Precipitation of genomic DNA

Sodium chloride (NaCl) precipitation was performed in order to concentrate the genomic DNA. 350 µL of sterile water and 350 µL of 6 M saturated NaCl was added to the eluted DNA and the mixture incubated on ice for 5 minutes. To precipitate the DNA 900 µL of isopropanol was added to the mixture and mixed gently by inverting the tube

4-6 times. The solution was spun at 14,000 rpm in a 4 °C microcentrifuge for 30 minutes to pellet the DNA. The supernatant was removed; the pellet washed with 350 μ L of 70% ethanol and then spun at 14,000 rpm for 30 minutes as in the previous step. The supernatant was then removed and the pellet was allowed to dry until it appeared flaky. The pellet was resuspended in 10 μ L of sterile water (pH \sim 8.5) by pipetting up and down gently. Genomic DNA was then stored in the -20 °C freezer.

4.2.5: Genomic DNA amplification using GenomiPhi system

The GenomiPhi kit (GE Healthcare; Amersham Biosciences) was used in order to amplify the amount of genomic DNA for the PCR genotyping reaction. The GenomiPhi kit utilizes random primers that bind to the genomic DNA strand and the Phi DNA polymerase replicates a genomic DNA strand initiating at each primer (Figure 4-3). The Phi enzyme system is unique since the polymerase does not fall off of the DNA strand upon reaching a newly formed replicated DNA strand, but rather displaces this newly replicated DNA strand and continues replication. This allows high molecular weight genomic DNA to be amplified. This amplification can be visualized in Figure 4-4, which shows genomic DNA isolated from three different mice before and after amplification with the GenomiPhi kit. The amount of DNA as observed with ethidium bromide staining was increased and the high molecular weight of the genomic DNA was retained.

In order to prevent repeated freeze-thawing, the GenomiPhi kit was aliquoted out into small 10 reaction aliquots and stored at -80 °C. The GenomiPhi kit was used exactly as described in the manufacturer's protocol. Briefly, 1 μ L of precipitated DNA (\sim 0.1 μ g/ μ L) was added to 9 μ L of sample buffer and denatured for 3 minutes at 95 °C. The

mixture was cooled on ice to 4 °C and then added to a 9:1 mixture of reaction buffer: Phi enzyme mix. The reaction was placed at 30 °C for a minimum of 18 hours and then the enzyme was heat-inactivated at 65 °C for 10 minutes. The reaction was cooled to 4 °C and used for PCR as described in Section 4.2.6.

4.2.6: Genotyping of animals by PCR

Primers used for genotyping were designed against the MCD sequence and were produced by the University of Alberta, Department of Biochemistry DNA core facility. The Blast (NCBI) database was used to check the specificity and accuracy of the primer sequences by showing all potential interaction sites within the database of known genomic sequences. The primers used for PCR had 10-100 potential interactions, but the first few predicted interactions were for the MCD gene. The sequences of primers used for genotyping (in 5' to 3' order) are found in the following Table:

Primer	Sequence
Fgn2	CCT ACG CTA GAT CCG AAC CCT AGC
Rgn2	AGA TAG GTG TCA ACC GAA AGG ACA
PGK-1	GCT AAA GCG CAT GCT CCA GAC TGC CTT G
Rgn4	AGG GCC TGC GCC TCC AGC AGA TCG
MCD NstF	CAA GCC AAG AGG GCG AGT CAG GTG
MCD NstR	TGG CCA TGC CTG TTT CAA GCA GGT C

Table 4-1: Primer sequences for genotyping of the MCD knockout mice by PCR (5' to 3' order)

The primer naming scheme is as follows: ‘F’ (forward) denotes a primer at the ATG start site running in the 5’-3’ direction; ‘R’ (reverse) denotes a primer at the stop sequence running in the 3’-5’ direction; genotyping primers are denoted by gn (genotyping) while nested primers are denoted by Nst (nested). The PGK-1 primer is a universal neomycin cassette primer reproduced from Jishage et al ¹¹.

The Fgn2/Rgn2 primer set was used to differentiate knockout, wild-type and heterozygous animals. A mouse containing only wild-type alleles produced a 1.6 Kb band, while a mouse containing only mutant alleles produced a 1.8 Kb band. A heterozygous mouse with one of each allele produced both the 1.8 and 1.6 Kb bands. The PCR protocol for the Fgn2/Rgn2 primer set is as follows:

MCD Fgn2 (0.1 µg/µL)	1 µL
MCD Rgn2 (0.1 µg/µL)	1 µL
10x PCR Buffer	10 µL
10x PCR enhancer	10 µL
50 mM MgSO ₄	1 µL
10 mM dNTPs	2 µL
ddH ₂ O	23.5 µL
Genomic DNA	1 µL
Platinum Pfx Polymerase	0.5 µL

Denature: 95 °C 2 minutes (1 cycle)

Denature: 95 °C 30 seconds

Anneal: 60 °C 1 minute

Extend: 68 °C 1 minute 30 seconds

x 35 cycles

The PCR products were cut out of the agarose gel, cleaned using a QIAEX II gel purification kit and sequenced by the Department of Biochemistry DNA core facility to determine that the products were correct. In order to further confirm that these primers were specific for the intron region of MCD, nested primers (MCD Nst) were used as

controls to re-amplify the Fgn2/Rgn2 amplified fragments. The nested primers were located approximately 40-50 bp inside of the Fgn2/Rgn2 primer region and produced a band of approximately 1.5 Kb. The PCR protocol for the nested primers was identical to the Fgn2/Rgn2 primer set described above.

The Fgn2/PGK-1 primer set was used to confirm the presence of the neomycin cassette of knockout and heterozygous animals. These primers produced a band of approximately 500 bp but since the PGK-1 primer was specific for the neomycin cassette, a band was not detected in DNA from wild-type animals. The PCR protocol used for the Fgn2/PGK-1 primer set is as follows:

MCD Fgn2 (0.1 µg/µL)	1 µL
PGK-1 (0.1 µg/µL)	1 µL
10x Buffer	5 µL
10 mM dNTPs	1 µL
DMSO	1 µL
Genomic DNA	1 µL
ddH ₂ O	23.5 µL
Herculase (Stratagene)	0.5 µL

Denature: 95 °C 2 minutes (1 cycle)

Denature: 95 °C 30 seconds

Anneal: 58 °C 30 seconds

Extend: 72 °C 1 minute 50 seconds

x10 cycles

Denature: 95 °C 30 seconds

Anneal: 58 °C 30 seconds

Extend: 72 °C 5 minutes

x25 cycles

Similarly, the Fgn2/Rgn4 primer set is specific for Exon 1 of the MCD gene and served as a control for the wild-type and heterozygous animals. This primer set produced a band of approximately 850 bp using the following PCR protocol:

MCD Fgn2 (0.1 µg/µL)	1 µL
Rgn4 (0.1 µg/µL)	1 µL
10x Buffer	5 µL
10 mM dNTPs	1 µL
DMSO	1 µL
Genomic DNA	0.06 µg (~7-9 µL)
ddH ₂ O	bring total volume to 50 µL
Herculase	0.5 µL

The cycles used for the Fgn2/PGK-1 primer set were identical to the Fgn2/Rgn4 primer set (shown above). PCR reaction products were run on 1% agarose gels at 90 V for approximately 45 minutes, stained with 1 µg/mL ethidium bromide and band size was determined using a 1 Kb DNA ladder (Invitrogen).

4.2.7: Back-crossing strategy for MCD knockout mouse breeding lines

MCD knockout mice were back-crossed for six generations to a C57 BL6 wild-type animal, in order to produce a background >99% similar to the genetic background of a C57 BL6 animal¹². The backcross strategy is depicted in Figure 4-6 and offspring were genotyped as described in Section 4.2.5. The back-crosses were initiated by the breeding of a female MCD knockout mouse with a wild-type C57 BL6 male mouse. The offspring from this mating were genotyped and a heterozygous female was mated with the same wild-type male (i.e. her father). This step was repeated five times and after the sixth backcross littermate heterozygous breeding pairs were initiated. The offspring of these heterozygous intercross pairs were genotyped and isolated for further matings, such that a littermate mating pair of knockout mice (and wild-type mice) were generated. These homozygous pairs allowed congenic lines of knockout and littermate wild-type animals to propagate.

4.2.8: Isolated working mouse heart model

Isolated working mouse hearts (male mice; age 3-4 months) were perfused as described by Belke *et al* ¹³. Briefly, hearts were aerobically perfused at a preload of 11.5 mmHg and an aortic afterload of 50 mmHg for 30 minutes with Krebs-Henselet solution containing 1.2 mM palmitate, 3% BSA, 5 mM glucose, 2.5 mM calcium, and 100 μ U/mL insulin. Fatty acid oxidation and glucose oxidation rates were measured as previously described by Saddik and Lopaschuk ¹⁴. Glucose oxidation rates were determined by measuring ¹⁴CO₂ release from the metabolism of U-¹⁴C glucose. Palmitate oxidation rates were measured either by measuring ¹⁴CO₂ production from hearts perfused with 1-¹⁴C palmitate or when hearts were simultaneously perfused with U-¹⁴C glucose through ³H₂O released from hearts perfused with 9,10-³H palmitate.

4.2.9: Isolation of tissue from MCD knockout mice

The light/dark cycle of the housed animals was reversed for a three week period prior to animal sacrifice and mice were maintained on a 12 hour dark; 12 hour light cycle. Three control mice and three MCD knockout mice (male mice; age 3-4 months) were sacrificed by a 60 mg·kg⁻¹ sodium pentobarbital injection at the middle of the dark cycle to control for circadian rhythm changes in expression. The hearts and livers were excised and immediately frozen in liquid nitrogen. The frozen tissues were powdered using a mortar and pestle followed by storage at -80°C.

4.2.10: Quantitative RT-PCR analysis of gene expression for PPAR α regulated genes

Quantitative real time PCR was performed by the laboratory of Dr. Martin E. Young (University of Texas; Houston, Texas), as previously described¹⁵. Briefly, reverse transcription was performed for 30 minutes at 42 °C with a gene specific primer for PDK-4, uncoupling protein-3 (UCP3), fatty acyl CoA synthetase (FACS), fatty acid transport protein (FATP-1), medium chain acyl CoA dehydrogenase (MCAD), or FAT/CD36. Reverse transcribed cDNA was used for quantitative two-step PCR (a 1 minute step at 95 °C, followed by 40 cycles of a 12 second step at 95 °C and a 1 minute step at 60 °C), in the presence of 400 nM specific forward and reverse primers, 100 nM specific fluorogenic probe, 2.5 mM MgCl₂, 50 mM KCl, 10 mM Tris buffer (pH 8.3 at 20 °C), 200 mM deoxynucleotides and 1.2 U *Taq* polymerase (Boehringer) in a final volume of 50 μ l. The fluorescence generated by each PCR reaction was compared to fluorescence obtained by RNA standards of known concentrations. A gene that is expressed constitutively with stable mRNA expression (cyclophilin) was used as an internal standard for RNA transcript loading and mRNA expression of metabolic genes were normalized to this cyclophilin expression.

4.2.11: Immunoblotting protocol for protein expression

Heart tissue, from 4-month old male mice, (15 mg) was homogenized for 30 seconds on level 3 of a PowerGen- 125 homogenizer (Fisher Scientific) in 100 μ L homogenization buffer (20 mM Tris, 50 mM NaCl, 0.25 M sucrose, 5 mM NaF; pH 7.4). Protein content was assayed using Biorad™ Reagent and 40 μ g of protein was loaded

onto either a 5% gel (for ACC and phospho-ACC) or a 10% SDS-PAGE gel (all other antibodies). Following electrophoresis at 120 V, samples were transferred to nitrocellulose membrane (2 hours at 100 V) and then blocked overnight in 5% (w/v) milk in tris-buffered saline (TBS). Membranes were incubated in primary antibody (in 5% (w/v) milk) for a minimum of 2 hours at room temperature and then washed once for 5 minutes in TBS containing 0.05% Tween-20 (TBS-T). Nitrocellulose was washed twice more in TBS for 5 minutes each and then incubated in the appropriate secondary antibody (in 5% (w/v) milk) for 1 hour at room temperature. Membranes were washed twice in TBS-T and then three times in TBS for 5 minutes each. Bound antibody was visualized using ECL[®] according to the manufacturer's instructions. Antibody dilutions for immunoblotting are summarized in Table 4-2.

Primary Antibody	Duration	Secondary Antibody	Duration
ACC; 1/1000	1hour	None	n/a
Phospho-ACC; 1/1000	Overnight	Goat anti-rabbit; 1/2000	1hour
AMPK; 1/1000	Overnight	Goat anti-rabbit; 1/2000	1hour
Phospho-AMPK; 1/1000	Overnight	Goat anti-rabbit; 1/2000	1hour
H240 MCD; 1/1000	Overnight	Goat anti-rabbit; 1/2000	1hour
Actin; 1/500	Overnight	Donkey Anti-Goat; 1/2000	1hour
FACS; 1/1500	2hours	Goat anti-rabbit; 1/2000	1hour
FABPpm; 1/3000	2hours	Goat anti-rabbit; 1/2000	1hour
FAT/CD36; 1/1000	Overnight	Goat anti-mouse; 1/2000	1hour

Table 4-2: Antibody dilutions and protocols for immunoblotting discussed in this chapter

4.2.12: PDC activity measurements

PDC activities were measured using a revised protocol based on the radiometric assay described by Constantin-Teodosiu *et al*¹⁶. Briefly, for measurement of ‘active’ PDC, frozen mouse heart tissue was homogenized in buffer containing 200 mM sucrose, 50 mM KCl, 5 mM ethylene glycol-bis(β -aminoethyl ether)-N,N,N',N'-tetraacetic acid

(EGTA), 50 mM tris(hydroxymethyl)aminomethane (Tris)-HCl, 50 mM sodium fluoride (NaF), 50 mM sodium pyrophosphate (NaPPi), 5 mM dichloroacetate and 0.1% Triton X-100, pH 7.8.

For assay of 'total' PDC activity (dephosphorylated form of PDC), frozen tissue was homogenized in buffer containing 1 mM calcium chloride (CaCl₂), but in the absence of NaF, NaPPi, and EGTA to increase the activity of the PDC phosphatase. The 'total' PDC samples were incubated in 0.8 mM magnesium chloride (MgCl₂) at 37 °C for 20 minutes.

Both 'active' and 'total' samples were then incubated in assay buffer (150 mM Tris-HCl, 0.75 mM EDTA, 0.75 mM nicotinamide adenine dinucleotide (NAD), 1.5 mM thiamine pyrophosphate (TPP), 5 mM EGTA, 5 mM dichloroacetate, and 0.75 mM coenzyme-A (CoA) and the reaction initiated by the addition of pyruvate. The reaction was terminated by 40 µL of 0.5 M perchloric acid. Samples were neutralized, centrifuged, and the resulting supernatant was used to determine acetyl-CoA content. Following the conversion of acetyl CoA to ¹⁴C citrate, the unreacted ¹⁴C oxaloacetate was converted back to ¹⁴C aspartic acid. The aspartate and citrate radioactivity were separated using Dowex resin (50WX8, 100-200 mesh; Sigma). The amount of acetyl CoA was determined by comparison of acetyl CoA standard curves run in parallel in each experiment.

4.2.13: Statistics

Statistical analysis of metabolic rates, malonyl CoA levels, mRNA expression and PDC activity of the two animal groups (wild-type and MCD knockout mice) was

performed using a two-tailed Student's t-test ($p < 0.05$ considered significant). Densitometry was performed using Quantity One software (Biorad) and statistical analysis was performed using a two-tailed Student's t-test ($p < 0.05$ considered significant).

4.3 Results

4.3.1: Production of MCD knockout mice and genomic primer design

Knockout mice were generated by targeted homologous recombination performed by Chugai Pharmaceuticals (Japan) as depicted in Figure 4-1. The MCD knockout mice were generated using a C57 BL6 background mouse line. The MCD gene was knocked out in all tissues and was not organ-specific. Knockout animals survived until adulthood, were capable of reproduction, and had no obvious phenotype.

In order to determine the genotype of these animals it was necessary to design a genotyping strategy that was both accurate and efficient. Due to the small amount of tissue provided by the Health Sciences Lab Animal Services (HSLAS) a PCR strategy was favored over a Southern blot detection strategy. Fgn2/Rgn2 PCR primers were designed outside of the region containing either the neomycin cassette or MCD exon 1, which allowed the simultaneous detection of both bands in heterozygous mice using one PCR reaction. The neomycin cassette was 200 bp longer than the existing exon 1 of MCD, therefore PCR with Fgn2/Rgn2 produced a 1.6 Kb band if the MCD exon was present and a 1.8 Kb band if the neomycin cassette was present. Figure 4-2 shows the location of the primers designed for genotyping and the size of band expected from PCR. To confirm the accuracy of the Fgn2/Rgn2 primer set, strand specific primers were designed within the MCD exon or the neomycin cassette and were designated Rgn4 (MCD exon specific) and PGK-1 (neomycin cassette specific). The Fgn2/Rgn4 primer set produced an 854 bp fragment, while PCR with the Fgn2/PGK-1 primer set produced a 500 bp fragment. All of the PCR products were sequenced to confirm that they were amplified from the MCD gene. Although the primers utilized for PCR required a

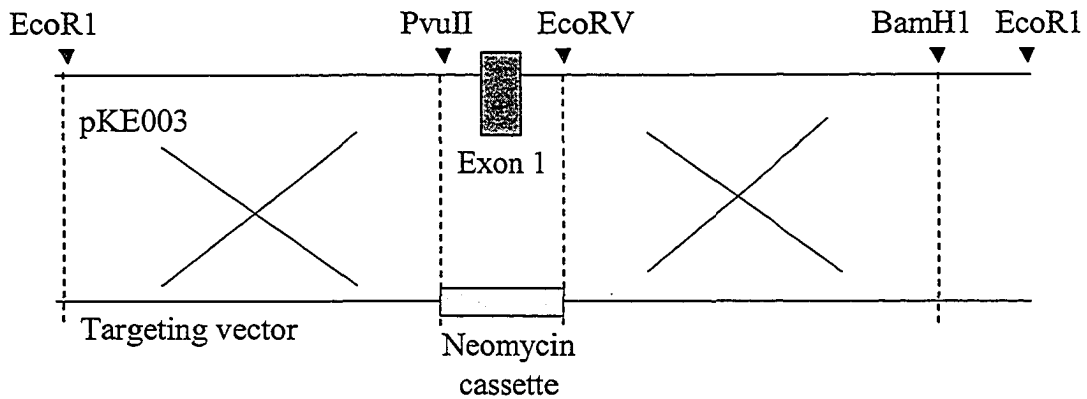
minimum amount of starting material, often the tissue provided did not meet this minimum requirement. Therefore, in order to amplify the amount of genomic starting material the GenomiPhi kit was utilized as described in Figure 4-3b. The GenomiPhi kit allowed amplification of the genomic DNA as shown in Figure 4-4.

4.3.2: Genotyping of the MCD knockout mice by PCR is accurate

Figure 4-5a shows the PCR fragments produced from a wild-type mouse (1.6 Kb), knockout mouse (1.8 Kb) and a heterozygous mouse (1.6 Kb and 1.8 Kb) using the Fgn2/Rgn2 primer set. The genotypes determined by these PCR reactions were confirmed by Western Blot analysis of liver tissue as indicated in Figure 4-5b. These MCD immunoblots show the absence of the 50.7 kDa band of MCD in knockout mouse liver, and the reduction in density of the MCD band in the heterozygous liver compared to livers from wild-type mice. These immunoblots confirm that the PCR reactions using the Fgn2/Rgn2 primers are accurate predictors of the genotype of the animal.

In addition, all PCR products were sequenced to determine that the bands were derived from the MCD gene (data not shown). The accuracy of the Fgn2/Rgn2 primer set was further confirmed by re-amplification of cleaned PCR fragments. Bands from wild-type and knockout mice were purified from a 1% agarose gel and re-amplified using either the Fgn2/Rgn2 primer set to show that the PCR bands are real or with the Fgn2/PGK-1 primer set to show the presence of the neomycin cassette. Figure 4-5c shows that both the 1.6 and 1.8 Kb band can be amplified using the Fgn2/Rgn2 primers, while only the 1.8 Kb band can be further amplified using the neomycin cassette specific primer (PGK-1). These data suggest that the bands produced by the Fgn2/Rgn2 primers

(a)



(b)

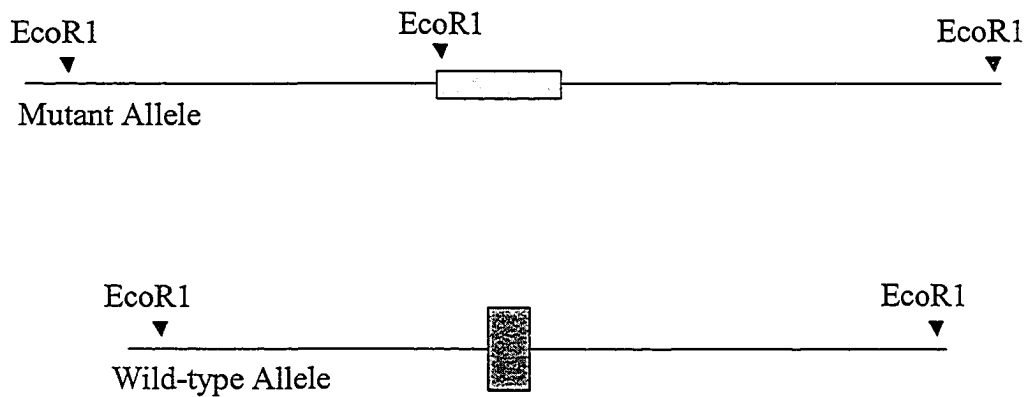


Figure 4-1: Production of MCD knockout mice by a directed homologous recombination event, which removes exon 1 of the MCD gene and replaces it with a neomycin cassette (a). The neomycin cassette is 200bp larger than the existing exon of MCD generating two different size alleles in the heterozygous animal (b).

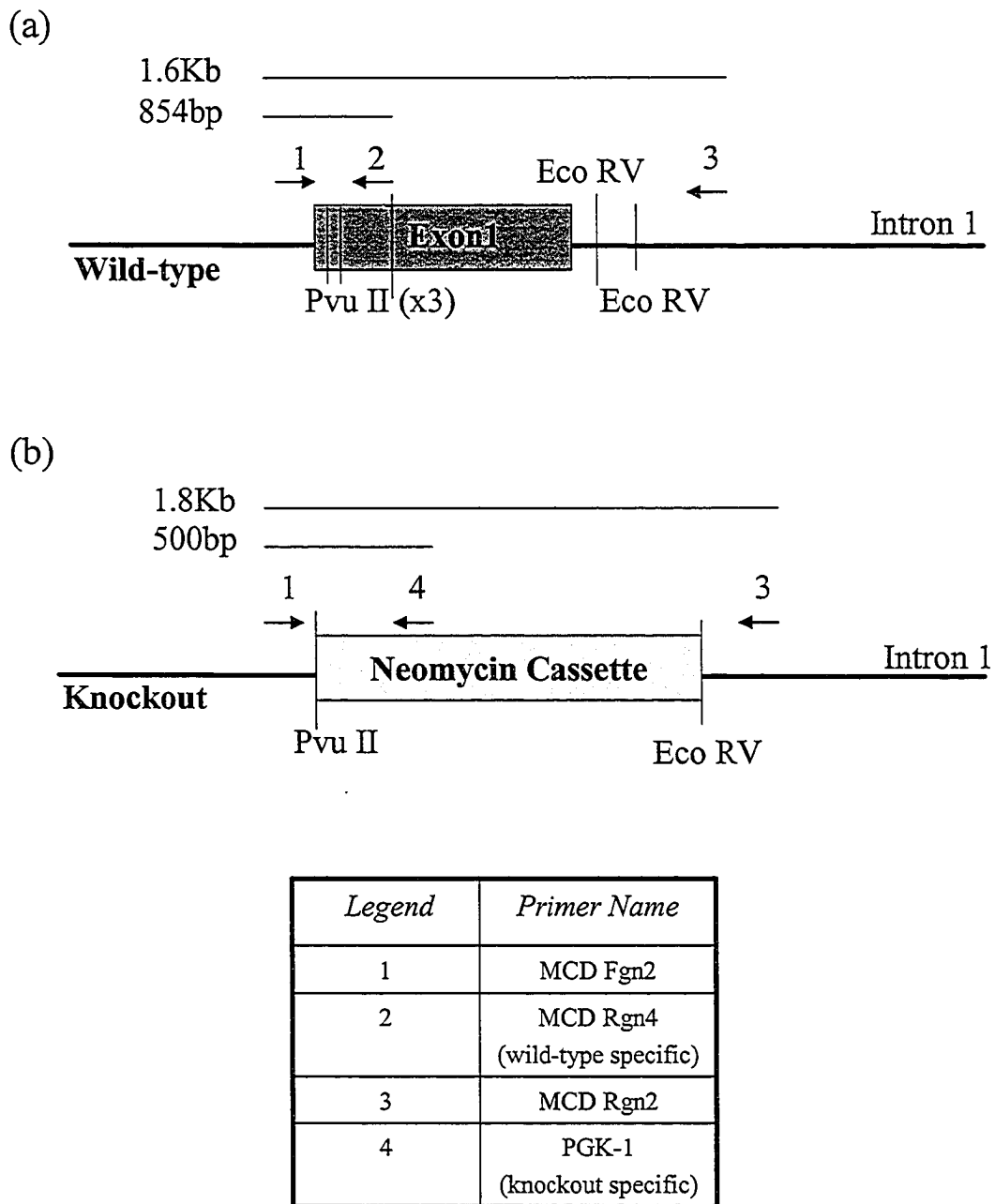
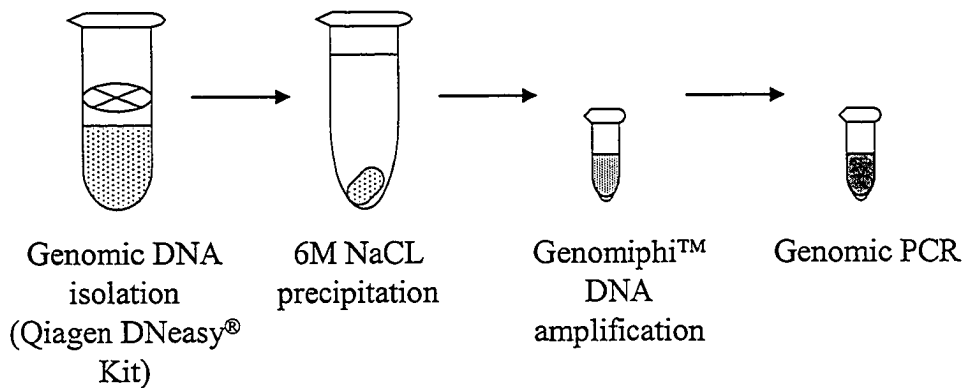


Figure 4-2: Primer design for specific genotyping of each allele. The wild-type allele is recognized by PCR with the Fgn2/Rgn2 primer set that produces a 1.6Kb band and the Fgn2/Rgn4 primer set that produces an 854bp band (a). The knockout allele is recognized by PCR with the Fgn2/Rgn2 primer set that produces a 1.8Kb band and the Fgn2/PGK-1 primer set that produces a 500bp band (b).

(a)



(b)

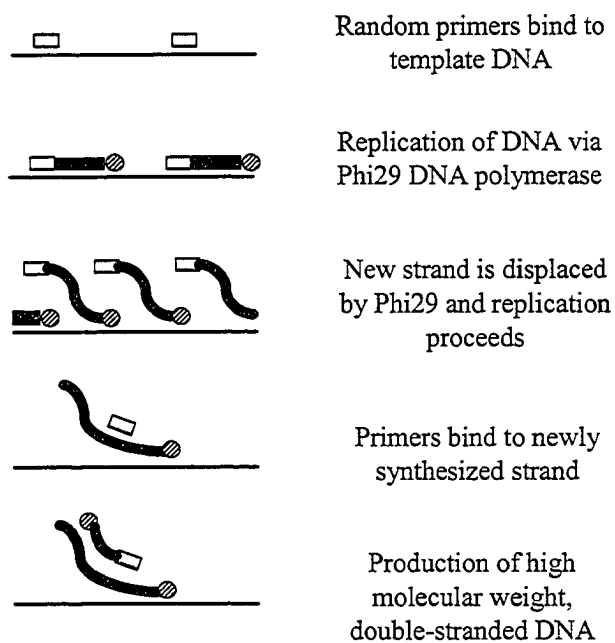
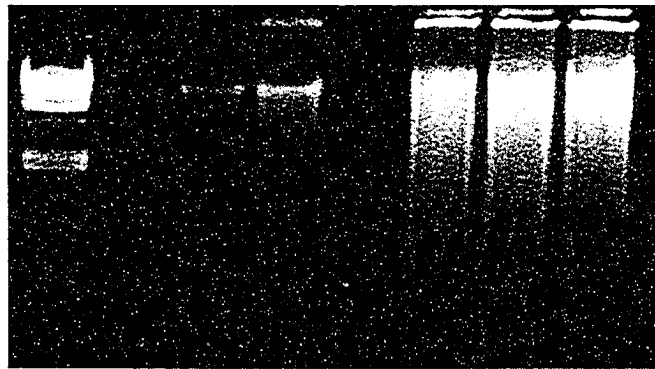


Figure 4-3: The genomic DNA isolation protocol for the MCD knockout mice (a) and detailed mechanism of action of the Genomiphi™ kit (b).



M Genomic DNA Genomiphi amplification

Figure 4-4: GenomiPhi™ amplification of isolated genomic DNA from MCD knockout mice.

are not a result of mis-priming, or short-strand amplification of the same product, and that only the 1.8 Kb band contains a neomycin cassette. Similar results are obtained by the genotyping of heterozygous mice with all three sets of primers, such that the Fgn2/Rgn2 primers produce two bands (1.6 and 1.8 Kb), the Fgn2/Rgn4 primers produce an 854 bp band, and the Fgn2/PGK-1 primers produce a 500 bp band (Figure 4-5d). The 1.8 Kb band re-amplified in Figure 4-5c is faint, however the appearance of the band on the gel was more apparent. The visualization of bands using a digital camera produced a dampening of the brightness of each band.

Taken together, these data demonstrate that the PCR protocol is accurate for the genotyping of the MCD knockout mouse breeding lines, and that this can be achieved using minimal quantities of tissue. The backcross strategy to produce congenic breeding lines of MCD knockout mice and wild-type controls is shown in Figure 4-6.

4.3.3: Metabolic profile of isolated working mouse hearts from MCD knockout mice and control mice

Figure 4-7 shows the loss of both MCD activity and protein in hearts from MCD knockout mice compared to control, as well as the high malonyl CoA levels observed in hearts from the MCD knockout mice. To determine if the lack of MCD protein has an effect on cardiac metabolic substrate preference, isolated working hearts were aerobically perfused for 30 min to measure metabolic rates. Palmitate oxidation rates were significantly higher in wild-type mouse hearts compared to the MCD knockout mouse hearts (Figure 4-8). As well, glucose oxidation rates of MCD knockout mouse hearts were significantly increased compared to wild-type mouse hearts (2.0 ± 0.9 vs. 1.2 ± 0.2

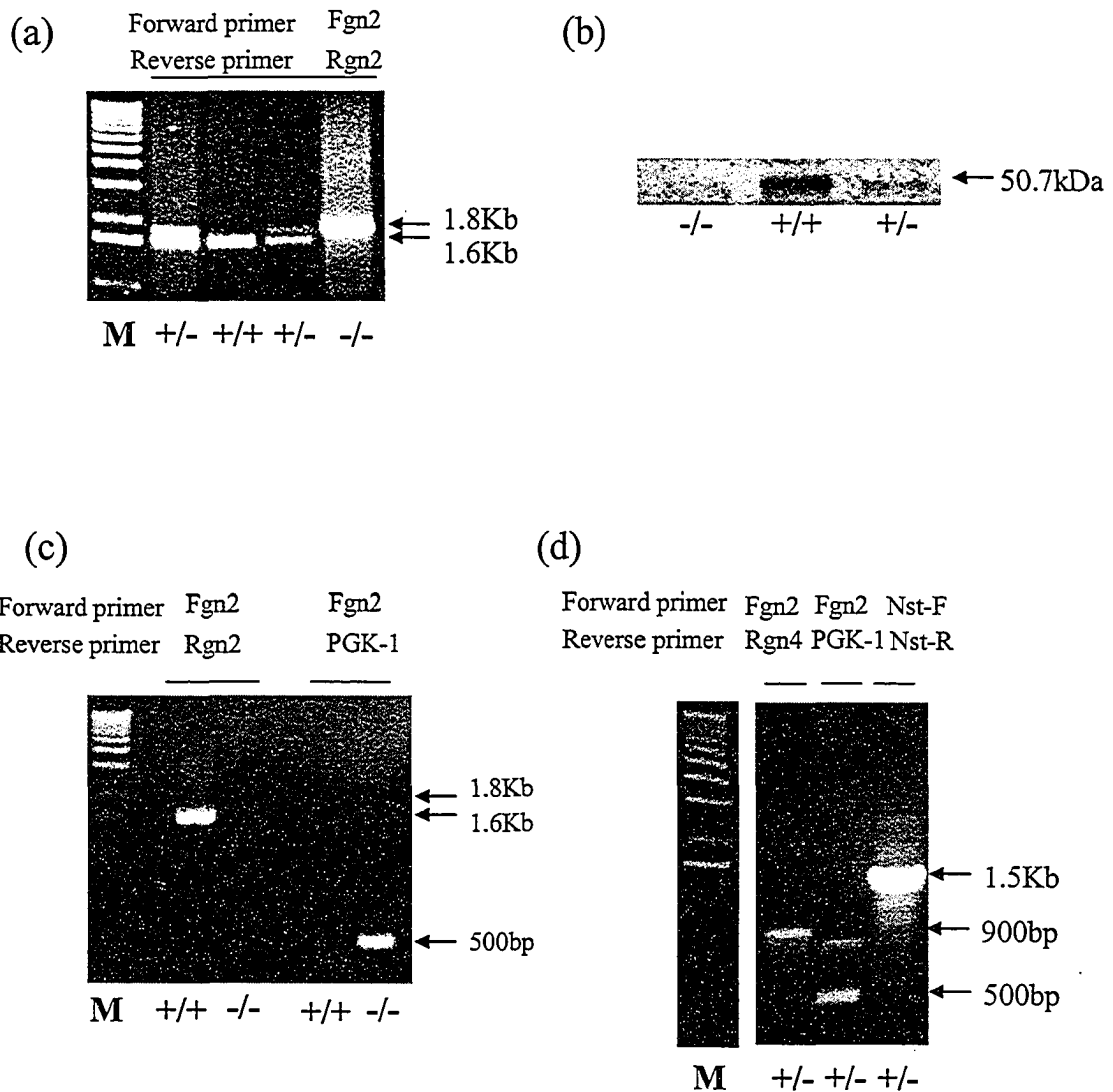


Figure 4-5: Confirmation of genotyping strategy. PCR fragments of wild-type, knockout and heterozygous animals using the Fgn2/Rgn2 primer set (a), Western blots of wild-type, knockout and heterozygous mouse livers using Anti-MCD antibody detects MCD in only wild-type and heterozygous animals (b), Re-amplification of Fgn2/Rgn2 PCR products indicates that only the 1.8Kb band contains a neomycin cassette (c), and confirmation of genotyping strategy using heterozygous animals and control primer sets indicates that the Fgn2/Rgn2 PCR protocol is accurate (d).

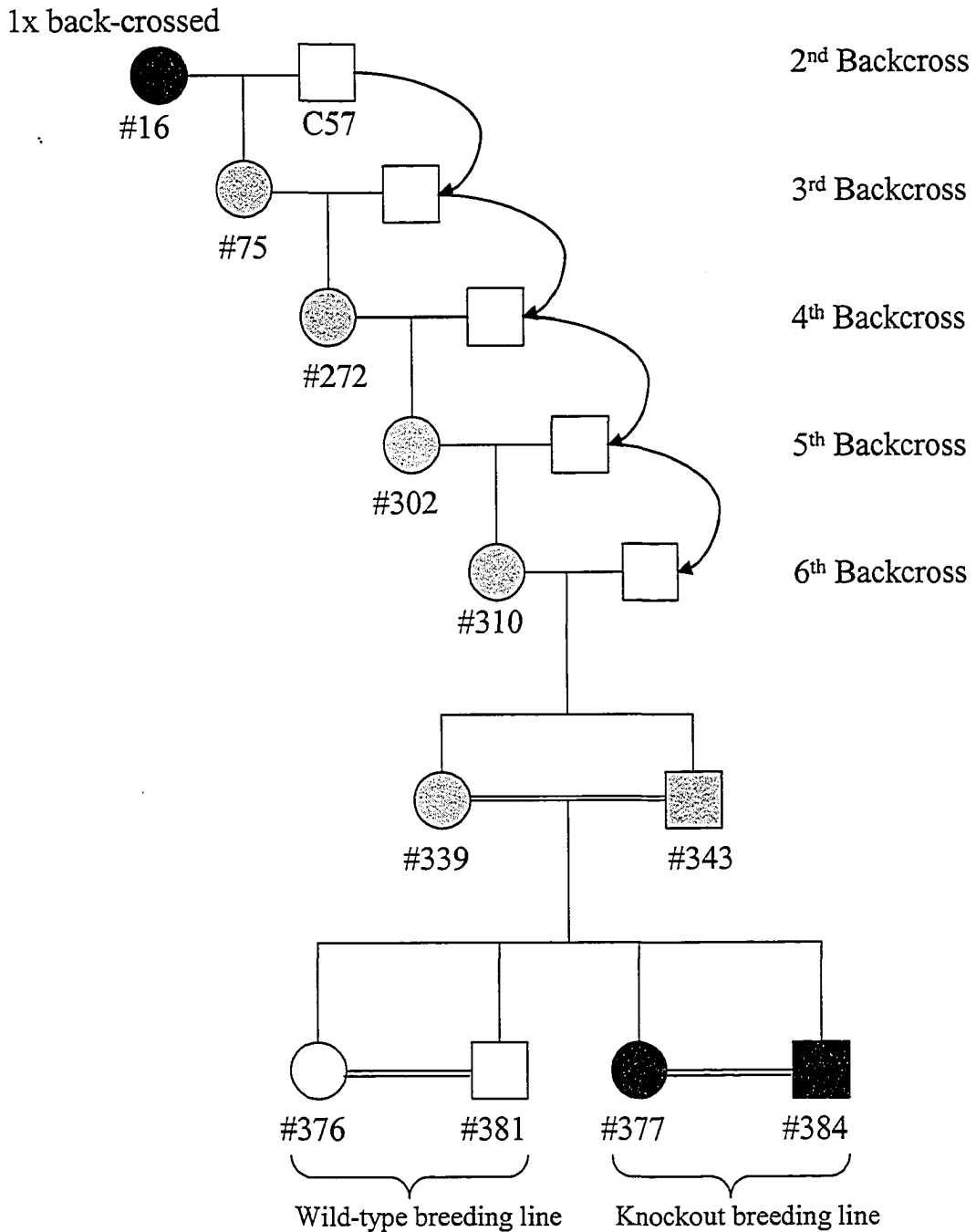


Figure 4-6: MCD knockout mouse backcross strategy. MCD knockout mice were back-crossed six times to a wild-type animal before establishing knockout and wild-type breeding lines. Female animals are represented by circles, while male animals are represented by squares. Gray shapes indicate heterozygous mice, white indicates wild-type and black indicates knockout mice.

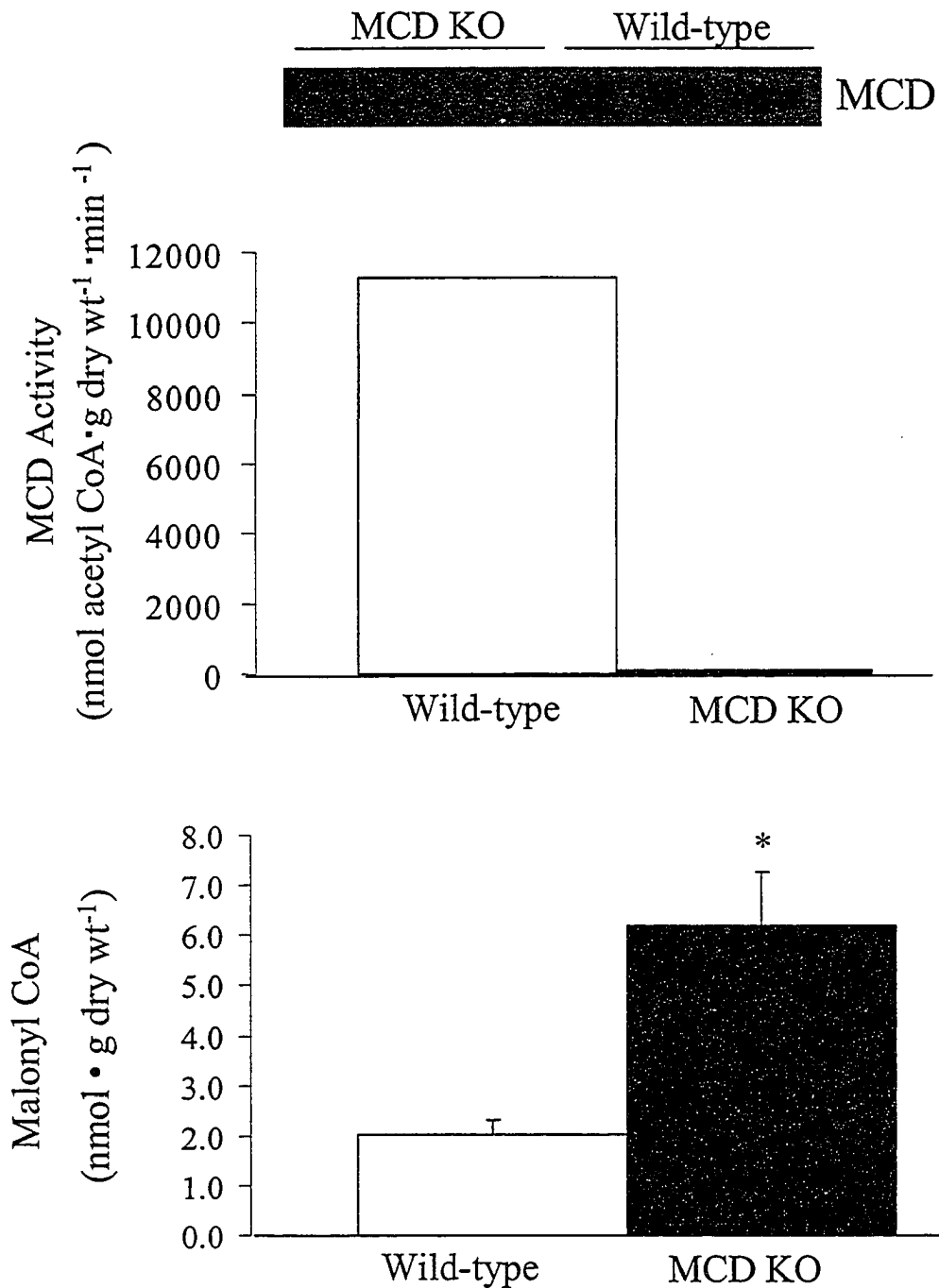


Figure 4-7: Characterization of the MCD knockout mice shows (1) the absence of MCD protein by immunoblot analysis (upper panel), (2) a lack of MCD activity in hearts from MCD knockout mice (middle panel), and (3) malonyl CoA levels were increased in MCD knockout mice compared to control (lower panel). *Significantly different from wild-type hearts; $p < 0.05$.

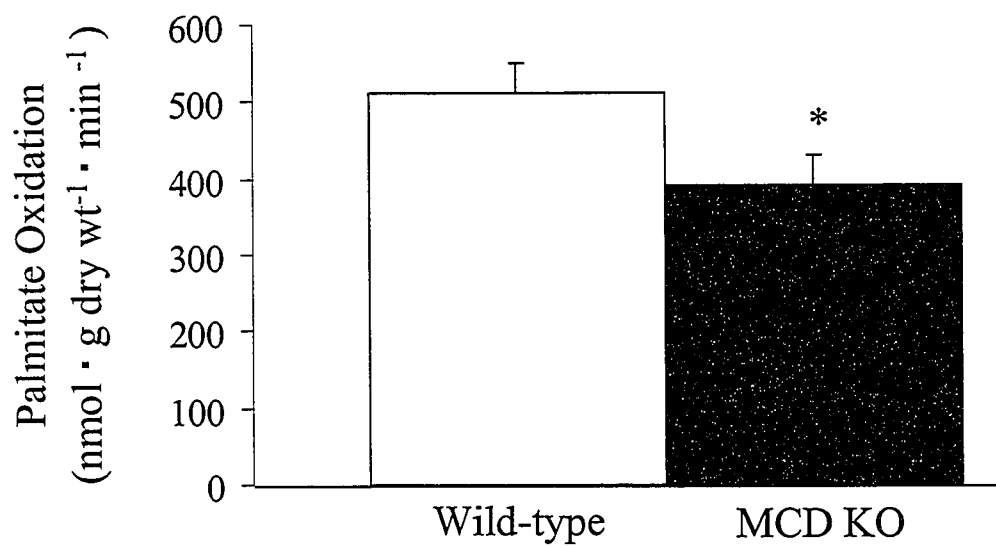


Figure 4-8: Steady state palmitate oxidation rates of wild-type mice (white bars) and MCD knockout mice (black bars) were measured as described in Section 4.2.7 and consist of n=12 wild-type animals and n=14 knockout animals. * Significantly different from wild-type hearts; p<0.05.

$\mu\text{mol}\cdot\text{g dry weight}^{-1}\cdot\text{min}^{-1}$, respectively). Therefore, hearts of mice lacking the MCD protein have a decreased reliance on fatty acids for energy.

4.3.4: mRNA expression analysis by quantitative RT-PCR of PPAR α regulated genes

To determine if these changes in metabolic substrate use were due to alterations in gene expression of metabolic enzymes, real time PCR was used to determine changes in mRNA expression of PPAR α regulated genes including PDK-4, FAT/CD36, UCP-3, FATP, MCAD and FACS. PDK-4 mRNA was increased over 3-fold in the MCD knockout mice vs. wild-type controls (as shown in Figure 4-9a; $p<0.05$). Similarly, mRNA for UCP-3 was increased 100% (Figure 4-9b) and mRNA of FAT/CD36 was increased by approximately 60% (Figure 4-9c) in MCD knockout hearts compared to control hearts ($p<0.05$). The mRNA expression of FATP-1 (Figure 4-9d), FACS (Figure 4-9e) and medium chain acyl CoA dehydrogenase (MCAD) (Figure 4-9f) was not different between MCD knockout mouse hearts compared to wild-type mouse hearts. Increased mRNA expression of a few of these PPAR α regulated genes is increased in the MCD knockout mice, suggesting a possible activation of PPAR α in these animals.

4.3.5: Protein expression of PPAR α regulated enzymes

Since the mRNA expression of PDK4, UCP-3 and FAT/CD36 is increased, we assessed the cardiac protein expression of several PPAR α regulated gene products in hearts from the MCD knockout mice. The protein expression of the PPAR α regulated genes FABPpm, FACS, and FAT/CD36 were not statistically different in MCD knockout mice vs. control as shown in Figure 4-10.

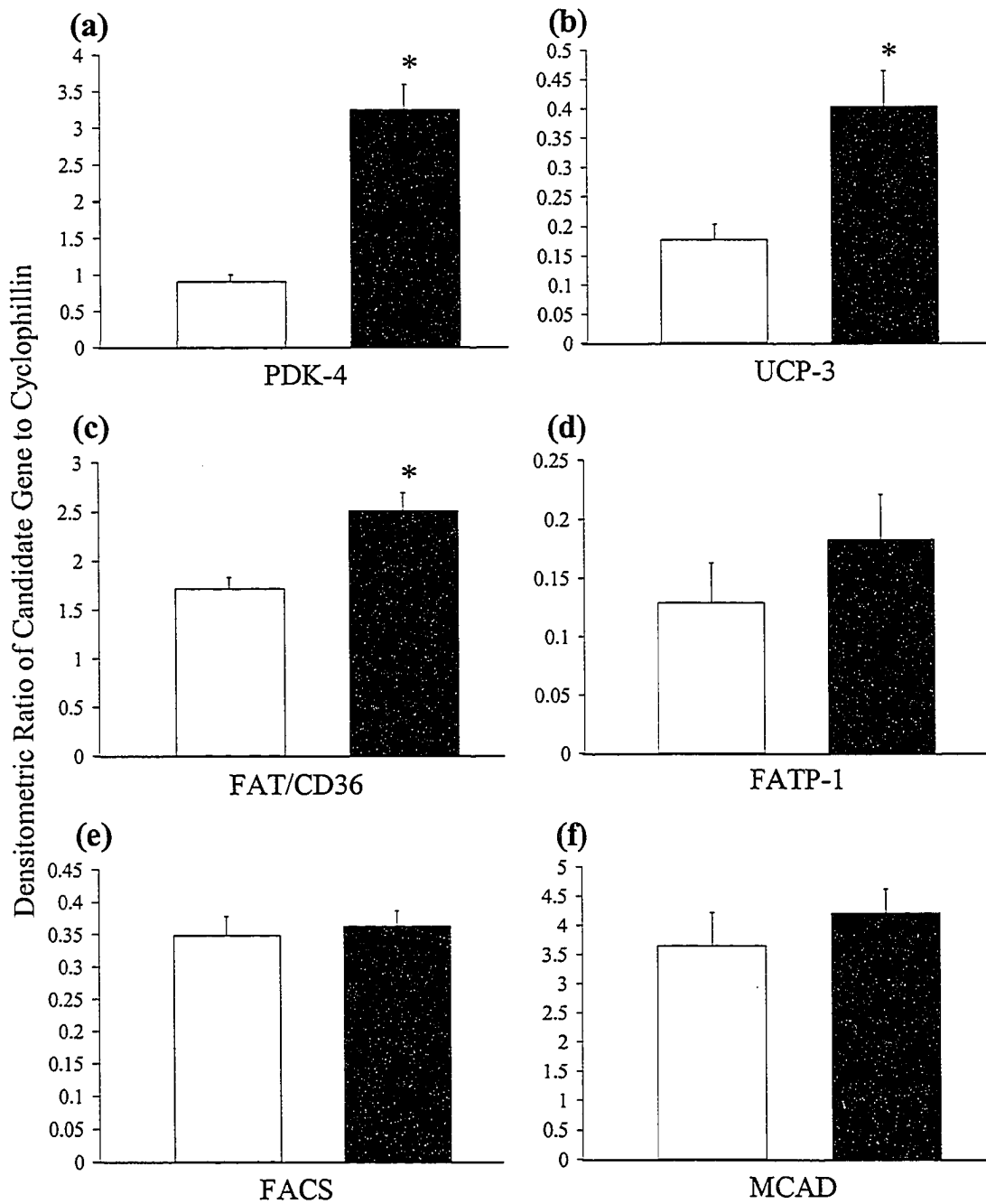


Figure 4-9: Cardiac mRNA expression of several metabolic genes expressed as a ratio to the housekeeping gene cyclophilin. Wild-type mice are represented by the white bars, while the MCD knockout mice are represented by the black bars. Values are expressed as ratio \pm SEM and represent an n of 3 animals in each group. *Significantly different from wild-type hearts; $p < 0.05$.

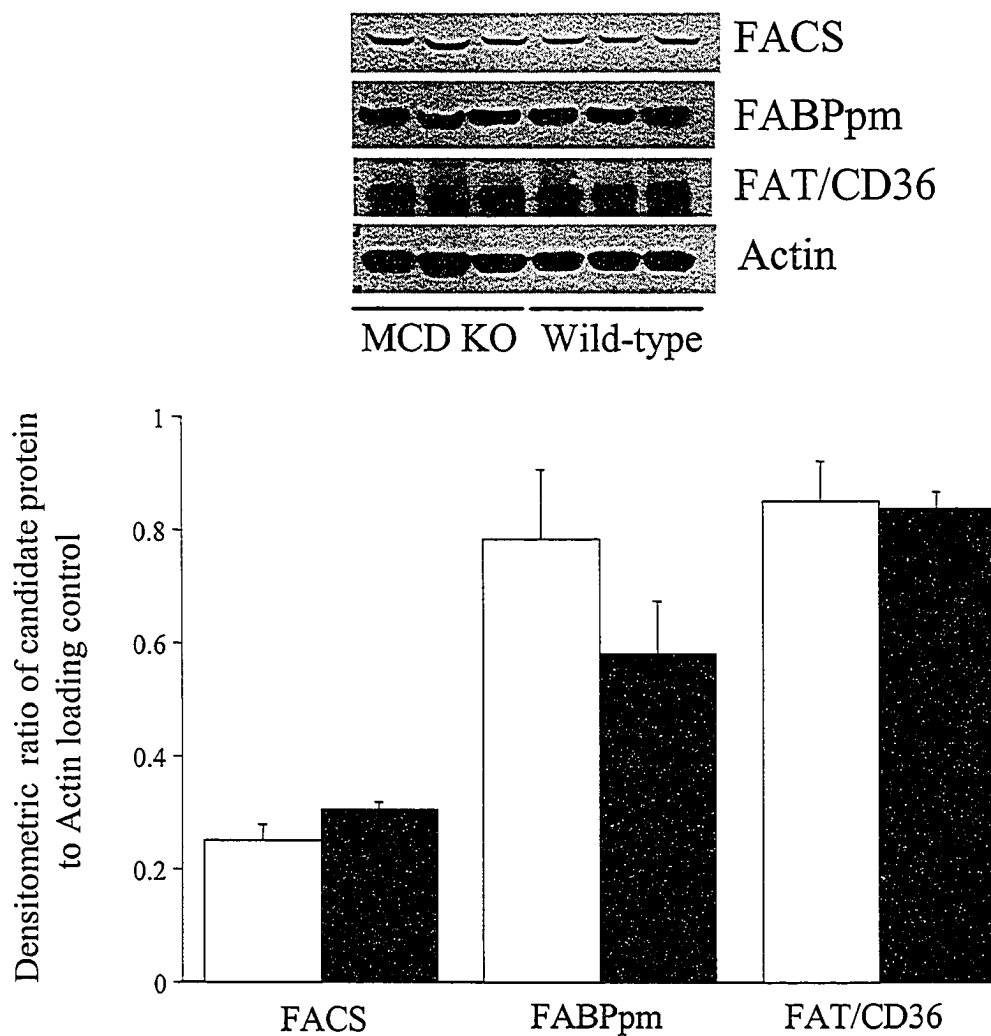


Figure 4-10: Immunoblot analysis of PPAR α regulated genes is not changed in MCD knockout mice compared to control animals (a) and densitometry of the immunoblots normalized to an Actin loading control; white bars represent wild-type mice, while black bars represent MCD knockout mice. (b) (n=3 in each group).

4.3.6: Protein expression of the enzymes involved in regulation of malonyl

CoA levels

Since MCD is an important determinant of malonyl CoA levels in the heart (see Figure 4-7) the MCD knockout mice were evaluated for compensatory changes in expression of ACC and AMPK, which are the enzymes responsible for the rate of malonyl CoA production in the heart. Western blots for ACC, AMPK, phosphorylated ACC, and phosphorylated AMPK of hearts from MCD knockout mice and their wild-type counterparts are shown in Figure 4-11 with densitometry depicted in Figure 4-12. There were no statistically significant changes in protein expression or phosphorylation status of ACC and AMPK between MCD knockout mice and backcrossed control mice. These data suggest that the MCD knockout mice do not compensate for high malonyl CoA levels by reducing the production of malonyl CoA.

4.3.7: PDC activity in MCD knockout mice

Hearts from MCD knockout mice utilize less fatty acids for oxidation, and as expected these hearts also utilize more glucose. Despite this increased reliance on glucose mRNA levels of PDK4 were increased in the mouse hearts. Since a good antibody was not available for us to detect PDK4 expression, we used an indirect measure of PDK4 activity by looking at the amount of PDC in the active form. Therefore, PDC activity was examined in hearts from MCD knockout mice and wild-type mice to determine the effect of increased PDK4 mRNA on PDC activation. Figure 4-13 shows the endogenous and maximal PDC activity in hearts from MCD knockout mice and their control counterparts. The maximal tissue activity of the PDC complex was not different between the wild-type

and MCD knockout mice, suggesting that there was no change in tissue expression of PDC in the heart. However, there was almost a three-fold increase in the amount of PDC in the active form in hearts from the MCD knockout mice vs. control mice. This change in PDC active was not significant as measured by the student's t-test and is likely a result of the small sample number assayed. However, it appears that the phosphorylated form of PDC may be decreased in the MCD knockout mouse hearts. These data do not agree with the mRNA expression of PDK4 obtained. This discrepancy may be due to the lack of change in PDK4 protein levels, which were not measured due to antibody availability. Further studies are required to elucidate the protein level of PDK4 and to determine the control of PDC in MCD knockout mouse hearts compared to control.

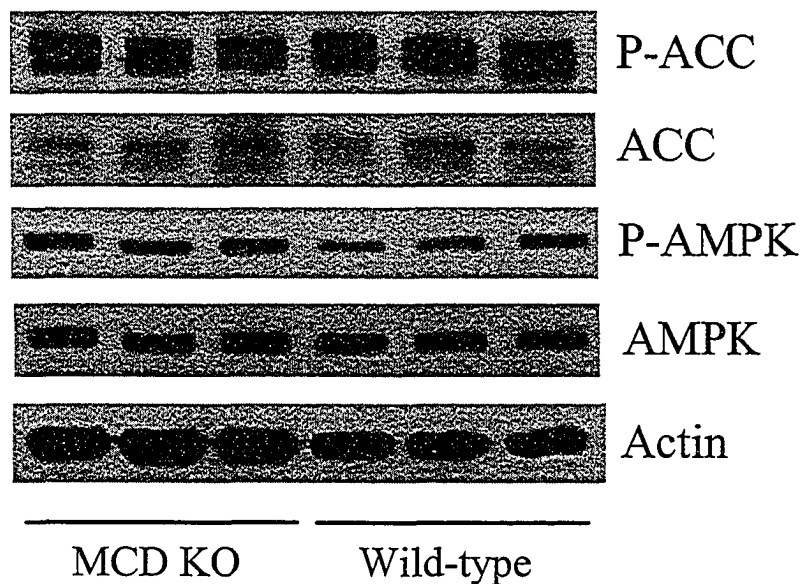


Figure 4-11: Immunoblots to determine expression of enzymes involved in malonyl CoA synthesis in the heart. There are no changes in ACC, AMPK or their phosphorylated forms in the knockout animal when compared to control (n=3 in each group).

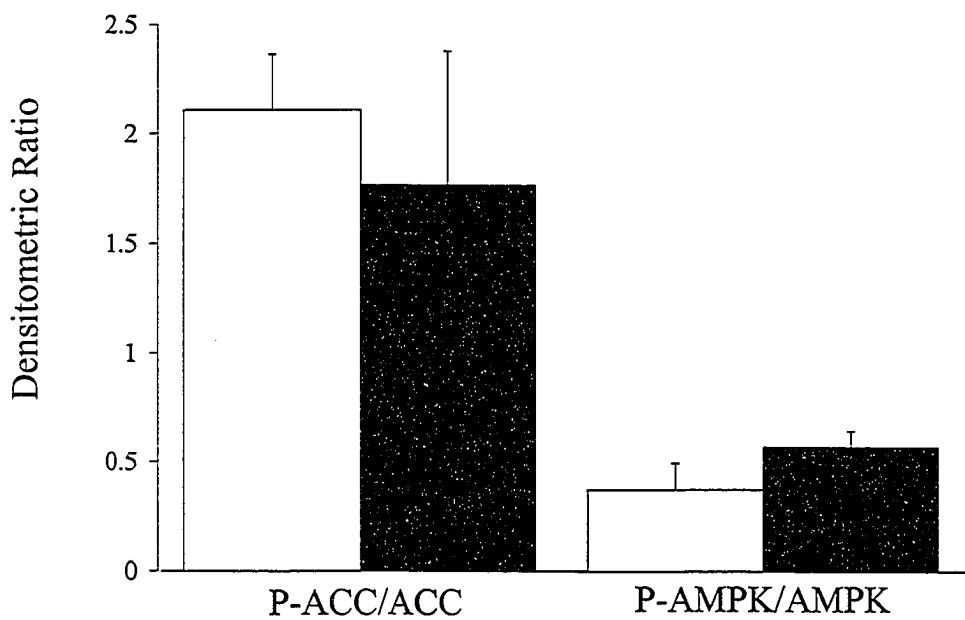
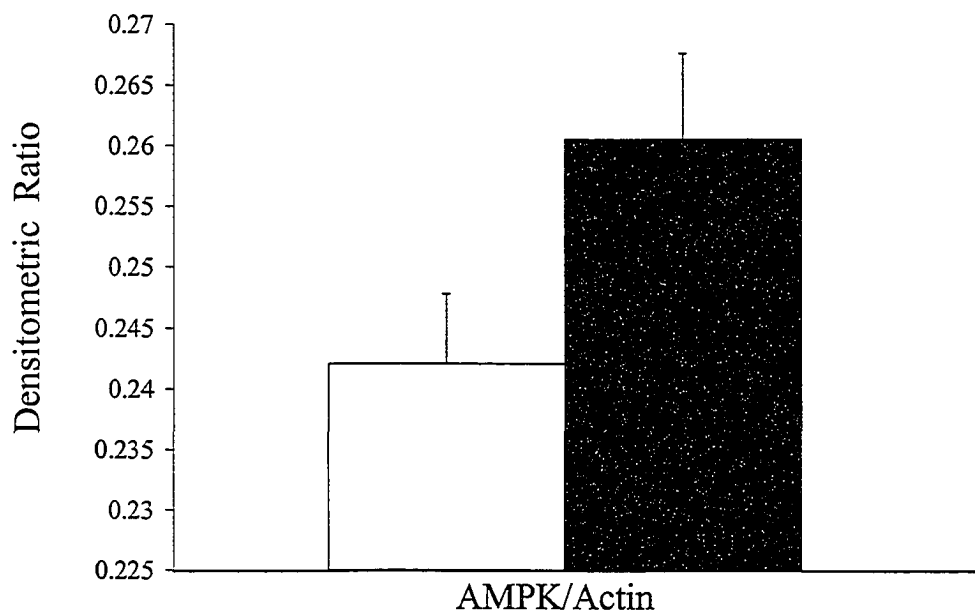


Figure 4-12: Densitometry for immunoblots from Figure 4-11 showing expression of AMPK normalized to Actin expression (a) and showing changes in the level of phosphorylation of ACC and AMPK (b) (n=3 in each group).

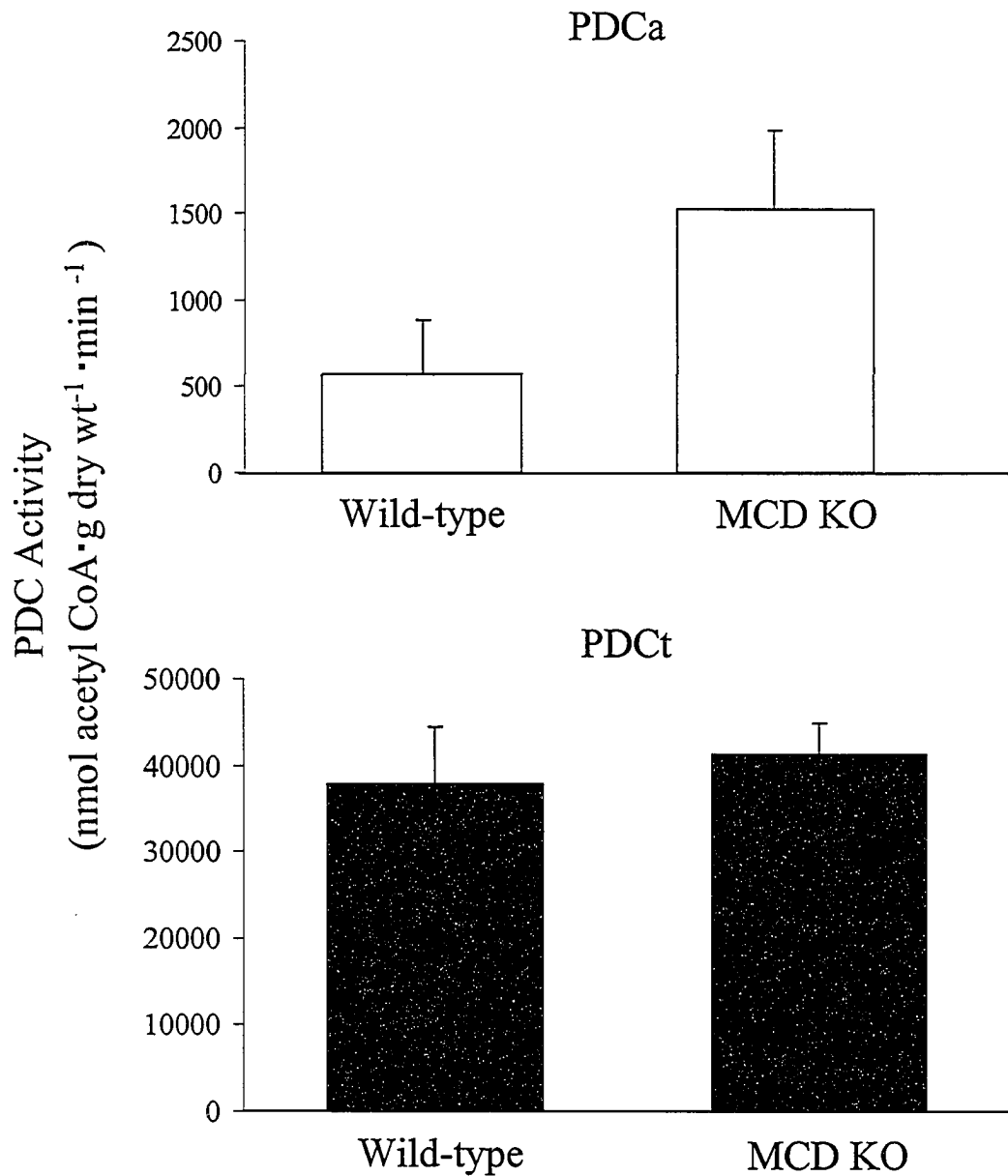


Figure 4-13: Cardiac PDC activity of 3 wild-type mice and 4 MCD knockout mice; PDC in the active form is shown in the upper panel (white bars), while maximal PDC activity (PDC total) is indicated by the black bars in the lower panel. (n=3 in each group)

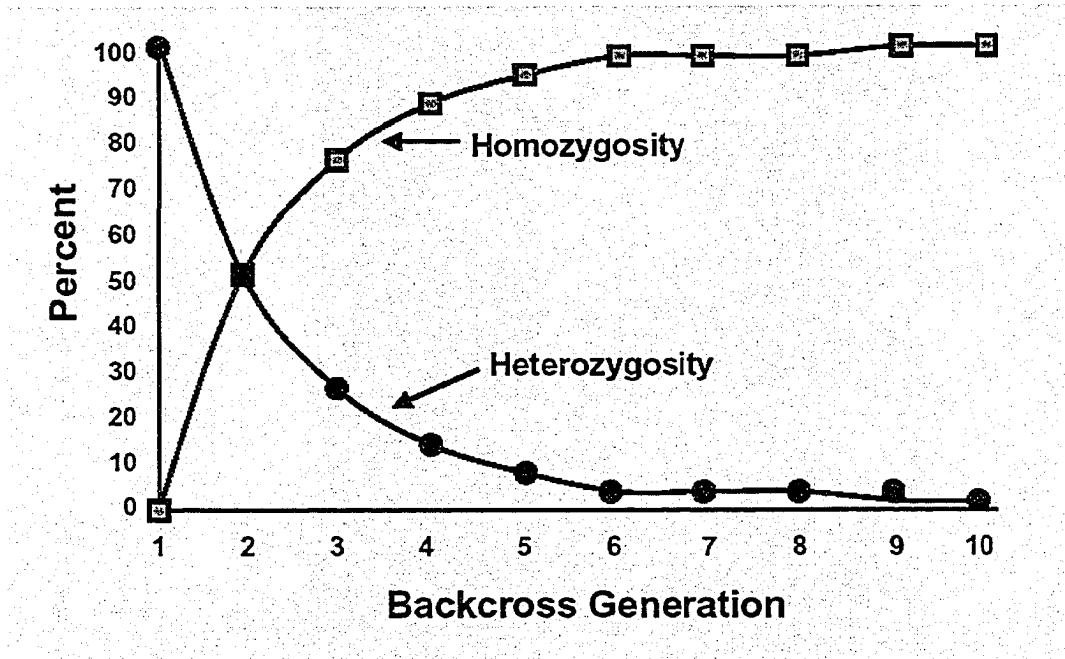


Figure 4-14: The relationship between the number of backcrosses and the level of homozygosity to the background strain of mice (Figure from Silver, L; 1995¹²).

4.4 Discussion

4.4.1: Accuracy of the PCR genotyping method

The PCR protocol developed for the genotyping of the MCD knockout mice is an accurate and efficient protocol that uses small tissue quantities. The use of one PCR reaction (Fgn2/Rgn2) to determine all three possible genotypes is an efficient strategy that allows quick genotyping of animal offspring. The 1.6 Kb and 1.8 Kb bands produced by the Fgn2/Rgn2 primers are reproducible and are specific for the region of DNA around the exon 1 region of MCD. The strand-specific primers (Rgn4 and PGK-1) indicate that only the 1.8 Kb band contains a neomycin cassette and only the 1.6 Kb band contains the exon 1 of MCD, which suggests that the genotyping strategy is correct. To further confirm this accuracy western blots were performed on wild-type and knockout mice, showing the presence of MCD only in the wild-type and heterozygous mice. Taken together, the genotyping strategy developed for these mice is capable of rapid and reproducible results for determining the genotype of each animal.

4.4.2: Phenotype of MCD knockout mice

The MCD knockout mice have no noticeable abnormalities and no overt phenotype. The mice do not develop diabetes as might be expected since MCD overexpression has been shown to improve insulin sensitivity⁸. MCD activation has been proposed as a potential therapy for diabetes by lowering malonyl CoA levels, accelerating fatty acid oxidation rates and reducing lipotoxicity. However, the lack of diabetic phenotype in the MCD knockout mice suggests that the high levels of malonyl CoA observed in diabetes are not causative for the pathological progression of diabetes.

Since MCD activation should accelerate fatty acid oxidation in the heart, this therapy may worsen ischemia/reperfusion injury, and evidence from our lab suggests that MCD inhibitors are a novel therapy for patients with ischemic heart disease ⁶. The hearts of MCD knockout mice are more resistant to ischemia/reperfusion injury and are more reliant on glucose for energy ¹⁷, suggesting that MCD inhibition is a good therapy for the prevention of ischemia/reperfusion injury. Taken together, these data suggest that the MCD knockout mice do not have any observable disease phenotype, despite the persistent elevation in malonyl CoA levels, suggesting that chronic MCD inhibition may be a safe and effective therapy.

In humans a very severe metabolic disorder has been attributed to a loss of MCD activity ¹⁸⁻²⁰. However, the MCD knockout mice generated do not appear to have these metabolic symptoms, suggesting that the human disorder may be the result of multiple gene mutations. Some studies have reported cases of malonic aciduria in the absence of a malonyl CoA decarboxylase deficiency ^{18,21,22}. It is also possible that the MCD knockout mice have a method to compensate for elevated malonyl CoA levels, although it does not appear to be due to a reduction in malonyl CoA production by ACC. Despite these possible compensation mechanisms, the MCD knockout mice are an important tool to help determine the role of MCD in cardiac function, as well as whole body metabolism.

4.4.3: Backcrosses

Most knockout animals are generated using donor mouse embryonic stem cells from a different strain of mice than the recipient strain to enhance homologous recombination ^{23, 24}. Although the preferred background for the MCD knockout mice

were the C57 BL6 mice, the MCD knockout mice were made with AB2.2-prime stem cells. While the AB2.2-prime stem cells lacking the MCD gene were injected into C57 BL6 blastocysts, the donor stem cell line still maintains the genotype of the AB2.2-prime stem cells. Therefore, in order to have the knockout mice on the desired C57 BL6 background, the knockout line must be backcrossed to a wild-type C57 BL6 background at least four times. Figure 4-15 shows the number of backcross generations required to reach homozygosity with the recipient mouse strain. At least six backcrosses are required to have a line approximately 99% identical to the C57 BL6 background and a further four backcrosses to reach 99.25-99.95% similarity ¹². For our purposes, we backcrossed the MCD knockout mice six times, but used four times backcrossed animals for immunoblot and RT-PCR analysis. However, since we used congenic wild-type lines produced from littermates with the same number of backcrosses we could determine changes due to the lack of MCD in the four times backcrossed knockout mice.

4.4.4: Metabolic profile of MCD knockout mice

Hearts from the MCD knockout mice have a decreased reliance on fatty acids as a source of energy, presumably due to the high levels of cardiac malonyl CoA and inhibition of mitochondrial fatty acid uptake. These low rates of fatty acid oxidation may relieve Randle cycle inhibition of the PDC complex and as expected the MCD knockout mice have increased rates of glucose oxidation compared to control. Due to both this metabolic profile and the improved recovery of hearts treated with MCD inhibitors ⁶, we can speculate that hearts from these mice would have improved functional recovery following an ischemic episode. Presumably the glucose utilization pathways would be

matched in the MCD knockout mice to prevent proton accumulation and calcium overload in the heart. Therefore, these data further confirm that MCD inhibition may be an important therapy for ischemic heart disease. Since these animals appear healthy and their hearts are not energy compromised, chronic MCD inhibition may be a safe method for treating ischemic heart disease.

4.4.5: Expression of proteins involved in malonyl CoA regulation

Immunoblot analysis of the MCD knockout mice was performed in order to determine if there are any long-term changes in gene expression with chronic MCD inhibition. There was no compensation for the absence of MCD with changes in protein expression or phosphorylation status of ACC or AMPK, suggesting that chronic inhibition of MCD does not lead to compensational changes in the control of malonyl CoA levels that may limit the usefulness of the therapy.

4.4.6: mRNA and protein expression of PPAR α regulated genes

Other long-term changes in enzymes of cardiac energy metabolism were also determined. The protein expression of several PPAR α regulated genes, including FAT/CD36, FACS and FABPpm were not altered in the MCD knockout mice versus control mice. However the mRNA expression of PDK-4, FAT/CD36, and UCP-3 were increased in the MCD knockout mice, suggesting that the reduced fatty acid oxidation rates cause an accumulation of free fatty acids that activate PPAR α and up-regulate genes involved in fatty acid oxidation. The reason for the discrepancy between protein expression and mRNA expression is likely due to the sensitivity of the protocols, such

that RT-PCR analysis of mRNA expression is much more sensitive than immunoblotting for protein expression. Similarly, changes in mRNA expression are often more dramatic than the changes in protein expression observed. Therefore, large changes in mRNA expression may translate to only a small degree of change in the level of protein expression.

This effect was also observed with the increased mRNA expression of PDK4 in the MCD knockout mice, which is not accompanied by a decrease in PDCa activity. Either the increased mRNA of PDK4 does not translate to a change in protein expression or there is a mismatch between PDK4 expression and PDC activity as shown in Chapter 2 of this thesis.

A further explanation for increased mRNA expression in the absence of enhanced protein expression is the circadian rhythm of mRNA expression observed in the heart²⁵,²⁶. Since mRNA levels can change dramatically over the course of a 24 hour period²⁷, the animals were sacrificed at the peak of mRNA expression for metabolic genes. Therefore, there may be a lag time due to protein synthesis and protein expression may not be evident at this time point. Whether these changes in mRNA expression are maintained for enough time to alter protein expression is unknown.

4.4.7: Limitations

As with every study, there were several limitations to the characterization of the MCD knockout mice. Transgenic animals have limitations, which arise from compensation that may not be directly attributed to the change in genotype. As well, our study utilized mRNA analysis that was not followed directly by protein expression

measurements of these same gene products. The protein levels of PDK4 and UCP3 were not investigated due to the lack of commercial antibody availability. In addition, PDK4 mRNA appears to increase almost 4-fold but there is also a potential increase in the activity of PDC in the active form. An increase in 'n' numbers of the PDC measurements or an investigation of PDK4 protein level in the MCD knockout mice may help explain this discrepancy. The limitations in this study make it difficult to interpret the data but we suggest that the metabolic profile of MCD knockout mice is more reliant on glucose than their wild-type counterparts.

4.4.8: Summary

In summary, the MCD knockout mice exhibit a decreased reliance on fatty acids as a cardiac substrate vs. control hearts. The alteration in metabolic substrate preference of MCD knockout mouse hearts is associated with a significantly increased mRNA expression of PDK4, UCP-3 and FAT/CD36, which suggests that PPAR α activation may occur in these animals. However, the protein levels of FAT/CD36, FACS, and FABPpm were not significantly altered in hearts from MCD knockout mice compared to control. The increase in PDK4 expression observed in hearts from MCD knockout mice was not associated with a change in PDCa activity in the MCD knockout hearts. The lack of protein expression changes and PDCa activity suggest that the mRNA expressional changes may not lead to functional alterations in metabolic substrate use in these hearts. The MCD knockout mice will be an important tool for future studies examining the role of MCD in various tissues and pathologies.

Literature Cited

1. McGarry, J.D., Leatherman, G.F., & Foster, D.W. Carnitine palmitoyltransferase I. The site of inhibition of hepatic fatty acid oxidation by malonyl-CoA. *J. Biol. Chem.* **253**, 4128-4136 (1978).
2. Dyck, J.R., Barr, A.J., Barr, R.L., Kolattukudy, P.E., & Lopaschuk, G.D. Characterization of cardiac malonyl-CoA decarboxylase and its putative role in regulating fatty acid oxidation. *Am. J. Physiol.* **275**, H2122-H2129 (1998).
3. Kudo, N., Barr, A.J., Barr, R.L., Desai, S., & Lopaschuk, G.D. High rates of fatty acid oxidation during reperfusion of ischemic hearts are associated with a decrease in malonyl-CoA levels due to an increase in 5'-AMP-activated protein kinase inhibition of acetyl-CoA carboxylase. *J. Biol. Chem.* **270**, 17513-17520 (1995).
4. Kudo, N. *et al.* Characterization of 5'AMP-activated protein kinase activity in the heart and its role in inhibiting acetyl-CoA carboxylase during reperfusion following ischemia. *Biochim. Biophys. Acta* **1301**, 67-75 (1996).
5. Saddik, M., Gamble, J., Witters, L.A., & Lopaschuk, G.D. Acetyl-CoA carboxylase regulation of fatty acid oxidation in the heart. *J. Biol. Chem.* **268**, 25836-25845 (1993).
6. Dyck, J.R. *et al.* Malonyl coenzyme a decarboxylase inhibition protects the ischemic heart by inhibiting fatty acid oxidation and stimulating glucose oxidation. *Circ. Res.* **94**, e78-e84 (2004).
7. Yano, S., Sweetman, L., Thorburn, D.R., Mofidi, S., & Williams, J.C. A new case of malonyl coenzyme A decarboxylase deficiency presenting with cardiomyopathy. *Eur. J. Pediatr.* **156**, 382-383 (1997).
8. An, J. *et al.* Hepatic expression of malonyl-CoA decarboxylase reverses muscle, liver and whole-animal insulin resistance. *Nat. Med.* **10**, 268-274 (2004).
9. King, M.T., Reiss, P.D., & Cornell, N.W. Determination of short-chain coenzyme A compounds by reversed-phase high-performance liquid chromatography. *Methods Enzymol.* **166**, 70-79 (1988).
10. Lopaschuk, G.D., Witters, L.A., Itoi, T., Barr, R., & Barr, A. Acetyl-CoA carboxylase involvement in the rapid maturation of fatty acid oxidation in the newborn rabbit heart. *J. Biol. Chem.* **269**, 25871-25878 (1994).
11. Jishage, K. *et al.* Alpha-tocopherol transfer protein is important for the normal development of placental labyrinthine trophoblasts in mice. *J. Biol. Chem.* **276**, 1669-1672 (2001).

12. Silver,L. Laboratory Mice in *Mouse Genetics: Concepts and Applications* 32-61 (Oxford University Press, New York, New York, 1995).
13. Belke,D.D., Larsen,T.S., Lopaschuk,G.D., & Severson,D.L. Glucose and fatty acid metabolism in the isolated working mouse heart. *Am. J. Physiol.* **277**, R1210-R1217 (1999).
14. Saddik,M. & Lopaschuk,G.D. Myocardial triglyceride turnover and contribution to energy substrate utilization in isolated working rat hearts. *J. Biol. Chem.* **266**, 8162-8170 (1991).
15. Depre,C. *et al.* Unloaded heart in vivo replicates fetal gene expression of cardiac hypertrophy. *Nat. Med.* **4**, 1269-1275 (1998).
16. Constantin-Teodosiu,D., Cederblad,G., & Hultman,E. A sensitive radioisotopic assay of pyruvate dehydrogenase complex in human muscle tissue. *Anal. Biochem.* **198**, 347-351 (1991).
17. Dyck,J.R.B. *et al.* Hearts from Malonyl CoA Decarboxylase Null Mice are Protected from Ischemic Damage. *Circulation* . 2004.
Ref Type: Abstract
18. Gregg,A.R., Warman,A.W., Thorburn,D.R., & O'Brien,W.E. Combined malonic and methylmalonic aciduria with normal malonyl-coenzyme A decarboxylase activity: a case supporting multiple aetiologies. *J. Inherit. Metab. Dis.* **21**, 382-390 (1998).
19. MacPhee,G.B. *et al.* Malonyl coenzyme A decarboxylase deficiency. *Arch. Dis. Child* **69**, 433-436 (1993).
20. Wightman,P.J. *et al.* MLYCD mutation analysis: evidence for protein mistargeting as a cause of MLYCD deficiency. *Hum. Mutat.* **22**, 288-300 (2003).
21. O'Brien,D.P. *et al.* Malonic aciduria in Maltese dogs: normal methylmalonic acid concentrations and malonyl-CoA decarboxylase activity in fibroblasts. *J. Inherit. Metab Dis.* **22**, 883-890 (1999).
22. Ozand,P.T., Nyhan,W.L., al,A.A., & Christodoulou,J. Malonic aciduria. *Brain Dev.* **16 Suppl**, 7-11 (1994).
23. Leiter,E.H. Mice with targeted gene disruptions or gene insertions for diabetes research: problems, pitfalls, and potential solutions. *Diabetologia* **45**, 296-308 (2002).
24. Sigmund,C.D. Viewpoint: are studies in genetically altered mice out of control? *Arterioscler. Thromb. Vasc. Biol.* **20**, 1425-1429 (2000).

25. Young, M.E., Razeghi, P., & Taegtmeier, H. Clock genes in the heart: characterization and attenuation with hypertrophy. *Circ. Res.* **88**, 1142-1150 (2001).
26. Young, M.E., Wilson, C.R., Razeghi, P., Guthrie, P.H., & Taegtmeier, H. Alterations of the circadian clock in the heart by streptozotocin-induced diabetes. *J. Mol. Cell. Cardiol.* **34**, 223-231 (2002).
27. Stavinoha, M.A. *et al.* Diurnal variations in the responsiveness of cardiac and skeletal muscle to fatty acids. *Am. J. Physiol. Endocrinol. Metab.* **287**, E878-E887 (2004).

Chapter 5

General Discussion

This chapter summarizes some of the findings presented in the previous chapters; relates them to the current understanding in the field and to possible therapeutic applications, as well as to propose future research goals.

5.1 MCD localization, control of MCD activity and the role of peroxisomal MCD

5.1.1: Peroxisomal oxidation and MCD

The studies described in Chapter 3 show that the majority of MCD in neonatal rat cardiac myocytes is present in cardiac peroxisomes. Although a post-translational cleavage event may occur, the retention of the MYC tag on our fusion proteins suggest that the smaller isoform of MCD present in neonatal rat cardiac myocytes is likely the result of translation from the second translational start site similar to MCD produced in the goose uropygial gland ¹.

While our data suggest that cardiac MCD appears to be located predominantly in the peroxisomes, the role of MCD in the peroxisome remains unclear. Emerging evidence suggests that peroxisomal oxidation is an important source of acetyl CoA for malonyl CoA production ². This peroxisomal derived malonyl CoA regulates CPT-1, suggesting that peroxisomal oxidation regulates mitochondrial fatty acid oxidation ². In order to understand the function of peroxisomal MCD, further studies are required to elucidate substrate transport and control of metabolism in the peroxisome. Therefore, studies into peroxisome function may involve the search for a malonyl CoA shuttle mechanism which would facilitate malonyl CoA import into peroxisomes.

Alternatively, it is possible that malonyl CoA does not need to be transported into the peroxisome but rather is produced within the peroxisome itself. Production of malonyl CoA may occur within peroxisomes by the presence of a yet unidentified peroxisomal ACC isoform or by oxidation of odd-chain dicarboxylic acids. Mitochondrial production of malonyl CoA is postulated to be the result of propionyl CoA carboxylase (PCC) activity on acetyl CoA³, which may in turn inhibit methylmalonyl CoA mutase³⁻⁵. However, it is unknown if the oxidation of fatty acids in the peroxisome could also result in the production of malonyl CoA through this mechanism or whether enzymes sensitive to malonyl CoA inhibition are present in the peroxisome.

Current evidence suggests that malonyl CoA production by ACC can only occur in the cytosol⁶, thus as acetyl CoA is not membrane permeable, a mechanism is required to export acetyl CoA from the peroxisome for malonyl CoA production. The mechanism for acetyl CoA export does not appear to be due to acetylcarnitine or acetate export in the rat heart². This area of investigation warrants further study and may help to understand the regulation and compartmentalization of malonyl CoA in the heart. The role of the cardiac peroxisome in oxidation of fatty acids is poorly understood, but in light of the high expression of MCD in these organelles future experiments should be directed to the study of peroxisomal oxidation and how it regulates mitochondrial fatty acid oxidation rates in the heart. These issues of substrate transport and metabolic regulation are depicted in Figure 5-1. These studies may provide insight into the role of MCD and peroxisomal metabolism in the heart.

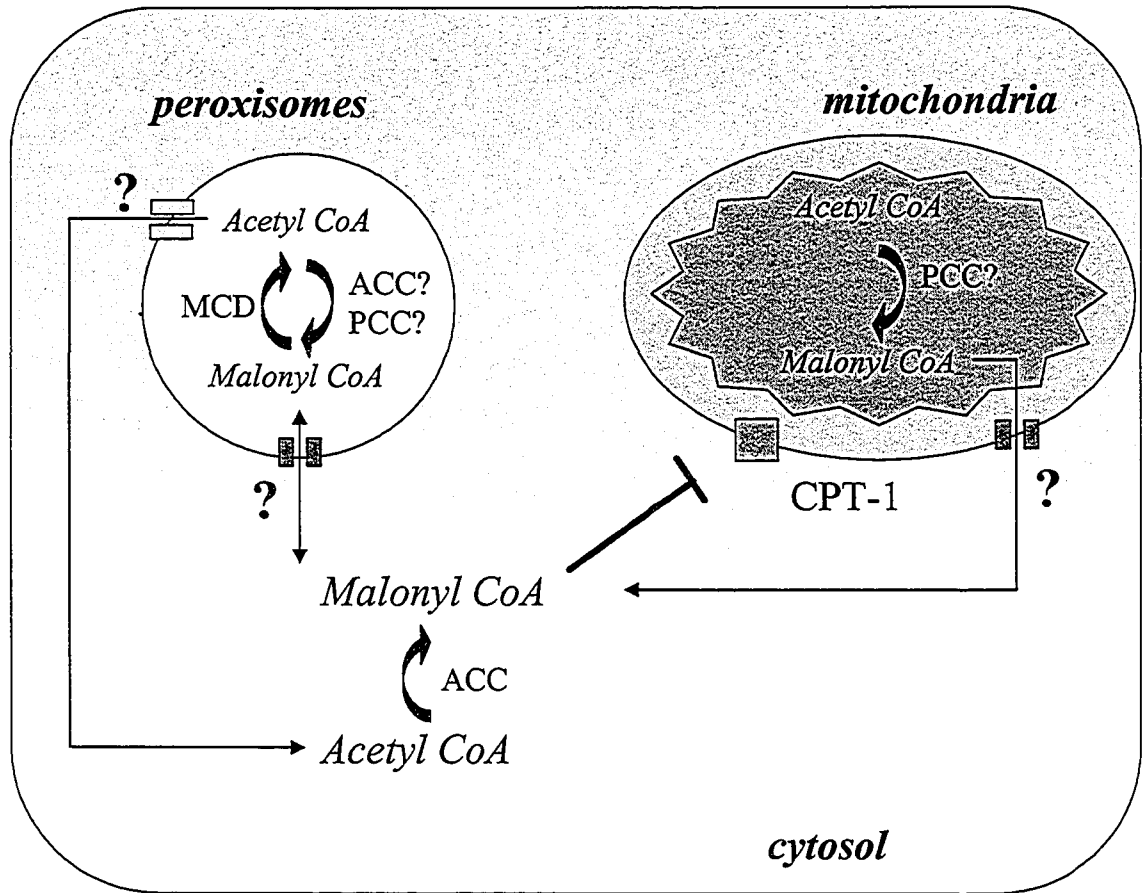


Figure 5-1: Summary of subcellular control of malonyl CoA levels in the myocyte at the current level of understanding assuming a peroxisomal distribution of MCD.

5.1.2: Malonyl CoA compartmentalization issues

The peroxisomal localization of MCD raises a major issue into the subcellular control of malonyl CoA levels. The total tissue level of malonyl CoA in the heart is enough to completely inhibit CPT-1 activity at the cytosolic face of the CPT-1 protein. However, extensive evidence shows that fatty acid oxidation is an important source of energy for the heart and thus CPT-1 is not completely inhibited. This discrepancy led to the hypothesis that malonyl CoA exists in distinct subcellular compartments such that only a small proportion of malonyl CoA resides in the cytosol. The question that arises is how peroxisomal MCD can dramatically alter malonyl CoA levels in the cytosol in the absence of a known malonyl CoA shuttle. MCD is currently thought to be the main method of malonyl CoA disposal potentially implying that peroxisomes act as a malonyl CoA sink, protecting CPT-1 by lowering cytosolic malonyl CoA levels. The data presented in Chapter 3 cannot rule out the possibility of MCD associated with the external surface of the peroxisome with access to cytosolic malonyl CoA, despite hydrophobicity studies of MCD which suggest that MCD is a hydrophilic protein with no membrane spanning regions (data not shown). How malonyl CoA is sequestered into various compartments is unknown and it is not possible at this time to visualize malonyl CoA in the cell. Thus future studies are required to determine the movement of malonyl CoA across the peroxisomal membrane, the exposure of MCD to the cytosol, and the regulation of cytosolic malonyl CoA levels.

5.1.3: Control of MCD localization

Although cardiac MCD is predominantly peroxisomal, the control of MCD localization may be tissue-specific. For example, the cDNA sequence of rat islet cells is very similar to that of the rat heart sequence, but the rat pancreatic islet cells express two MCD isoforms (50.7 and 54.7 kDa), while the rat heart expresses only the 50.7 kDa isoform. This suggests that a level of translational control exists for MCD isoform expression in different tissues.

Since both MCD isoforms are a result of one MCD gene in all tissues ⁷, the question remains what signals the production of one or both of the MCD isoforms. There appears to be only one mRNA transcript produced in various tissues ⁸ suggesting that the translation of the protein mediated by the Kozak sequence may be one determinant of MCD isoform expression. For example, in the heart the second start site may have a better Kozak consensus sequence to initiate translation, which may be more efficient than the first ATG on the MCD transcript ⁹. Thus, the second translational start site may be preferentially used in the rat heart, while the first translational start site may be more important for translation of the islet MCD isoforms. Initiation of translation generally occurs at the first Kozak sequence beginning at the 5' end of an mRNA transcript, however a Kozak sequence may be bypassed in a process known as 'leaky scanning' ¹⁰. This could lead to the production of two proteins, which may differ at the N-terminus and therefore may have different targeting to intracellular organelles or different levels of activity. Although our studies show that the different length MCD fusion proteins have altered intracellular targeting, the activity of the fusion proteins did not differ. Further studies are needed to elucidate the control of translation on the MCD transcript.

Assuming that only the first translational start site is functional on each mRNA transcript it is tempting to suggest that the presence of two MCD isoforms in islet cells is due to post-translational cleavage of the full-length MCD similar to that observed with the goose liver MCD protein ¹. Although our data suggest that the smaller isoform of cardiac MCD is not cleaved following translation, we cannot rule out the possibility that entry into the mitochondria involves a cleavage event that may render a smaller MCD product that may not react with the H240 MCD antibody. In such a case, lack of mitochondrial MCD visualization may be due to the loss of the H240 epitope by the formation of protein complexes or cleavage. Therefore, the immunocytochemistry studies performed may be unable to detect mitochondrial MCD. Perhaps immunogold labeling of purified mitochondria will indicate the presence of MCD in cardiac mitochondria. Future studies are needed to determine if there is a mitochondrial form of MCD in the heart and whether this mitochondrial MCD is modified by post-translational modification.

Although it is believed that only one mRNA transcript of MCD is produced ^{1,8}, it is possible that alternate splicing may occur in certain tissues or under certain conditions. Activation of nuclear receptors including PPAR α may regulate the transcription of different mRNA species. Since these transcription factors may be activated under different nutritional states, it is plausible that the composition of fats in the diet may affect the isoform of MCD expressed and localized. For example, one might expect that diets rich in omega-3 fatty acids, which are oxidized in the peroxisome and activate PPAR α , may increase MCD expression in the peroxisome. Diets richer in short to medium chain fatty acids may encourage high MCD expression in the mitochondria where they are oxidized. Future studies using animals treated with various diets are

needed to show whether changes in expression or localization of MCD occur and how MCD localization is controlled.

5.2 MCD Knockout mice

MCD plays an important role in the degradation of malonyl CoA, which in turn influences fatty acid oxidation rates. MCD inhibition has been proposed as a potential treatment for ischemic heart disease and MCD inhibitors protect the heart following ischemia ¹¹. Thus, the MCD knockout mice were created to further explore the contribution of MCD to fatty acid oxidation rates in the aerobic and ischemic heart.

Preliminary studies (described in Chapter 4) indicate that PPAR α may be activated in hearts from the MCD knockout mice. However, since not all of the genes measured were up-regulated it is unknown if PPAR α is responsible for these observed changes in expression. Indeed PDK4 is also regulated by thyroid hormone ¹², PPAR δ ¹³ and the farnesoid X receptor ¹⁴. FAT/CD36 may also be regulated by PPAR γ ¹⁵ and UCP3 mRNA may be controlled by thyroid hormone ¹⁶. Therefore, it may be premature to suggest that PPAR α activity is the only reason for increased expression of these proteins in the MCD knockout mice.

Despite this unresolved issue, the continued use of MCD knockout mice may provide insight into the role of MCD in cardiac metabolism as well as metabolism in other tissues. Since MCD inhibition has been shown to prevent ischemia/reperfusion injury ¹¹, this therapy may also reduce infarct size following a myocardial infarction. Left anterior descending artery occlusion of MCD knockout mice could predict the effect of MCD inhibition on infarct size generation. Since MCD inhibition appears to prevent

cardiac injury, likely due to a reduction in proton and lactate accumulation, it is expected that MCD knockout mice will have a reduced infarct size compared to control. This may lead to the possible future use of MCD inhibitors in the treatment of myocardial infarction.

Another observation regarding the MCD knockout is the lack of evidence of a global detrimental metabolic disorder, although MCD deficiency has been implicated as a factor for malonic aciduria in humans. The MCD knockout mice have shown that a global loss of MCD is not sufficient to cause the formation of a metabolic disorder, which is consistent with some studies indicating the presence of malonic aciduria with normal MCD activity in humans¹⁷⁻¹⁹. Therefore, future studies should be directed at determining the cause of malonic aciduria in humans, which appear to be the result of mutations in more than one gene. The MCD knockout mice may be a good tool to study polygenic causes of malonic aciduria through pharmacological manipulation using selective inhibitors, or dominant negative gene transfer studies. These studies would target other gene products involved in oxidation of fatty acids that when combined with MCD deficiency may lead to this metabolic disorder.

5.3 Treatment of ischemic heart disease

5.3.1: Metabolic modulation in the treatment of ischemic heart disease

Metabolic modulation in the treatment of ischemic heart disease has a very promising future. The use of metabolic agents may be superior to other treatments, since there are few effects on cardiovascular function including blood pressure and heart rate. This unique feature allows metabolic modulators to be used as an adjunct therapy to

existing therapies with few problems. Metabolic modulation has potential applications beyond preventing injury following ischemia/reperfusion, as discussed throughout this thesis, including the prevention of anginal pain, diabetic cardiomyopathy and reduction in infarct size. These forms of ischemic heart disease may benefit from the use of partial fatty acid oxidation inhibitors to enhance glucose use and improve cardiac efficiency.

Pharmacological agents that partially inhibit fatty acid oxidation such as trimetazidine and ranolazine are currently on the market in several countries world-wide for the treatment of angina. Several other agents have shown efficacy in the research setting, including etomoxir (a CPT-1 inhibitor), propionyl L-carnitine and dichloroacetate (a PDK inhibitor). However, the search continues for new agents and new pharmacological targets to treat ischemic heart disease. Therefore, the pharmacological potential of agents directed at the modulation of PDK, MCD and PPAR α activity will need to be explored.

5.3.2: Modulation of PDK activity

The studies in Chapter 2 of this thesis show that in mice over-expressing PPAR α , PDC phosphorylation does not control glucose oxidation rates as effectively as the action of the Randle cycle on PDC activity. This study suggests that a multi-level control of PDC activity exists in the heart. The impact of this end-product regulation of PDC is not fully understood and further studies could elucidate the contribution of allosteric regulation of PDC to glucose oxidation rates. The evidence from our study and others ²⁰, ²¹ suggest that the amount of PDC in the active form is not an accurate predictor of glucose oxidation rates and a direct metabolic measurement of glucose utilization may be

required for an accurate assessment. Therefore since there is more than one level of glucose oxidation control at the level of PDC, the question remains whether PDK inhibition would be a reliable pharmacological target for treatment of ischemic heart disease.

The PDK inhibitor dichloroacetate appears to be efficacious in enhancing glucose oxidation rates and cardiac recovery of working hearts both *in vitro* and *in vivo*^{20, 22-32}. This wealth of evidence regarding dichloroacetate use in enhancing glucose oxidation rates and cardiac recovery cannot be ignored. In order to reconcile our study with these previous studies, further experiments involving treatment of the MHC-PPAR α mice with dichloroacetate would determine if glucose oxidation rates can be enhanced in these animals via PDK inhibition. It is possible that under the control of dichloroacetate, the allosteric regulation of PDC may become only a minor component of glucose oxidation rate control. In addition, perfusions of the MHC-PPAR α mouse hearts in the presence of high fat (1.2 mM palmitate vs. 0.4 mM palmitate used previously) may increase PDK activity via increased acetyl CoA and NADH levels^{33, 34}. Therefore, the contribution of PDK phosphorylation to glucose oxidation rates may become more evident. Since diabetic hearts and previously ischemic hearts are exposed to high levels of fatty acids, this model may be a better method to determine whether phosphorylation or allosteric control of PDC is more important for controlling glucose oxidation rates.

5.3.3: Modulation of PPAR α activity

PPAR α agonists from the fibrate family cause an up-regulation of fatty acid oxidizing enzymes and PDK4 expression, which exerts a coordinated control over the

two opposing metabolic pathways to promote fatty acid utilization. The efficacy of PPAR α agonists in the treatment of various forms of ischemic heart disease is unknown and may be difficult due to the multiplicity of PPAR α agonism on whole body metabolism. For instance, one study shows that 24 hour pre-treatment with PPAR α agonists protects the heart during ischemia/reperfusion injury in a mouse model ³⁵. However, the reduction in plasma lipids in the treated mice may be the mechanism of cardioprotection in this setting rather than a direct effect of PPAR α upregulation in the heart ³⁵. A second study suggests that PPAR α agonists reduce infarct size in a transiently ligated mouse model of myocardial infarction ^{36, 37}. However, the agonists were given only 30 minutes prior to the insult ^{36, 37}, suggesting that this might not be an effect of protein upregulation by PPAR α and the agonist may have a direct action on the myocardium itself independent of PPAR α . Both of these studies involve acute treatments with a PPAR α agonist for less than a week. Therefore the cardioprotective role of PPAR α is unclear and although these agonists appear to reduce cardiac injury, the long term effects of PPAR α activation were not examined in these studies. We might suspect that chronic PPAR α activation may lead to a diabetic cardiomyopathy as is observed in mice over-expressing cardiac PPAR α ³⁸. Taken together, the therapeutic potential of PPAR α agonists in the treatment of ischemic heart disease is difficult to predict. Acute PPAR α activation appears to reduce infarct size ^{35-37, 39}. However, the long-term effects of PPAR α activation on fatty acid oxidation in the heart may have the opposite effect. With evidence to indicate that high fatty acid oxidation rates impair cardiac recovery following ischemia, it seems that inhibition of PPAR α may be more

effective than activation. However, a loss of PPAR α activity has been associated with cardiac hypertrophy⁴⁰ and will likely limit the use of PPAR α inhibitors. The role of PPAR α in the setting of heart failure and diabetic cardiomyopathy is still being debated. While the success of PPAR α agonism is unknown, the inhibition of MCD may be a better pharmacological therapy for ischemic heart disease.

5.4.4: Modulation of MCD activity

Fatty acid oxidation rates can be manipulated by treatment with MCD inhibitors, which prevents malonyl CoA degradation and inhibits CPT-1 mediated mitochondrial fatty acid uptake. Acute inhibition of MCD has already shown promise in the treatment of ischemia/reperfusion injury in a rat model, while chronic loss of MCD (as evidenced by the MCD knockout mice) does not appear to have a negative impact on cardiac function nor cause compensatory mechanisms that would limit the usefulness of MCD inhibition therapy. MCD inhibitors do not affect pre-perfusion cardiac function of *ex vivo* working rat hearts suggesting that these inhibitors have negligible cardiac side effects. Both acute and chronic inhibition of MCD in rodents suggests that MCD inhibition may be a safe and effective treatment for angina, myocardial infarction and surgical ischemia. While there is insufficient evidence regarding toxicity from the use of MCD inhibitors in humans, the health and vitality of the MCD knockout mice in terms of cardiac recovery and insulin sensitivity (See Section 5.4) suggests that MCD inhibition may be a promising new therapy for ischemic heart disease. Of the three pharmacological targets described in these studies MCD appears to have the most promise in the treatment of ischemic heart disease.

5.4 Metabolic modulation of insulin sensitivity

Pharmacological treatments directed at PDK, MCD and PPAR α modulation may also be effective in the treatment of other disease states including insulin resistance and diabetes. Pharmacological inhibition of PDK in diabetes may increase glucose disposal and lower plasma glucose levels. However, whether PDK inhibition may be an effective pharmacological target for diabetes is unknown. One complicating factor is the presence of four different isoforms of PDK, which display distinct characteristics. The expression of PDK4 is dramatically increased during diabetes and fasting⁴¹⁻⁴⁴. However, PDK4 is less sensitive to inhibition by pyruvate than the other isoforms⁴⁵, and the effect of dichloroacetate (a pyruvate analog) may be similarly decreased⁴⁶. Therefore, further study into the role of PDK in the treatment of diabetes is required.

PPAR α agonists have a potent lipid-lowering effect and the role of PPAR α in the treatment of diabetes is emerging. PPAR α activation has been suggested to promote fatty acid oxidation rates, decrease the high plasma free fatty acids levels associated with diabetes and improve insulin sensitivity. In fact PPAR α activation has been shown to improve plasma glucose levels in *db/db* mice^{47, 48} and improve insulin sensitivity in fatty rats⁴⁹. A reduction in lipid accumulation in skeletal muscle due to enhanced fatty acid oxidation is associated with improved insulin sensitivity^{50, 51}. Unfortunately, since PPAR α activation would also enhance fatty acid oxidation rates in the heart, the effect of these agents on diabetic cardiomyopathies and ischemic heart disease may be detrimental. Similarly, PPAR α has a potential role in cardiac lipotoxicity and progression of diabetic cardiomyopathy⁵⁰⁻⁵². Pharmacological activation of PPAR α should therefore be used with caution in diabetic patients with cardiomyopathies or increased risk of

cardiovascular disease. Indeed, PPAR α agonists may worsen lipotoxicity via increased uptake of fatty acids, which may accumulate in the form of triglycerides. Further studies are needed to determine the best treatment for insulin sensitivity with the least side effects. Activation of PPAR γ may remain the best treatment for diabetes, since there are less direct effects on the myocardium.

MCD activation may be another possible treatment for diabetes and to prevent diabetic cardiomyopathy⁵³. However, the MCD knockout mice have persistently elevated levels of malonyl CoA, but this does not appear to cause diabetes. Another study utilizing overexpression of MCD confirms this observation and shows an increased rate of fatty acid oxidation in the islet cell, which may prevent glucose stimulated insulin secretion^{54, 55}. This suggests that MCD inhibition may improve insulin secretion but whether insulin sensitivity would also be improved was not determined. Another factor affecting the pathogenesis of insulin resistance and diabetes is the presence of obesity. Inhibition of MCD in the hypothalamus may raise malonyl CoA levels and promote satiety. The lack of diabetes observed in the MCD knockout mice may also be due to a difference in food uptake and satiety. Previous work has shown that high malonyl CoA levels in the hypothalamus reduce food intake in mice⁵⁶⁻⁵⁸. Since the MCD knockout mice would be expected to have high hypothalamic malonyl CoA levels, the lack of diabetes onset may be due to differences in fuel intake. Therefore, MCD inhibition may also reduce the incidence of obesity, which is a risk factor for the pathogenesis of diabetes and ischemic heart disease. High fat feeding studies of the MCD knockout mice or cross-breeding the MCD knockout mice with an obesity mouse model may provide further insight into the role of MCD in obesity and insulin resistance. Future studies of

the MCD knockout mice regarding food intake, metabolic disposal of fuels and uptake of fat by the gut may increase the understanding of MCD in food intake regulation.

Although the mechanism of improved insulin sensitivity in the MCD knockout mice is unknown, the control of fatty acid oxidation rates in skeletal muscle may be an important determinant of insulin sensitivity. A reduction in fatty acid oxidation rates may increase glucose utilization and disposal from plasma, thereby reducing glucose levels and improving insulin sensitivity. Further studies are needed to determine whether inhibiting fatty acid oxidation rates by inhibiting MCD will be a successful treatment strategy for diabetes.

5.5 Summary

In summary, the novel observations of these studies have helped discover some important points regarding enzymatic control of glucose and fatty acid oxidation. The studies involving the control of the PDC complex using PPAR α over-expressing mice indicate that the Randle cycle plays a substantial role in the regulation of PDC activity. Novel approaches into the study of MCD localization suggest that while both putative targeting sequences are functional, MCD is localized mainly to the peroxisomes in the heart. Studies of the MCD knockout mice show that these mice have lower rates of fatty acid oxidation than wild-type mice and this may be associated with an activation of PPAR α . Overall the results from the MCD knockout mice provide further support that MCD may be a promising pharmacological treatment for ischemic heart disease and diabetes. However, the role of PDK and PPAR α modulation requires further

investigation. Hopefully the data shown in this thesis will provide knowledge that will further aid in the treatment of ischemic heart disease.

Literature Cited

1. Courchesne-Smith, C. *et al.* Cytoplasmic accumulation of a normally mitochondrial malonyl-CoA decarboxylase by the use of an alternate transcription start site. *Arch. Biochem. Biophys.* **298**, 576-586 (1992).
2. Reszko, A.E. *et al.* Peroxisomal fatty acid oxidation is a substantial source of the acetyl moiety of malonyl-CoA in rat heart. *J. Biol. Chem.* **279**, 19574-19579 (2004).
3. Scholte, H.R. The intracellular and intramitochondrial distribution of malonyl-CoA decarboxylase and propionyl-CoA carboxylase in rat liver. *Biochim. Biophys. Acta* **178**, 137-144 (1969).
4. Kim, Y.S. & Kolattukudy, P.E. Purification and properties of malonyl-CoA decarboxylase from rat liver mitochondria and its immunological comparison with the enzymes from rat brain, heart, and mammary gland. *Arch. Biochem. Biophys.* **190**, 234-246 (1978).
5. Landriscina, C., Gnoni, G.V., & Quagliariello, E. Properties of malonyl-CoA decarboxylase and its relation with malonyl-CoA incorporation into fatty acids by rat liver mitochondria. *Eur. J. Biochem.* **19**, 573-580 (1971).
6. Abu-Elheiga, L. *et al.* The subcellular localization of acetyl-CoA carboxylase 2. *Proc. Natl. Acad. Sci. U. S. A* **97**, 1444-1449 (2000).
7. Jang, S.H., Cheesbrough, T.M., & Kolattukudy, P.E. Molecular cloning, nucleotide sequence, and tissue distribution of malonyl-CoA decarboxylase. *J. Biol. Chem.* **264**, 3500-3505 (1989).
8. Voilley, N. *et al.* Cloning and expression of rat pancreatic beta-cell malonyl-CoA decarboxylase. *Biochem. J.* **340** (Pt 1), 213-217 (1999).
9. Sacksteder, K.A., Morrell, J.C., Wanders, R.J., Matalon, R., & Gould, S.J. MCD encodes peroxisomal and cytoplasmic forms of malonyl-CoA decarboxylase and is mutated in malonyl-CoA decarboxylase deficiency. *J. Biol. Chem.* **274**, 24461-24468 (1999).
10. Kozak, M. Pushing the limits of the scanning mechanism for initiation of translation. *Gene* **299**, 1-34 (2002).
11. Dyck, J.R. *et al.* Malonyl coenzyme a decarboxylase inhibition protects the ischemic heart by inhibiting fatty acid oxidation and stimulating glucose oxidation. *Circ. Res.* **94**, e78-e84 (2004).

12. Holness, M.J., Bulmer, K., Smith, N.D., & Sugden, M.C. Investigation of potential mechanisms regulating protein expression of hepatic pyruvate dehydrogenase kinase isoforms 2 and 4 by fatty acids and thyroid hormone. *Biochem. J.* **369**, 687-695 (2003).
13. Abbot, E.L. *et al.* Diverging regulation of pyruvate dehydrogenase kinase isoform gene expression in cultured human muscle cells. *FEBS J.* **272**, 3004-3014 (2005).
14. Savkur, R.S., Bramlett, K.S., Michael, L.F., & Burris, T.P. Regulation of pyruvate dehydrogenase kinase expression by the farnesoid X receptor. *Biochem. Biophys. Res. Commun.* **329**, 391-396 (2005).
15. Wilmsen, H.M. *et al.* Thiazolidinediones upregulate impaired fatty acid uptake in skeletal muscle of type 2 diabetic subjects. *Am. J. Physiol. Endocrinol. Metab.* **285**, E354-E362 (2003).
16. Acin, A. *et al.* Cloning and characterization of the 5' flanking region of the human uncoupling protein 3 (UCP3) gene. *Biochem. Biophys. Res. Commun.* **258**, 278-283 (1999).
17. Gregg, A.R., Warman, A.W., Thorburn, D.R., & O'Brien, W.E. Combined malonic and methylmalonic aciduria with normal malonyl-coenzyme A decarboxylase activity: a case supporting multiple aetiologies. *J. Inherit. Metab. Dis.* **21**, 382-390 (1998).
18. O'Brien, D.P. *et al.* Malonic aciduria in Maltese dogs: normal methylmalonic acid concentrations and malonyl-CoA decarboxylase activity in fibroblasts. *J. Inherit. Metab. Dis.* **22**, 883-890 (1999).
19. Ozand, P.T., Nyhan, W.L., al, A.A., & Christodoulou, J. Malonic aciduria. *Brain Dev.* **16 Suppl**, 7-11 (1994).
20. Schoder, H., Knight, R.J., Kofoed, K.F., Schelbert, H.R., & Buxton, D.B. Regulation of pyruvate dehydrogenase activity and glucose metabolism in post-ischaemic myocardium. *Biochim. Biophys. Acta* **1406**, 62-72 (1998).
21. Stanley, W.C. *et al.* Pyruvate dehydrogenase activity and malonyl CoA levels in normal and ischemic swine myocardium: effects of dichloroacetate. *J. Mol. Cell. Cardiol.* **28**, 905-914 (1996).
22. Barak, C. *et al.* Effects of dichloroacetate on mechanical recovery and oxidation of physiologic substrates after ischemia and reperfusion in the isolated heart. *J. Cardiovasc. Pharmacol.* **31**, 336-344 (1998).
23. Bersin, R.M. & Stacpoole, P.W. Dichloroacetate as metabolic therapy for myocardial ischemia and failure. *Am. Heart J.* **134**, 841-855 (1997).

24. Lewandowski,E.D. & White,L.T. Pyruvate dehydrogenase influences postischemic heart function. *Circulation* **91**, 2071-2079 (1995).
25. Liu,B., Clanachan,A.S., Schulz,R., & Lopaschuk,G.D. Cardiac efficiency is improved after ischemia by altering both the source and fate of protons. *Circ. Res.* **79**, 940-948 (1996).
26. Lopaschuk,G.D., Wambolt,R.B., & Barr,R.L. An imbalance between glycolysis and glucose oxidation is a possible explanation for the detrimental effects of high levels of fatty acids during aerobic reperfusion of ischemic hearts. *J. Pharmacol. Exp. Ther.* **264**, 135-144 (1993).
27. McVeigh,J.J. & Lopaschuk,G.D. Dichloroacetate stimulation of glucose oxidation improves recovery of ischemic rat hearts. *Am. J. Physiol.* **259**, H1079-H1085 (1990).
28. Smolenski,R.T. *et al.* Pyruvate/dichloroacetate supply during reperfusion accelerates recovery of cardiac energetics and improves mechanical function following cardioplegic arrest. *Eur. J. Cardiothorac. Surg.* **19**, 865-872 (2001).
29. Taniguchi,M. *et al.* Dichloroacetate improves cardiac efficiency after ischemia independent of changes in mitochondrial proton leak. *Am. J. Physiol. Heart Circ. Physiol.* **280**, H1762-H1769 (2001).
30. Vanoverschelde,J.L., Janier,M.F., Bakke,J.E., Marshall,D.R., & Bergmann,S.R. Rate of glycolysis during ischemia determines extent of ischemic injury and functional recovery after reperfusion. *Am. J. Physiol.* **267**, H1785-H1794 (1994).
31. Wahr,J.A., Childs,K.F., & Bolling,S.F. Dichloroacetate enhances myocardial functional and metabolic recovery following global ischemia. *J. Cardiothorac. Vasc. Anesth.* **8**, 192-197 (1994).
32. Wahr,J.A., Olszanski,D., Childs,K.F., & Bolling,S.F. Dichloroacetate enhanced myocardial functional recovery post-ischemia : ATP and NADH recovery. *J. Surg. Res.* **63**, 220-224 (1996).
33. Cooper,R.H., Randle,P.J., & Denton,R.M. Regulation of heart muscle pyruvate dehydrogenase kinase. *Biochem. J.* **143**, 625-641 (1974).
34. Cooper,R.H., Randle,P.J., & Denton,R.M. Stimulation of phosphorylation and inactivation of pyruvate dehydrogenase by physiological inhibitors of the pyruvate dehydrogenase reaction. *Nature* **257**, 808-809 (1975).
35. Yue,T.L. *et al.* Activation of peroxisome proliferator-activated receptor-alpha protects the heart from ischemia/reperfusion injury. *Circulation* **108**, 2393-2399 (2003).

36. Wayman,N.S., Ellis,B.L., & Thiemermann,C. Ligands of the peroxisome proliferator-activated receptor-PPAR- α reduce myocardial infarct size. *Med. Sci. Monit.* **8**, BR243-BR247 (2002).
37. Wayman,N.S. *et al.* Ligands of the peroxisome proliferator-activated receptors (PPAR- γ and PPAR- α) reduce myocardial infarct size. *FASEB J.* **16**, 1027-1040 (2002).
38. Finck,B.N. *et al.* The cardiac phenotype induced by PPAR α overexpression mimics that caused by diabetes mellitus. *J Clin. Invest.* **109**, 121-130 (2002).
39. Yue,T.L. *et al.* Rosiglitazone treatment in Zucker diabetic Fatty rats is associated with ameliorated cardiac insulin resistance and protection from ischemia/reperfusion-induced myocardial injury. *Diabetes* **54**, 554-562 (2005).
40. Barger,P.M., Brandt,J.M., Leone,T.C., Weinheimer,C.J., & Kelly,D.P. Deactivation of peroxisome proliferator-activated receptor- α during cardiac hypertrophic growth. *J. Clin. Invest.* **105**, 1723-1730 (2000).
41. Wu,P. *et al.* Starvation and diabetes increase the amount of pyruvate dehydrogenase kinase isoenzyme 4 in rat heart. *Biochem. J.* **329** (Pt 1), 197-201 (1998).
42. Wu,P., Inskeep,K., Bowker-Kinley,M.M., Popov,K.M., & Harris,R.A. Mechanism responsible for inactivation of skeletal muscle pyruvate dehydrogenase complex in starvation and diabetes. *Diabetes* **48**, 1593-1599 (1999).
43. Wu,P. *et al.* Starvation increases the amount of pyruvate dehydrogenase kinase in several mammalian tissues. *Arch. Biochem. Biophys.* **381**, 1-7 (2000).
44. Wu,P., Peters,J.M., & Harris,R.A. Adaptive increase in pyruvate dehydrogenase kinase 4 during starvation is mediated by peroxisome proliferator-activated receptor α . *Biochem. Biophys. Res. Commun.* **287**, 391-396 (2001).
45. Baker,J.C., Yan,X., Peng,T., Kasten,S., & Roche,T.E. Marked differences between two isoforms of human pyruvate dehydrogenase kinase. *J. Biol. Chem.* **275**, 15773-15781 (2000).
46. Bowker-Kinley,M.M., Davis,W.I., Wu,P., Harris,R.A., & Popov,K.M. Evidence for existence of tissue-specific regulation of the mammalian pyruvate dehydrogenase complex. *Biochem. J.* **329** (Pt 1), 191-196 (1998).
47. Aasum,E. *et al.* Cardiac function and metabolism in Type 2 diabetic mice after treatment with BM 17.0744, a novel PPAR- α activator. *Am. J. Physiol. Heart Circ. Physiol.* **283**, H949-H957 (2002).

48. Aasum,E., Cooper,M., Severson,D.L., & Larsen,T.S. Effect of BM 17.0744, a PPAR α ligand, on the metabolism of perfused hearts from control and diabetic mice. *Can. J. Physiol. Pharmacol.* **83**, 183-190 (2005).
49. Kim,S.K. *et al.* Left-ventricular diastolic dysfunction may be prevented by chronic treatment with PPAR-alpha or -gamma agonists in a type 2 diabetic animal model. *Diabetes Metab. Res. Rev.* **19**, 487-493 (2003).
50. Muoio,D.M. *et al.* Peroxisome proliferator-activated receptor-alpha regulates fatty acid utilization in primary human skeletal muscle cells. *Diabetes* **51**, 901-909 (2002).
51. Ye,J.M. *et al.* Peroxisome proliferator-activated receptor (PPAR)-alpha activation lowers muscle lipids and improves insulin sensitivity in high fat-fed rats: comparison with PPAR-gamma activation. *Diabetes* **50**, 411-417 (2001).
52. Finck,B.N. *et al.* A critical role for PPARalpha-mediated lipotoxicity in the pathogenesis of diabetic cardiomyopathy: modulation by dietary fat content. *Proc. Natl. Acad. Sci. U. S. A* **100**, 1226-1231 (2003).
53. Kim,H.J. *et al.* Tissue-specific regulation of malonyl CoA decarboxylase activity in OLETF rats. *Diabetes, Obesity and Metabolism*(2005).
54. Herrero,L. *et al.* Alteration of the malonyl-CoA/carnitine palmitoyltransferase I interaction in the beta-cell impairs glucose-induced insulin secretion. *Diabetes* **54**, 462-471 (2005).
55. Roduit,R. *et al.* A role for the malonyl-CoA/long-chain acyl-CoA pathway of lipid signaling in the regulation of insulin secretion in response to both fuel and nonfuel stimuli. *Diabetes* **53**, 1007-1019 (2004).
56. Hu,Z., Cha,S.H., Chohnan,S., & Lane,M.D. Hypothalamic malonyl-CoA as a mediator of feeding behavior. *Proc. Natl. Acad. Sci. U. S. A* **100**, 12624-12629 (2003).
57. Hu,Z., Cha,S.H., van,H.G., Wang,J., & Lane,M.D. Effect of centrally administered C75, a fatty acid synthase inhibitor, on ghrelin secretion and its downstream effects. *Proc. Natl. Acad. Sci. U. S. A* **102**, 3972-3977 (2005).
58. Loftus,T.M. *et al.* Reduced food intake and body weight in mice treated with fatty acid synthase inhibitors. *Science* **288**, 2379-2381 (2000).